

**Unlocking proteomic and ecological
heterogeneity between *Schizophyllum
commune* and *Trametes versicolor* as early
sapwood colonizers on wood**

Amjad Zia

ORCID



0000-0002-3034-3181

**Unlocking proteomic and ecological
heterogeneity between *Schizophyllum
commune* and *Trametes versicolor* as early
sapwood colonizers on wood**

Dissertation

for the award of the degree

"Doctor rerum naturalium" (Dr.rer.nat.)

"Doctor of Philosophy" (PhD.) Division of Natural Sciences, Mathematics and
Informatics

Of the Georg-August-University of Göttingen

within the doctoral program "Materialforschung Holz"

Of the Georg-August University School of Science (GAUSS)

Submitted by

Amjad Zia

from Faisalabad, Pakistan

Göttingen, 2021

Thesis committee

1. **Prof. Dr. Carsten Mai**
Department of Wood Biology and Wood Products,
Georg-August University Göttingen, Göttingen

2. **Prof. Dr. Andrea Polle**
Department of Forest Botany and Tree Physiology,
Georg-August University Göttingen, Göttingen

3. **PD. Dr. Markus Euring**
Department of Wood Technology and Wood-based Composites,
Georg-August University Göttingen, Göttingen

Members of the Examination Board

4. **Prof. Dr. Christian Ammer**
Department of Silviculture and Forest Ecology of the Temperate Zones
Georg-August University Göttingen, Göttingen

5. **Prof. Dr. Holger Militz**
Department of Wood Biology and Wood Products
Georg-August University Göttingen, Göttingen

6. **Prof. Dr. Oliver Gailing**
Department of Forest Genetics and Forest Tree Breeding
Georg-August University Göttingen, Göttingen

Date of oral examination: July 23, 2021

Unlocking proteomic and ecological heterogeneity between *Schizophyllum commune* and *Trametes versicolor* as early sapwood colonizers on wood

Copyright © 2021 by Amjad Zia.

All rights reserved.

Printed in Germany.

No part of this book may be used or reproduced in any manner whatsoever without written permission except in the case of brief quotations embodied in critical articles or reviews.

For information contact; amjadzia1877@gmail.com

Book layout and cover were designed by the author.

ISBN:

DOI: [doi:10.53846/goediss-9372](https://doi.org/10.53846/goediss-9372)

JULY 2021

Dedicated to my family

Table of contents

Table of contents	V
Summary	IX
Zusammenfassung	XIII
1 General introduction	19
1.1 Background and purpose of this thesis	19
1.2 Chemical composition of wood and enzymatic degradation of its polymers	21
1.2.1 Cellulose and cellulases	22
1.2.2 Hemicellulose and hemicellulases	24
1.2.3 Pectin and pectinases	26
1.2.4 Lignin and Lignin-modifying enzymes	28
1.3 Wood decay fungi and early sapwood colonizers	30
1.3.1 <i>Trametes versicolor</i> (turkey tail mushroom)	31
1.3.2 <i>Schizophyllum commune</i> (split gill mushroom)	32
1.4 Interactions of wood decay basidiomycetes and mycoparasitism	34
1.5 Medium-free inoculation method	35
1.6 Proteomics – a modern approach to study the wood decay mechanisms	36
1.7 Objectives for this study	37
2 Materials and methods	39
2.1 Fungal strains	39
2.2 Growth conditions	39
2.3 Wood substrate collection	40
2.3.1 Sapwood collection	40
2.3.2 Bark collection	40
2.3.3 Wood decay tests	40
2.4 Interactions between <i>S. commune</i> and <i>T. versicolor</i>	42

2.4.1	Dual interactions on natural substrate _____	42
2.4.2	Dual interactions on artificial substrate _____	43
2.5	Medium-free pellets production _____	44
2.5.1	Protocol _____	44
2.6	A new method for secretome isolation from fungus-wood sample _____	45
2.6.1	Fungus-wood sample preparation and inoculation _____	45
2.6.2	Testing of extraction buffers for secretome isolation _____	45
2.6.3	Protocol for secretome isolation from fungus-wood sample _____	46
2.7	Extracellular protein purification and digestion _____	47
2.8	Sodium dodecyl sulfate–polyacrylamide gel electrophoresis _____	48
2.9	Intracellular protein purification and digestion _____	48
2.10	MS analysis and protein identification _____	49
2.11	Dual interactions on glass-fiber filters _____	51
2.11.1	Protein extraction from glass-fiber filters _____	51
2.12	Statistical analysis _____	51
3	Results _____	53
3.1	Wood decay by <i>S. commune</i> and <i>T. versicolor</i> _____	53
3.1.1	Comparison of sapwood weight losses by both fungi in different light schemes	54
3.1.2	Comparison of bark and sapwood weight losses of both fungi under light and dark conditions _____	59
3.1.3	Assessment the growth of both early sapwood colonizers on wood wash-out	62
3.2	Fungal interactions between <i>S. commune</i> and <i>T. versicolor</i> _____	64
3.2.1	Dual interactions on natural substrate _____	64
3.2.2	Dual interactions on artificial substrate _____	74
3.3	Medium-free pellets production _____	78
3.4	Protein profiling of <i>T. versicolor</i> grown on beech wood _____	80
3.4.1	Comparison of extraction buffers for secretome isolation _____	80
3.4.2	Comparing the secretome extraction buffers for 10- and 28- days old samples	81

3.4.3	Comparison of the <i>T. versicolor</i> (Tv-D) secretomes at early (10 days) and late (28 days) stages of decay _____	82
3.4.4	Intracellular proteins of <i>T. versicolor</i> (Tv-D) grown on beech wood _____	96
3.5	Secretome of <i>S. commune</i> grown on beech wood _____	100
3.6	Secretome analysis of <i>T. versicolor</i> and <i>S. commune</i> in dual culture _____	110
3.6.1	Fungal cell wall-degrading proteins _____	112
3.6.2	Chitinases _____	116
3.6.3	Proteins with potential antimicrobial activities _____	116
3.6.4	Ribonucleases _____	122
3.6.5	Oxidases and peroxidases _____	122
3.6.6	Proteases and peptidases _____	128
3.6.7	Potentially plant cell wall degrading enzymes _____	130
3.6.8	Miscellaneous identified proteins _____	130
4	Discussion _____	131
4.1	Comparison of beech bark and sapwood weight losses in decay tests _____	131
4.1.1	Wood decay by <i>T. versicolor</i> _____	131
4.1.2	Wood decay by <i>S. commune</i> _____	132
4.1.3	Fungal growth on wood wash-out _____	147
4.2	Fungal interactions between <i>S. commune</i> and <i>T. versicolor</i> on natural and artificial substrates _____	147
4.3	The <i>T. versicolor</i> secretome on beech wood _____	151
4.4	Secretome of <i>S. commune</i> on beech wood _____	152
4.5	Secretome analysis of <i>T. versicolor</i> and <i>S. commune</i> in dual culture _____	154
5	Conclusion and outlook _____	157
6	Supplementary data _____	161
7	Literature Cited _____	254
	Acknowledgements _____	302
	Curriculum Vitae _____	304

Summary

Fungi are an essential part of forest ecosystems and wood decay fungi play key roles in degradation of wood and in nutrient recycling. The complete degradation of wood by a single fungal species is a challenge due to the reluctant physical structure and chemical composition of wood. In nature, therefore, decaying wood is a harbor for multiple wood decaying fungi. These fungi, among others, are key players in the wood decay process. Certain wood-decay fungi colonize early the wood and start the decay process. In this context, two early sapwood colonizers *Schizophyllum commune* and *Trametes versicolor* are often found together in the form of mushrooms on branches of living trees, on freshly fallen dead wood and also on cut stems. In previously reported and in own observations, fruiting bodies of both fungi appeared on the decaying wood first during the early decay stage. However, *S. commune* is a weak degrader with features in between white and brown rot (grey rot), and may take advantages from co-resident fungi better able to degrade wood. *T. versicolor* in contrast is an aggressive white rot. Interactions between these two early sapwood colonizers exist which might be competitive or cooperative. In this thesis work, the central focus was to understand better the interactions between the early sapwood colonizers (*S. commune* and *T. versicolor*) in laboratory experiments in dual cultures on beech wood, and to isolate the secretomes/ proteomes from single and dual cultures grown on beech sapwood or artificial substrate to define functions in growth on wood, in detoxification of harmful wood compounds and in defense to other fungi.

Beech sapwood and bark decay tests were performed to test and compare the decay capacity of two early sapwood colonizers, *S. commune* and *T. versicolor*, under different light schemes. Three strains of *S. commune* (dikaryon *Sc-D*; the two parental monokaryons *Sc-M1* and *Sc-M2*) and two strains of *T. versicolor* (dikaryon *Tv-D*; monokaryon *Tv-M*) were inoculated on beech particles (ca. 4 x 1 mm) and incubated at 25 °C under different light conditions (in continuous dark - CD, in dark - D, in continuous light - CL, and in 12 h dark/12 h light cycles – 12L/12D) for 30 and 90 days. The aggressive behavior of *T. versicolor* has been verified by beech sapwood and bark decay tests. Overall, *T. versicolor* caused higher reduction in bark and sapwood weights than *S. commune*. In sapwood, *T. versicolor* reduced the weight at maximum 53% (*Tv-D*) and 24% (*Tv-M*) within 90 days, while *S. commune* achieved the weight loss in the same time only up to 6% (*Sc-D*: 4%; *Sc-M1*: 5%, and *Sc-M2*: 6%). All strains of *S. commune* reduced only a same

minor amount of the weight under all light and dark conditions. Differences have been observed in the weight losses by both strains of *T. versicolor* between all tested light schemes. The maximum reduction in weight losses caused by the *Tv*-M strain were 19%, 9%, 24%, and 24% under CL, 12L/12D, D and CD conditions, respectively. Maximum 44%, 48%, 53%, and 52% sapwood weight losses by the *Tv*-D strain were recorded under CL, 12L/12D, D and CD, respectively. In bark, the weight loss by *T. versicolor* was maximum 33% with 60 days of incubation in dark. In contrast, 4% bark weight was reduced by *S. commune* in dark and in light. In dark, both monokaryotic and dikaryotic strains of *T. versicolor* showed higher reduction in bark weights (*Tv*-M: 10 %, *Tv*-D: 33 %) in comparison to light condition (*Tv*-M: 8 %, *Tv*-D: 28 %).

In the tests of fungal growth on wood wash-out collected from European ash tree log, three *S. commune* (*Sc*-M1, *Sc*-M2, and *Sc*-D) and two *T. versicolor* (*Tv*-M, and *Tv*-D) strains were grown on different dilutions (1:1, 1:4, and 1:10) in dark/light at 25 °C. The growth of *Sc*-M2, *Sc*-D, *Tv*-M, and *Tv*-D were also tested on wood wash-out with the addition of thiamine, glucose and nitrogen. *S. commune* grew under all the conditions tested but *T. versicolor* could not grow on concentrated wood wash-out (1:1 dilution) with and without thiamine. With the presence of carbon, *Sc*-M2, *Tv*-M, and *Tv*-D produce dense mycelium except *Sc*-D. The tested strains (*Sc*-M2, *Sc*-D, *Tv*-M, and *Tv*-D) gave thin mycelial growth in the presence of nitrogen.

The interactions between both early sapwood colonizers were studied on natural (beech sapwood particles) and artificial (*S. commune* minimal medium) substrates. All possible interactions between three strains of *S. commune* (*Sc*-M1, *Sc*-M2, and *Sc*-D) and two strains of *T. versicolor* (*Tv*-M, and *Tv*-D) were observed on both substrates under continuous light and continuous dark conditions at 25 °C for 16 days. The dikaryotic strain of *T. versicolor* (*Tv*-D) was encountered with the monokaryotic strains of *S. commune* (*Sc*-M1 and *Sc*-M2) on day 6 and with the dikaryotic strain (*Sc*-D) on day 8, and dense mycelia appeared in the interaction zone. After that, the *Tv*-D strain overgrew throughout the *S. commune* (all strains) colonized compartments while growing on wood. However, on *S. commune* minimal medium, the *Tv*-D strain overgrew the *S. commune* strains while forming barriers of dense mycelia. In contrast, deadlocks were formed between the monokaryotic strain of *T. versicolor* (*Tv*-M) and the three strains of *S. commune* which were sustained till the end of the experiment on both natural and artificial substrates. In the dark, *T. versicolor* grew faster over the wood with *S. commune* as compared to in light. Therefore, *S. commune* inhabited wood particles were invaded by *T. versicolor* over time in the interactional

studies. *S. commune* also produced specialized hyphal structures i.e., spicules (small needle-like anatomical structures on hyphae) and hyphal coils in the interaction with *T. versicolor*. Deadlocks (mutual inhibition after mycelial contact), barrage formation (barrier zone of hyphal growth), and pigmentation of different colors and intensities were observed in the interactions on agar media.

For production of medium-free pellets, two strains of *T. versicolor* (*Tv-M* and *Tv-D*) and three strains of *S. commune* (*Sc-D*, *Sc-M1* and *Sc-M2*) were grown on liquid BSM and *S. commune* minimal medium, respectively in dark conditions at 25 °C. In submerged cultures, medium-free pellets of all strains of both fungi were produced successfully to inoculate the wood for the secretome/ proteome isolations. These pellets were stored at 4 °C in fridge.

Four different buffers were tested for the isolation of the *T. versicolor* (*Tv-D*) secretome from fungus-wood samples which were incubated at 25 °C in dark. In the experiment performed, buffer 1 was the best to isolate the secretome as it extracted a low number of contaminating intracellular proteins. The *T. versicolor* secretomes from early (10 days) and late (28 days) stages of decay were isolated and compared. 206 and 217 secreted proteins with signal peptides (identified by using SignalP 4.1) were then identified from 10- and 28- days old *T. versicolor* wood samples, respectively. In the experiment, at the early decay stage more laccases were found than at the late stage of decay at which more chitinases were found. The secreted proteins (183) shared between early and late decay stages were grouped according to their putative functions. The potential function of an enzyme was identified from the databases of JGI, InterPro, UniProt, HMMER web server, Pfam, NCBI blastp and NCBI conserved domain database (CDD). Enzymes and proteins secreted by *T. versicolor* were grouped according to their potential functions, like; lignin-modifying enzymes (e.g., peroxidases, laccases), cellulose-degrading enzymes (e.g., β -glucosidases, exo- and endo-glucanases), enzymes cleaving main and side chains of hemicellulose (e.g., endo-1,4- β -xylanases, β -galactosidases), pectinases (e.g., endo-polygalacturonase, pectinesterase), chitinases, auxiliary activity enzymes, proteases and peptidases, (e.g. aspartyl peptidases, and serine proteases), a few enzymes of other functions and some proteins of no known function.

After extracting the *T. versicolor* (*Tv-D*) secretome from the fungus-wood samples, the remaining samples were processed for the intracellular proteins to identify the proteins involved in different metabolisms while growing on wood. The potential function of an enzyme was

identified from the databases of JGI, InterPro, UniProt, HMMER web server, Pfam, NCBI blastp and NCBI conserved domain database (CDD). In the analysis of *T. versicolor* intracellular proteins, the identified proteins were involved in the following different pathways: amino acid metabolism, biodegradation of xenobiotics, biosynthesis of secondary metabolites, energy metabolism, metabolism of carbohydrates and complex carbohydrates, metabolism of lipids and complex lipids, metabolism of cofactors and vitamins, metabolism of other amino acids, nucleotide metabolism, sorting and degradation, transcription, and translation.

For the secretomic analysis of *S. commune*, the *Sc*-M1 (monokaryotic) strain was grown on beech sapwood particles for 2 weeks in dark at 25 °C. In the secretome of *S. commune*, 197 proteins with signal peptides were identified, and lignin-modifying enzymes (laccases and other multi-copper oxidases) were not expressed. According to the potential functions of proteins, the identified proteins were involved in the degradation of cellulose (found all three-essential group of enzymes i.e., exoglucanases, endoglucanases and β -glucosidases), hemicellulose (identified enzymes involved in the cleavage of xylan, mannans, and others), and pectin (identified enzymes acting on main and side chains). Besides these, chitinases, amylases, lipases, proteases and peptidases, auxiliary activities enzymes (identified members of AA3 (glucose-methanol-choline family of oxidoreductases), AA6 (reduction of the quinones by 1,4-benzoquinone reductases), and AA9 (copper-dependent lytic polysaccharide monooxygenase - copper dependent cleavage of cellulose with oxidation of carbons)), enzymes of other functions, and some proteins of unknown function were found in the secretome.

In the dual culture interaction of dikaryotic *S. commune* (*Sc*-D) and *T. versicolor* (*Tv*-D) strains on glass-fiber filters, the interaction was carried out on two layers of glass-fiber filters soaked in *S. commune* minimal medium which were placed in Petri-dish having solid *S. commune* minimal medium and incubated in dark for 10 days at 25 °C. From 453 identified proteins in the secretome, 284 and 169 proteins were from *T. versicolor* and *S. commune* respectively. The identified proteins from both fungi in the secretome were grouped as fungal cell wall degrading enzymes (glucanases and mannanases), chitinases, oxidases and peroxidases (e.g., laccases, peroxidases), proteases and peptidases (aspartic, metallo and serine peptidases), nucleases, and proteins with potential antimicrobial activities.

Zusammenfassung

Pilze sind ein wesentlicher Bestandteil von Waldökosystemen und holzzerstörende Pilze spielen eine Schlüsselrolle beim Abbau von Holz und beim Nährstoffrecycling. Der vollständige Abbau von Holz durch eine einzelne Pilzart ist aufgrund der widerspenstigen physikalischen Struktur und chemischen Zusammensetzung von Holz eine Herausforderung. In der Natur ist verrottendes Holz daher ein Unterschlupf für mehrere holzzerstrende Pilze. Diese Pilze sind neben anderen die Hauptakteure im Holzerfallsprozess. Bestimmte holzzerstörende Pilze besiedeln früh das Holz und starten den Zerfallsprozess. In diesem Zusammenhang werden zwei frühe Splintholzbesiedler, *Schizophyllum commune* und *Trametes versicolor*, oft gemeinsam in Form von Pilzen auf Ästen lebender Bäume, auf frisch gefallenem Totholz und auch auf geschnittenen Stämmen gefunden. In früheren Berichten und in eigenen Beobachtungen erschienen die Fruchtkörper beider Pilze zuerst in der frühen Fäulnisphase auf dem morschen Holz. Allerdings ist *S. commune* ein schwacher Zersetzer mit Merkmalen zwischen Weiß- und Braunfäule (Graufäule) und könnte Vorteile von mitbewohnenden Pilzen haben, die besser in der Lage sind, Holz abzubauen. *T. versicolor* hingegen ist eine aggressive Weißfäule. Zwischen diesen beiden frühen Splintholzbesiedlern bestehen Interaktionen, die sowohl kompetitiv als auch kooperativ sein können. In dieser Arbeit ging es darum, die Interaktionen zwischen den frühen Splintholzbesiedlern (*S. commune* und *T. versicolor*) in Laborexperimenten in Doppelkulturen auf Buchenholz besser zu verstehen und die Sekretome/Proteome aus Einzel- und Doppelkulturen, die auf Buchensplintholz oder künstlichem Substrat gewachsen sind, zu isolieren, um Funktionen beim Wachstum auf Holz, bei der Entgiftung schädlicher Holzinhaltstoffe und bei der Verteidigung gegen andere Pilze zu definieren.

Buchen-Splintholz- und Rindenfäulnisversuche wurden durchgeführt, um die Fäulniskapazität von zwei frühen Splintholzbesiedlern, *S. commune* und *T. versicolor*, unter verschiedenen Beleuchtungsschemata zu testen und zu vergleichen. Drei Stämme von *S. commune* (Dikaryon *Sc-D*; die beiden elterlichen Monokaryonen *Sc-M1* und *Sc-M2*) und zwei Stämme von *T. versicolor* (Dikaryon *Tv-D*; Monokaryon *Tv-M*) wurden auf Buchenpartikel (ca. 4 x 1 mm) inokuliert und bei 25 °C unter verschiedenen Lichtbedingungen (in kontinuierlicher Dunkelheit - CD, in Dunkelheit - D, in kontinuierlichem Licht - CL, und in 12 h Dunkelheit/12 h Licht-Zyklen - 12L/12D) für 30 und 90 Tage bebrütet. Das aggressive Verhalten von *T. versicolor* wurde durch

Tests an Buchensplintholz und Rindenfäule verifiziert. Insgesamt verursachte *T. versicolor* eine höhere Reduktion des Rinden- und Splintholzgewichts als *S. commune*. Im Splintholz reduzierte *T. versicolor* das Gewicht innerhalb von 90 Tagen um maximal 53 % (*Tv-D*) und 24 % (*Tv-M*), während *S. commune* den Gewichtsverlust in der gleichen Zeit nur bis zu 6 % erreichte (*Sc-D*: 4 %; *Sc-M1*: 5 % und *Sc-M2*: 6 %). Alle Stämme von *S. commune* reduzierten unter allen Licht- und Dunkelbedingungen nur einen gleich geringen Anteil des Gewichts. Es wurden Unterschiede in den Gewichtsverlusten durch beide Stämme von *T. versicolor* zwischen allen getesteten Lichtschemata beobachtet. Die maximale Reduktion der Gewichtsverluste durch den *Tv-M*-Stamm betrug 19 %, 9 %, 24 % und 24 % unter CL-, 12L/12D-, D- bzw. CD-Bedingungen. Die maximalen Gewichtsverluste im Splintholz durch den *Tv-D*-Stamm betrugen 44 %, 48 %, 53 % und 52 % unter CL, 12L/12D, D bzw. CD. In der Rinde betrug der Gewichtsverlust durch *T. versicolor* maximal 33 % bei 60 Tagen Inkubation im Dunkeln. Im Gegensatz dazu wurden 4% Rindengewicht durch *S. commune* im Dunkeln und im Licht reduziert. Im Dunkeln zeigten sowohl monokaryotische als auch dikaryotische Stämme von *T. versicolor* eine höhere Reduktion des Rindengewichts (*Tv-M*: 10 %, *Tv-D*: 33 %) im Vergleich zu hellen Bedingungen (*Tv-M*: 8 %, *Tv-D*: 28 %).

Bei den Tests des Pilzwachstums auf ausgewaschenem Holz, das aus dem Stamm der europäischen Esche gesammelt wurde, wurden drei *S. commune* (*Sc-M1*, *Sc-M2* und *Sc-D*) und zwei *T. versicolor* (*Tv-M* und *Tv-D*) Stämme in verschiedenen Verdünnungen (1:1, 1:4 und 1:10) im Dunkeln/Licht bei 25 °C gezüchtet. Das Wachstum von *Sc-M2*, *Sc-D*, *Tv-M* und *Tv-D* wurde auch auf Holzauswaschung unter Zugabe von Thiamin, Glukose und Stickstoff getestet. *S. commune* wuchs unter allen getesteten Bedingungen, aber *T. versicolor* konnte auf konzentrierter Holzauswaschung (1:1 Verdünnung) mit und ohne Thiamin nicht wachsen. Bei Anwesenheit von Kohlenstoff produzieren *Sc-M2*, *Tv-M* und *Tv-D* ein dichtes Myzel, außer *Sc-D*. Die getesteten Stämme (*Sc-M2*, *Sc-D*, *Tv-M* und *Tv-D*) bildeten in Anwesenheit von Stickstoff ein dünnes Myzelwachstum.

Die Interaktionen zwischen den beiden frühen Splintholzbesiedlern wurden auf natürlichen (Buchensplintholzpartikel) und künstlichen (*S. commune* Minimalmedium) Substraten untersucht. Alle möglichen Interaktionen zwischen drei Stämmen von *S. commune* (*Sc-M1*, *Sc-M2* und *Sc-D*) und zwei Stämmen von *T. versicolor* (*Tv-M* und *Tv-D*) wurden auf beiden Substraten unter Dauerlicht- und Dauerdunkelbedingungen bei 25 °C für 16 Tage beobachtet. Der dikaryotische

Stamm von *T. versicolor* (Tv-D) wurde am 6. Tag mit den monokaryotischen Stämmen von *S. commune* (Sc-M1 und Sc-M2) und am 8. Tag mit dem dikaryotischen Stamm (Sc-D) zusammengebracht, und in der Interaktionszone erschienen dichte Myzelien. Danach wuchs der Tv-D-Stamm in allen von *S. commune* (alle Stämme) kolonisierten Kompartimenten über, während er auf Holz wuchs. Auf *S. commune*-Minimalmedium wuchs der Tv-D-Stamm jedoch über die *S. commune*-Stämme hinaus und bildete Barrieren aus dichten Myzelien. Im Gegensatz dazu bildeten sich Deadlocks zwischen dem monokaryotischen Stamm von *T. versicolor* (Tv-M) und den drei Stämmen von *S. commune*, die bis zum Ende des Experiments sowohl auf natürlichen als auch auf künstlichen Substraten aufrechterhalten wurden. Im Dunkeln wuchs *T. versicolor* schneller über das Holz mit *S. commune* als im Licht. Daher wurden die von *S. commune* bewohnten Holzpartikel in den Interaktionsstudien im Laufe der Zeit von *T. versicolor* besiedelt. *S. commune* produzierte in der Interaktion mit *T. versicolor* auch spezialisierte Hyphenstrukturen, d. h. Spicula (kleine nadelartige anatomische Strukturen auf Hyphen) und Hyphenwindungen. Deadlocks (gegenseitige Hemmung nach Myzelkontakt), Barrierebildung (Sperrzone des Hyphenwachstums) und Pigmentierung unterschiedlicher Farben und Intensitäten wurden bei den Interaktionen auf Agarmedien beobachtet.

Zur Herstellung von medienfreien Pellets wurden zwei Stämme von *T. versicolor* (Tv-M und Tv-D) und drei Stämme von *S. commune* (Sc-D, Sc-M1 und Sc-M2) auf flüssigem BSM bzw. *S. commune*-Minimalmedium unter dunklen Bedingungen bei 25 °C kultiviert. In submersen Kulturen wurden von allen Stämmen beider Pilze erfolgreich medienfreie Pellets hergestellt, um das Holz für die Sekretom-/Proteomisolierungen zu beimpfen. Diese Pellets wurden bei 4 °C im Kühlschrank gelagert.

Vier verschiedene Puffer wurden für die Isolierung des *T. versicolor* (Tv-D) Sekretoms aus Pilz-Holz-Proben getestet, die bei 25 °C im Dunkeln inkubiert wurden. In dem durchgeführten Experiment war Puffer 1 der beste zur Isolierung des Sekretoms, da er eine geringe Anzahl kontaminierender intrazellulärer Proteine extrahierte. Die *T. versicolor*-Sekretome aus frühen (10 Tage) und späten (28 Tage) Stadien des Zerfalls wurden isoliert und verglichen. 206 und 217 sekretierte Proteine mit Signalpeptiden (identifiziert mit SignalP 4.1) wurden dann aus 10 bzw. 28 Tage alten *T. versicolor* Holzproben identifiziert. Im Experiment wurden im frühen Zerfallsstadium mehr Laccasen gefunden als im späten Zerfallsstadium, in dem mehr Chitinasen gefunden wurden. Die sekretierten Proteine (183), die sich die frühen und späten Fäulnisstadien

teilen, wurden entsprechend ihrer vermuteten Funktionen gruppiert. Die potentielle Funktion eines Enzyms wurde aus den Datenbanken von JGI, InterPro, UniProt, HMMER-Webserver, Pfam, NCBI blastp und NCBI conserved domain database (CDD) identifiziert. Die von *T. versicolor* sezernierten Enzyme und Proteine wurden nach ihren potenziellen Funktionen gruppiert, wie z. B. ligninmodifizierende Enzyme (z. B. Peroxidasen, Laccasen), celluloseabbauende Enzyme (z. B. β -Glucosidasen, Exo- und Endo-Glucanasen), Enzyme, die Haupt- und Seitenketten von Hemicellulose spalten (z. B., Endo-1,4- β -Xylanasen, β -Galaktosidasen), Pektinasen (z. B. Endo-Polygalakturonase, Pektinesterase), Chitinasen, Enzyme mit Hilfsaktivitäten, Proteasen und Peptidasen (z. B. Aspartylpeptidasen, Serinproteasen), einige Enzyme mit anderen Funktionen und einige Proteine ohne bekannte Funktion.

Nach der Extraktion des *T. versicolor* (*Tv-D*) Sekretoms aus den Pilz-Holz-Proben wurden die verbleibenden Proben für die intrazellulären Proteine aufbereitet, um die Proteine zu identifizieren, die an verschiedenen Stoffwechselfvorgängen während des Wachstums auf Holz beteiligt sind. Die potentielle Funktion eines Enzyms wurde aus den Datenbanken von JGI, InterPro, UniProt, HMMER-Webserver, Pfam, NCBI blastp und NCBI conserved domain database (CDD) identifiziert. Bei der Analyse der intrazellulären Proteine von *T. versicolor* waren die identifizierten Proteine an den folgenden verschiedenen Stoffwechselwegen beteiligt: Aminosäurestoffwechsel, biologischer Abbau von Xenobiotika, Biosynthese von Sekundärmetaboliten, Kohlenhydratstoffwechsel, Energiestoffwechsel, Lipidstoffwechsel, Stoffwechsel von Cofaktoren und Vitaminen, Stoffwechsel komplexer Kohlenhydrate, Stoffwechsel komplexer Lipide, Stoffwechsel anderer Aminosäuren, Nukleotidstoffwechsel, Sortierung und Abbau, Transkription und Translation.

Für die Sekretomanalyse von *S. commune* wurde der Stamm *Sc-M1* (monokaryotisch) für 2 Wochen im Dunkeln bei 25 °C auf Buchensplintholzpartikeln kultiviert. Im Sekretom von *S. commune* wurden 197 Proteine mit Signalpeptiden identifiziert, wobei Lignin-modifizierende Enzyme (Laccasen und andere Multi-Kupfer-Oxidasen) nicht exprimiert wurden. Entsprechend den potentiellen Funktionen der Proteine waren die identifizierten Proteine am Abbau von Cellulose (alle drei essentiellen Enzymgruppen, d.h. Exoglucanasen, Endoglucanasen und β -Glucosidasen, wurden gefunden), Hemicellulose (identifizierte Enzyme, die an der Spaltung von Xylan, Mannanen und anderen beteiligt sind) und Pektin (identifizierte Enzyme, die auf Haupt- und Seitenketten wirken) beteiligt. Außerdem Chitinasen, Amylasen, Lipasen, Proteasen und

Peptidasen, Enzyme mit Hilfsaktivitäten (identifizierte Mitglieder der AA3 (Glucose-Methanol-Cholin-Familie der Oxidoreduktasen), AA6 (Reduktion der Chinone durch 1,4-Benzochinon-Reduktasen), und AA9 (kupferabhängige lytische Polysaccharid-Monooxygenase - kupferabhängige Spaltung von Cellulose mit Oxidation von Kohlenstoffen)), Enzyme anderer Funktionen und einige Proteine mit unbekannter Funktion wurden im Sekretom gefunden.

Bei der dualen Kulturinteraktion von dikaryotischen *S. commune* (Sc-D) und *T. versicolor* (Tv-D) Stämmen auf Glasfaserfiltern wurde die Interaktion auf zwei Schichten von Glasfaserfiltern durchgeführt, die mit *S. commune*-Minimalmedium getränkt waren. Diese wurden in Petri-Schalen mit festem *S. commune*-Minimalmedium platziert und 10 Tage bei 25 °C im Dunkeln inkubiert. Von 453 identifizierten Proteinen im Sekretom stammten 284 bzw. 169 Proteine aus *T. versicolor* und *S. commune*. Die identifizierten Proteine aus beiden Pilzen im Sekretom wurden als pilzliche zellwandabbauende Enzyme (Glucanasen und Mannanasen), Chitinasen, Oxidasen und Peroxidasen (z. B. Laccasen, Peroxidasen), Proteasen und Peptidasen (Asparagin-, Metallo- und Serinpeptidasen), Nukleasen und Proteine mit potenziellen antimikrobiellen Aktivitäten gruppiert.

1 General introduction

1.1 Background and purpose of this thesis

Wood decay is a challenge for a fungus due to the physical properties and the complex chemical structure of recalcitrant lignocellulosic biomass (Floudas et al. 2012; Deacon 2013). In nature, therefore, a variety of wood decaying fungi harbor the deadwood and appear as sporocarps (fruiting bodies) on the decaying wood (Jang et al. 2015; Sefidi and Etemad 2015; Blinkova and Ivanenko 2016; Krause et al. 2020). Key players from wood decaying fungi are early wood colonizers which most probably start the decay process of recalcitrant lignocellulose and may influence the subsequent colonizers (Dickie et al. 2012; Hiscox et al. 2015; Song et al. 2015; Song et al. 2017). Especially members of Basidiomycota (Agaricomycetes) are the main agents of wood decay, and play crucial roles in carbon and nutrients recycling (Krah et al. 2018; Leonhardt et al. 2019). Two members of the basidiomycetous fungi, *Schizophyllum commune* and *Trametes versicolor* are early sapwood colonizers and often in nature found (as fruiting bodies) together on freshly fallen dead wood of broadleaf trees (Lakkireddy et al. 2017; Zia et al. 2018).

Wood decay has traditionally been categorized into three broad groups: white, brown, and soft rot (Schwarze et al. 2000; Schmidt and Czeschlik 2006). In nature, the majority of wood decay is carried out by Basidiomycetes, from which more than 90% belonged to white rot group and less than 10% are brown rot fungi (Rytioja et al. 2014). Brown-rot fungi generally depolymerize cellulose and hemicellulose without attacking lignin or degrading only a small part of it (because of complete or partial lack of class II peroxidases), and brown color appears because of the remaining lignin (Yelle et al. 2008; Eastwood et al. 2011; Rytioja et al. 2014). All components of lignocellulosic material including lignin are degraded by a massive attack of white-rot fungi (because the fungus have multiple lignin-degrading peroxidases and ranges of enzymes acting on crystalline cellulose), either simultaneous or sequentially first the lignin and then the polysaccharides. White rot fungi mainly break down the lignin by leaving behind cellulose, gives a whitish appearance on decayed wood (Hammel and Cullen 2008; Hofrichter 2010; Rytioja et al. 2014). Soft rot fungi mainly belong to Ascomycetes, degrade wood by creating a series of successive cavities within the S2 layer of wood (known as type 1) or degrade wood layers outwards

from the lumen by creating V-shaped eroded channels (known as type 2) by mainly degrading cellulose of wood (Schmidt and Czeschlik 2006; Schwarze et al. 2000).

T. versicolor is an aggressive white rot degrader and broadly distributed throughout the world (Janjušević et al. 2017). On the other hand, *S. commune* is a weak pathogen and wood degrader (Lakkireddy et al. 2017; Jusoh et al. 2014; Suprapti and Djarwanto 2014; Suprapti et al. 2011; Takemoto et al. 2010; Peddireddi 2008; Schmidt and Liese 1980), and with features in between white and brown rot (a fungus lacks genes for ligninolytic peroxidases (like brown-rot fungi) but (like white-rot fungi) have diverse ranges of enzymes attacking crystalline cellulose, Riley et al. 2014). The fungus is now also known as grey rot fungus, a wood decay fungus acts like a white rotter but lacks majority of ligninolytic class II peroxidases (Riley et al. 2014; Zhu et al. 2016; Krah et al. 2018; Villavicencio et al. 2020). The fungus has been reported from every part of the world including Antarctica (Gonçalves et al. 2015). *T. versicolor* can depolymerize lignin, cellulose and hemicellulose, and leave excessive cellulose which can be utilized by other (or weak) degraders. Therefore, *S. commune* may take advantage from co-resident fungi better able to degrade wood (Essig 1922; Erwin et al. 2008; Floudas et al. 2015) such as *T. versicolor* (Lakkireddy et al. 2017). To understand better the mechanisms of wood decay by white-rot and brown-rot basidiomycetes, the genomes of 31 fungi (24 basidiomycetes, 5 ascomycetes, and 2 other) (Floudas et al. 2012), and 22 genomes of wood-decaying fungi were compared (Riley et al. 2014), which made it clear that *T. versicolor* is a white-rot fungus but *S. commune* is in between white-rot and brown-rot species. *T. versicolor* (strain FP-101664, SS1, genome version 1.0, sequenced as a part of Saprotrrophic Agaricomycotina Project, <https://mycocosm.jgi.doe.gov/Travel/Travel.home.html>) has 14,296 predicted genes in its genome and 1462 predicted proteins have a secretion signal (10% of total), from which 138 are potential enzymes for lignocellulose-degradation (Floudas et al. 2012). *S. commune* (strain H4-8, genome version 3.0, sequenced as a part of 1000 Fungal Genomes Project <https://mycocosm.jgi.doe.gov/Schco3/Schco3.home.html>), on the other hand, has in total 16,319 predicted genes and 1549 predicted proteins with a signal peptide, from which 111 are potential enzymes for lignocellulose-degradation (Floudas et al. 2012). In the absence of protein-coding genes for lignin peroxidases, manganese peroxidases and versatile peroxidases in the *S. commune* genome, it is interesting to study the secretome and the mechanism of lignocellulosic biomass biodegradation.

In our observations (Lakkireddy et al. 2017), *S. commune* as mushrooms appears as a first fungus on freshly fallen deadwood and starts to decay (Koyani et al. 2016; Floudas et al. 2015; Padhiar and Albert 2011; Erwin et al. 2008), which is probably due to presence of a distinct set of enzymes. After the appearance of *S. commune*, *T. versicolor* appears besides *S. commune* on the same wood. As known from literature, *S. commune* is a weak degrader and *T. versicolor* is a strong degrader, it is interesting to explore their cooperative/ competing interactions and at the same time how both fungi contribute to decay process (early and later decay stages). The fungi are expected to produce a distinct range of extra- and intracellular proteins for the growth on wood and for the accompanying process of the wood decay. These enzymes and enzymatic cocktails could improve and enhance the biotechnological processes and products e.g., the production of biofuel, enzymes and schizophyllan (extracellular polysaccharide produced by *S. commune*) (Tovar-Herrera et al. 2018). Therefore, it is also important to analyze the proteomes (the secretomes as well as the intracellular proteomes) of the two fungi grown in single culture and in combination on wood.

1.2 Chemical composition of wood and enzymatic degradation of its polymers

Stem wood of trees is the most useful naturally occurring organic matter, consists of two major fractions – the bark (periderm, cortex, phloem) and the wood (sapwood, heartwood). Bark, the outermost layer, protects the inner parts from outer extremes and attacks. Bark varies from tree to tree in thickness and structure, and weighs 10 – 20% (dry wt) of the total woody biomass (Vane et al. 2006). As the wood fraction comprised of sapwood and heartwood, they differ in chemical composition, function, physical strength and thickness. The wood fraction is composed of different biopolymers (cellulose 42 – 52 %, hemicellulose 25 – 32 %, lignin 20 – 30 %), extractives (2 – 9 %), and inorganic material which vary from softwood to hardwood (Herz 2015; Tarasov et al. 2018). Although the main constituents (cellulose, hemicellulose, lignin, pectin, and extractives) of bark and wood are similar but their proportions and quantities differ among trees (Sjöström 1993; Ek et al. 2009; Rowell et al. 2012; Dhyani and Bhaskar 2018). Due to the complex nature of wood, it is highly recalcitrant to decay. Therefore, a repertoire of enzymes has been identified and described for each polymer (cellulose, hemicellulose, lignin, and pectin) degradation. A fungus in wood decay process produces a cocktail of lignocellulolytic enzymes, which depends on the microorganism, the type of substrate and the environment. This cocktail contains cellulases,

hemicellulases, pectinases, and ligninases. In the following sections, major wood polymers are briefly described with the enzymes involved in their degradation.

1.2.1 Cellulose and cellulases

Cellulose is the main component of plant cell walls and wood, and the most abundant biopolymer on the earth (Klemm et al. 2005). Cellulose surrounds plant cells as being a major part of tough plant cell wall and provides structural strength to cell to maintain cell shape and turgor pressure. Primarily, cellulose is composed of several hundred to many thousands glucose units – $(C_6H_{10}O_5)_n$ which are connected with $\beta(1\rightarrow4)$ glycosidic linkage in a linear chain (Figure 1-1). Two glucose molecules unite to form cellobiose (Figure 1-1 - the repeating unit of cellulose) and these cellobiose units assemble in a linear chain of glucan polymer which is known as cellulose. A native cellulose molecule contains 10,000 to 15,000 glucose units (DP – the degree of polymerization refers to glucose units per cellulose molecule) depending on the tree species. On average, a 5 μm wood cellulose fragment is made from 10,000 (DP) glucose units (Klemm et al. 2005; Schmidt and Czeschlik 2006; Rowell et al. 2012). The linear chain of cellulose (20 to 300) connect to build cellulose fibers. These fibers aggregate together by hydrogen bonding and van der Waals forces to create microfibrils. In the plant cell wall, fabrication of these microfibrils in a crisscross pattern provides structural support to the cell (Dhyani and Bhaskar 2019).

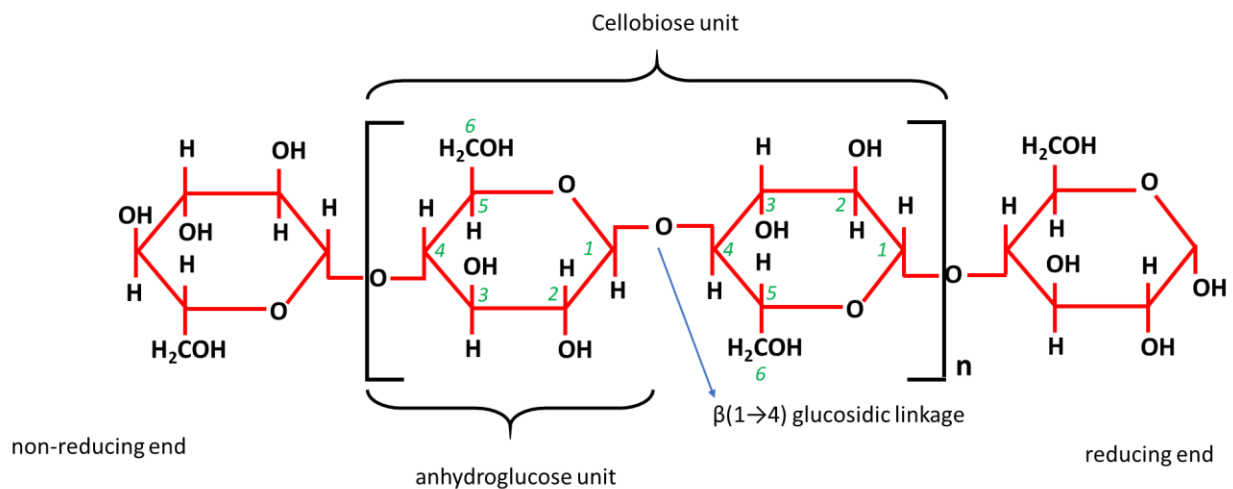


Figure 1-1 Chemical structure and glycosidic bonding of cellobiose in cellulose (redrawn from Olsson and Westm 2013).

Cellulose-degrading enzymes are classified into three major categories: endoglucanases, exoglucanases, and β -glucosidases (Figure 1-2). Exoglucanases cleave the 1 \rightarrow 4 linkages from the reducing or nonreducing ends of cellulose polysaccharides and oligosaccharides. These enzymes are further categorized into cellobiohydrolases (CBHs) and cellodextrinases. CBHs (cellobiohydrolases or cellulose 1,4- β -cellobiosidases) hydrolyze the 1 \rightarrow 4 linkages and release cellobiose from the cellulose ends. CBHIs (EC 3.2.1.176) from glycoside hydrolase (GH) 7 (formerly known as cellulase family C) and GH 48 (formerly known as cellulase family L) families cleave the cellulose chain reducing ends, and CBHIIIs (e.g., EC 3.2.1.91) belong to GH 5 (formerly known as cellulase family A), GH 6 (formerly known as cellulase family B) and GH 9 (formerly known as cellulase family E) families act on the nonreducing ends of the cellulose chains, processively. Cellodextrinases from GH 1, GH 3, GH 5, and GH 9 families cut (1 \rightarrow 4)-linkages in cellulose and cellodextrins with the removal of successive glucose units. Glucan 1,4- β -glucosidase (EC 3.2.1.74) is the example of cellodextrinase (Kubicek et al. 2014; Gupta 2016; Ceballos 2018).

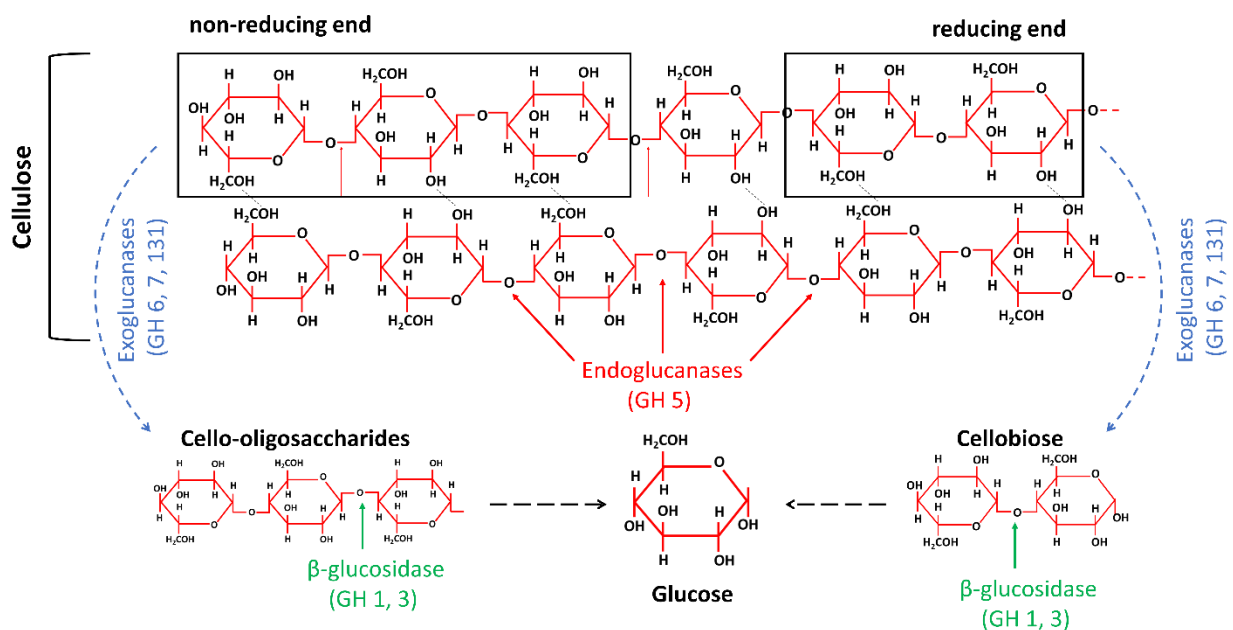


Figure 1-2 The enzymatic degradation of cellulose to glucose based on the secretome of *S. commune* (the information is taken from Ceballos 2018).

Endoglucanases (like; 4- β -D-glucan 4-glucohydrolase, EC 3.2.1.4) cut randomly internal 1,4- β -d-glycosidic linkages of cellulose chains and generate short chains with new ends. Enzymes with endoglucanase activities are found in GH 5, GH 6, GH 7, GH 9, GH 12, GH 44,

GH 45, GH 48, GH 51, GH 74, and GH 124 families. β -glucosidases (e.g., EC 3.2.1.21) release β -D-glucose units by hydrolyzing the nonreducing ends of oligosaccharides (cellobiose and cellodextrin). These enzymes are found in GH 1, GH 3, GH 5, GH 9, GH 30, and GH 116 families (Kubicek et al. 2014; Gupta 2016; Ceballos 2018).

1.2.2 Hemicellulose and hemicellulases

From the branched heteropolymers, hemicelluloses are the second abundant polysaccharides of wood, containing mainly arabinoxylan, glucomannan, glucuronoxylan, xyloglucan and xylan polymers (Figure 1-3) which are bonded by a complex combination of relatively short polymers (built of arabinose, galactose, glucose mannose, and xylose). The combination and composition of these polymers differ from species to species. These polymers are relatively short polymers compared to cellulose with an average DP of 50–200 (Dhyani and Bhaskar 2018, 2019). Hemicellulose encapsulates cellulose fibrils by hydrogen bonds and is connected with lignin covalently (Schmidt and Czeschlik 2006; Ceballos 2018). Sugar units in hemicellulose are usually linked β -(1 \rightarrow 4) for a backbone of the polymer and (1 \rightarrow 2), (1 \rightarrow 3), and/or (1 \rightarrow 6) for the branching points. As the core chains linkages are different in the major polysaccharides (galactomannans, xylans, and xyloglucans - Figure 1-3) due to different sugars, and the side-chains often have the same linkages and contained the same sugars. Hence, the enzymes involved in the depolymerization of these polymers are same (Kubicek et al. 2014).

For the complete depolymerization of xylans, xylanases are distributed in families GH3, GH10, GH11, GH30, GH43, and GH54. However, fungal xylanases are mostly members of GH 10 and GH 11 families, and the highest number of fungal xylanases are from GH 10 family. The backbone of xylan is cleaved by endo-1,4- β -xylanases (EC 3.2.1.8). Further cleavages of the main chain and the side-groups are done by xylan 1,4- β -xylosidase (EC 3.2.1.37), acetylerase (EC 3.1.1.6), xylan α -1,2-glucuronidase (EC 3.2.1.131), and α -arabinosidase (EC 3.2.1.55). To act on xyloglucans, the back bone is hydrolyzed by endo- β -(1 \rightarrow 4)-glucanases (both specific and nonspecific). Mostly xyloglucanases are from GH5, GH12, GH16, GH44 and GH74 families, which cleave the polymer main and side chains (Schmidt and Czeschlik 2006; Kubicek et al. 2014; Rytioja et al. 2014).

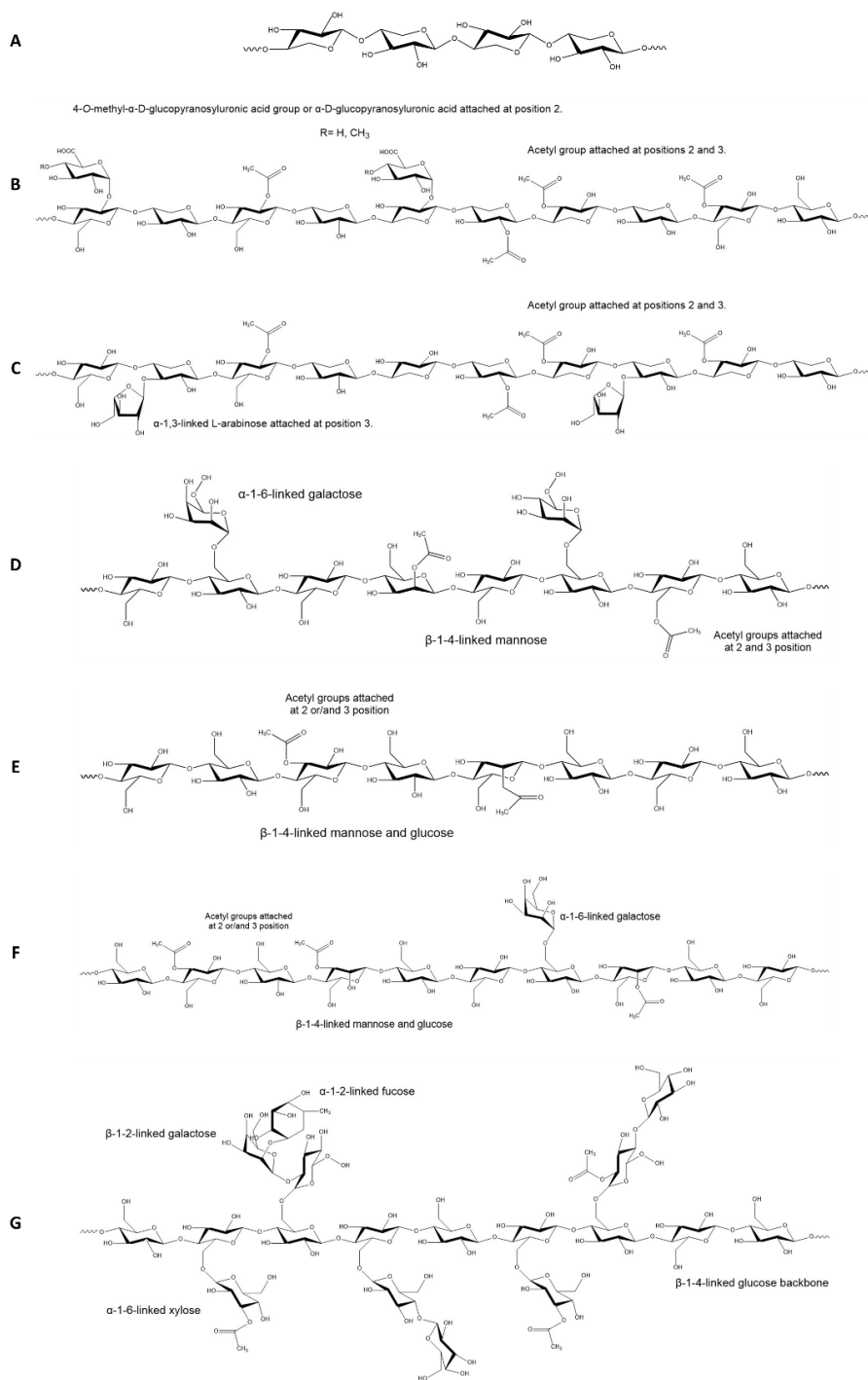


Figure 1-3 Schematic structures of different hemicellulose polysaccharides of A: β -1,4-D-xylan, B: glucuronoxylan, C: arabinoxylan, D: galactomannan, E: glucomannan, F: galactoglucomannan, and G: xyloglucan. These structures were redrawn from Zhou et al. 2017 by using ChemDraw Professional version 20.0.

The mannan-containing polymers (galactomannans, glucomannans, and galactoglucomannans, Figure 1-3 D, E and F) are hydrolyzed by β -mannanase (EC 3.2.1.78) and β -mannosidase (EC 3.2.1.25) belong to GH26 and GH5 families, respectively. β -Mannosidases are also members of GH1 and GH2 families. Besides these enzymes, α -glucosidase from GH27 and GH36, β -galactosidase from GH35, and esterases as accessory enzymes are involved in the depolymerization. α -Arabinosidases activity can be found in GH43, GH51, GH54 and GH62 families which act on arabinans and arabinogalactans polymers (Schmidt and Czeschlik 2006; Kubicek et al. 2014; Rytioja et al. 2014).

1.2.3 Pectin and pectinases

Pectin, another major heteropolysaccharide of lignocellulosic material, is mainly made of α -(1 \rightarrow 4) linked galacturonic acid (GalA) units with varying proportions of various monosaccharides (17 different sugars) as side chains (Figure 1-4). This complex macromolecule plays quite diverse functions in a plant, like; providing support and strength to a plant, cell differentiation and growth, activation of plant defense mechanisms, stimulate the accumulation of antimicrobial substances (phytoalexin) and protease inhibitors, and lignification (Voragen et al. 2009; Yapo 2011; Lara-Espinoza et al. 2018). Pectin polysaccharides are divided into four groups (Figure 1-4) viz. homogalacturonan, rhamnogalacturonan-I, rhamnogalacturonan-II, and xylogalacturonan, which are inter-linked covalently (Yapo 2011). In homogalacturonan, galacturonic acid residues in a backbone are α -1,4-linked in a linear chain. Rhamnogalacturonan-I is a branched heteropolymer and composed of galacturonic acid units with other sugars residues (α -L- Araf, β -D-Galp, and α -L-Rhap) in its backbone and side chains. The most complex polysaccharide of pectin is rhamnogalacturonan-II, which has homogalacturonan in backbone and interconnected covalently by 20 different linkages with individual sugars (28–36 units). Xylogalacturonans are composed of homogalacturonans connected at the O-3 position with xylose (Voragen et al. 2009; Yapo 2011; Ceballos 2018; Lara-Espinoza et al. 2018).

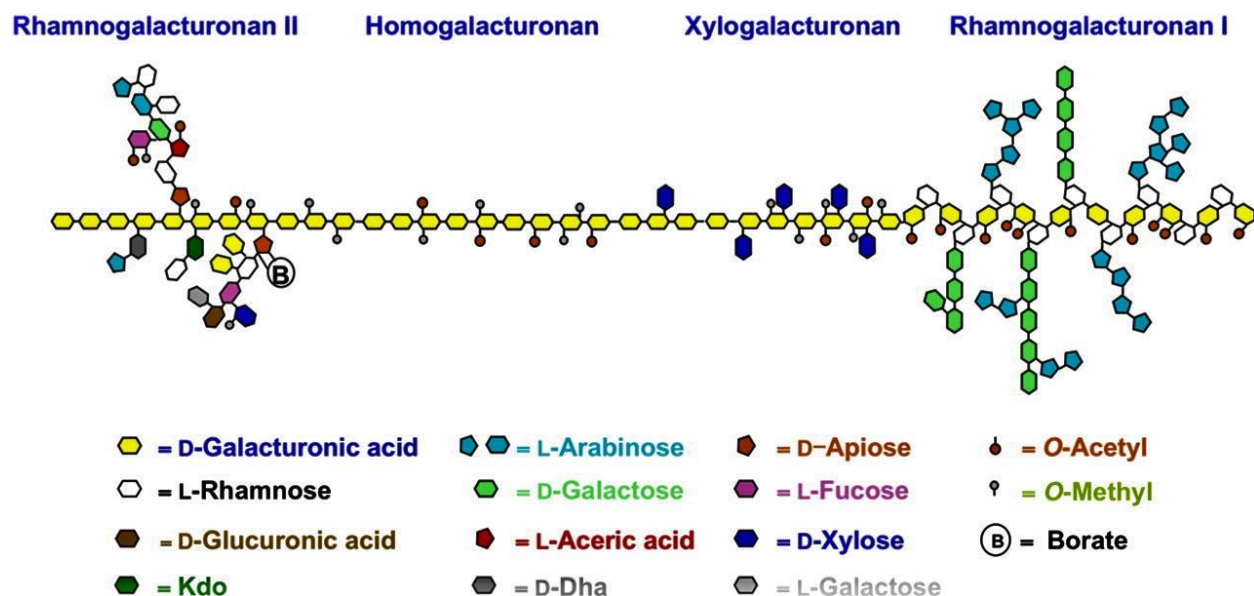


Figure 1-4 Graphical representations of pectin and its polysaccharides. Kdo: 3-Deoxy-D-manno-oct-2-ulosonic acid, and Dha: 3-deoxy-D-lyxo-heptopyran-2-ularic acid (taken from Harholt et al. 2010).

The degradation of this complex macromolecule is carried out by pectinases which include several esterases, hydrolases and lyases. Here, pectin degrading enzymes are categorized according to pectin groups. In literature, numerous enzymes are described for the cleavage of homogalacturonan which include exopolygalacturonase (EC 3.2.1.67 and EC 3.2.1.82; GH 28), endo-polygalacturonase (EC 3.2.1.15; GH 28), polysaccharide lyases (EC 4.2.2.2 and EC 4.2.2.10), pectin methylesterase, and pectin acetyl esterase (EC 3.1.1.11; CE 8). For rhamnogalacturonan-I, the participating enzymes in breakdown are rhamnogalacturonan hydrolase (EC 3.2.1.171; GH 28), rhamnogalacturonan lyase (EC 4.2.2.23), rhamnogalacturonan rhamnhydrolase (EC 3.2.1.174), rhamnogalacturonan galacturono hydrolase (EC 3.2.1.173; GH 28), and rhamnogalacturonan acetylerase (EC 3.1.1.86). Endo xylogalacturonan hydrolase (EC 3.2.1.-; GH 28) and exopolygalacturonase are the main enzymes involved in the depolymerization of xylogalacturonan. In addition to above pectinolytic enzymes, the following enzymes also involve in rhamnogalacturonan-II depolymerization, include: exogalactanase, endogalactanases (EC 3.2.1.89), α -D-galactoside galactohydrolase (EC 3.2.1.22), β -D-galactoside galactohydrolase (EC 3.2.1.23), feruloyl esterase (EC 3.1.1.73), arabinan endo-1,5- α -L-arabinanase (EC 3.2.1.99),

α -L-arabinofuranosidase (EC 3.2.1.55), and exoarabinases (de Vries and Visser 2001; Voragen et al. 2009; Yapo 2011; Sharma et al. 2013; Kubicek et al. 2014; Rytioja et al. 2014; Ceballos 2018; Mellinas et al. 2020).

1.2.4 Lignin and Lignin-modifying enzymes

Lignin is the third component of lignocellulosic material, the second most abundant organic material after cellulose and the most abundant source of aromatic heteropolymers on earth. This noncarbohydrate polymer is crucial in the plant cell wall formation of bark and wood by linking covalently to different plant polysaccharides. These cross-links provide mechanical strength, rigidity and hydrophobicity to the plant cell wall. The quantity of lignin varies plant to plant, like; 25 – 35% lignin in softwood, 20 – 25% lignin in hardwood, and 10 – 15% lignin in grass of the total biomass. This tridimensional polymer is composed of three phenylpropane monomers (Figure 1-5A): *p*-coumaryl (*p*-hydroxyphenyl / 4-hydroxycinnamyl) alcohol, coniferyl (guaiacyl / 3-methoxy 4-hydroxycinnamyl) alcohol, and sinapyl (syringyl / 3,5-dimethoxy 4-hydroxycinnamyl) alcohol linked by ether, carbon to carbon and ester bonds (Figure 1-5B). The ratio of these units in lignin varies species to species (Boerjan et al. 2003; Dashtban et al. 2010; Wang et al. 2017).

Lignin is extremely difficult to biodegrade due to the presence of aromatic rings and different types of bonding, irregular chemical structure compared to carbohydrates and hydrophobic nature. Exclusively, white-rot fungi have ability to cleave the aromatic ring of natural lignin by extracellular oxidative enzymes, which include heme peroxidases and phenol oxidases. The heme peroxidases, also known as peroxidases, are members of fungal class II peroxidases (only enzymes which are potentially active on lignin) and further divided into four major groups: lignin peroxidases (LiPs, EC 1.11.1.4, AA2), manganese peroxidases (MnPs, EC 1.11.1.13, AA2), versatile peroxidases (VPs, EC 1.11.1.16, AA2), and dye-decolorizing peroxidases (DyPs, EC 1.11.1.19). These enzymes in the presence of H₂O₂ catalyze the oxidation of the substrate. There are more fungal class II peroxidases available than those acting with lignin, such as the well-studied (Kudanga 2012) enzyme CiP (*Coprinopsis cinerea* peroxidase, EC 1.11.1.7). From phenol oxidases, laccases (EC 1.10.3.2, AA1) are members of multicopper phenoloxidase family. They can oxidize a variety of substrates (such as aromatic amines, aminophenols, ortho- and para-di- and polyphenols, lignins, and nonphenolic compounds) by the single-electron oxidation instead of using hydrogen peroxide which is used by the peroxidases (Christopher et al. 2014).

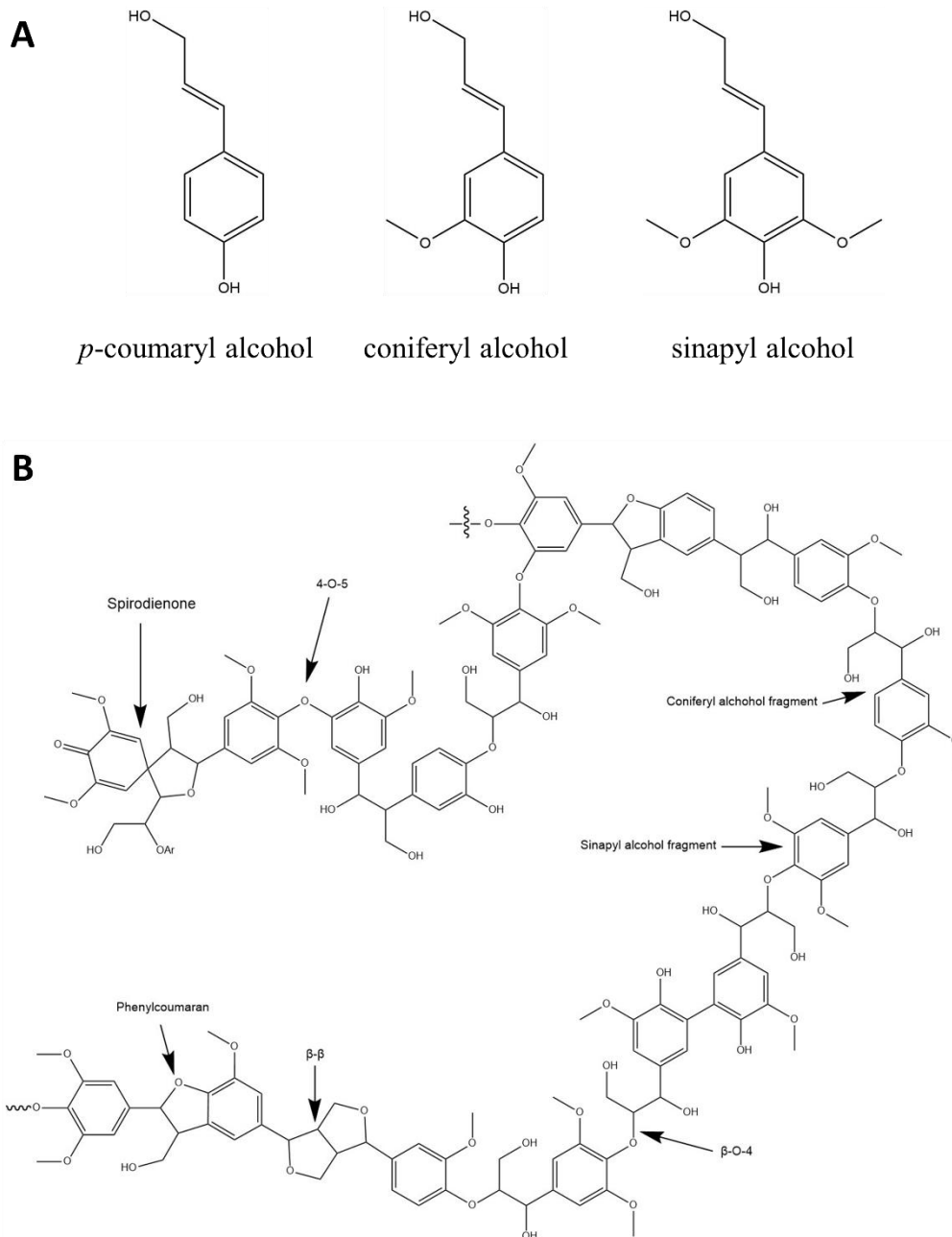


Figure 1-5 Graphical representations of the three common building blocks (monolignols) of lignin (A), and schematic structure of a hardwood lignin (B). These structures were redrawn from Zakzeski et al. 2010 by using ChemDraw Professional version 20.0.

A laccase has four copper ions which are classified into three types: type-1 (T1, one copper ion), type-2 (T2, one copper ion), and type-3 (T3, two copper ions). The function of T1 is to give the blue color of the enzyme, and the function of the trinuclear cluster of T2 and T3 is the catalytic activity of laccase. T1 is connected to two sulphur-containing amino acids (cysteine and

methionine) and two histidine ligands. T2 is connected to water and two histidine ligands whereas two T3 copper ions are connected to three histidine ligands. In the oxidation process of a substrate by laccase, T1 site receives one-electron near the protein surface which then transferred to the trinuclear cluster (T2/T3 site) within the protein. A laccase's total reduced form has four electrons which are transferred to oxygen (O₂) to form water (H₂O) (Hamidi 2013; Durán et al. 2002; Xu et al. 1996; Cole et al. 1990).

The lignin degradation process is further supported by other extracellular accessory enzymes, which include glucose oxidase (GLOX; EC 1.1.3.4), glyoxylate oxidase (EC 1.2.3.5), aryl-alcohol oxidase (AAO; EC 1.1.3.7), aryl-alcohol dehydrogenase (AAD; EC 1.1.1.90), and quinone reductases (EC 1.6.5.5) (Wong 2009; Dashtban et al. 2010; Fraaije and van Bloois 2012; Pollegioni et al. 2015; Stajić et al. 2016; Falade et al. 2017; Ceballos 2018).

1.3 Wood decay fungi and early sapwood colonizers

As a foe to wood, wood decay fungi cause reduction in wood weights, depolymerize chemical constituents, and diminish the wood physical and mechanical strengths, density, electrical conduction, compression, bending strength, and stiffness (Cowling 1961; Curling et al. 2002; Schmidt and Czeschlik 2006; Bari et al. 2015a). On the other hand, they are facilitating the global environment by degrading the wood to release carbon (annually about 80 Tg carbon confiscate in wood) and nutrients blocked in wood (Hiscox et al. 2018; Krah et al. 2018). Among the potential usages of these fungi are the production of myco-wood (e.g., *T. versicolor* used for myco-wood pencils), myco-fodder/ palo podrido (e.g., *Lentinula edodes*), edible mushrooms (e.g., *S. commune*, *Pleurotus* spp.), biopulping (*Phanerochaete chrysosporium*), and wood saccharification (Schmidt and Czeschlik 2006).

The fungal community in decaying wood changes over the time and develops by successions of different wood decay fungi. Hiscox et al. (2016) classified these fungi based on their arrival on the substrate into “*primary, secondary, late secondary, and end-stage colonizers*”. The virgin wood is usually colonized by saprotrophic or opportunistic decay fungi (primary colonizers), existing as endophytes or land as spores on the wood, which are replaced by strong wood degraders (secondary colonizers), possibly land as spores at the wood or enter from the soil. Later, these colonizers are replaced by more aggressive colonizers with higher confrontational abilities, known as late secondary and end-stage colonizers (Boddy 2000; Lindahl and Finlay 2006;

Boddy and Heilmann-Clausen 2008; Hiscox et al. 2016; 2018). Also, primary colonizers have the weakest confrontational abilities but they develop rapidly in the wood (Boddy 2000; Lindahl and Finlay 2006; Parfitt et al. 2010; Hiscox et al. 2016; Hiscox and Boddy 2017). Primary and early secondary colonizers (early sapwood colonizers) are the key players which start the decay process of recalcitrant lignocellulose. These primary colonizers combat for the territory and the resources, but they probably benefit each other indirectly by degrading the wood constitutions partially and leaving the rest for other colonizers. The secondary colonizers utilize these degraded products directly or indirectly, and depolymerize other chemical constitutes to gain required nutrients. In the same contest, wood is a weak source of nitrogen, can be especially assessed by the members of wood decaying basidiomycetes (Lindahl and Finlay 2006; White 2012). It is considered that the primary colonizers mobilize the nitrogen, bonded within the wood, and secondary colonizers can utilize the nitrogen (Lindahl and Finlay 2006). Similarly, in case of *S. commune* (primary colonizers) and *T. versicolor* (secondary colonizers) maybe take advantages from the degraded products, as first is grey rot and other is white-rot. Therefore, it is quite interesting to study the secretomes of both fungi in single culture on natural substrate.

1.3.1 *Trametes versicolor* (turkey tail mushroom)

T. versicolor (Polyporaceae, Polyporales, Agaricomycetes) – synonyms: *Coriolus versicolor* and *Polyporus versicolor* – is a worldwide distributed polypore mushroom, inhabits on standing or fallen dead wood and a strong wood degrader (Schmidt and Czeschlik 2006). According to US national fungus collection database, *T. versicolor* has been observed on 129 different genera and at least 259 different plant species (Farr and Rossman 2020). In nature, the *T. versicolor* mature fruiting bodies (mushrooms) have leathery texture with concentric zones of various colors and with fine hairs on upper surface of the cap. The lower surface of the cap has pores (angular to circular) and cream-white to yellow in color (Schmidt and Czeschlik 2006). However, young stages in fruiting (stroma formation or hymenium formation) are in white color in nature, and under controlled conditions (own observations of stroma development as presented later in the thesis).

T. versicolor has been used as traditional Chinese medicine (such as in form of teas) from thousands of years (Wasser 2002; Chang et al. 2017). Antitumor activities of the isolated peptidoglycans (proteins bind to polysaccharides) from the *T. versicolor* fruiting bodies have been

studied against various cancers (breast, colorectal, gastric, lung and hepatoma cancers) for many years (Sun et al. 2014; Dou et al. 2019). Besides these, other beneficial effects like; analgesia, antiatherosclerosis, anti-chronic bronchitis, anti-inflammation, anti-hyperlipidemia, anti-hepatopathy, immunoregulation, and liver protection have been observed with the application of the *T. versicolor* polysaccharides (Yamaç and Bilgili 2006; Sun et al. 2014; Chang et al. 2017; Dou et al. 2019). Also, the ethanolic extracts from mycelium and basidiocarp of *T. versicolor* have shown antifungal potentials against various species (Yamaç and Bilgili 2006; Knežević et al. 2018).

Besides above extensively studied topics related to this fungus, its enzymatic depolymerization, degradation of plant cell wall components at microscopic level, and weight losses of numerous wood species have also been significantly investigated and still under focus. The fungus degrades lignocellulosic biomass in a typical manner of white rot fungi, initialize the degradation from the lumen of wood cells (tracheids), then penetrate plant cell walls via pits, make holes by erosion, and continue through the S-layers across the middle lamella (Cowling 1961; Highley and Murmanis 1987; Bari et al. 2015a; Chen et al. 2017). Due to its strong abilities to degrade the lignin in addition to other wood polymers (Cowling 1961; Bari et al. 2015a), this fungus has been included in European (DIN EN 113) and American (ASTM D2017-05) wood decay test for basidiomycetes. To know the wood degradation mechanism of *T. versicolor*, the genome has been sequenced which shed light on the presence of genes for diverse classes of lignocellulose degrading enzymes such as glycoside hydrolases, carbohydrate esterases, polysaccharide lyases, class II peroxidases (lignin peroxidases, dye-decolorizing peroxidases, heme-thiolate peroxidases, manganese peroxidases, and versatile peroxidases), multicopper oxidases (e.g., laccases), cellobiose dehydrogenase, oxalate oxidase/decarboxylases, quinone reductases and auxiliary activities enzymes (Floudas et al. 2012; Carabajal et al. 2013; Rytioja et al. 2014; Kersten and Cullen 2014; Gao et al. 2017b; Dai et al. 2018).

1.3.2 *Schizophyllum commune* (split gill mushroom)

S. commune (Schizophyllaceae, Agaricales, Agaricomycetes) is a versatile opportunist fungus distributed throughout the world including Antarctica, which colonizes mainly on dead wood and as well as herbaceous plants, and often appears as a weak plant pathogen (Cooke 1961; Schmidt and Liese 1978; Gonçalves et al. 2015; Farr and Rossman 2017; Lakkireddy et al. 2017).

This xerotolerant fungus had been identified from 291 botanical species (belong to 162 genera) as host (Cooke 1961) which meanwhile has reached up to 630 species (belong to 278 genera and 88 families) (Khonsuntia et al. unpublished). This cosmopolitan fungus has been recovered from a repertoire of substrates and habitats (Takemoto et al. 2010), like on dead wood (Cooke 1961; French and Keirle 1969; Schmidt and Liese 1980; Ginns 1986; Motiejūnaitė et al. 2014; Lakkireddy et al. 2017; Suliaman et al. 2017), infecting living plants (Essig 1922; Poole 1929; Ledebour 1946; Erwin et al. 2008; Takemoto et al. 2010; GLTMS 2015; Stravinskienė et al. 2015; Lakkireddy et al. 2017), as endophyte (Agusta et al. 2006; You et al. 2012; Jin et al. 2013; Qadri et al. 2013; Bourdel et al. 2016), spores in air (Shams-Ghahfarokhi et al. 2014; Kim et al. 2015; 2016), in marine environment (You et al. 2012; Panno et al. 2013; Supaphon et al. 2014; Maduranga et al. 2018; Xu et al. 2018), on glaciers sediments (Gonçalves et al. 2015), causing diseases in humans (Kligman 1950; Kamei et al. 1999; Chowdhary et al. 2013a; Jeyaprakasam et al. 2016; Siqueira et al. 2016; Oguma et al. 2018; Cavanna et al. 2019), infecting animals (Kano et al. 2002; Tanaka et al. 2008; Mori et al. 2009; Hanafusa et al. 2016; Yoshizawa et al. 2017), and living on non-living materials like; coals and rocks (Fakoussa and Hofrichter 1999; Wengel et al. 2006; Kirtzel et al. 2017; Kirtzel et al. 2018).

Despite of these impacts, the mushrooms of this fungus serves as food in Central-American states, in tropical African territories and tropical South-East-Asian countries (Cooke 1961; Lipp 1971; de León 2003; Abdullah and Rusea 2009; Okhuoya et al. 2010; Chen et al. 2014; Choudhary et al. 2015; Preecha et al. 2016; Tantengco 2018; Kamalebo et al. 2018). The small fan-shaped annual mushrooms are leathery and grow usually in groups. The upper surface of the cap is whitish-beige-colored and hairy. Gills (pseudolamellae) are present on the lower surface of the cap, usually whitish to beige in color which split lengthwise and bent outward (in dried state). These hygroscopic controlled splits can be rolled-in or -out depending on dryness of mushrooms. Basidiospores are produced on and released from the surfaces of the (pseudo)gills which can stay for years without water and revive when again moist (Schmidt and Czeschlik 2006; Almási et al. 2019; Carreño-Ruiz et al. 2019).

Due to its abundance in nature, the wood decay abilities of *S. commune* have been tested against many tree species with various mono- and dikaryotic strains, different incubation temperatures and periods, and with different test systems. From literature, it is found that the reduction in weight by this fungus varied from 0 % (Humar et al. 2001; 2002; Schirp et al. 2003;

Ujang et al. 2007) to 68 % (Reis et al. 2017). *S. commune* before its genome sequencing was generally believed as a white-rot fungus (Schmidt and Czeschlik 2006; Ohm et al. 2010) because of whitish appearance of the inhabiting wood under its fruiting bodies. But, the *S. commune* wood decay tests in laboratory and the sequenced genome have made it clear that this fungus is intermediate between white and brown rot (Riley et al. 2014; Floudas et al. 2015; Lakkireddy et al. 2017; Nagy et al. 2017). Therefore, it is now listed in a separate group as a ‘grey rot’ (Riley et al. 2014; Zhu et al. 2016; Krah et al. 2018; Kües et al. 2018). The sequenced genome of *S. commune* has revealed, its genome contains genes for glycoside hydrolases (240 candidates), glycosyl transferases (75), carbohydrate esterases (30), polysaccharide lyases (16) expansin- related proteins (17), and auxiliary enzymes (23) but lack of genes for ligninolytic peroxidases (Ohm et al. 2010; Kersten and Cullen 2014; Rytioja et al. 2014). The *S. commune* genome has also revealed the presence of laccase genes and tannase genes. These facts make this fungus more interesting especially for biologists to explore its enzymes and enzymes- cocktails for degradation of various lignocellulosic substrate, which can be a potential source for bioethanol production, and biodegradation of pollutants and xenobiotics (Tovar-Herrera et al. 2018).

1.4 Interactions of wood decay basidiomycetes and mycoparasitism

In nature, the decomposition of wood is mainly carried out by the members of basidiomycetes. These wood decay basidiomycetes colonize together in/on a decaying wood and interact with each other. Interactions between them can be facilitative or competitive (is the most observed type between wood decay basidiomycetes) and determine the community composition in the decaying wood (Boddy 2000; Hiscox et al. 2018). The environmental conditions and the nutrients availability influence also the fungal interactions (Ferreira et al. 2010; Schöneberg et al. 2015; Morón-Ríos et al. 2017). Combative interactions can be carried out at a distance via diffusible or volatile compounds (DOCs and VOCs), or by close contact at the hyphal level (Boddy 2000; Hiscox et al. 2018). In the results of these interactions, one fungus can be replaced by the other (known as replacement), or both fungi restrict to its territory (known as deadlock). Else, one or both fungi enter other’s territory but later deadlock arises (known as partial replacement) with barrage formation (Rayner et al. 1994; Rayner et al. 1996; Boddy 2000). Besides the effects of interactions on fungal growth, combative interactions have shown different effects on the substrates (organic or inorganic) e.g., change in the decay rate of lignocellulosic substrates by

interspecific interactions (Boddy 2000; Morón-Ríos et al. 2017; Hiscox et al. 2018). Possible contributions of these interactions to weathering process and biomineralization have been suggested and studied in recent years (Gadd 2001, 2007; Morón-Ríos et al. 2017).

Mycoparasitism occurs when one fungus directly attacks on other fungus and acquires nutrition from it. Mycoparasites are either biotrophic (utilize nutrients from the mycelium of living host without killing it) or necrotrophic, gain nutrition from the host mycelium after killing it by unspecialized mechanisms (Jeffries 1995; Boddy 2000). Before and during the mediation of these interactions, the involved fungi are using physical and chemical weapons to win or survive. In the interaction zone, up- and down-regulation of several genes (e.g., for cytochrome P450, glutathione-S-transferases, serine/threonine protein kinases and oxidoreductases) and enzymes (e.g., chitinases, laccases, and peroxidases), and production of secondary metabolites (e.g., members of benzenoids, carboxylic acids, sesquiterpenes, monoterpene) have been reported (Verma and Madamwar 2002; Baldrian 2004; Chi et al. 2007; Peiris et al. 2008; Eyre et al. 2010; Hiscox et al. 2010a; Arfi et al. 2013; Chen et al. 2015; Sánchez-Fernández et al. 2016) to attack or defend a fungus against an opponent. Overall, these interactions are an innovative and potential field of study. Fungal interactions can be helpful in finding new enzymes, enzymes complexes and secondary metabolites for pharmacology, agriculture, and industrial applications such as, the production of useful enzymes, antibiotics and antifungals, and use as biological control of pathogenic fungi (Boddy 2000; Susi et al. 2011; Hiscox and Boddy 2017; Hiscox et al. 2018; Speckbacher and Zeilinger 2018).

1.5 Medium-free inoculation method

Numerous laboratory techniques are available for fungal multiplication and inoculation but none of them is media-free inoculation method. Fungal multiplication in the laboratory is usually carried out on solid (agar plates/ slants) or liquid (shake flasks, bench top fermenters) media depending on the purpose. The obtained inoculum is normally with the media ingredients which supplies extra nutrients to the fungus and may make the fungus stronger in decay (Peddireddi 2008). On the other hand, inoculum with old media contents can bring with it previously secreted proteins which may create a false identification of proteins in proteomic analysis (e.g., the protein profiling of a wood decay fungus at early stage of decay). It may alter the fungal metabolism and trigger a different set of proteases and peptidases to degrade previously secreted proteins which

may also lead to false results. Therefore, media-free inoculum is the prerequisite to solve the above said complications.

Fungal spores are used as (media-free) inoculum (Nevalainen et al. 2014), but in the absence of usable spores (e.g., *S. commune* and *T. versicolor*) this option is not applicable. Therefore, a media-free inoculation method for the filamentous fungi is necessary to overcome the problem of media ingredients with inoculum. The above stated problems are solved by fungal pelletization (formation of fungal pellets), which is described in this thesis (protocol presented in section 2.5). Pellets are an alternative mycelial growth form to the mycelial colony growth on agar of filamentous fungi and are formed in submerged culture (Pirt 1966; van Suijdam et al. 1980). Pellet formation of filamentous fungi has been used since decades for the production of a surfeit of food, pharmaceutical and industrial products (Veiter et al. 2018; Nair et al. 2016).

1.6 Proteomics – a modern approach to study the wood decay mechanisms

Current international fungal genome projects address the task to identify catalogs of genes for lignocellulose degradation in numerous basidiomycetous fungi of different properties (white and brown rots, aggressive and weak wood degraders, and pathogens) with targets such as to 1. generally better elucidate the yet little understood mechanisms of wood decay and the differences between them, 2. to identify useful enzymes for biotechnological purposes such as for converting energy-rich lignocellulose into bioenergy, and 3. to identify strategies as how pathogens might be hindered to attack valuable trees (Ohm et al. 2014). By now, the MycoCosm portal of the JGI (Joint Genome Institute, Walnut Creek, CA) offers multiple annotated fungal genomes (with each more than 10,000 different genes) to the international research community to study biological problems such as wood decay (Grigoriev et al. 2014). These resources can now be taken for functional approaches in fungal research such as by using modern proteomic techniques to identify those proteins that act in early or later decay stages, that attack lignin or that convert polysaccharides into their individual sugars (Aguilar-Pontes et al. 2014). These enzymes and enzymatic complexes could improve and enhance the biotechnological processes and products (Tovar-Herrera et al. 2018).

Genomes of *S. commune* and *T. versicolor* have been sequenced under the Saprotrophic Agaricomycotina Project (SAP), and available under the MycoCosm portal of the JGI. The genomes analysis of both fungi revealed diverse types of enzymes repertoires for the degradation

of lignocellulosic substrates. The study of the expressed secretomes and proteomes on natural substrate (wood) can offer better understanding for the lignocellulose-degrading enzymes participating in its depolymerization, and for the involved proteins in nutrient acquisition. Furthermore, the co-culture secretomes can divulge the proteins repertoires potentially secreted in mycoparasitism and in defense response.

1.7 Objectives for this study

Based on above scenario, the following objectives were set to be answered in this project:

- 1- To assess and compare the decay capabilities of *S. commune* and *T. versicolor* grown on beech sapwood and bark under different light schemes
- 2- To study the interactions between both fungi on natural and artificial substrates and to describe the proteins involved in dual interactions
- 3- To develop a medium-free inoculation method and a protocol for the secretome extraction from fungus-wood samples for proteomic studies
- 4- To profile the secretomes of both fungi grown on beech sapwood at early and late stages of wood decay

2 Materials and methods

2.1 Fungal strains

One dikaryotic (having two genetically different nuclei in the cell) and the two parental monokaryotic (possess only one nucleus per cell) strains of *S. commune* (Wessels et al. 1987) were used which have been sequenced by Ohm et al. 2010 (Table 2-1). The *S. commune* dikaryotic strain *Sc* (*S. commune*) 4-39 x 4-40 (*matA41 matB41* x *matA43 matB43*) which was originated from the two parental monokaryotic strains *Sc* 4-39 (*matA41 matB41*; CBS 341.81) and *Sc* 4-40 (*matA43 matB43*; CBS 340.81) were used. One sequenced monokaryotic (*Tv*-FP-101664 SS1, Floudas et al. 2012) and one dikaryotic strain (*Tv*-6) of *T. versicolor* were used in this study (Table 2-1). *T. versicolor* dikaryotic strain (*Tv*-6) originated from the collection of the Institute of Molecular Wood Biotechnology and Technical Mycology, Georg August Universität, Göttingen. All strains were collected from the institute's collection, except *Sc* 4-40 which was provided by Prof. dr. H.A.B. (Han) Wösten, Utrecht University, Utrecht, The Netherlands.

Table 2-1 Fungal strains and their abbreviations used in this study

Fungus	Type	Fungal strains	Abbreviation
<i>Schizophyllum commune</i> (<i>Sc</i>)	Monokaryons	<i>Sc</i> 4-39 wt	<i>Sc</i> -M1
		<i>Sc</i> 4-40 wt	<i>Sc</i> -M2
	Dikaryon	<i>Sc</i> 4-39 x 4-40	<i>Sc</i> -D
<i>Trametes versicolor</i> (<i>Tv</i>)	Monokaryon	<i>Tv</i> -FP-101664, SS1	<i>Tv</i> -M
	Dikaryon	<i>Tv</i> -6	<i>Tv</i> -D

2.2 Growth conditions

Cultivation of *S. commune* strains were carried out on *S. commune* (*Sc*) minimal medium (Dons et al. 1979), comprising (per liter) 20 g glucose, 1.5 g L-asparagine monohydrate, 1 g dipotassium phosphate (K₂HPO₄), 1 g yeast extract, 0.5 g magnesium sulphate heptahydrate (MgSO₄ x 7H₂O), 0.46 g monopotassium phosphate (KH₂PO₄), 0.12 mg thiamine-HCl, 0.1 mg

pyridoxine HCl, 0.005 mg biotin, 0.2 mg copper(II) sulfate pentahydrate ($\text{CuSO}_4 \times 5\text{H}_2\text{O}$), 0.08 mg manganese(II) chloride tetrahydrate ($\text{MnCl}_2 \times 4\text{H}_2\text{O}$), 0.4 mg cobaltous chloride hexahydrate ($\text{CoCl}_2 \times 6\text{H}_2\text{O}$), 1.2 mg calcium nitrate tetrahydrate ($\text{Ca}(\text{NO}_3)_2 \times 4 \text{H}_2\text{O}$) and 10 g (1%) agar. *T. versicolor* strains were grown on Basidiomycete standard medium (BSM), containing (per liter) 5 g glucose, 0.65 g L-asparagine monohydrate, 1 g monopotassium phosphate (KH_2PO_4), 0.5 g magnesium sulphate heptahydrate ($\text{MgSO}_4 \times 7\text{H}_2\text{O}$), 0.5 g potassium chloride (KCl), 0.5 g yeast extract, 50 ml stock solution I (0.2 g ferrous sulphate heptahydrate ($\text{FeSO}_4 \times 7\text{H}_2\text{O}$) per liter), 50 ml stock solution II (0.16 g manganese(II) acetate tetrahydrate ($\text{Mn}(\text{CH}_3\text{COO})_2 \times 4\text{H}_2\text{O}$), 0.04 g zinc nitrate tetrahydrate ($\text{Zn}(\text{NO}_3)_2 \times 4\text{H}_2\text{O}$), 1 g calcium nitrate tetrahydrate ($\text{Ca}(\text{NO}_3)_2 \times 4\text{H}_2\text{O}$), 0.06 g copper sulfate pentahydrate ($\text{CuSO}_4 \times 5\text{H}_2\text{O}$) and 10 g (1 %) agar (Peddireddi 2008). All cultures were incubated at 25 °C in dark.

2.3 Wood substrate collection

2.3.1 Sapwood collection

A wood log from Beech (*Fagus sylvatica* L.) was cut in November 2015 from Forstbotanischer Garten of Göttingen university. Thin bark from freshly cut beech log (dia. 9 cm) was removed and sapwood was separated from inner core (heartwood). Sapwood, free of nodes, was crushed into particles of size ca. 4 x 1 mm by crusher (electra, France). The sapwood particles were dried at 25 °C for one week on greenhouse benches to achieve a moisture level of <10% to cease the attack of microorganisms and stored in grey plastic bag at room temperature.

2.3.2 Bark collection

Beech bark was provided by the district forester (Mr. Dietmar Raab, Revierförster) of the Göttingen region. Bark was dried in oven at 60 °C and grinded by crusher (electra, France). Bark particles was stored at room temperature (RT) in glass jars.

2.3.3 Wood decay tests

2.3.3.1 Sapwood decay test

For decay tests, glass vials of dia. 3 cm, volume 45 ml were used. Each vial was filled with the sapwood particles (3 g dry weight) and distilled water (4.5 ml, 150 % of the particles weight, based on my observations for the optimum moisture level for the fungal growth). Glass vial was

closed with cotton plug covered by aluminum foil. After autoclaving at 121 °C for 20 min, the vials were kept overnight on room temperature to cool down. Inoculation was done by agar block (dia. 0.7 cm) of 7 days old culture and vials were incubated at 25 °C. Four light schemes (continuous light, 12 h light + 12 h dark, dark (open to record observations) and continuous dark (open at the end of experiment)) and 5 replicates were tested for each fungal strain (Table 2-1). Vials with sapwood particles but without fungus were served as control. After incubation of 30 and 90 days, cotton plugs were removed, vials were placed in oven at 105 °C for 72 h and weighed to record the final weight. Wood weight loss (%) was calculated as $((\text{initial weight} - \text{final weight}) / \text{initial weight}) \times 100$. Decay tests for 30- and 90-days incubation periods were performed separately and repeated twice.

2.3.3.2 Bark vs sapwood decay test

The method as explained above in sapwood decay test was exercised here with 2 g of sample (bark/ sapwood particles) and with two light schemes (continuous light and continuous dark). Three replicates for each fungal strain (Table 2-1) were inoculated by agar block (dia. 0.7 cm) of 7 days old culture, and incubated for 60 days at 25 °C. Weight losses of bark and sapwood were calculated as mentioned in the sapwood decay test.

2.3.3.3 Fungal growth on wood wash-out

Wood wash-out was collected on several days after rain from a cavity in a recently cut European ash (*Fraxinus excelsior*) tree log. After mixing the collected wood wash-outs, heavy particles were removed by centrifugation (centrifuge 5810R, Eppendorf AG, Germany) at 4000 rpm (3220 g) for 15 min. The pH of the wash-out was 9. For the testing of fungal growth, different dilutions (1:1, 1:4, and 1:10) of the wash-out were made with distilled water. For solidification of the wood wash-out, 1.5% agar was added and autoclaved at 121 °C for 20 min. Upon cooling, the wash-out was poured in test tubes and placed in slanting position. Glucose (2%) and nitrogen (0.04% w/v) were autoclaved separately and were mixed in the medium before pouring in test tubes. Thiamine (0.12 mg per liter) was sterilized by filtration and mixed before pouring. Two strains of *T. versicolor* and three strains of *S. commune* were tested (Table 2-1). Three test tubes for each fungal strain were inoculated with agar block (0.3 cm dia) from freshly growing cultures and were incubated at 25 °C in dark/ light.

2.4 Interactions between *S. commune* and *T. versicolor*

2.4.1 Dual interactions on natural substrate

Dual interactions were carried out on beech sapwood particles (natural substrate for both fungi) in 3-partitions Petri dishes (Ø 9 cm). Sapwood particles and water were separately sterilized by autoclaving at 121 °C for 20 min before using. Under sterilized conditions, two chambers of Petri dish were filled with autoclaved sapwood particles (2 g each portion) and 3 ml water (150 % of the particles weight), and one filled with 10 ml sterilized water (Figure 2-1).

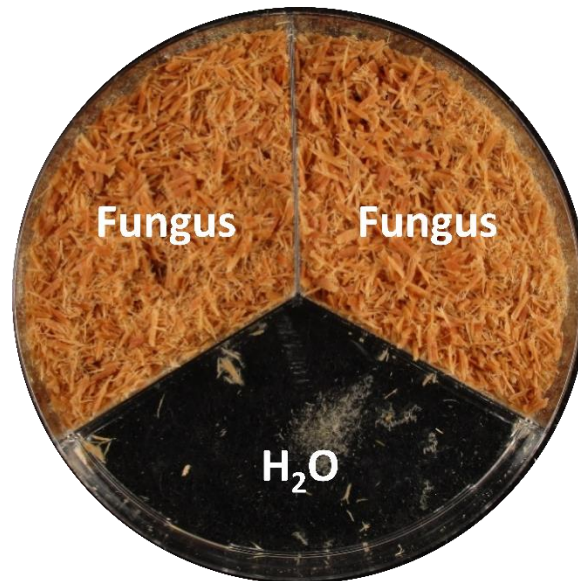


Figure 2-1 Three partition Petri dish (Ø 9 cm), two chambers filled with autoclaved sapwood particles and one with sterilized water.

Table 2-2 List of fungal interactions tested

Interaction #	Fungus 1	Fungus 2
1	<i>Tv</i> -D	<i>Sc</i> -M1
2	<i>Tv</i> -D	<i>Sc</i> -M2
3	<i>Tv</i> -D	<i>Sc</i> -D
4	<i>Tv</i> -D	<i>Tv</i> -M
5	<i>Tv</i> -M	<i>Sc</i> -M1
6	<i>Tv</i> -M	<i>Sc</i> -M2
7	<i>Tv</i> -M	<i>Sc</i> -D
8	<i>Sc</i> -M1	<i>Sc</i> -M2
9	<i>Sc</i> -M1	<i>Sc</i> -D

10	<i>Sc</i> -M2	<i>Sc</i> -D
11	<i>Tv</i> -D	<i>Tv</i> -D
12	<i>Tv</i> -M	<i>Tv</i> -M
13	<i>Sc</i> -M1	<i>Sc</i> -M1
14	<i>Sc</i> -M2	<i>Sc</i> -M2
15	<i>Sc</i> -D	<i>Sc</i> -D
16	Uninoculated control	

Agar blocks of size Ø 0.6 cm were sectioned with sterilized cork-borer from 7 days old cultures grown on *S. commune* minimal medium under dark condition. Each chamber with sapwood particles were inoculated with one agar block of same or different strain. All interactions listed in Table 2-2 were carried out under two different light patterns (continuous light and continuous dark). Five replicates of each interaction were inoculated and incubated for 16 days at 25 °C. Plates were left unsealed for gas exchange. Two sets of whole experiment were studied. *S. commune* and *T. versicolor* were identified by morphology of hyphae. Hyphae of *S. commune* were nondichotomously branched, septate, hyaline, having spicules, and clamp connections (only in dikaryotic strain). Hyphae of *T. versicolor* were hyaline with two types of hyphae (generative hyphae with clamp connections and skeletal hyphae) and with clamp connections (only in dikaryotic strain). Spicules are short acute thin lateral hyphal projections or tubercules and 1-2 µm in length and 0.4-0.5 µm in width (Nobles 1965).

2.4.2 Dual interactions on artificial substrate

Petri dishes (Ø 9 cm) filled with *S. commune* minimal medium (Dons et al. 1979) were used to investigate the fungal interactions. All possible combinations of all 5 strains as shown in Table 2-2 were tested. Using aseptic conditions, agar blocks of 0.7 cm Ø were cut with cork-borer from 7 days old freshly grown cultures on *S. commune* minimal medium under dark condition. Each plate was inoculated with two agar blocks of same or of different strains, placed ca. 4 cm apart from each other. Three replicates of each interaction were inoculated and incubated for 16 days at 25 °C. All interactions were carried out against two different light patterns (continuous light and continuous dark). Plates were left unsealed for gas exchange. Two sets of whole experiment were studied.

2.5 Medium-free pellets production

Pellets production was carried out with two strains of *T. versicolor* and three strains of *S. commune* (Table 2-1) in dark at 25 °C. The *T. versicolor* and *S. commune* strains were grown on BSM and *S. commune* minimal medium, respectively. The fungal pellet formation was carried out by the following protocol and a graphical diagram is given in Figure 2-2.

2.5.1 Protocol

1. Grow fresh fungal culture on agar medium (in sterilized Petri dish - dia. 9 cm with ventilation cams) in dark.
2. Cut blocks with the help of sterilized cork-borer (dia. 0.7 cm) from 7-days old fungal culture, grown on agar medium.
3. Prepare liquid medium and autoclave it at 121 °C for 20 min.
4. Pour 50 ml autoclaved liquid medium in sterilized 250 ml Erlenmeyer (conical) flask fitted with cotton plug.
5. Transfer three agar blocks in conical flask containing sterilized 50 ml liquid medium and cover the plug and flask neck with aluminum foil.
6. Incubate inoculated flask at 25 °C in dark for 7 days (or when mycelia completely cover medium surface).
7. Mince the fungal mycelia within liquid medium in the flask with the help of handheld homogenizer.
8. Take a new sterilized 250 ml conical flask, fill with 100 ml of autoclaved liquid medium, and inoculate with 1 ml of fragmented mycelia.
9. Incubate the flask on a rotatory shaker with a speed of 120 rpm at 25 °C for 7 days.
10. Harvest pellets with medium in 50 ml sterilized Falcon tube (catalog number - 62.547.254, Sarstedt).
11. Centrifuge tube at 1000 rpm (201 g) for 2 min at room temperature (RT) to separate the pellets and aqueous phase.
Note: Centrifuge on higher speed may create a compact mass of pellets or pellets deformation.
12. Carefully discard the aqueous phase.
13. Wash pellets with sterilized dH₂O (make volume up to 45 ml of tube) and vortex to re-suspended pellets.

Note: If pellets do not disperse by vortex, shake tube vigorously by hand.

14. Repeat steps 10 to 12 for three times to wash pellets.

15. Store washed pellets in sterilized dH₂O at 10 °C till further use.

Note: All steps performed under sterilized conditions.

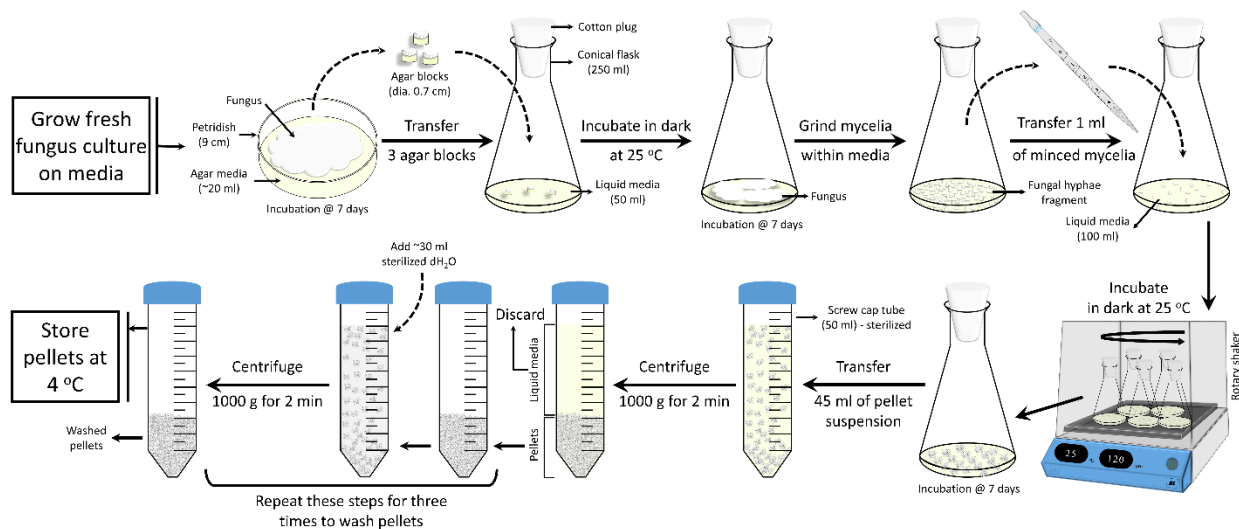


Figure 2-2 Graphical representation of medium-free pellet production

2.6 A new method for secretome isolation from fungus-wood sample

2.6.1 Fungus-wood sample preparation and inoculation

Sterilized polypropylene tube (25 ml, catalog number - 60.9922.243, Sarstedt) with screw cap was filled with 2 g sterilized sapwood particles and 150 % (3 ml) autoclaved water. Sapwood particles and distilled water were autoclaved before pouring in tubes, separately. Each tube was inoculated with one medium-free pellet, closed with the cap (set loose for air circulation), and incubated at 25 °C in dark.

2.6.2 Testing of extraction buffers for secretome isolation

Four different extraction buffers containing protease inhibitor were tested (Table 2-3) to extract the secretomes from the fresh fungus-wood samples.

Table 2-3 Extraction buffer combinations for secretome isolation

No.	Buffer	Volume
Buffer 1 [†]	a) 10mM KH ₂ PO ₄ with dithiothreitol (DTT)* – pH 7.4**	3ml
	b) 10mM phenylmethylsulfonyl fluoride (PMSF)***	3ml
Buffer 2	a) Phosphate buffer [†] (6.7 mM KH ₂ PO ₄ + 6.7 mM Na ₂ HPO ₄ ·2H ₂ O) – pH 7.4	3ml
	b) 10mM PMSF	3ml
Buffer 3	a) 20mM NH ₄ HCO ₃ (ammonium bicarbonate, ABC)	3ml
	b) 10mM PMSF	3ml
Buffer 4	a) 50% 20mM NH ₄ HCO ₃ with DTT	3ml
	b) 50% Tri-fluoroethanol (TFE)	3ml

[†]Buffer 1: Fernández-Acero et al. 2006; buffer 2, 3 and 4: suggested by Dr. Andrzej Majcherczyk

* added 7 mg/2.5 ml (18.2 mM) stock solution before use.

** adjusted with 4M NaOH and 6M HCl

*** The stock solution was made up in isopropanol.

[†] further details at <http://www.aeisner.de/rezept/puffer2.html>

Note: LC-MS quality water was used to prepare the buffers.

2.6.3 Protocol for secretome isolation from fungus-wood sample

1. Prepare both solutions (a and b) of a buffer separately and mix them just before use.
2. Add 6 ml of the buffer to the wood-fungus sample tube and place in vacuum chamber without cap.
3. Apply vacuum to replace air spaces of the sample with buffer solution, and release vacuum after bubble formation (repeat vacuum application till all or maximum solution absorb in the sample). Then, close the tube with cap again.
4. Incubate samples for 30 min in ice. After 30 min, ultra-sonicate samples for 3 min.
5. Make two holes at bottom of sample tube with red-hot needle and place in 50 ml sterilized Falcon tubes.
6. Centrifuge the sample tube (loose the cap before centrifuge) while still inside 50 ml Falcon tube at 1000 rpm (201 g) for 3 min to get all liquid from the sample to 50 ml Falcon tube.

7. Remove the sample tube, fasten the cap and store the fungus-wood samples at -20 °C or freeze-dried for further processing of intracellular proteins.
8. Close Falcon tube containing liquid extract and centrifuge at 4000 rpm (3220 g) for 30 min to get all solid wood particles at the bottom.
9. Transfer the supernatant (7 ml – typically regained volume) to new 15 ml tube (catalog number - 62.554.502, Sarstedt) and discard 50 ml Falcon tube with pellet.
10. Freeze dry the liquid sample for further processing for extracellular proteins.

2.7 Extracellular protein purification and digestion

The freeze-dried sample (in 15 ml tube) was dissolved in 75 µl ABC/DTT (as reducing agent) buffer (4 parts of 100 mM ABC and 1 part of 100 mM DTT) and centrifuged (centrifuge 5810R, Eppendorf AG, Germany) at 2000 rpm (805 g) for 3 min to separate the solids from liquid phase. The liquid phase (75 µl) was collected in 1.5 ml E-cup (catalog number – 72.690.001, Sarstedt, Germany), mixed with 75 µl TFE (2,2,2-trifluoroethanol), and incubated for 30 min at 60 °C to increase the solubility of proteins. Then the E-cup was centrifuged (centrifuge 5415R, Eppendorf AG, Germany) for 10 min at 13200 rpm (16100 g) and 100 µl supernatant was collected carefully into a new 1.5 ml LoBind tube (catalog number – 0030 108.116, Eppendorf AG, Germany). The suspension containing reduced proteins were alkylated by the addition of 5 µl of 500mM iodoacetamide and incubated in dark for 30 min at RT. After the incubation period, 50 µl water was added to dilute TFE in the sample and the proteins were precipitated with 620 µl methanol, 200 µl chloroform 70 µl NaCl and 395 µl water as described in a protocol by Wessel and Flügge (1984). The LoBind tube was shaken vigorously and centrifuged for 20 min at 16100 g. The proteins suspension in LoBind tube was separated into three phases. Upper phase was removed carefully without removing precipitate formed between two phases. The precipitate was converted to pellet by addition of 500 µl MeOH and centrifugation for 20 min at 16100 g. Precipitated proteins were dissolved in 50 µl 100 mM Tris-HCl (pH 8.0) buffer and digested by 5 µl (100ng/µl) trypsin (Thermo Scientific) at 37 °C overnight. Next day, the protein digestion was stopped by the addition of 20 µl 20 mM ammonium formate (AF – pH 10). For the purification of the digested peptides, self-made C18 StageTip (a pipette tip fitted with 3-layers of 3M-C18 filter; Rappsilber et al. 2007) was used after washing with 10 µl MeOH, 20 µl 100% acetonitrile (ACN) and 20 µl 20mM AF, respectively. Sample aliquot (60 µl) was added to StageTip and centrifuged

for 10 min at 1800 g. The StageTip loaded with the peptides was washed with 15 µl 20mM AF. The peptides were eluted with 30 µl 60% ACN (prepared in 20mM AF – pH 10) in a 0.5 ml LoBind E-cup (catalog number – 0030 108.094, Eppendorf AG, Germany) by centrifugation for 4 min at 1800 g followed by 2 min at 3000 g. The E-cup was placed in speedvac (Concentrator plus, Eppendorf AG, Germany) for 1 h at 45 °C to evaporate the solution and the dried sample was stored at -20 °C till further analysis. This protocol was supplied by Dr. Andrzej Majcherczyk.

2.8 Sodium dodecyl sulfate–polyacrylamide gel electrophoresis

To estimate the quality of the isolated proteins from four buffers, proteins were separated using one-dimensional sodium dodecyl sulfate-polyacrylamide gel electrophoresis (1D SDS-PAGE) according to Laemmli (1970). The proteins were stacked in stacking (4 %) gel and separated in resolving (12 %) gels according to their molecular weights. The electrophoresis was set to 20 mA until the samples reached the separating gel, followed by 36 mA (for 3-4 hours) until the bromophenol blue dye reached the bottom of the gel. After removing the gel from the electrophoresis, the gel was fixed in trichloroacetic acid (12 % - w/v) for 2 h and stained overnight in the Coomassie Brilliant Blue solution (Herz 2015). The gel was washed with and dipped in water overnight to remove the excess dye. Stained gel was scanned with a scanner (ScanMaker 9800XL Plus – Microtek).

2.9 Intracellular protein purification and digestion

The freeze-dried fungus-wood sample (30 mg) was grinded in 2 ml tube (catalog number – 0030 120.094, Eppendorf AG, Germany) with stainless steel balls (5 balls of 3 mm, and 2 balls of 4 mm balls – respectively, catalog numbers 22.455.0011 and 22.455.0001 from Retsch, Germany) by mixer mill MM 400 (Retsch, Germany) at 25Hz for 2 min, chilled in liquid nitrogen and repeated four times to achieve very fine powder. The sample powder without removing the stainless-steel balls was dissolved in 150 µl ammonium bicarbonate/ D-1,4-dithiothreitol (as reducing agent) buffer and 150 µl TFE (2,2,2-trifluoroethanol). Then, the tube was placed in Thermomixer at 50 °C, 1500 rpm for 60 min. After incubation, the tubes were chilled in ice to room temperature. Then, the suspension was transferred to a new 1.5 ml normal tube (catalog number – 72.690.001, Sarstedt, Germany) and centrifuged (centrifuge 5415R, Eppendorf AG, Germany) for 15 min at 16100 g (13200 rpm). From liquid phase, 75 µl sample was transferred into in a new LoBind1.5 ml E-cup (catalog number – 0030 108.116, Eppendorf AG, Germany),

mixed with 75 μ l TFE (2,2,2-trifluoroethanol), and incubated for 30 min at 60 °C to increase the solubility of proteins. Then the E-cup was centrifuged for 10 min at 13200 rpm (16100 g) and 100 μ l supernatant was collected carefully into a new 1.5 ml LoBind tube. The suspension containing reduced proteins were alkylated by the addition of 5 μ l of 500mM iodoacetamide and incubated in dark for 30 min at RT. After the incubation period, 50 μ l water was added to dilute TFE in the sample and the proteins were precipitated with 620 μ l methanol, 200 μ l chloroform 70 μ l NaCl and 395 μ l water as described in a protocol by Wessel and Flügge (1984). The LoBind tube was shaken vigorously and centrifuged for 20 min at 16100 g. The proteins suspension in LoBind tube was separated into three phases. Upper phase was removed carefully without removing precipitate formed between two phases. The precipitate was converted to pellet by addition of 500 μ l MeOH and centrifugation for 20 min at 16100 g. Precipitated proteins were dissolved in 50 μ l 100 mM Tris-HCl (pH 8.0) buffer and digested by 5 μ l (100ng/ μ l) trypsin (Thermo Scientific) at 37 °C overnight. Next day, the protein digestion was stopped by the addition of 20 μ l 20 mM ammonium formate (AF – pH 10). For the purification of the digested peptides, self-made C18 StageTip (a pipette tip fitted with 3-layers of 3M-C18 filter; Rappsilber et al. 2007) was used after washing with 10 μ l MeOH, 20 μ l 100% acetonitrile (ACN) and 20 μ l 20mM AF, respectively. Sample aliquot (60 μ l) was added to StageTip and centrifuged for 10 min at 1800 g. The StageTip loaded with the peptides was washed with 15 μ l 20mM AF. The peptides were eluted with 30 μ l 60% ACN (prepared in 20mM AF – pH 10) in a 0.5 ml LoBind E-cup (catalog number – 0030 108.094, Eppendorf AG, Germany) by centrifugation for 4 min at 1800 g followed by 2 min at 3000 g. The E-cup was placed in speedvac (Concentrator plus, Eppendorf AG, Germany) for 1 h at 45 °C to evaporate the solution and the dried sample was stored at -20 °C till further analysis.

2.10 MS analysis and protein identification

The dried peptides were resuspended into 25 μ l acetonitrile (2%) with formic acid (0.1%) in water, and 10 μ l from the peptide suspension was packed in 300 μ l mass-spec quality kinesis-vials (catalog number KVP6124, Kinesis GmbH, Germany). For nanoLC-MS/MS analysis, 5 μ l peptide suspension was set up to elute the peptides by nanoLC (Eksigent 425, SCIEX) fitted with C-18 column and were analyzed with a high-resolution TripleTOF 5600+ mass spectrometer (SCIEX, Darmstadt, Germany). In MS/MS analysis under the information dependent acquisition mode, top 30 multiple charged ions in each MS cycle were subjected to execute MS/MS

fragmentation. Generated raw MS/MS data was processed using ProteinPilot software (version: 5.0.1 – SCIEX) with the adjusted parameters of cysteine alkylation to iodoacetamide and digestion by trypsin to infer the proteins in the sample. The MS data was searched against a self-made database containing the protein fasta-files of *T. versicolor* (<https://mycocosm.jgi.doe.gov/Travel/Travel.home.html>, strain FP-101664 SS1, version 1.0,) and *S. commune* (<https://mycocosm.jgi.doe.gov/Schco3/Schco3.home.html>, strain H4-8, version 3,) which were downloaded from the website of Joint Genome Institute (DOE Joint Genome Institute, Walnut Creek, CA, USA). The sequences of common contaminants (156 proteins including common laboratory proteins, proteins added by accident through dust or physical contact, and proteins commonly used as molecular weight standards) were also included in the database. Cut-off value for protein identification was set to values corresponding to maximum False Discovery Rate (FDR) of 0.05 and at least two identified peptides with confidence of 99%.

The list of the identified proteins generated by the software was combined with the annotations provided by JGI. However, each identified protein was crosschecked with the JGI databases for the user created models of protein sequence and for the user annotations. Further, each protein sequence was analyzed to obtain additional information e.g., putative function, and localization of protein. SignalP (v. 4.1 – Nielsen 2017, <http://www.cbs.dtu.dk/services/SignalP-4.1/>) was used for the prediction of signal peptides from the amino acid sequences. For prediction of transmembrane helices and the subcellular localization of the identified proteins, TMHMM (Server v. 2.0; Krogh et al. 2001, <http://www.cbs.dtu.dk/services/TMHMM/>) and DeepLoc-1.0 (<http://www.cbs.dtu.dk/services/DeepLoc/>) were used (Armenteros et al. 2017). For further confirmation of defined putative function of a protein or to define a putative function of unknown protein, the protein sequence was searched against InterPro (<https://www.ebi.ac.uk/interpro/>, Mitchell et al. 2019), UniProt (<https://www.uniprot.org/>, The UniProt Consortium 2019), and NCBI blastp (<https://blast.ncbi.nlm.nih.gov/Blast.cgi>). The sequences of protein with unknown function were also searched in HMMER web server (<https://www.ebi.ac.uk/Tools/hmmer/>, Potter et al. 2018), Pfam database (<http://pfam.xfam.org/>, El-Gebali et al. 2019), and NCBI conserved domain database (CDD, <https://www.ncbi.nlm.nih.gov/Structure/cdd/wrpsb.cgi>) to identify a putative domain and a putative function. For the classification of proteases and proteinases, the peptidase database MEROPS (release 12.3; Rawlings et al. 2018, <https://www.ebi.ac.uk/merops/>), and for the classification of proteins acting on carbohydrates, the CAZy (Carbohydrate-Active

enZYMes, <http://www.cazy.org/>) database (Lombard et al. 2014) were used. The enzyme database (ExplorEnz; McDonald et al. 2009, <https://www.enzyme-database.org/>) was used to identify the correct name and the EC number of a protein according to IUBMB enzyme nomenclature, and to keep the standard chemical names format according to IUPAC standards. All Venn diagrams were drawn by Venny 2.1 on-line software (Oliveros 2007-2015).

2.11 Dual interactions on glass-fiber filters

Dikaryotic strains of *T. versicolor* (Tv-D) and *S. commune* (Sc-D) were selected for this interactional study. Glass-fiber filters were washed twice in distilled water to remove the effects of any chemical contaminant. Then, these glass-fiber filters soaked in liquid *S. commune* minimal medium and autoclaved with it. One, two and three layers of the filters placed on Petri dish (9 cm Ø) having solid *S. commune* minimal medium. Agar blocks of size 0.7 cm Ø were cut from freshly grown cultures. Each replicate was inoculated with two agar blocks of different fungus ca. 4 cm apart from each. Three replicates per case were incubated in dark for 10 days at 25 °C.

2.11.1 Protein extraction from glass-fiber filters

After 10 days, glass-fiber filters were cut with a sterilized cutter to separate the interaction zone. The middle part (the interaction zone) was placed separately in 15 ml tubes and centrifuged for 5 min at 1000 rpm (201 g) to extract liquid. Samples were frozen at -20 °C, followed by freeze-drying. The freeze-dried sample (in 15 ml tube) was dissolved in 75 µl ammonium bicarbonate/D-1,4-dithiothreitol (as reducing agent) buffer and followed the protocol as described above in section 2.7.

2.12 Statistical analysis

Statistical significance and pairwise comparisons of the data were determined using ANOVA and Tukey HSD (Honestly Significant Difference) post hoc tests ($p < 0.001$) executed in R (version-4.0.3, R Core Team 2020) using agricolae library (Mendiburu and Simon 2015).

3 Results

S. commune is an opportunistic fungus with wide host range of tree species. Fruiting bodies of this fungus as a weak pathogen and as a saprotroph on different broadleaf tree species alone and with other wood-colonizing fungi were observed in nature. *S. commune* was found as one of the first species in the form of fruiting bodies on deadwood and was replaced by other wood-decaying fungi over time (observations based on fruiting bodies). As *S. commune* is a poor wood degrader, it may take advantage from co-resident fungi better able to degrade wood. *S. commune* fruiting bodies were often observed on deadwood together with basidiomes of polypores such as *T. versicolor* (Figure 3-1). The detailed results were presented in Lakkireddy et al. (2017). Cooperative and competing interactions might exist between different species in the wood. To understand such interactions better, these interactions between both early sapwood fungi (*S. commune* and *T. versicolor*) were investigated in this study in laboratory conditions in single and dual cultures, grown on natural and artificial substrates. Wood (bark and sapwood) decay testes were carried out to determine the decay by each fungus alone.



Figure 3-1 *S. commune* fruiting bodies replaced by *T. versicolor* mushrooms on the cut site of a poplar log over a year (dated: A = 10/2016, B = 03/2017, C = 10/2017)

3.1 Wood decay by *S. commune* and *T. versicolor*

For the decay tests under laboratory conditions, beech sapwood particles were inoculated with monokaryotic and dikaryotic strains of *S. commune* and *T. versicolor* in glass vials and delved into the effects of both fungi on wood decay under different light and dark schemes.

3.1.1 Comparison of sapwood weight losses by both fungi in different light schemes

All monokaryotic and dikaryotic strains of both fungi, *S. commune* and *T. versicolor* were able to grow on beech sapwood particles under all light schemes, albeit overall growth of mycelium was different. The reduction in sapwood weight by *T. versicolor* monokaryotic (*Tv-M*) and dikaryotic (*Tv-D*) strains were considerably higher compared to *S. commune* strains (monokaryotic *Sc-M1* and *Sc-M2*, and dikaryotic *Sc-D*) in both (30 and 90 days) decay periods (Figure 3-2 and Figure 3-3). Dark and light conditions had different effects on mycelial surface growth of all *S. commune* and *T. versicolor* strains, but light induced fruiting body development only on the established mycelium of *Tv-D* (Figure 3-4).

The weight losses between all *S. commune* strains under all light schemes were ranged from 2 to 4 % and 3 to 6 % within 30 and 90 days respectively. There were no statistically significant differences in the amounts of weight losses by the *S. commune* monokaryotic (*Sc-M1* and *Sc-M2*) and dikaryotic (*Sc-D*) strains, and there was no significant increase over the time (30 to 90 days). More interestingly, the weight losses caused by all tested *S. commune* strains under the four light schemes were neglectable within the given time (Figure 3-2, 3-3).

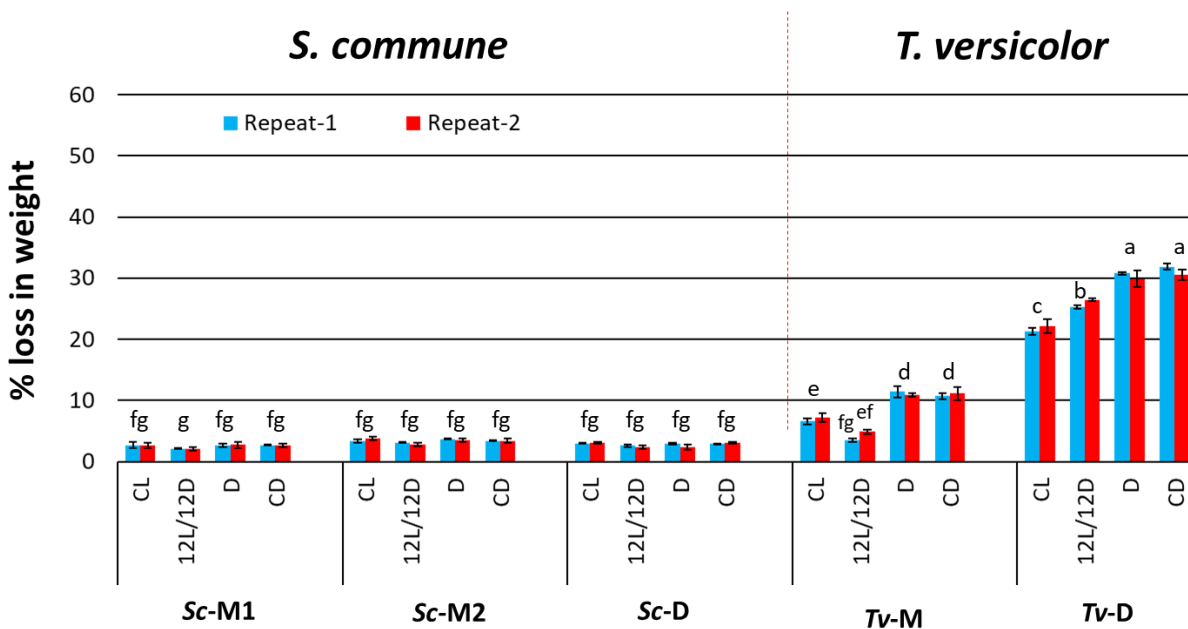


Figure 3-2 Weight losses of beech sapwood particles in 30 days by *S. commune* and *T. versicolor* under different environmental conditions (CL = Continuous Light, 12L/12D = 12h Light

+ 12h Dark, D = Dark, CD = Continuous Dark). Values of 5 replicates were averaged. The error bars show standard deviations from the average values. Bars with the same letter are not significantly different from each other ($p < 0.001$, ANOVA followed by Tukey's HSD test).

On the other hand, the weight losses caused by the *T. versicolor* monokaryotic (*Tv-M*) and dikaryotic (*Tv-D*) strains were comparable higher over the *S. commune* strains. The *Tv-M* strain reduced beech sapwood weight within 30 days by 11% in dark and continuous dark, by 7% in light and by 4-5% in a 12 h dark/12 h light scheme (Figure 3-2). By the increase of decay period, the weight losses reached within 90 days to 24% in dark and continuous dark schemes, 19% in light and 9% in a 12 h dark/12 h light schemes (Figure 3-3). The *T. versicolor* dikaryotic strain (*Tv-D*) strongly decayed beech sapwood under all light schemes. However higher weight losses were detected under dark and continuous dark schemes compared to the 12 h light/ 12 h dark, and continuous light schemes (Figure 3-2 and Figure 3-3). Up to 32% and 53% reduction in weights within 30 and 90 days respectively were observed under the influence of dark conditions, which were significantly higher than the weight losses of beech sapwood in continuous light (21-22% within 30 days and 44% within 90 days), and in 12 h light/12 h dark scheme (25-26% within 30 days and 47-48% within 90 days) (Figure 3-2, 3-3).

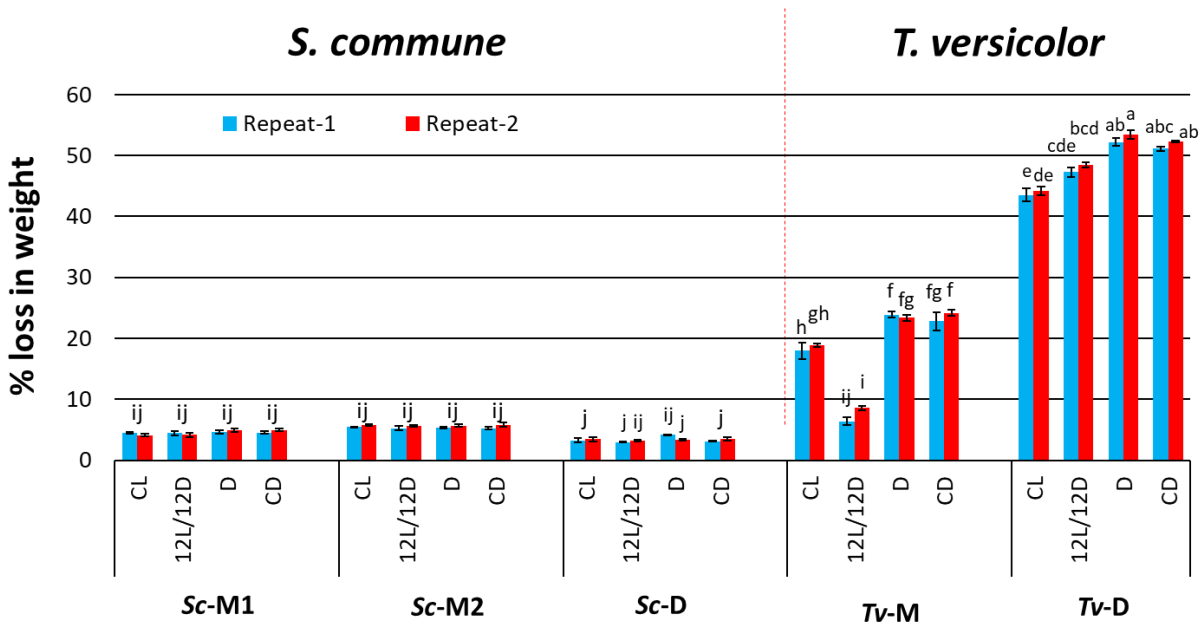


Figure 3-3 Weight losses of beech sapwood particles in 90 days by *S. commune* and *T. versicolor* under different environmental conditions (CL = Continuous Light, 12L/12D = 12h Light + 12h Dark, D = Dark, CD = Continuous Dark). Values of 5 replicates were averaged. The error bars show standard deviations from the average values. Bars with the same letter are not significantly different from each other ($p < 0.001$, ANOVA followed by Tukey's HSD test).

3.1.1.1 Mycelium growth and fruiting body development on wood particles

T. versicolor (dikaryotic strain – Tv-D) was chosen due to the high decay rate observed in the former experiments as well as that in nature, the dikaryon as it is the typical life form of the fungus, and to describe the different fruiting development stages of the fungus. *T. versicolor* in dark and light conditions had different effects on mycelial surface growth (Figure 3-4). Complete darkness led to good mycelial growth around all wood particles throughout the samples (checked the wood particles inside the sample). Contrariwise, light induced formation of thick mycelium on the surface of the samples, and low mycelium density around the wood particles inside the samples. In dark (with short periods of illumination), surface mycelium produced aggregated structures due to light. However, in continuous light and in 12 h light/ 12 h dark schemes, the surface mycelium was massive with different fruiting structures (Figure 3-4).

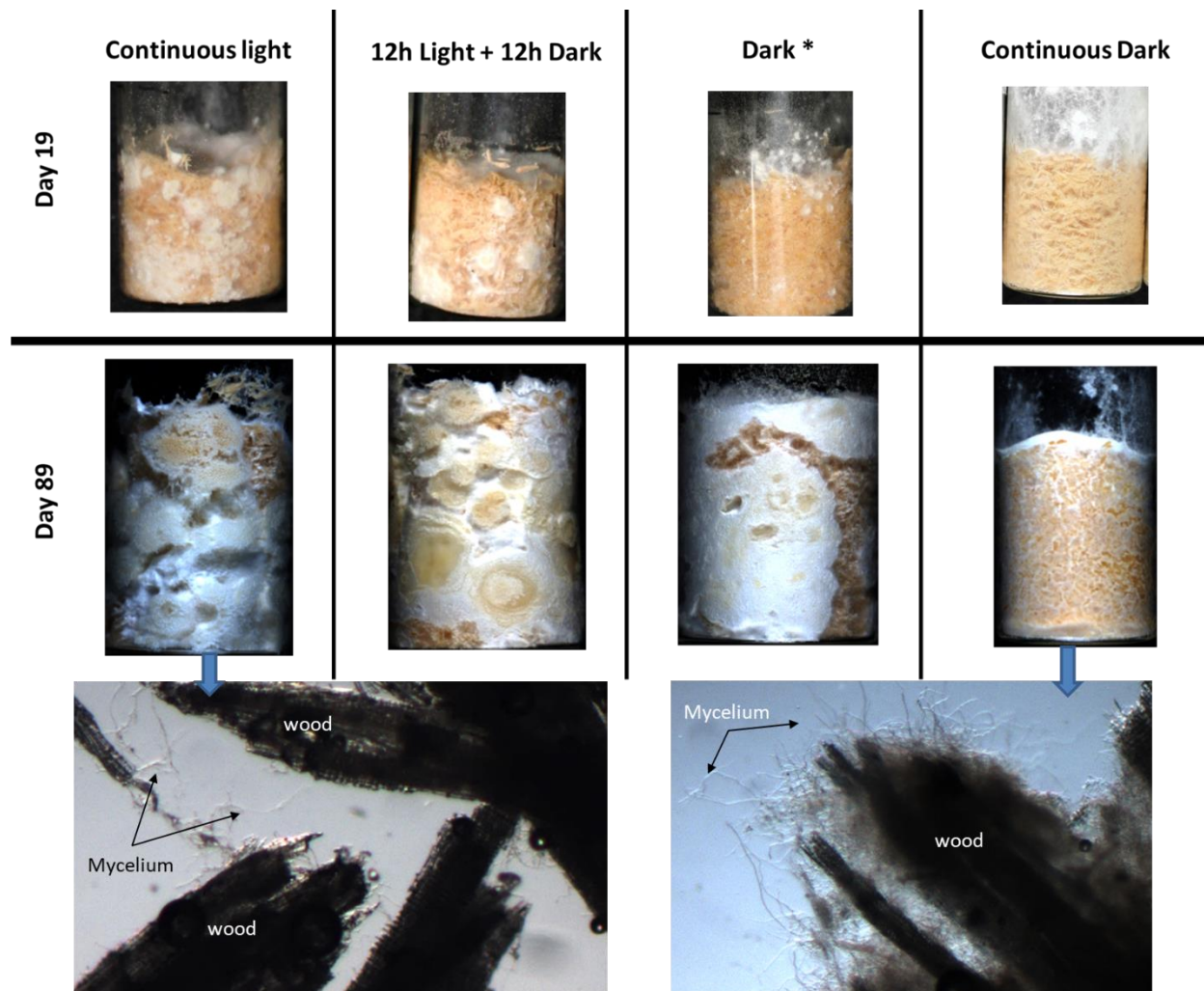


Figure 3-4 Comparison of *T. versicolor* (*Tv*-D strain) mycelia and fruiting structures grown on beech sapwood particles at 25 °C under different light conditions (* dark conditions with short periods of illumination).

Moreover, light induced fruiting body development on the established mycelium. The observed *T. versicolor* fruiting body development on beech sapwood particles started with secondary hyphal knots (SHKs – a compact mass of undifferentiated hyphae as an early fruiting body developmental stage, Liu et al. 2006) which formed thick mycelium on the surface of the sample. Later these SHKs differentiated into different tissues and edges of mycelium grew perpendicular to surface mycelium by pushing substrate into the opposite direction. This process created a cup-shaped structure. The inner side of the cup transformed to differentiated tubes (possibly the spore-bearing structures). The developed stromata (compact mass of mycelial tissues having the spore producing structures) were of various shapes as shown in Figure 3-5. SHKs were

regularly spotted on the fungus-wood samples exposed to illumination which later transformed to stromata on the established mycelium (Figure 3-4 and Figure 3-5). More of these structures were produced under continuous light than in a 12 h light/ 12 h dark regime and in cultures kept in dark with short periods of illumination (received during daily samples evaluation).

The *T. versicolor* monokaryotic strain (*Tv-M*) had a thin mycelial growth on the sample surface and within the particles under all light schemes. The monokaryotic cultures did not form SHKs and therefore also no more advanced structures were developed. It was also observed that *T. versicolor* (in both, monokaryotic *Tv-M* and dikaryotic *Tv-D* stains) changed the color of beech sapwood to dark brown and later yellow, indicating the lignin degradation by the decay action of the fungus.

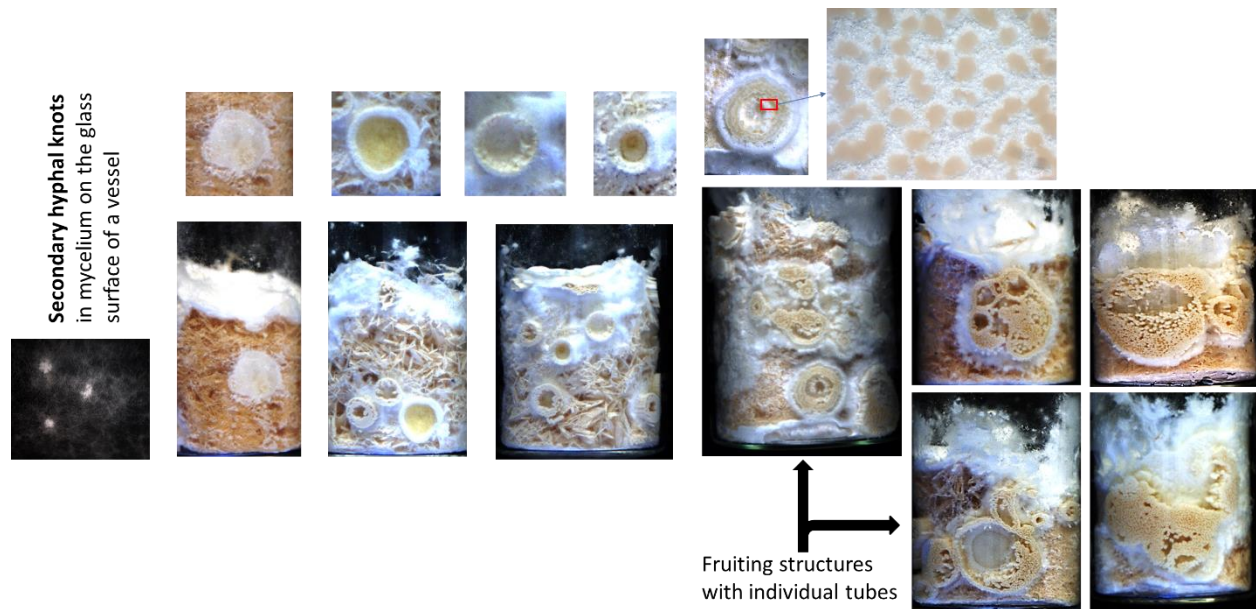


Figure 3-5 Development of *T. versicolor* (strain *Tv-D*) fruiting bodies on beech sapwood particles at 25 °C under light

The surface mycelium of all *S. commune* strains on beech sapwood particles under all conditions was thin, and no SHKs and fruiting body were developed. The *S. commune* monokaryotic strains (*Sc-M1* and *Sc-M2*) were comparatively fast growing than the dikaryotic strain (*Sc-D*) and formed aerial mycelium on the glass surface of the tubes. Furthermore, the monokaryotic *S. commune* strains had a relatively thin mycelium within the sapwood particles

unlike the dikaryotic strain. Although light can induce fruiting bodies in the dikaryotic strains of *S. commune* as reported previously by Perkins (1969) and Raudaskoski and Viitanen (1982) but in this study no fruiting body structure was observed. No change in the color of the wood was observed during all three *S. commune* (monokaryotic and dikaryotic) strains growth on beech sapwood particles.

3.1.2 Comparison of bark and sapwood weight losses of both fungi under light and dark conditions

In nature, *S. commune* appeared first on deadwood and later replaced by *T. versicolor* when the bark was still present. This indicated a relationship between bark and both fungi (Figure 3-1). Therefore, the decay abilities of *S. commune* and *T. versicolor* were assessed on beech bark particles and compared with beech sapwood particles under continuous light (L) and dark (D) conditions.

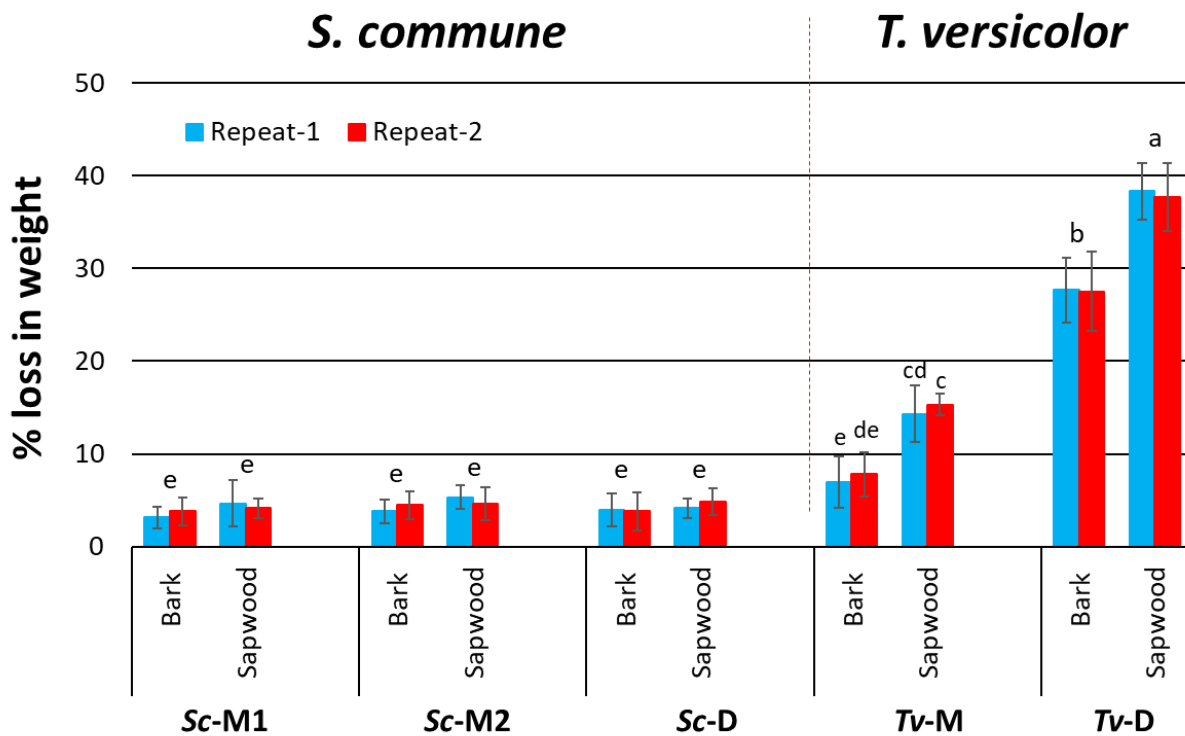


Figure 3-6 Comparison of weight losses of beech bark and sapwood particles in 60 days by *S. commune* and *T. versicolor* under light condition at 25 °C. Values of 3 replicates were averaged. The error bars show standard deviations from the average values. Bars with

the same letter are not significantly different from each other ($p < 0.001$, ANOVA followed by Tukey's HSD test).

All strains (monokaryotic and dikaryotic) of both fungi were able to colonize the beech bark and sapwood particles under light and dark conditions. Continuous light and dark conditions had an influence on the weight losses of bark and sapwood particles. The reduction in weights of all tested strains were statistically non-significant under dark condition compared to light condition (Figure 3-6, 3-7). Among all the tested strains of both fungi, the overall highest bark and sapwood weight losses were caused up to 33% and 43% respectively, by the *Tv*-D strain. Up to 28% (L) and 33% (D) bark weight losses were done by the *Tv*-D strain which were statistically significant less than weight losses of sapwood (38% – L and 43% – D). The *Tv*-M strain reduced the bark weights by 7 to 8% (L) and by 9 to 10% (D). But, 14 to 15% (L) and 18 to 20% (D) reduction in sapwood weights were observed by the action of the *Tv*-M strain (Figure 3-6, 3-7).

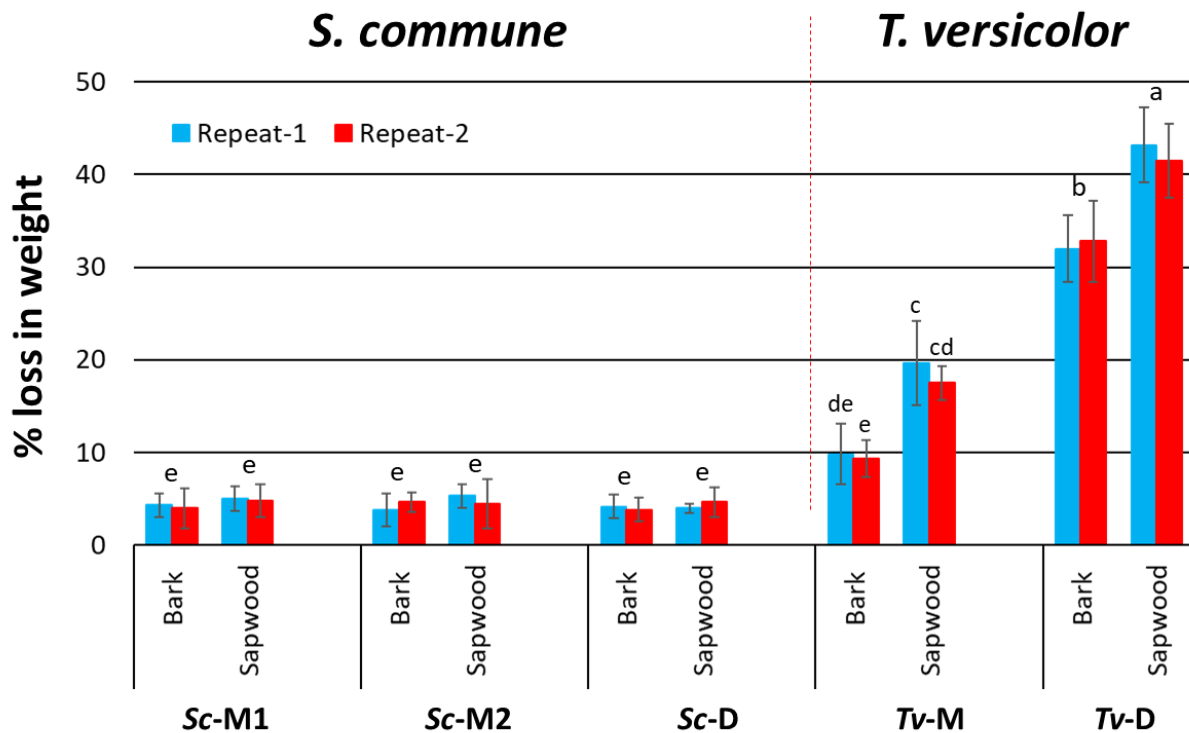


Figure 3-7 Comparison of weight losses of beech bark and sapwood particles in 60 days by *S. commune* and *T. versicolor* under dark condition at 25 °C. Values of 3 replicates were averaged. The error bars show standard deviations from the average values. Bars with

the same letter are not significantly different from each other ($p < 0.001$, ANOVA followed by Tukey's HSD test).

However, overall weight losses were low in bark and sapwood colonized by all *S. commune* strains under both (light and dark) conditions. The decay caused by the *S. commune* strains in bark was between 3 to 5% under light and dark conditions. In contrast, under same conditions, between 4 to 5% reduction in weights were observed in sapwood particles inhabited by monokaryotic (*Sc-M1* & *Sc-M2*) and dikaryotic (*Sc-D*) *S. commune* strains (Figure 3-6, 3-7). The strong decay ability of *T. versicolor* was evident by the much higher weight losses in bark and sapwood compared to *S. commune*.

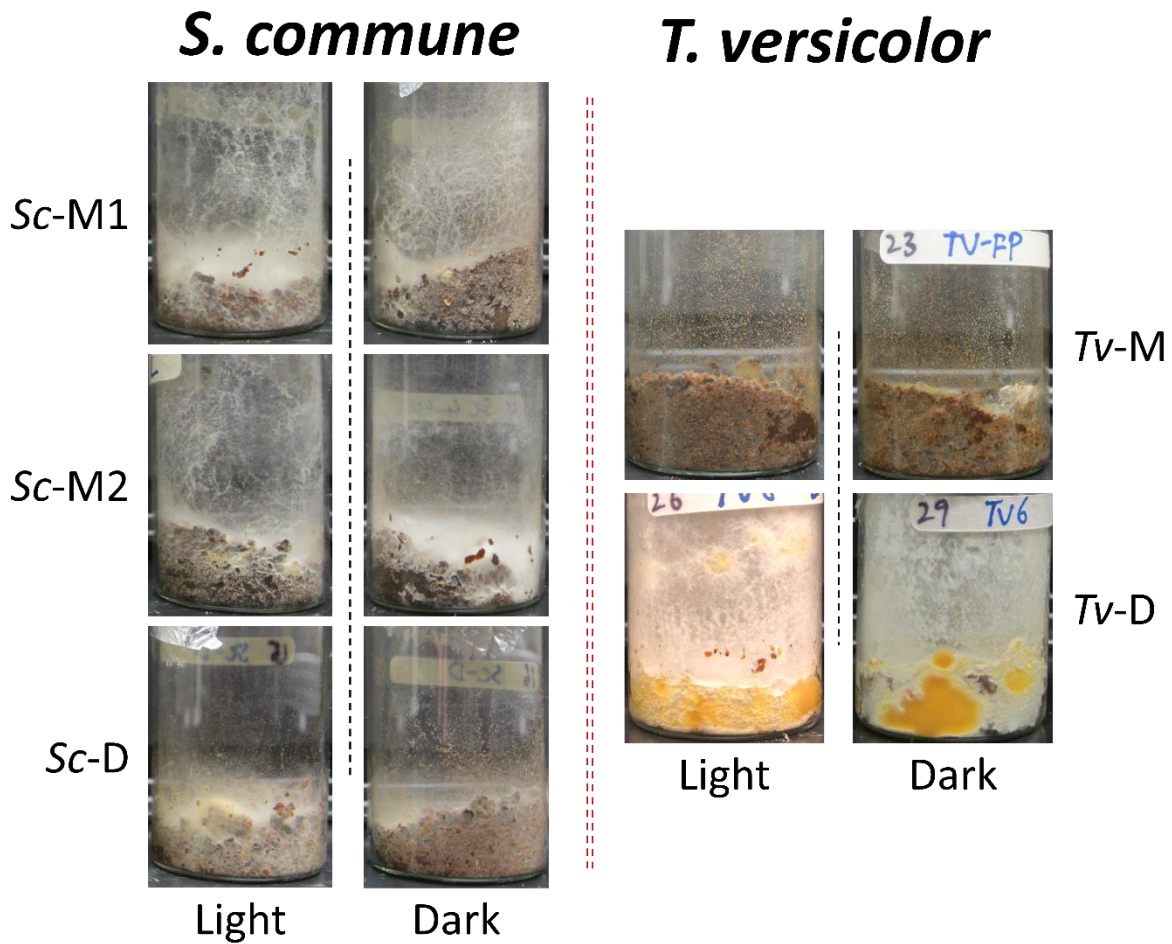


Figure 3-8 Comparison of mycelial growth by monokaryotic and dikaryotic *S. commune* and *T. versicolor* strains grown on beech bark particles under light and dark conditions for 60 days at 25 °C.

Mycelial growth of all tested strains on beech bark particles showed obvious differences in the growth in light and dark conditions, there was more mycelium on the surfaces in light and noticeable differences among the tested strains of both fungi. In case of *S. commune* monokaryotic strains (*Sc-M1* & *Sc-M2*), dense mycelia on the sample surface (top surface of culture) and on the wall of the glass vials were observed (Figure 3-8). On the other side, dikaryotic *S. commune* strain (*Sc-D*) did not grow on the glass walls and did not produce any fruiting body structure. Overall growth of the *S. commune* dikaryon on bark particles was better than the monokaryons. In deeper layers of the sample, the mycelium of all *S. commune* strains grew around bark particles under both light conditions, but comparatively more mycelial growth in light condition than dark. Furthermore, the monokaryotic strains grew in a thinner manner on bark particles inside the sample layers unlike the *S. commune* dikaryotic strain *Sc-D*.

The mycelial growth by the *Tv-M* strain was scant on bark particles (on the sample surface and throughout the sample) and did not grow on the glass walls under both light and dark conditions (Figure 3-8). In contrast, the *Tv-D* strain produced massive surface mycelia on the substrate surface and on the glass walls along with yellow-orange spots (probably fused mycelium) (Figure 3-8). The strain also grew with a denser mycelium within the bark particles under both light conditions.

3.1.3 Assessment the growth of both early sapwood colonizers on wood wash-out

The purpose was to test the growth of both early sapwood colonizers (*S. commune* and *T. versicolor*) on the wood wash-out. Different dilutions of wood wash-out with and without addition of nutrients (carbon and nitrogen) and vitamin (thiamin) were tested for fungal growth. All strains of *S. commune* grew on wood wash-out with and without additions but not the *T. versicolor* strains.

Table 3-1 Fungal growth of *S. commune* and *T. versicolor* on different dilutions of wood wash-out

Wood wash-out dilutions	Mycelial density				
	<i>S. commune</i>			<i>T. versicolor</i>	
	<i>Sc-M1</i>	<i>Sc-M2</i>	<i>Sc-D</i>	<i>Tv-M</i>	<i>Tv-D</i>
1:1	T	T	T	X	X
1:1 + thiamin	T	T	T	X	X
1:4	T	T	T	T	T
1:10	T	T	T	T	T
1:10 + carbon	-	C	T	C	C
1:10 + nitrogen	-	T	T	T	T
1:10 + carbon + nitrogen	-	C	T	C	C

T = thin, C = compact, X = no growth, - = not tested

On 1:1, 1:4 and 1:10 dilutions of wood wash-out, monokaryotic (*Sc-M1* and *Sc-M2*) and dikaryotic (*Sc-D*) strains of *S. commune* showed scattered and thin mycelial growth on the wood wash-out. Similar growth patterns were observed upon addition of thiamine to 1:1 dilution of wood wash-out. Addition of thiamine was tested because *S. commune* required supplementation of this vitamin for good mycelial growth and induction of fruiting (Jonathan and Fasidi 2001; Wessels 1965). Further the wood wash-out was tested with the addition of carbon (C) and nitrogen (N) sources with 1:10 dilution of wood wash-out. In the presence of C and C+N, monokaryotic strain of *S. commune* (*Sc-M2*) grew with compact mycelial density. On the contrary, thin and scattered mycelia of the *Sc-D* strain were observed in the presence of C and C+N. The nitrogen added to the wood wash-out had no effect on the mycelial growth of the *S. commune* strains compared to the wash-out control without additions, where the mycelia of all tested strains were thin and scattered in the presence of nitrogen (Table 3-1).

Both (monokaryotic and dikaryotic) strains of *T. versicolor* (*Tv-M* and *Tv-D*) did not show any mycelial growth on 1:1 dilution of wood wash-out with and without addition of thiamin even after 20 days of inoculation. Upon dilution of wood wash-out to 1:4 and 1:10, both *T. versicolor*

strains (*Tv*-D and *Tv*-M) were able to grow with thin and scattered mycelia. With the addition of carbon (C) and nitrogen (N) sources to 1:10 dilution of wood wash-out, compact mycelial density in both strains of *T. versicolor* were observed in the presence of C and C+N. However, addition of nitrogen alone to the wood wash-out had no change in mycelial growth (Table 3-1).

3.2 Fungal interactions between *S. commune* and *T. versicolor*

As in nature *S. commune* as early invader fruits regularly as the first on wood, may dwell with other species such as *T. versicolor* that will then later replace the fungus. It is considered, *S. commune* is taking advantage of other stronger wood degraders. Consequently, cooperative or/ and competing interactions might occur between *S. commune* and *T. versicolor* in the wood. Hence, these interactions were investigated between both species on natural and artificial substrates in laboratory.

3.2.1 Dual interactions on natural substrate

Interactions between the fungal species on wood were tested in 3-divided Petri-dishes where one chamber was filled with water and the two others with beech sapwood particles which were then inoculated with mycelium of a same or of different fungal strains (Figure 3-9 and Figure 3-10). Mono- and dikaryons of the two species were tested. All strains grew on and into the wood particles, albeit with different speed and amounts of mycelium production.

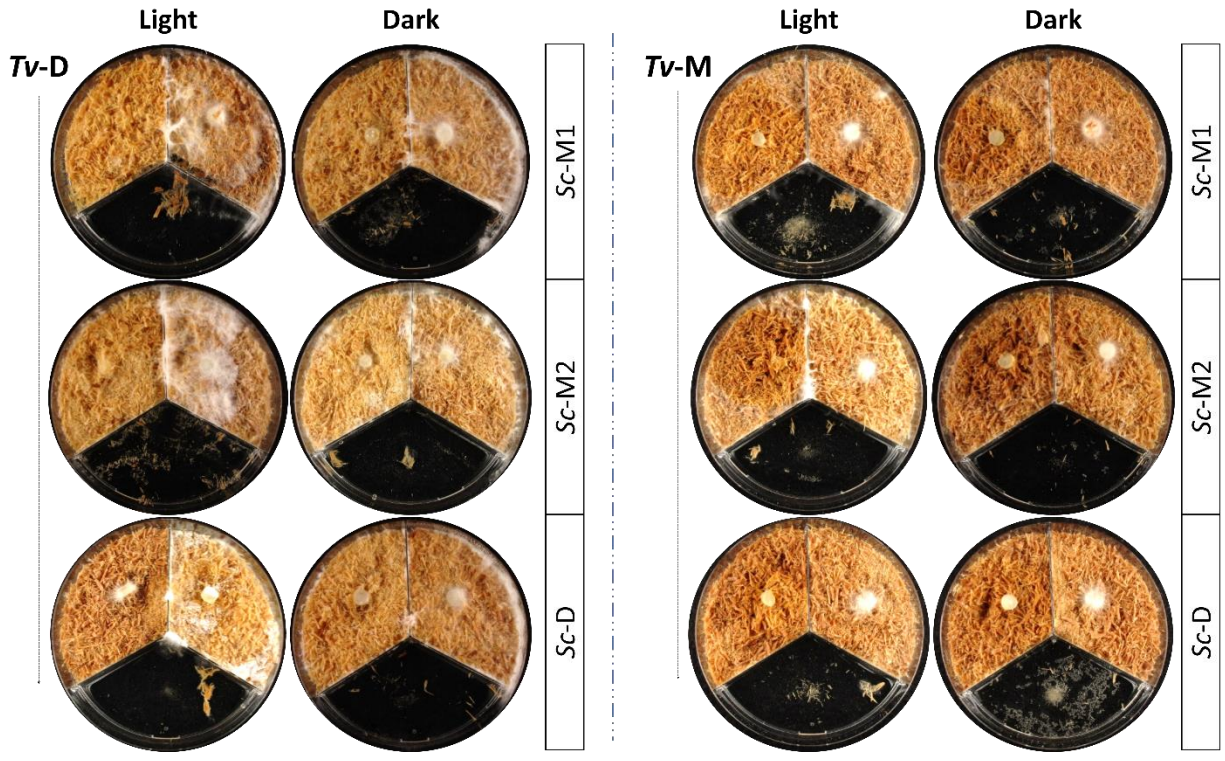
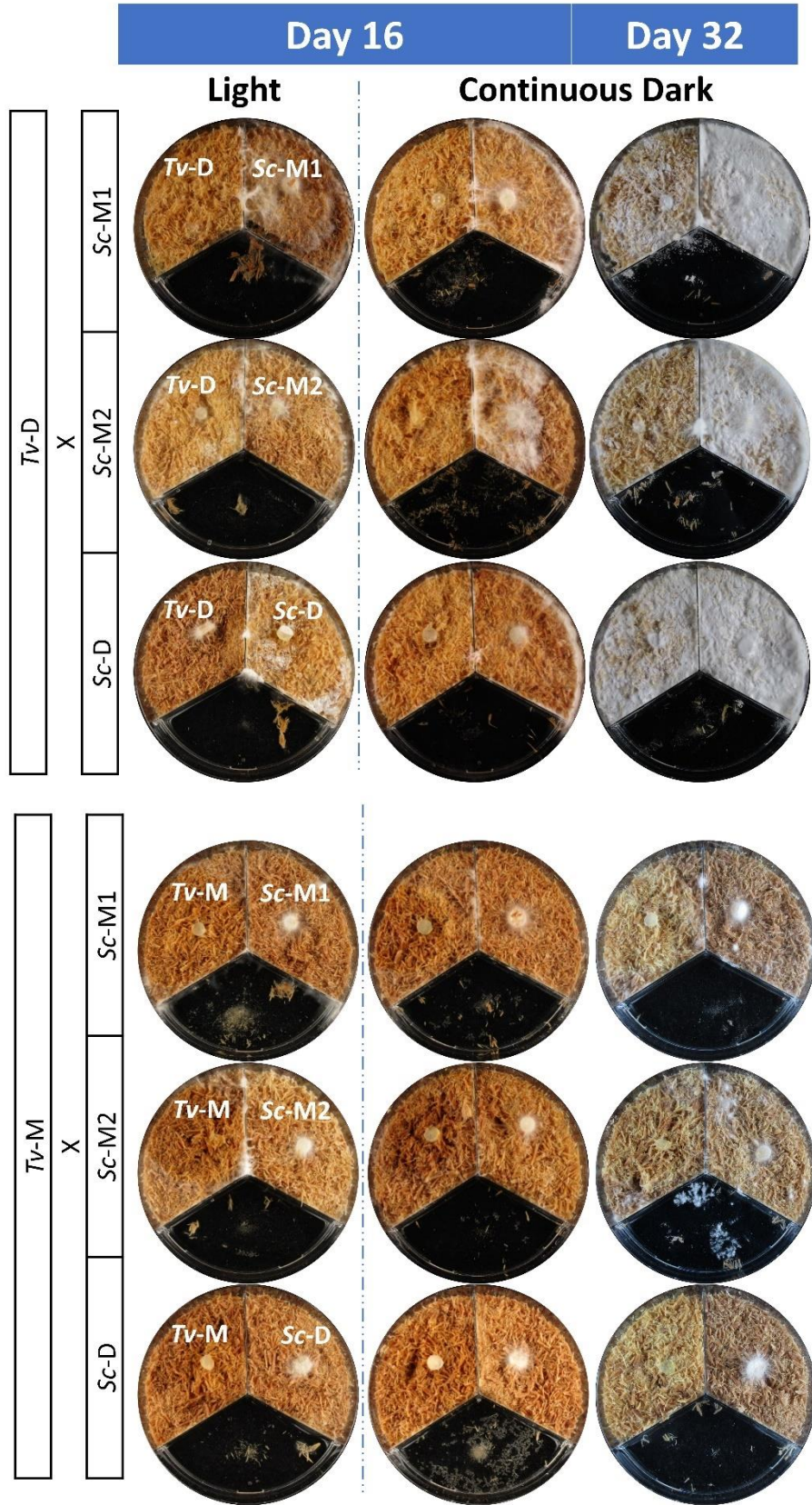
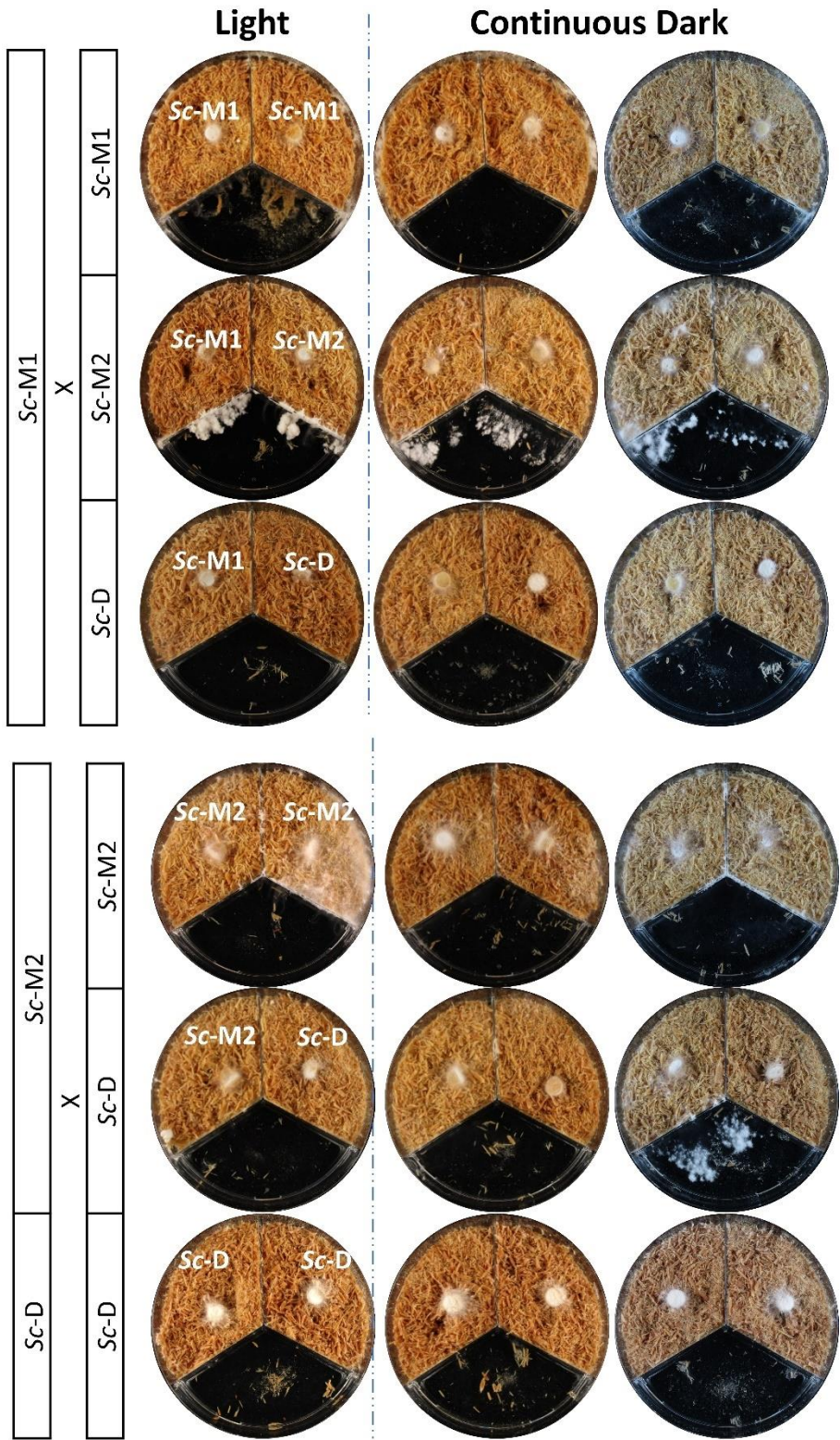


Figure 3-9 Interactions between monokaryotic and dikaryotic strains of *T. versicolor* and *S. commune* on beech sapwood particles after 16 days of incubation at 25 °C.



continue ---

Day 16 Day 32



continue ---

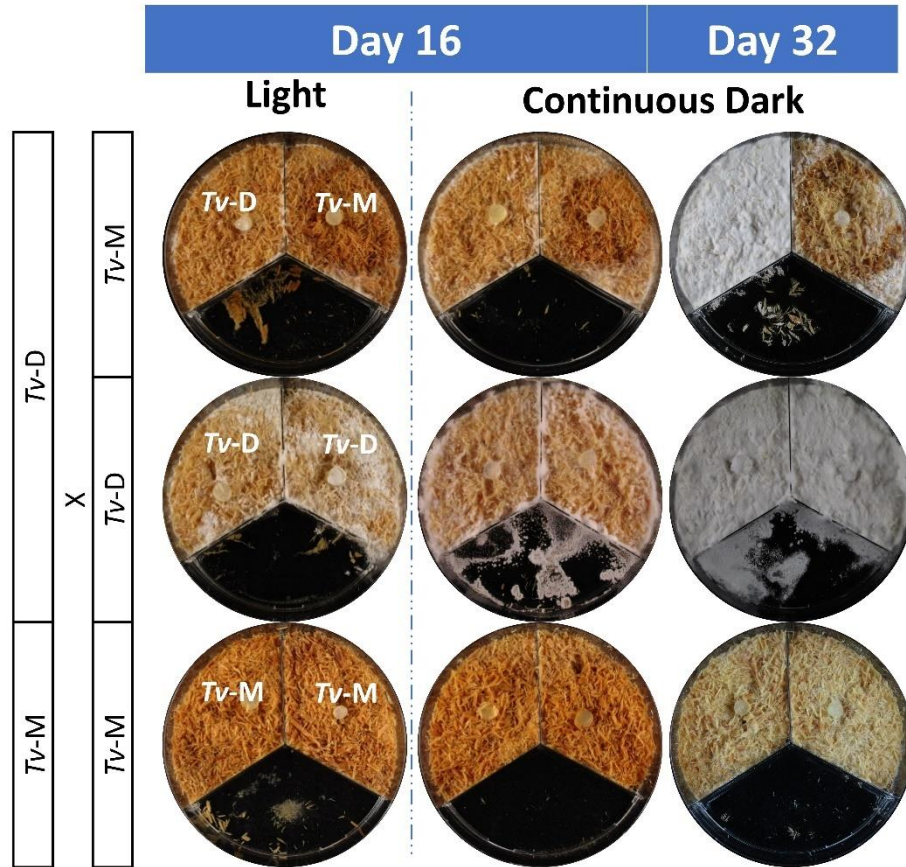


Figure 3-10 Intra- and interspecific interactions between mono- and dikaryotic strains of *T. versicolor* and *S. commune* developed over time on beech sapwood particles

In dual culture of the *Tv-D* strain with the individual *S. commune* strains (monokaryotic *Sc-M1* & *Sc-M2*, and dikaryotic *Sc-D*), all strains had the same growth speed irrespectively of species and type of mycelium. After 6 days of incubation, dense mycelia of mixed strains emerged at the point of interaction (at the central wall). Microscopy showed that further growth of *S. commune* was ceased by the *Tv-D* strain which then started to grow over the wood inhabited by *S. commune* with a much denser mycelium than in single culture. In comparison to light condition, the *Tv-D* strain grew in the dark faster over the wood inhabited with any *S. commune* strain, as observed at day 16 of incubation (Figure 3-9 and Figure 3-10). With the increase of incubation period (32 days), the *Tv-D* strain made more dense mycelia over the *S. commune* inhabited wood than the alone *T. versicolor* inhabited wood (Figure 3-11).

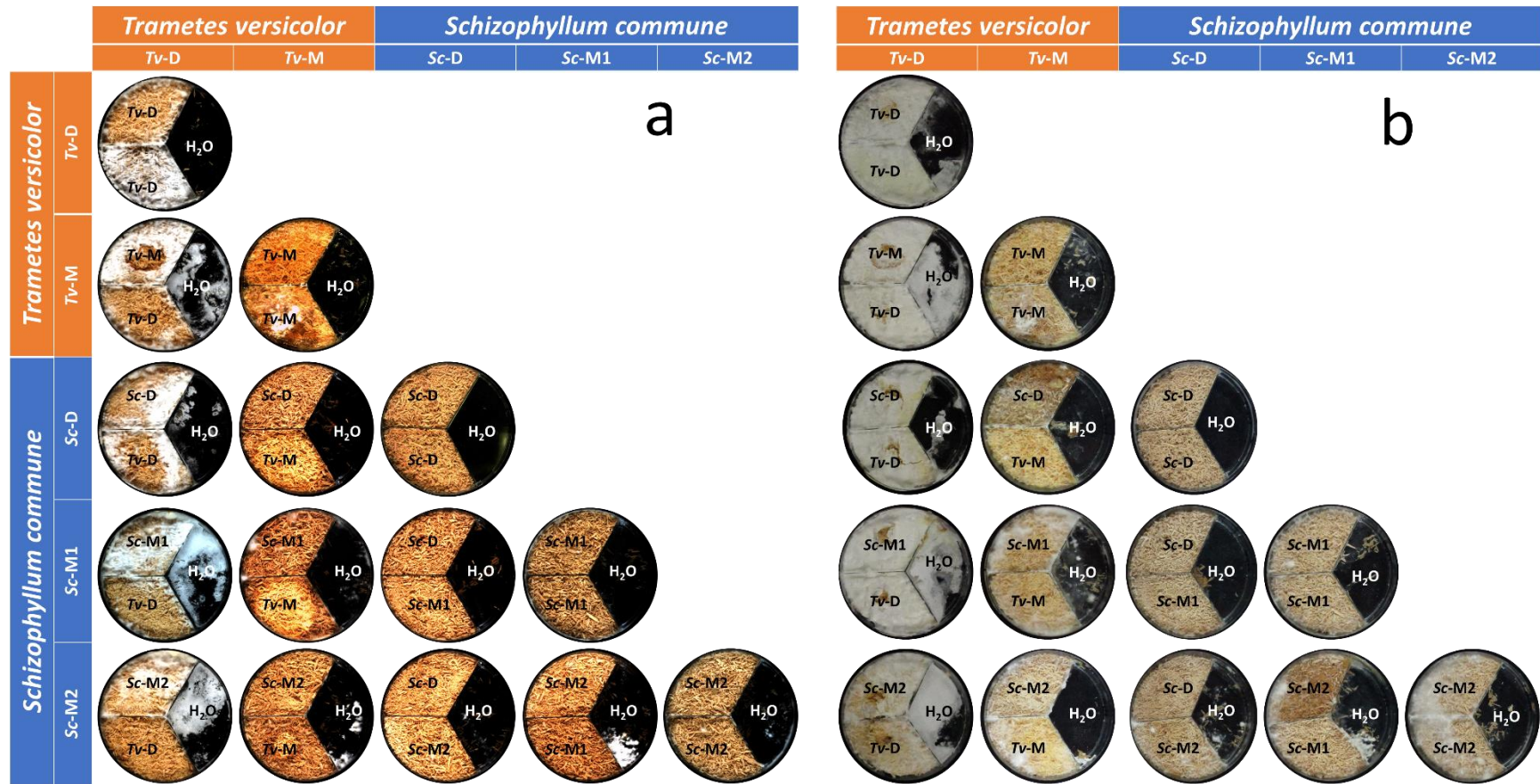


Figure 3-11 Interactions between combinations of strains of *T. versicolor* and *S. commune* on beech sapwood particles after 4 weeks (a) and 20 weeks (b) of incubation

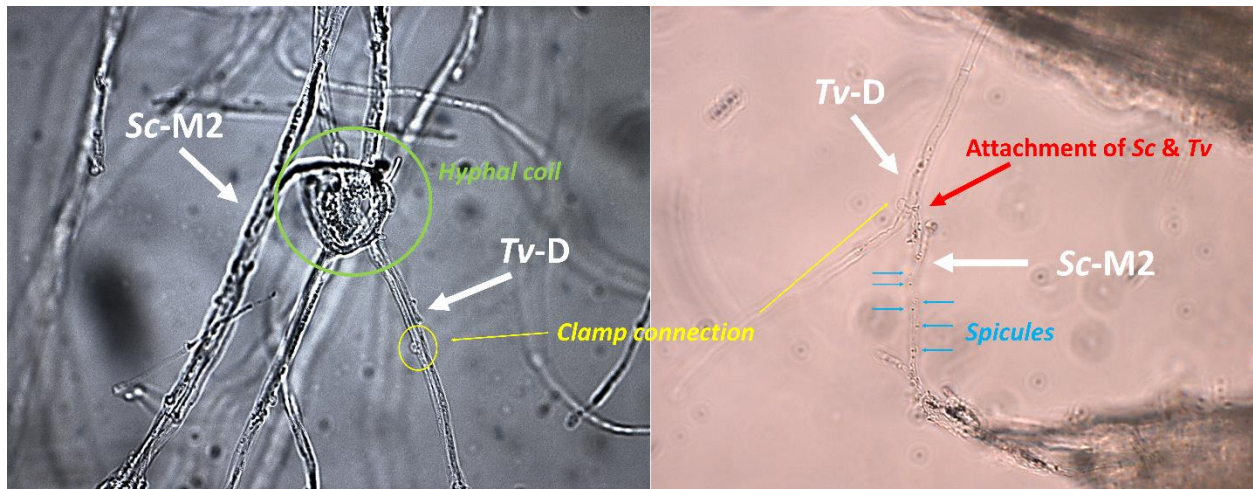


Figure 3-12 Hyphal interaction between *T. versicolor* dikaryotic strain (*Tv-D*) and *S. commune* monokaryotic strain (*Sc-M2*) on beech sapwood particles after 15 days cultivation at 25 °C (400X magnification). Hyphal coil and spicules were formed on the *Sc-M2* strain and clamp connections on the *Tv-D* strain.

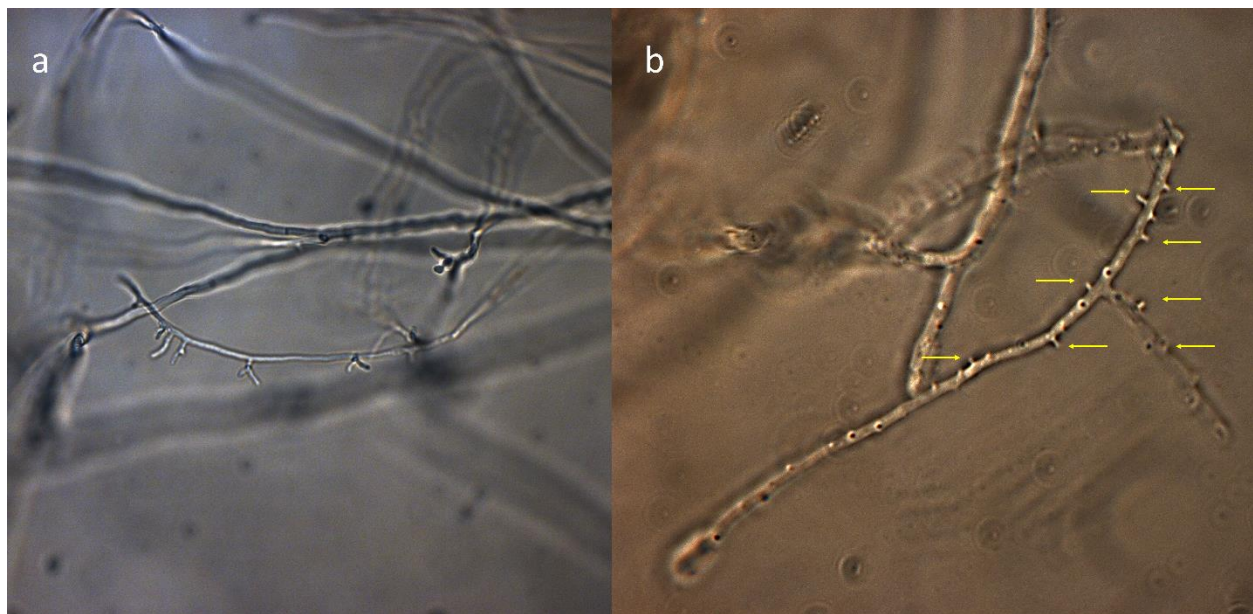


Figure 3-13 Mycelium of *S. commune* monokaryotic strain (*Sc-M1*) without spicules in single culture (a, 400X magnification), and with spicules (arrows) in dual culture of *Sc-M1* and *Tv-D* in the interaction region (b, 1000X magnification) after 8 days cultivation at 25 °C on beech wood particles.

After 20 weeks of incubation, dense mycelia of the *Tv*-D strain covered whole wood surface and constructed to a thick mycelial mat (Figure 3-11). Microscopy observations of growing mycelia showed that *S. commune* was replaced by *T. versicolor* over time. Typical features of *S. commune*, hyphal coils and spicules were found prominent in combat regions and rarely found on normal mycelia (mycelia in single strain cultures) and initial combat zones (Figure 3-12, Figure 3-13, Figure 3-14, and Figure 3-15).

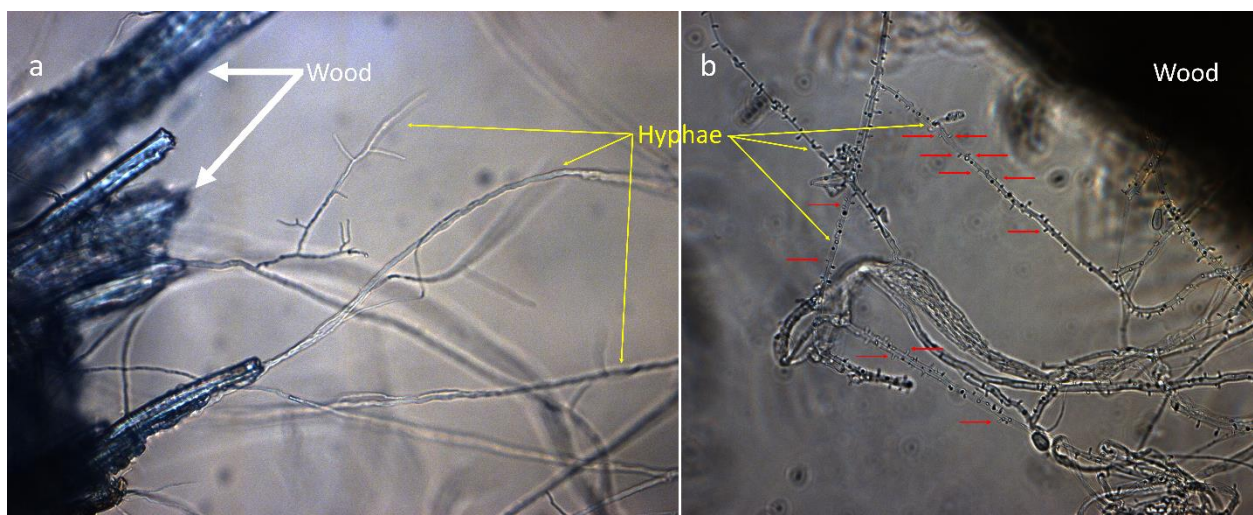


Figure 3-14 Mycelium of *S. commune* monokaryotic strain (*Sc*-M2) without spicules in single culture (a), and with spicules (red arrows) in dual culture of *Sc*-M2 and *Tv*-M (b) on beech sapwood particles after 15 days cultivation at 25 °C (400X magnification).

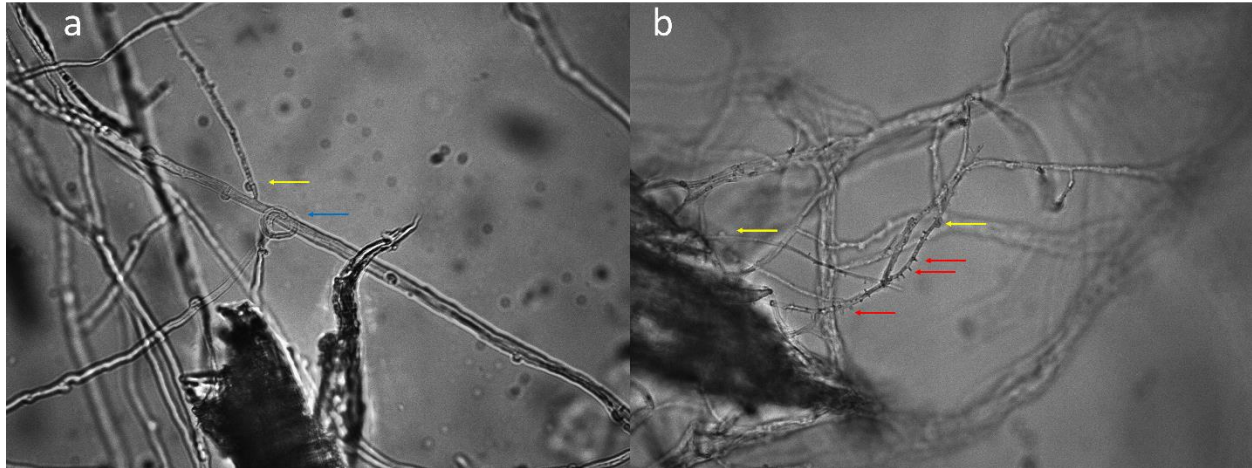


Figure 3-15 Mycelium of *S. commune* dikaryotic strain (*Sc-D*) without and with spicules (a) and with spicules (b, red arrows) in single culture on beech sapwood particles after 10 days cultivation at 25 °C (400X magnification). Yellow arrows indicate clamp connections, and blue arrow indicates hyphal coil.

On the other hand, in the interaction study of the *Tv-M* strain with the individual *S. commune* monokaryotic (*Sc-M1* & *Sc-M2*) and dikaryotic (*Sc-D*) strains, no barrier formation and no dense mycelia were developed at the point of interaction (Figure 3-9). The *Tv-M* strain grew slower than the *Tv-D* and all *S. commune* strains. Therefore, the *S. commune* strains grew over the central plastic wall of the tripartite Petri dishes into the *Tv-M* compartment and inhabited wood particles in the *Tv-M* compartment while the *Tv-M* strain inhabited only a part of its own compartment. However, none of the competing species (competing in the *Tv-M* compartment) grew over each other in both light and dark conditions, even with the increase of incubation period to 32 days and up until 20 weeks (Figure 3-10 and Figure 3-11). Spicules on the *S. commune* hyphae were developed near the interaction zone which were absent in single culture and non-combat regions (Figure 3-14). Change in color of wood particles from brown to yellow was detected in the wood inhabited by *T. versicolor* (both strains) but not in *S. commune* inhabited wood particles. *S. commune* fruiting structures were also discerned on water especially in the interaction of the *Tv-M* strain with *Sc-D* which might be due to survival strategy of *S. commune* in combat situation (Figure 3-16). Fruiting structures were also observed on water in the interaction of the *Sc-M1* and *Sc-M2* strains under light condition which was due to dikaryon formation of the two mating-compatible monokaryons (Figure 3-10). In the same strain interactions of the *Tv-M*

and all *S. commune* strains, all strains grew on and into the wood particles but without any prominent aerial mycelium production (Figure 3-10). Conversely, the *Tv*-D strain in self-confrontation produced dense mycelium which transformed to mycelial mat after longer (4 and 20 weeks) incubation periods (Figure 3-10 and Figure 3-11). Furthermore, aggregates and tube-like structures as potential primordial structures of fruiting bodies of the *Tv*-D strain appeared in aging beech sapwood cultures regardless of prior inoculation and growth of other fungal strains. Numbers of structures were higher in dual cultures with *S. commune* as compared to any *T. versicolor* strain combinations (Figure 3-17).

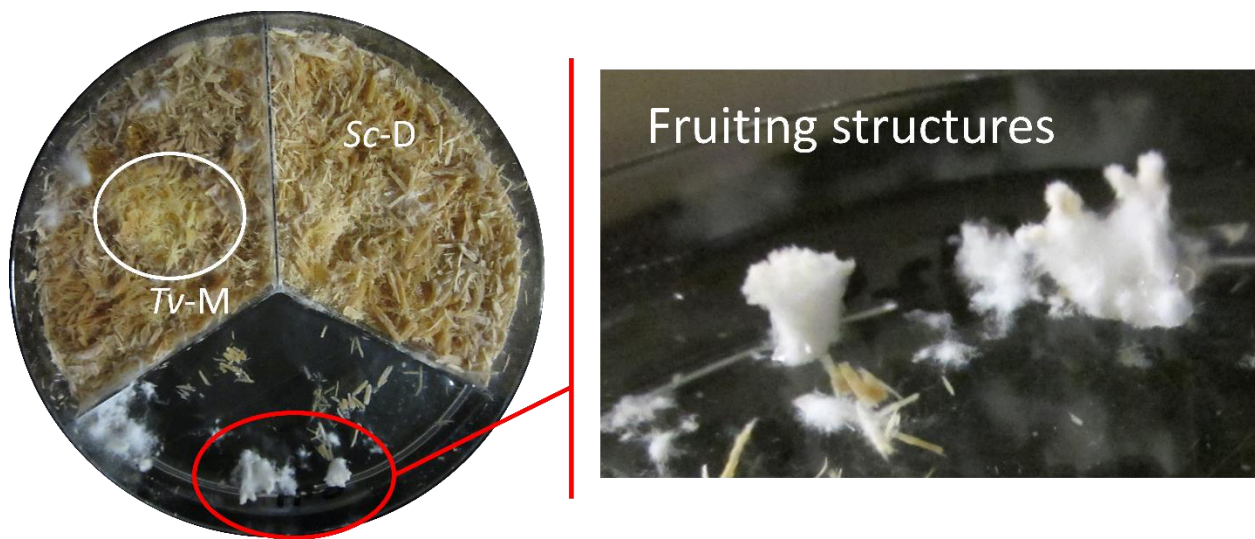


Figure 3-16 Fruiting initiation in *S. commune* dikaryotic strain (*Sc*-D) on water surface while interacting with *T. versicolor* monokaryotic strain (*Tv*-M) on beech sapwood particles after 16 days of incubation at 25 °C. *Tv*-M confined within white circle and surrounded by *Sc*-D as confirmed by microscopy of overgrown wood particles.

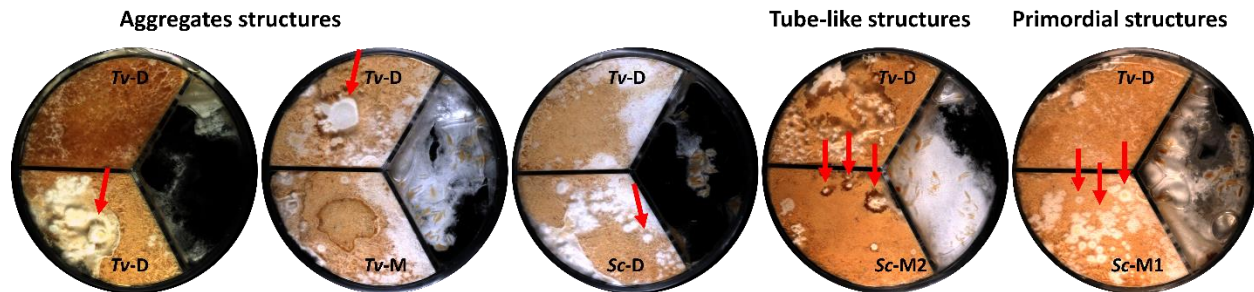
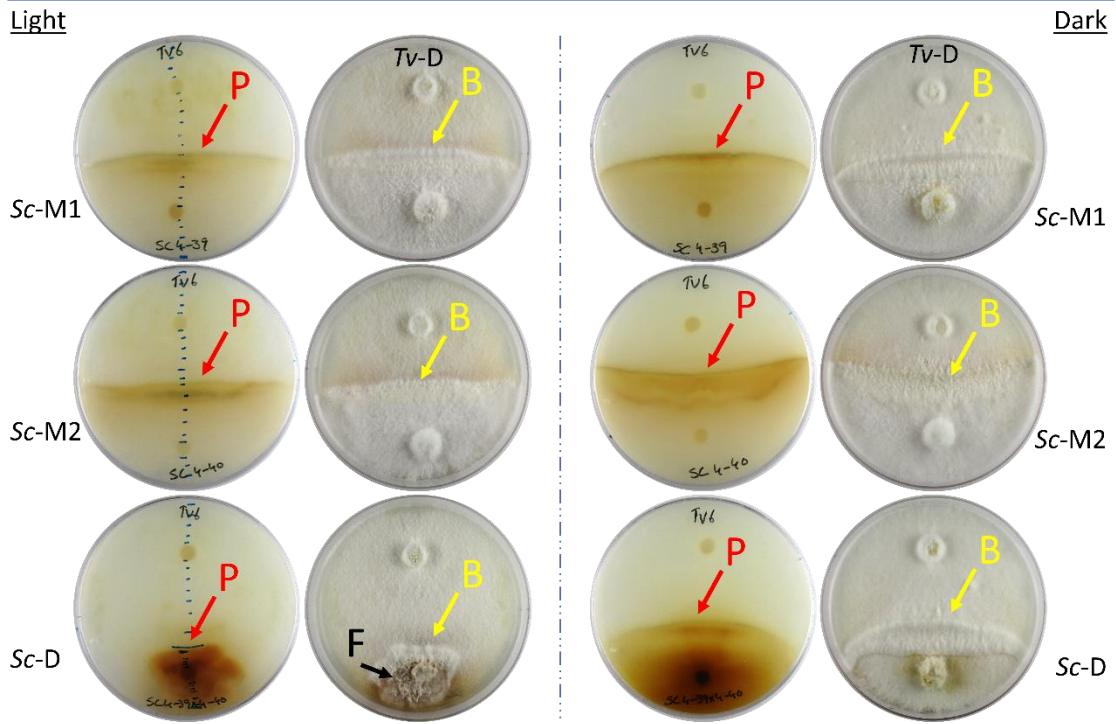


Figure 3-17 Aggregates and tube-like structures (marked by red arrows) as potential primordial structures of fruiting bodies appeared on the bottoms of Petri-dishes in all cultures inoculated with the dikaryotic *T. versicolor* after 20 weeks of incubation at 25 °C.

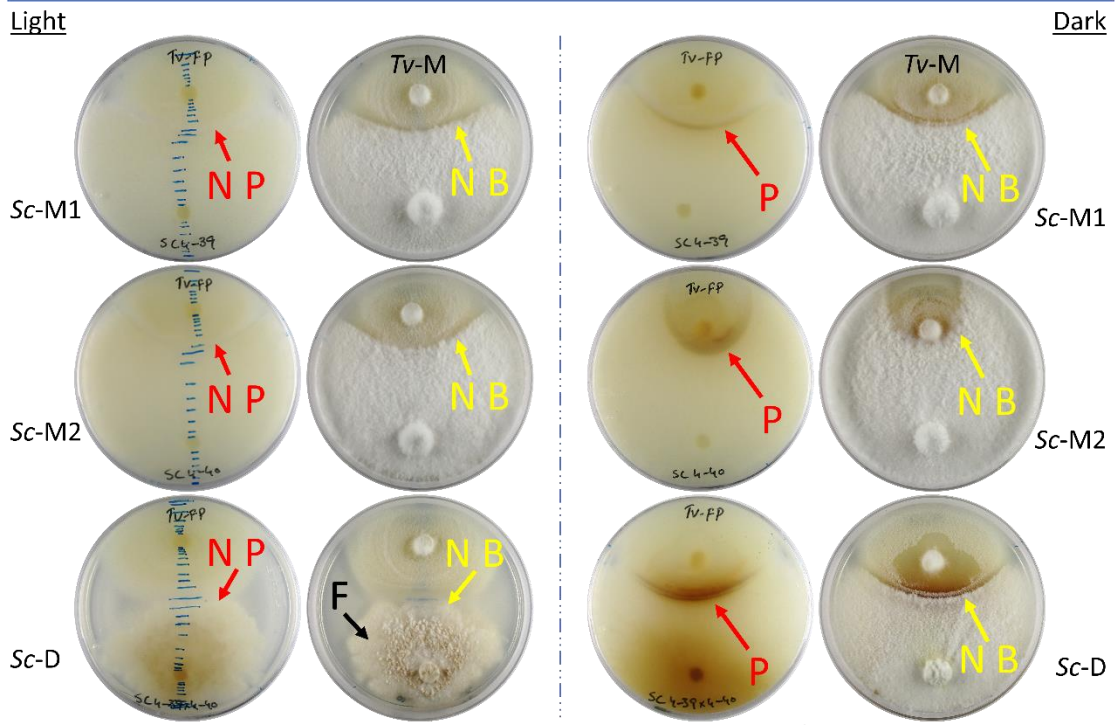
3.2.2 Dual interactions on artificial substrate

Interactions between the monokaryotic and dikaryotic strains of *T. versicolor* and *S. commune* were carried on *S. commune* minimal medium under light and dark conditions. In dual cultures on agar medium, deadlock, barrier formation and color reactions were observed at the regions of interactions between *T. versicolor* and *S. commune* (Figure 3-18A, B). Interactions of the *Tv-D* strain were started with deadlock on day 6 of incubation with both monokaryotic *S. commune* strains (*Sc-M1* and *Sc-M2*) but with the dikaryotic *S. commune* strain (*Sc-D*) on day 8 of incubation. Two days later, after an initial stage of barrage formation, the *Tv-D* strain grew over all three *S. commune* strains over the time as shown in Figure 3-18A. Broader barriers were formed by the *Tv-D* strain in the dark as compared to the light condition. Reactions involving dikaryons were usually stronger than those with monokaryons. Contrarily, deadlocks were formed between the interactions of the *Tv-M* strain with all three *S. commune* strains but no mycelial overlapping (barrage formation) was observed (Figure 3-18B). Like deadlocks, stoppages were observed in same strain dual inoculations of both species (Figure 3-18C - E).

T. versicolor (Tv-D) vs *S. commune* **A**



T. versicolor (Tv-M) vs *S. commune* **B**

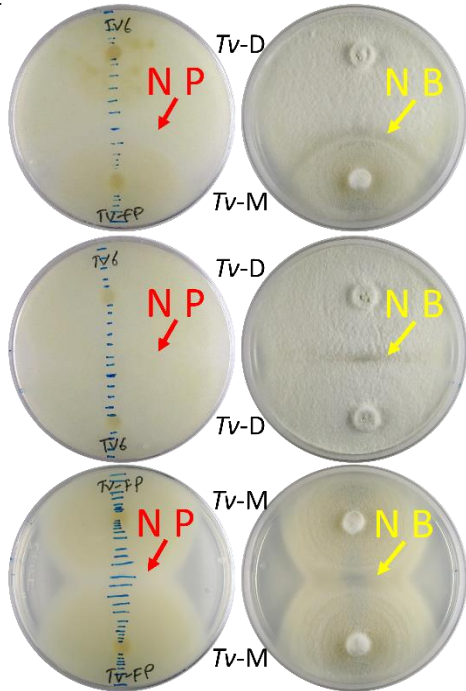


continue ---

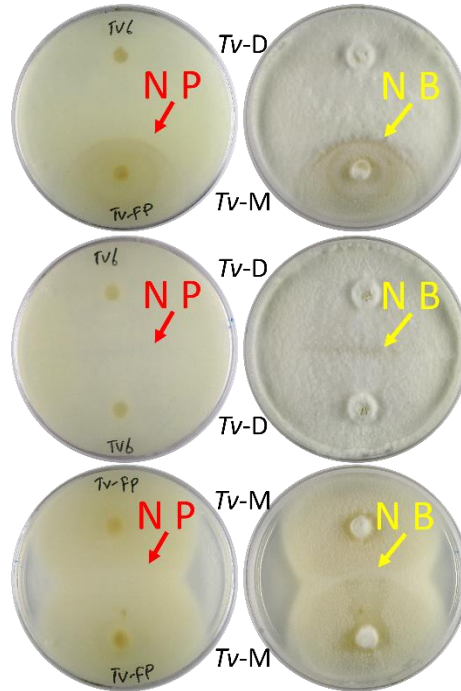
T. versicolor vs *T. versicolor*

C

Light



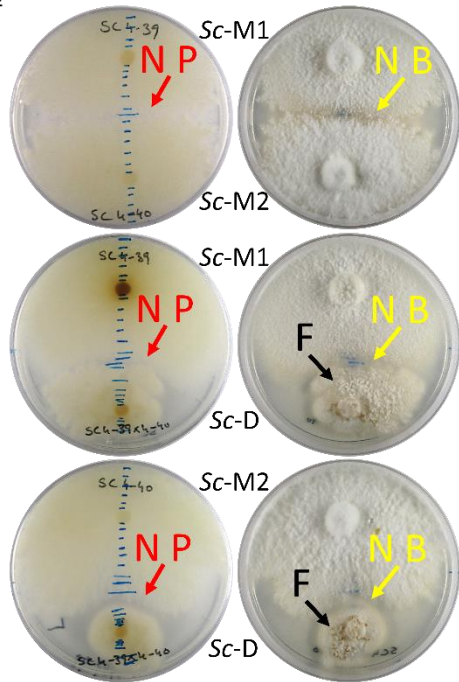
Dark



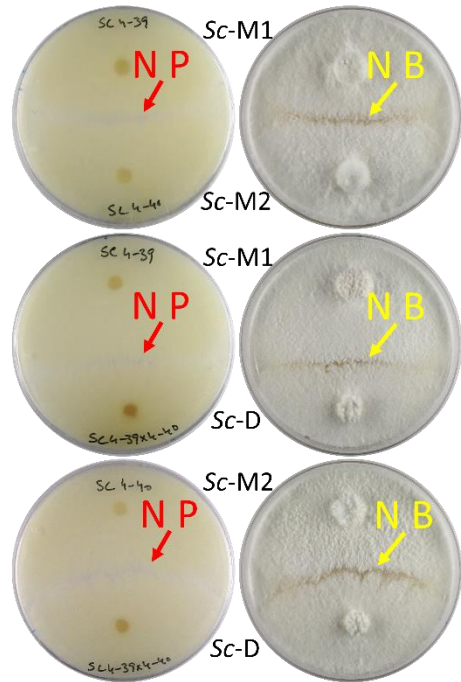
S. commune vs *S. commune*

D

Light



Dark



continue ---

S. commune vs *S. commune*

E

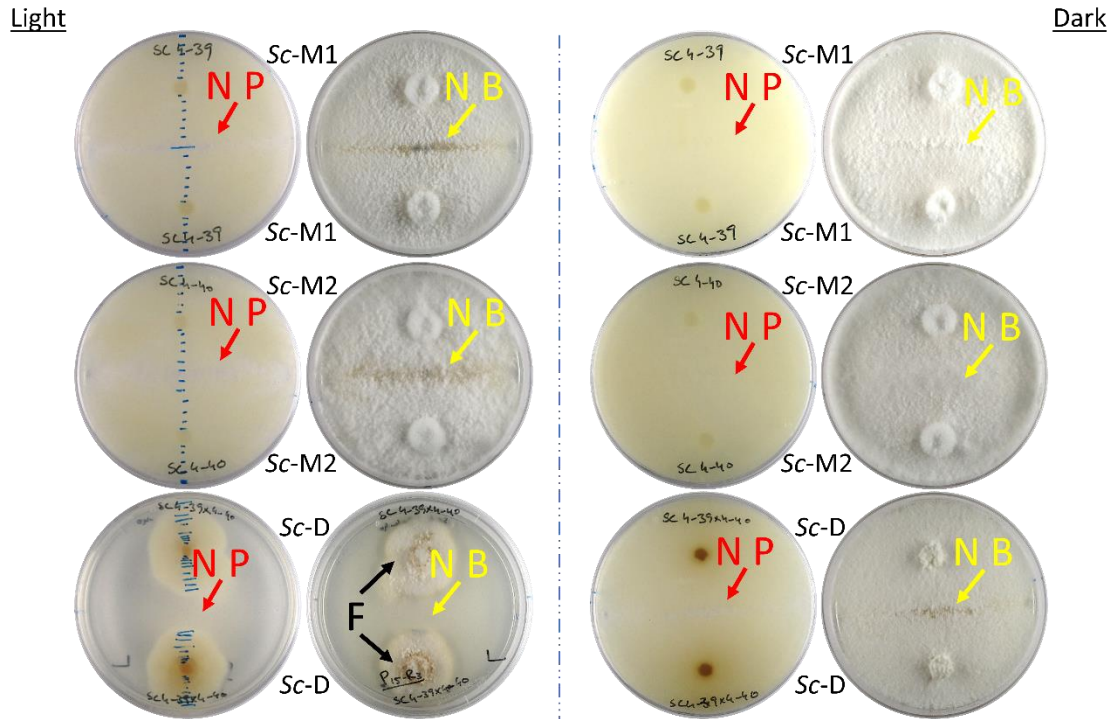


Figure 3-18 Intra- and interspecific interactions between mono- and dikaryotic strains of *T. versicolor* and *S. commune* on agar medium at 25 °C under light and dark conditions (12 days after inoculation). P – pigmentation, N P – no pigmentation, B – barrier formation, N B – no barrier formation, F – fruiting structures.

Interactions of *T. versicolor* and *S. commune* produced different types of pigmentations (blue, green, yellow and brown) with different intensities usually in the interaction region, but in the case of the *Sc-D* strain pigments produced underneath whole colonies while interacting with *T. versicolor* strains (*Tv-M* and *Tv-D*). The pigmentation colors were formed in the border regions and were lighter in the interactions of the *Tv-M* and *Tv-D* strains with the monokaryotic strains (*Sc-M1* and *Sc-M2*) whereas the dikaryotic strain (*Sc-D*) produced darker pigmentation in the border region (Figure 3-18A, B). Under the influence of light/dark condition, the light grown *Tv-D* strain gave pigmentation with all *S. commune* strains (in cases of *Sc-M1* and *Sc-M2* in the border region, and in case of *Sc-D* underneath its colony) but lighter as compared to dark grown samples. A thin layer of blue pigmentation was observed in the interaction of the *Tv-D* strain with the *Sc-*

M1 strain in the border region. But in the interaction of the *Tv*-D strain with the *Sc*-M2 and *Sc*-D strains, a thin layer of green pigmentation with multiple layers of brown and yellow pigmentations were observed in the border region (Figure 3-18A). In the interaction of the *Tv*-D strain with the *Sc*-D strain, pigmentation was produced underneath whole colony of *Sc*-D strain. In literature, blue pigments are identified as indigo (from *S. commune*; Miles et al. 1956), yellow belongs to carotenoids class, brown (melanin, Arun et al. 2015) and green (unknown; Krause et al. 2020).

On the contrary, under light, no pigmentation appeared when the *Tv*-M strain interacted with all *S. commune* strains. However, under dark conditions, light grey, light brown, and brown pigmentations were observed in the interactions of the *Tv*-M strain with the *Sc*-M1, and *Sc*-M2 strains in the interaction zone, respectively (Figure 3-18B). In the combat of *Tv*-M and *Sc*-D strains, pigmentation was produced in the border region and underneath whole colony of *Sc*-D strain. In same strain dual inoculations of both species, no pigmentation was observed (Figure 3-18C – E). Additionally, initial fruiting structures appeared in all cultures of the *S. commune* dikaryon (*Sc*-D) in light (Figure 3-18).

3.3 Medium-free pellets production

Pellets are aggregated spherical mycelial structures of filamentous fungi, forming in submerged culture. A protocol for medium-free pellets production was developed to use pellets as inoculum and inoculation for proteomic experiments. The pellets of two filamentous basidiomycete fungi, *S. commune* and *T. versicolor*, were produced in submerged culture from mycelial fragments because these fungi don't produce asexual spores.

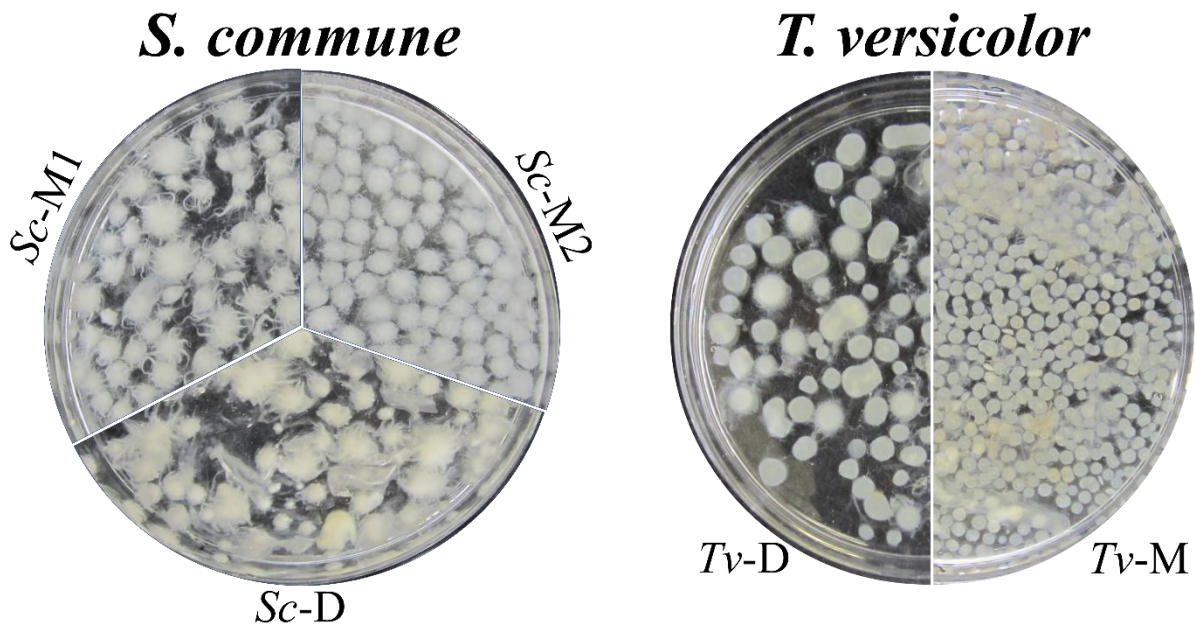


Figure 3-19 Comparison of medium-free pellets of the *S. commune* and *T. versicolor* monokaryotic and dikaryotic strains (after 7 days of incubation). The strains of *S. commune* were grown in liquid *S. commune* minimal medium and the strains of *T. versicolor* were grown in in liquid BSM medium. The flasks were incubated on a rotatory shaker with a speed of 120 rpm at 25 °C for 7 days.

The pellets were produced in submerged culture from hyphal fragments of the filamentous fungi. These pellets were separated from culture medium and washed with sterilized water to remove the medium contents. The obtained pellets were medium-free which were used as inoculum and stored at 4 °C for further use. The pellets of the *S. commune* monokaryotic and dikaryotic strains were variable in size but were comprised by a core region surrounded by a hairy region. The hairy region of the *Sc-M1* and *Sc-D* pellets were longer compared to the *Sc-M2* pellets (Figure 3-19). Contrarily, the pellets sizes of *T. versicolor* strains were not equal and did not possess a hairy region around the pellet core. Also, the size of *Tv-D* pellets was bigger than the *Tv-M* pellets (Figure 3-19).

3.4 Protein profiling of *T. versicolor* grown on beech wood

3.4.1 Comparison of extraction buffers for secretome isolation

For the comparison of the extraction buffers, autoclaved sapwood particles were inoculated with one medium-free pellet (grown on BSM medium) of *T. versicolor* (*Tv-D*), and incubated at 25 °C in dark for 10 days (see section 2.6.1 for details). Four extraction buffers (containing protease inhibitor) as described in Table 2-3 were used to extract the secretomes from the fresh fungus-wood samples (three biological replicates per buffer). The isolated proteins from the extraction buffers were separated according to their molecular weight and compared for protein concentration first using 1D-SDS-PAGE. The resolved bands in the 1D-SDS-PAGE gel represented the protein concentration for each extraction buffer. The number of visible bands were higher and the intensity stronger in protein extraction buffers 3 and 4 which indicated a higher number of proteins compared to buffers 1 and 2 (Figure 3-20). However, most of the protein bands were common with different intensity in the four protein extraction buffers as appeared in 1D gel.

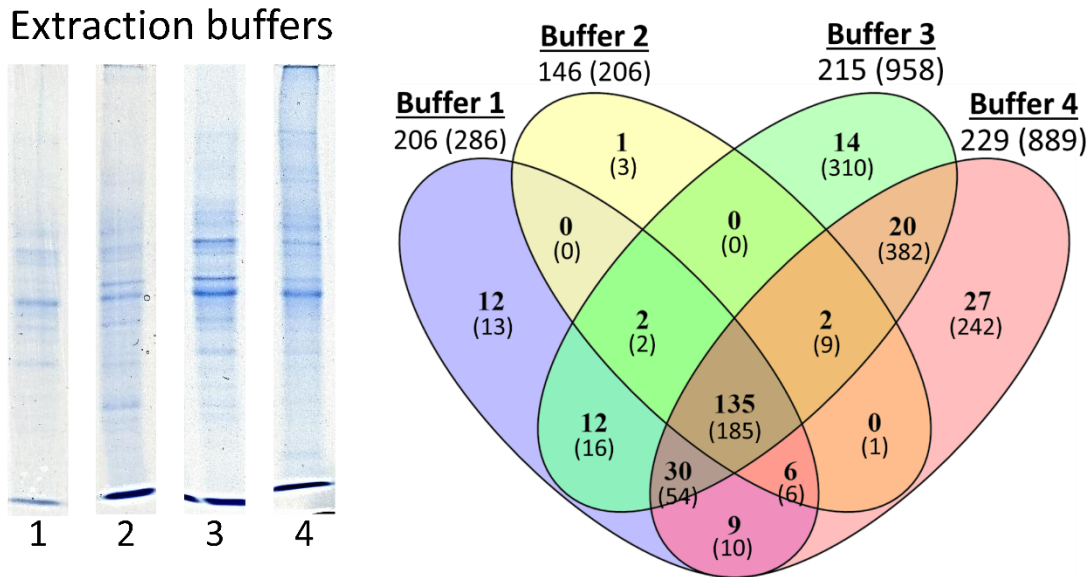


Figure 3-20 1D-SDS-PAGE gel and Venn diagram comparing secreted proteins isolated from *T. versicolor*-beech wood samples (10 days old samples). The values in parentheses are total proteins and without parentheses are proteins with signal peptide. *T. versicolor* (*Tv-D*) was grown on beech wood particles (inoculated with one medium-free pellet) and incubated in dark at 25 °C.

Afterwards, for protein identification and to confirm the quality of the four extraction buffers, the isolated proteins from the extraction buffers were digested by trypsin and the resulting peptides were analyzed by a high resolution TripleTOF 5600 (AB Sciex) mass-spectrometer. The identified proteins from MS/MS data reflected the findings that protein extraction buffers 3 and 4 were the buffers with the highest number of total proteins. From total identified proteins (286, 206, 958 and 889 from protein extraction buffers 1, 2, 3 and 4 respectively), 206, 146, 215 and 229 proteins with signal peptides were identified from *T. versicolor* with buffers 1, 2, 3 and 4, respectively (Figure 3-20, and Supplementary figure 1 - for the variation between three biological replicates), of which 135 were common among all. Numbers of contaminating intracellular proteins without signal peptides varied much between the samples while classes of these proteins were mostly shared between samples. In the experiment performed, buffer 1 was best for further secretome isolation with a low number of contaminating intracellular proteins (Figure 3-20, Venn diagram).

3.4.2 Comparing the secretome extraction buffers for 10- and 28- days old samples

For further validation and reliability of the protein extraction buffers results from 10 days old *T. versicolor* (*Tv*-D)-beech wood samples, the 28 days old samples (three biological replicates per buffer) were subjected for the isolation of secretomes with the buffers. From the 28 days old samples, protein extraction buffers 1, 2, 3 and 4 yielded 347, 752, 797 and 961 total proteins respectively as visualized in Figure 3-21 (Supplementary figure 2 - variation between three biological replicates). However, 217, 222, 248 and 277 proteins with signal peptide were identified from buffer 1, 2, 3 and 4 respectively. The buffer 4 had the highest number of proteins with signal peptide along with intracellular proteins followed by buffers 3 and 2. Conversely, the buffer 1 extracted a lower number of secreted proteins with low number of contaminating intracellular proteins in this experiment (Figure 3-20 and Figure 3-21).

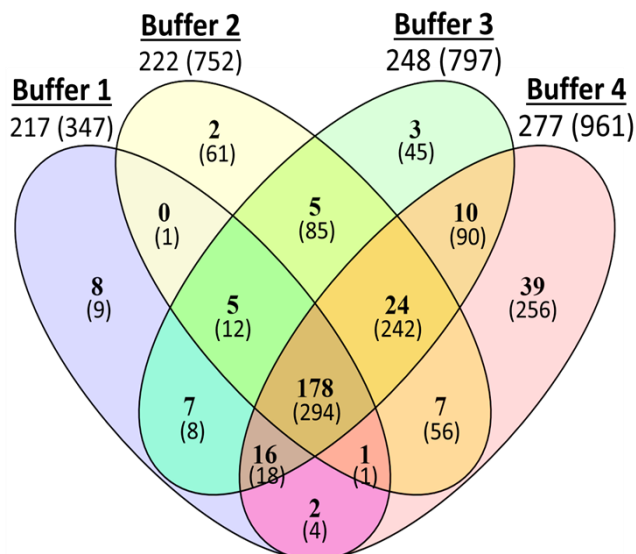


Figure 3-21 Venn diagram comparing secreted proteins isolated from 28 days old *T. versicolor*-beech wood samples. The *Tv*-D strain was grown on beech wood particles (inoculated with one medium-free pellet), and incubated in dark at 25 °C. (Numbers in brackets are total proteins, and numbers outside brackets are proteins with signal peptide).

In comparison of both extractions (from 10- and 28-days old samples), the buffers 3 and 4 were among the top protein isolating buffers in both extractions with the highest number of intracellular proteins which probably due to abrasive action of buffers on mycelium. The numbers of isolated proteins by the buffer 2 were different in 10 days and 28 days old samples, although each buffer had three biological replicates. Nevertheless, the buffer 1 extracted the lowest number of contaminating intracellular proteins in both extractions. Therefore, it was suggested that the buffer 1 was the optimum, stable and reliable buffer for secretome isolation.

3.4.3 Comparison of the *T. versicolor* (*Tv*-D) secretomes at early (10 days) and late (28 days) stages of decay

From the secretomes isolated by the buffer 1 from 10- and 28-days old *T. versicolor*-wood samples, 206 and 217 proteins with signal peptides were identified, respectively (Figure 3-21 and Figure 3-22). From total 240 proteins, 183 were common in both, while 23 were detected only from 10 days old secretome and 34 were exclusive to 28 days old secretome. Secreted proteins unique to the early decay (10 days) were categorized as laccases (3), proteins related to

carbohydrate metabolism (8), proteins of other functions (7), and proteins of unknown function (5). Chitinases (3), proteins related to carbohydrate metabolism (13), proteins of other functions (9), and proteins of unknown function (9) were only found in the late decay (28 days) secretome. The early decay samples contained a higher number of laccases with potential effects on lignin degradation while chitinases with possible functions in reuse of aged mycelium were unique to the older samples (Figure 3-22).

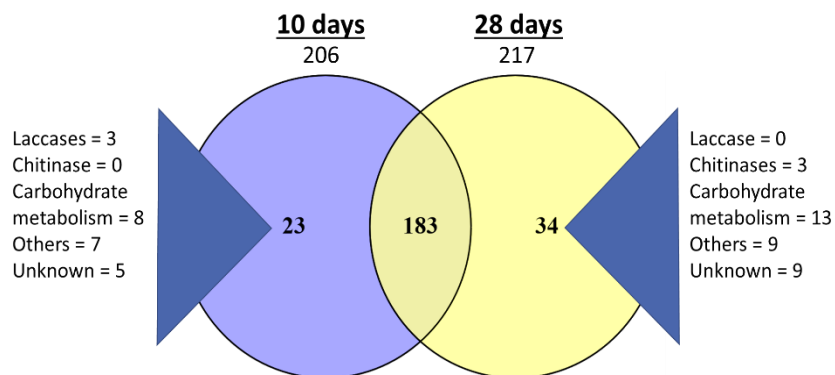


Figure 3-22 The *T. versicolor* (*Tv-D*) secretomes isolated at early (10 days) and late (28 days) stages of decay, grown on beech sapwood particles in dark at 25 °C.

T. versicolor secreted an exhaustive range of proteins with potential functions for the depolymerization of a three-dimensional biopolymer (wood). The 183 secreted proteins shared between 10- and 28-days were categorized into 9 functional groups after determining the probable role of each protein based on information obtained from the JGI, UniProt, NCBI, carbohydrate-active enzymes database (CAZy) and MEROPS databases. In line with a character of an aggressive white-rot fungus, approximately 13 % (23 proteins) of the total proteins possibly involved in lignin degradation, categorized as lignin-modifying enzymes. Possibly for the degradation of cellulose, hemicellulose and pectin, *T. versicolor* secreted about 13 % (24), 20 % (37) and 5 % (9) of the total proteins, respectively. For the categories of proteases and peptidases, chitinases and auxiliary activity (AA9; copper-dependent lytic polysaccharide monooxygenases), around 18 % (33), 4 % (7) and 3 % (6) proteins were found in the secretome, respectively. The 38 identified proteins (21 %) were secreted for miscellaneous functions categorized as others. Furthermore, in the secretome, 6 proteins (3 %) were identified with unknown function (Figure 3-23).

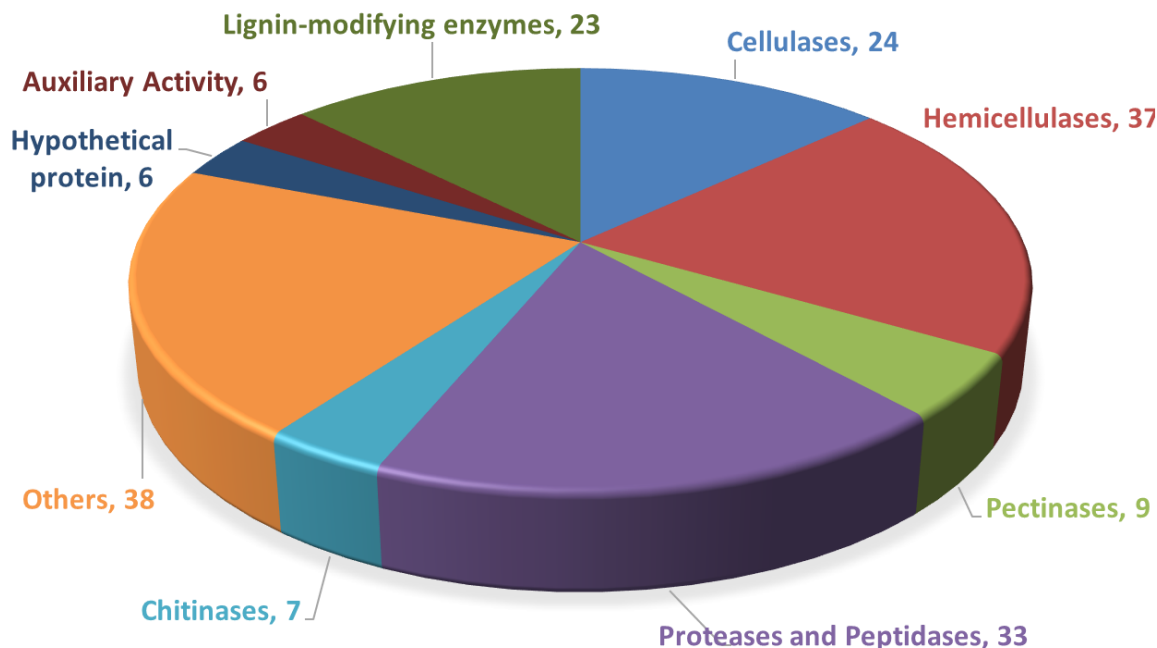


Figure 3-23 Classification of 183 secreted proteins shared between 10 and 28 days-old *T. versicolor*-beech wood samples. Dikaryotic *T. versicolor* strain (Tv-D) strain was grown on beech sapwood particles in dark at 25 °C.

3.4.3.1 Lignin-modifying enzymes

As *T. versicolor* is a wood-white rotting fungus, a wide range of enzymes were found in the secretome with the possible function in the breakdown of the complex aromatic heteropolymer, lignin. Six lignin peroxidases (LiP1, LiP2, LiP2s, LiP5, LiP9, and LiP10; EC 1.11.1.14; AA2), five manganese peroxidases (MnP1s, MnP2s, MnP3s, MnP5s and MnP6s; EC 1.11.1.13; AA2), one versatile peroxidase (VP2; EC 1.11.1.16; AA2), two laccases (TvLac3 and TvLac7; EC 1.10.3.2; AA1_1), five copper radical oxidases (AA5_1), two GMC oxidoreductases (AA3_2), and two proteins containing iron reductase domain (AA8-CBM1, AA8-AA3_1) were identified in the secretome of *T. versicolor* for the potential functions of the oxidative depolymerization of lignin (Table 3-2).

3.4.3.2 Cellulases

Likely for the complete depolymerization of cellulose, *T. versicolor* secreted several exoglucanases, endoglucanases and β -glucosidases. With the potential function to cut cellobiose from the reducing ends of cellulose, three cellulose 1,4- β -cellobiosidases (EC 3.2.1.176; GH7) were secreted. One cellulose 1,4- β -cellobiosidase (EC 3.2.1.91; GH6-CBM1) was found with the possible function to slice the non-reducing end of cellulose and to release cellobiose. Potentially for the depolymerization of the non-reducing ends from the cellulose chain, two glucan 1,4- α -glucosidases (EC 3.2.1.3; GH15-CBM20) were released by the fungus with possible function to hydrolyze successively the terminal (1 \rightarrow 4)-linked α -D-glucose units and produced β -D-glucose. Further, probably for the release of α -glucose from the non-reducing ends of (1 \rightarrow 3)- β -D-glucans, two glucan 1,3- β -glucosidases (EC 3.2.1.58; GH17 and GH55) were secreted likely for the hydrolysis of β -D-glucose units successively. In the category of endoglucanases, five endo- β -1,4-glucanases / cellulases (EC 3.2.1.4; GH5, GH10, and GH12) and one endo-1,3- β -glucanase (EC 3.2.1.39; GH16) were expressed by the fungus with possible functions to hydrolyze (1 \rightarrow 4)- β -D-glucosidic bonds and (1 \rightarrow 3)- β -D-glucosidic bonds in cellulose, respectively. Possibly for the release of terminal non-reducing β -D-glucose, seven β -glucosidases (EC 3.2.1.21; GH3) were identified. Besides these, *T. versicolor* also secreted three β -glucanases (GH131) of a broad specificity towards β -1,3, β -1,4 and β -1,6 glucosidic linkages which may act as endo- β -1,4-glucanase with exo- β -1,3/1,6-glucanase (Table 3-3).

Table 3-2 Identified enzymes with potential lignin-degrading activities in the dikaryotic *T. versicolor* (Tv-D) secretome shared between 10 and 28 days

JGI protein ID ^a	Putative protein function ^b	Family ^c	EC ^c	UP ^d (days)		<i>pI</i> ^e	<i>M_w</i> ^e
				10	28		
138261	Laccase (TvLac3)	AA1_1	1.10.3.2	16	9	5.09	55484.98
47314	Laccase (TvLac7)	AA1_1	1.10.3.2	4	2	6.04	56751.24
43576	Lignin peroxidase (LiP1)	AA2	1.11.1.14	78	60	4.88	39549.46
43578	Lignin peroxidase (LiP2)	AA2	1.11.1.14	67	77	4.4	38809.65
52333	Lignin peroxidase (LiP2s)	AA2	1.11.1.14	17	32	4.69	39547.28
134250	Lignin peroxidase (LiP5)	AA2	1.11.1.14	16	16	4.94	39367.28
134226	Lignin peroxidase (LiP9)	AA2	1.11.1.14	62	32	5.14	38866.76
134657	Lignin peroxidase (LiP10)	AA2	1.11.1.14	12	16	4.89	38878.82
51375	Manganese peroxidase (MnP1s)	AA2	1.11.1.13	5	3	4.44	37881.43
112835	Manganese peroxidase (MnP2s)	AA2	1.11.1.13	13	12	4.49	38360.91
131080	Manganese peroxidase (MnP3s)	AA2	1.11.1.13	18	6	4.93	37879.8
43477	Manganese peroxidase (MnP5s)	AA2	1.11.1.13	42	5	4.48	38168.85
51455	Manganese peroxidase (MnP6s)	AA2	1.11.1.13	22	5	5.06	38290.22
26239	Versatile peroxidase (VP2)	AA2	1.11.1.16	3	2	4.48	38147.82
115556	Copper radical oxidase	AA5_1	-	13	19	4.84	59386.57
116129	Copper radical oxidase	AA5_1	-	35	54	5.69	59108.58
117805	Copper radical oxidase	AA5_1	-	45	84	5.48	59963.48
118266	Copper radical oxidase	AA5_1	-	51	118	5.31	59998.3

130016	Copper radical oxidase	AA5_1	-	6	13	4.88	81435.55
122574	GMC oxidoreductase	AA3_2	-	4	12	5.29	64111.25
133945	GMC oxidoreductase	AA3_2	-	11	12	5.11	65362.5
	Iron reductase domain / carbohydrate-binding				4		
45408	module family 1 protein	AA8-CBM1	-	2		4.7	28123.47
73596	Iron reductase domain / GMC oxidoreductase	AA8, AA3_1	-	15	14	5.22	81404.96

^a with signal peptide (predicted with SignalP-5.0 database). ^b Putative function for identified proteins was obtained from the JGI, InterPro, UniProt and NCBI databases. ^c Carbohydrate-active enzymes database (CAZy) was used for the family information and for the enzyme commission number (EC number). ^d Unique peptides. ^e The theoretical *pI* (isoelectric point) and *M_w* (molecular weight) were computed based on protein sequence obtained from the JGI database.

Table 3-3 Identified enzymes with potential cellulose-degrading activities in the dikaryotic *T. versicolor* (Tv-D) secretome shared between 10 and 28 days

JGI protein ID ^a	Putative protein function ^b	Family ^c	EC ^c	UP ^d (days)		pI ^e	Mw ^e
				10	28		
Exoglucanases							
112163	Cellulose 1,4- β -cellobiosidase (reducing end)	GH7	3.2.1.176	29	77	4.6	49047.18
125941	Cellulose 1,4- β -cellobiosidase (reducing end)	GH7	3.2.1.176	29	52	4.87	48878.07
124366	Cellulose 1,4- β -cellobiosidase (reducing end)	GH7	3.2.1.176	5	8	4.43	48813.73
63826	Cellulose 1,4- β -cellobiosidase (non-reducing end)	GH6, CBM1	3.2.1.91	34	149	5.12	47341.99
37357	Glucan 1,4- α -glucosidase	GH15, CBM20	3.2.1.3	22	21	4.93	61189.81
54963	Glucan 1,4- α -glucosidase	GH15, CBM20	3.2.1.3	21	21	4.95	61300.74
62730	Glucan 1,3- β -glucosidase	GH17	3.2.1.58	6	17	5.36	40216.33
34683	Glucan 1,3- β -glucosidase	GH55	3.2.1.58	3	5	6.18	81149.78
Endoglucanases							
150608	Endo- β -1,4-glucanase / cellulase	GH5_5, CBM1	3.2.1.4	4	11	5.08	40672.63
151848	Endo- β -1,4-glucanase / cellulase	GH5_5, CBM1	3.2.1.4	7	54	4.57	43858.73
68212	Endo- β -1,4-glucanase / cellulase	GH5_7	3.2.1.4	6	5	5.64	48779.73
33948	Endo- β -1,4-glucanase / cellulase	GH10	3.2.1.4	11	3	6.08	37673.81
136117	Endo- β -1,4-glucanase / cellulase	GH12	3.2.1.4	5	8	5.17	26144.93
134721	Endo-1,3- β -glucanase	GH16	3.2.1.39	6	6	6.02	33748.08
β-glucosidases							
49760	β -glucosidase	GH3	3.2.1.21	7	7	5.27	94577.86
55634	β -glucosidase	GH3	3.2.1.21	5	9	5.86	76588.16

67879	β -glucosidase	GH3	3.2.1.21	6	8	6.13	83898.58
	β -glucosidase; carbohydrate-binding module				22		
68557	family 1 / glycoside hydrolase family 3 protein	GH3, CBM1	3.2.1.21	15		5.93	85398.53
70471	β -glucosidase	GH3	3.2.1.21	9	12	5.2	86982.53
132011	β -glucosidase	GH3	3.2.1.21	7	8	5.89	83851.56
170938	β -glucosidase	GH3	3.2.1.21	23	27	5.16	95750.9
Broad specificity glucanases							
	Glycoside hydrolase family 131 / carbohydrate-				9		
46975	binding module family 1 protein	GH131, CBM1	-	5		5.06	34947.8
62247	Glycoside hydrolase family 131 protein	GH131	-	4	4	6.27	27625.93
175614	Glycoside hydrolase family 131 protein	GH131	-	9	30	5.12	33680.76

^a with signal peptide (predicted with SignalP-5.0 database). ^b Putative function for identified proteins was obtained from the JGI, InterPro, UniProt and NCBI databases. ^c Carbohydrate-active enzymes database (CAZy) was used for the family information and for the enzyme commission number (EC number). ^d Unique peptides. ^e The theoretical *pI* (isoelectric point) and *M_w* (molecular weight) were computed based on protein sequence obtained from the JGI database.

3.4.3.3 Hemicellulases

The wood fraction hemicellulose comprises of main and side chains of diverse kinds of heteropolymers. Arabinoxylan, glucomannan, glucuronoxylan, xylan, and xyloglucan are some of the important hemicelluloses. Therefore, *T. versicolor* secreted a broad range of hemicellulases for the rigorous action on linear and branched hemicelluloses. From the 37 hemicellulases, three endo-1,4- β -xylanases (EC 3.2.1.8; GH10) were identified to possibly cleave xylans. To likely cleave mannans and associated polymers, one β -mannosidase (EC 3.2.1.25; GH2), three α -1,2-mannosidases (GH92), one mannan endo-1,4- β -mannosidase (EC 3.2.1.78; GH5), one exo- α -1,6-mannosidase (GH125), and one mannosyl-oligosaccharide 1,2- α -mannosidase (EC 3.2.1.113; GH47) were found in the secretome. Two α -galactosidases (EC 3.2.1.22; GH27), two β -galactosidases (EC 3.2.1.23; GH35), two glucan 1,3- β -glucosidases (EC 3.2.1.58; GH5), one galactan 1,3- β -galactosidase (EC 3.2.1.145; GH43), one galactan endo-1,6- β -galactosidase (EC 3.2.1.164, GH30), and one α -L-arabinofuranosidase (EC 3.2.1.55; GH51) were produced to possibly act on other mannan-type polysaccharides (glucomannan, and galactomannan, etc.). Moreover, seven carboxylesterases (EC 3.1.1.1; CE1), three acetylerases (EC 3.1.1.6; CE16), and one non-reducing end feruloyl esterase (EC 3.1.1.73; CE1) were produced to probably act on sides chains. Additionally, one protein member of GH10, GH72, GH74 and GH115 family protein and three members from CE1 were identified in the secretome (Table 3-4).

3.4.3.4 Pectinases

Possibly for the degradation of a complex and branched polymer of pectin, *T. versicolor* secreted two endo-polygalacturonases (EC 3.2.1.15; GH28), one galacturan 1,4- α -galacturonidase (EC 3.2.1.67; GH28), one rhamnogalacturonase (EC 3.2.1.171; GH28) which probably cleaved the main chain of pectin. Two pectinesterases (EC 3.1.1.11; CE8), two α -L-rhamnosidases (EC 3.2.1.40; GH78), and one β -L-arabinofuranosidase (EC 3.2.1.185; GH127) were released to possibly slice side groups (Table 3-5).

3.4.3.5 Proteases and peptidases

In the *T. versicolor* secretome, 7 aspartic peptidases, 6 metallo peptidases, 19 serine peptidases and 1 other peptidase were found. Seven proteins of aspartic peptidases group were from family A1, included three acid proteases, one aspartyl protease, one aspergillopepsin (EC 3.4.23.18), one saccharopepsin (EC 3.4.23.25) and one polyporopepsin (EC 3.4.23.29). From

metallo peptidases group, two Zn-dependent exopeptidases (M28), one leucine aminopeptidase-1 (EC 3.4.11.1; M28) and three fungalysins (M36) were found in the secretome. Seven serine carboxypeptidases (S10), two lysosomal Pro-X carboxypeptidases (EC 3.4.16.2; S28), one member of family S41, one C-terminal processing peptidase-like protein (S41A), and eight tripeptidyl-peptidases I (EC 3.4.14.9; S53) belonged to serine peptidases group. Furthermore, one peptide N-acetyl- β -D-glucosaminyl asparaginase amidase-A was also identified from the *T. versicolor* secretome (Supplementary table 1).

3.4.3.6 Other secreted proteins

Five lytic polysaccharide monooxygenases (LPMOs) of AA9 family and one member of carbohydrate-binding module 1 (CBM1) were identified in the *T. versicolor* secretome (Table 3-6). Likely for the degradation of chitin, three chitinases (EC 3.2.1.14; GH18) and four β -N-acetylhexosaminidases (EC 3.2.1.52; GH20) were found in the secretome (Table 3-6). The 38 identified proteins were detected to be involved in various functions (Supplementary table 2). Moreover, six proteins of unknown function were also found in the secretome (Supplementary table 20).

Table 3-4 Identified enzymes with potential hemicellulose-degrading activities in the dikaryotic *T. versicolor* (Tv-D) secretome shared between 10 and 28 days

JGI protein ID ^a	Putative protein function ^b	Family ^c	EC ^c	UP ^d (days)		pI ^e	Mw ^e
				10	28		
Main chain							
154147	Endo-1,4- β -xylanase	GH10	3.2.1.8	8	16	5.2	38764.96
38102	Endo-1,4- β -xylanase	GH10, CBM1	3.2.1.8	22	55	4.99	42541.04
48717	Endo-1,4- β -xylanase	GH10, CBM1	3.2.1.8	8	14	4.92	43305.6
61724	β -mannosidase	GH2	3.2.1.25	12	54	4.62	105255.35
Side chain							
159574	α -galactosidase	GH27	3.2.1.22	3	9	5.01	47537.33
60477	α -galactosidase	GH27	3.2.1.22	2	13	5.06	48191.45
37024	β -galactosidase	GH35	3.2.1.23	12	19	5.63	109089.91
75316	β -galactosidase	GH35	3.2.1.23	7	19	5.82	110304.6
59914	Non-reducing end α -L-arabinofuranosidase	GH51	3.2.1.55	22	36	5.43	68935.97
148125	Glucan 1,3- β -glucosidase	GH5_15	3.2.1.58	8	12	5.25	51527.26
25402	Glucan 1,3- β -glucosidase	GH5_9	3.2.1.58	9	9	5.42	46753.04
	Mannan endo-1,4- β -mannosidase / carbohydrate-binding module family 1				9		
161823		GH5_7, CBM1	3.2.1.78	3		4.85	46728.67
145953	Galactan 1,3- β -galactosidase	GH43, CBM35	3.2.1.145	9	12	5.66	47141.49
66957	Galactan endo-1,6- β -galactosidase	GH30	3.2.1.164	26	30	6.04	51572.55
	Glycoside hydrolase family 72 / carbohydrate-binding module family 43 protein				6		
68341		GH72, CBM43	-	2		4.56	82932.29
49304	Glycoside hydrolase family 115 protein	GH115	-	37	46	5.4	110788.05
115416	Exo- α -1,6-mannosidase	GH125	-	5	9	5.37	55880.75
51358	Feruloyl esterase-like protein	CE1	3.1.1.73	7	19	5.64	58439.67
109109	Carboxylesterase	CE1	3.1.1.1	26	62	5.35	53375.75
41392	Carboxylesterase	CE1	3.1.1.1	21	21	6.56	59200.19
47993	Carboxylesterase	CE1	3.1.1.1	14	12	5.62	58099.27

48030	Carboxylesterase	CE1	3.1.1.1	12	14	5.3	58130.2
68896	Carboxylesterase	CE1	3.1.1.1	18	4	4.82	57630.98
72294	Carboxylesterase	CE1	3.1.1.1	10	30	6.03	58239.61
164970	Carboxylesterase	CE1	3.1.1.1	10	8	4.94	58449.99
168624	Acetylesterase	CE16	3.1.1.6	18	23	5.42	34478.06
70662	Acetylesterase	CE16	3.1.1.6	7	5	5.75	32924.23
39742	Acetylesterase	CE16, CBM1	3.1.1.6	4	5	4.73	37502.73
Others							
	Carbohydrate-binding module family 1 / glycoside hydrolase family 10 protein				35		
144893		GH10, CBM1	-	18		6.99	39805.73
	Carbohydrate-binding module family 1 / glycoside hydrolase family 74 protein				27		
112178		GH74, CBM1	-	15		5.27	87540.26
131501	Mannosyl-oligosaccharide 1,2- α -mannosidase	GH47	3.2.1.113	50	51	4.83	59763.96
40820	α -1,2-mannosidase	GH92	-	13	28	5.37	90473.76
43566	α -1,2-mannosidase	GH92	-	12	13	5.25	90600.5
75494	α -1,2-mannosidase	GH92	-	7	30	5.02	89434.49
	Carbohydrate-binding module family 1 / carbohydrate esterase family 1 protein				18		
141077		CE1, CBM1	-	8		5.69	38718.45
	Carbohydrate-binding module family 1 / carbohydrate esterase family 1 protein				13		
43877		CE1, CBM1	-	10		7.03	37537.74
130597	Carboxylesterase and related proteins	-	-	28	29	6.11	73329.11

^a with signal peptide (predicted with SignalP-5.0 database). ^b Putative function for identified proteins was obtained from the JGI, InterPro, UniProt and NCBI databases. ^c Carbohydrate-active enzymes database (CAZy) was used for the family information and for the enzyme commission number (EC number). ^d Unique peptides. ^e The theoretical *pI* (isoelectric point) and *M_w* (molecular weight) were computed based on protein sequence obtained from the JGI database.

Table 3-5 Identified enzymes with potential pectin-degrading activities in the dikaryotic *T. versicolor* (Tv-D) secretome shared between 10 and 28 days

JGI protein ID ^a	Putative protein function ^b	Family ^c	EC ^c	UP ^d (days)		<i>pI</i> ^e	<i>Mw</i> ^e
				10	28		
Main chain							
52416	Endo-polygalacturonase	GH28	3.2.1.15	4	7	5.9	37582.77
24492	Endo-polygalacturonase	GH28	3.2.1.15	2	7	6.09	45375.08
131837	Galacturan 1,4- α -galacturonidase (exo-polygalacturonase)	GH28	3.2.1.67	2	6	4.84	43440.4
72935	Rhamnogalacturonase	GH28	3.2.1.171	3	2	6.62	46299.15
Side chain							
175476	Pectinesterase	CE8	3.1.1.11	3	10	4.99	42034.25
68175	Pectinesterase	CE8	3.1.1.11	2	3	7.32	32614.4
151427	α -L-rhamnosidase	GH78	3.2.1.40	5	24	6.09	70505.32
55703	α -L-rhamnosidase	GH78	3.2.1.40	11	28	5.83	71346.05
28809	β -L-arabinofuranosidase	GH127	3.2.1.185	11	28	5.49	72304.78

^a with signal peptide (predicted with SignalP-5.0 database). ^b Putative function for identified proteins was obtained from the JGI, InterPro, UniProt and NCBI databases. ^c Carbohydrate-active enzymes database (CAZy) was used for the family information and for the enzyme commission number (EC number). ^d Unique peptides. ^e The theoretical *pI* (isoelectric point) and *Mw* (molecular weight) were computed based on protein sequence obtained from the JGI database.

Table 3-6 Identified enzymes with potential activities as auxiliary activity enzymes and chitinases in the dikaryotic *T. versicolor* (Tv-D) secretome shared between 10 and 28 days

JGI protein ID ^a	Putative protein function ^b	Family ^c	EC ^c	UP ^d (days)		<i>pI</i> ^e	<i>Mw</i> ^e
				10	28		
Auxiliary activity enzymes							
162601	Lytic polysaccharide monooxygenase (formerly GH61)	AA9	-	10	15	7.11	24775.8
36998	Lytic polysaccharide monooxygenase (formerly GH61)	AA9	-	4	3	4.87	24695.69
51004	Lytic polysaccharide monooxygenase (formerly GH61)	AA9	-	10	7	5.42	28371.04
71674	Lytic polysaccharide monooxygenase (formerly GH61) / Carbohydrate-Binding Module Family 1 protein	AA9-CBM1	-	2	2	5.32	33123.33
143379	Lytic polysaccharide monooxygenase (formerly GH61) / carbohydrate-binding module family 1 protein	AA9-CBM1	-	4	4	4.83	32733.53
133420	Carbohydrate-binding module family 1 protein	CBM1	-	2	6	4.5	25655.4
Chitinases							
68104	β -N-acetylhexosaminidase	GH20	3.2.1.52	10	13	5.2	77083.52
135976	β -N-acetylhexosaminidase	GH20	3.2.1.52	15	14	5.48	59409.98
175547	β -N-acetylhexosaminidase	GH20	3.2.1.52	11	3	5.78	59281.88
60488	β -N-acetylhexosaminidase	GH20	3.2.1.52	17	18	5.37	61531.79
72257	Chitinase	GH18	3.2.1.14	9	6	5.65	36557.28
158931	Chitinase; glycoside hydrolase family 18 / carbohydrate-binding module family 5 protein	GH18, CBM5	3.2.1.14	2	3	5.15	51379.75
73594	Chitinase; glycoside hydrolase family 18 / carbohydrate-binding module family 5 protein	GH18, CBM5	3.2.1.14	10	2	5.7	55766.14

^a with signal peptide (predicted with SignalP-5.0 database). ^b Putative function for identified proteins was obtained from the JGI, InterPro, UniProt and NCBI databases. ^c Carbohydrate-active enzymes database (CAZy) was used for the family information and for the enzyme commission number (EC number). ^d Unique peptides. ^e The theoretical *pI* (isoelectric point) and *Mw* (molecular weight) were computed based on protein sequence obtained from the JGI database.

3.4.4 Intracellular proteins of *T. versicolor* (Tv-D) grown on beech wood

After the extraction of secretomes from 28 days old fungus wood samples by four extraction buffers (Table 2-3), the remaining samples were processed (as described above in section 2.9) for intracellular protein profiling. From buffer 1, 2, 3 and, 4, total identified proteins were 1399, 1405, 1252, and 1282, respectively (Figure 3-24, and Supplementary figure 3 - Venn diagrams with overlaps and differences between three biological replicates per buffer).

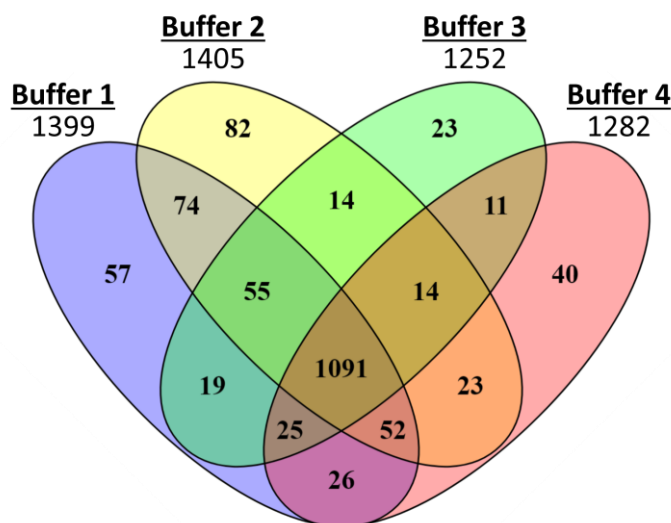


Figure 3-24 Venn diagram comparing numbers of identified intracellular proteins isolated from 28 days old *T. versicolor*-beech wood samples after the extraction of secretomes with four buffers. Dikaryotic *T. versicolor* strain (Tv-D) was grown on beech wood particles (inoculated with one medium-free pellet) and incubated in dark at 25 °C. Numbers are total identified proteins.

As described in section 3.4 above, buffer 1 is possibly the best for the isolation of secretome in the experiment performed, the remaining samples from buffer 1 were further analyzed for the intracellular protein profiling (Venn diagram comparing total identified proteins in three biological replicates - Supplementary figure 3A). The identified proteins were categorized according to their potential functions to identify the possible active metabolic pathways in various cellular functions of the fungus while growing on wood. The potential role of each protein was obtained from the JGI, UniProt, NCBI, carbohydrate-active enzymes database (CAZy) and MEROPS databases.

From the total identified proteins (1399), about 9% (128 proteins) belonged potentially to carbohydrate metabolism, 1% (17) to metabolism of complex carbohydrates, 8% (116) to amino acid metabolism, 3% (40) to nucleotide metabolism, 4% (51) to lipid metabolism, 1% (14) to metabolism of complex lipids, 6% (85) to energy metabolism, 25% (356) to cellular processes and signaling, 4% (58) to protein biosynthesis, 4% (55) to structural proteins, 1% (9) to inorganic ion transport and metabolism, 4% (55) to biodegradation of xenobiotics, 2% (22) to biosynthesis of secondary metabolites, 1% (19) to metabolism of cofactors and vitamins, 4% (54) to proteases and peptidases, 6% (80) to hypothetical protein, and 17% (240) to proteins with other functions (Figure 3-25).

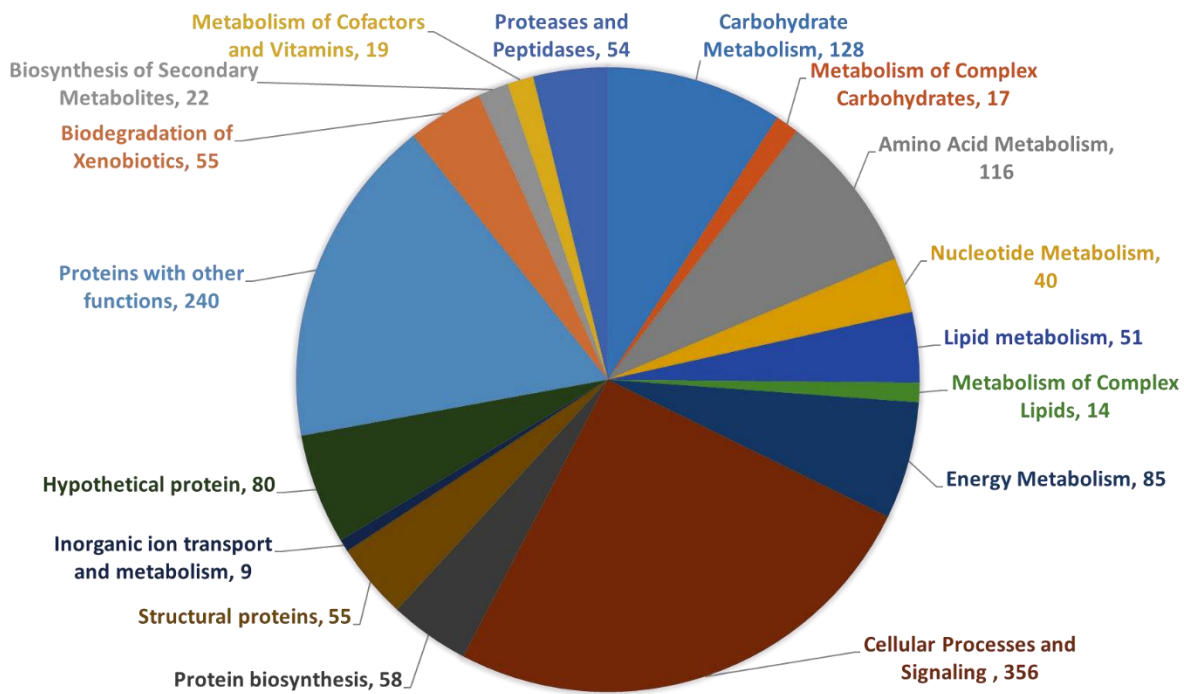


Figure 3-25 Classification of intracellular proteins from 28 days-old *T. versicolor*-beech wood samples Dikaryotic *T. versicolor* strain (*Tv*-D) was grown on beech sapwood particles in dark at 25 °C.

In the carbohydrate metabolism, the identified proteins were probably involved in 16 pathways (Supplementary table 3) i.e., ascorbate and aldarate metabolism (1 protein), butanoate metabolism (2), carbohydrate transport and metabolism (11), citrate cycle (TCA cycle) (22),

fructose and mannose metabolism (11), galactose metabolism (4), glycolysis/gluconeogenesis (32), glyoxylate and dicarboxylate metabolism (6), proteins with other functions (11), pentose and glucuronate interconversions (11), pentose phosphate pathway (8), propanoate metabolism (1), and pyruvate metabolism (7). In addition to these, proteins with potential functions in aminosugars metabolism (3 proteins), N-glycans biosynthesis (5), and starch and sucrose metabolism (9) were identified (Supplementary table 4 - metabolism of complex carbohydrates).

In the group of amino acid metabolism, the identified proteins were possibly active in various pathways (Supplementary table 5) i.e., alanine and aspartate metabolism (3 proteins), arginine and proline metabolism (4), cysteine metabolism (1), glutamate metabolism (1), glycine, serine and threonine metabolism (16), histidine metabolism (4), lysine biosynthesis (8) and degradation (2), methionine metabolism (4), phenylalanine, tyrosine and tryptophan biosynthesis (7), tryptophan metabolism (16), tyrosine metabolism (5), valine, leucine and isoleucine biosynthesis (8), valine, leucine and isoleucine degradation (5), urea cycle and metabolism of amino groups (6), and amino acid transport and metabolism (26). From 40 proteins potentially involved in the nucleotide metabolism (Supplementary table 6), 20 proteins were possibly participating in purine metabolism, 13 proteins in pyrimidine metabolism, and 7 proteins in nucleotide transport and metabolism.

Potentially, for the metabolisms of lipids (Supplementary table 7) and complex lipids (Supplementary table 8), the following pathways were found active; fatty acid metabolism (22 proteins), lipid transport and metabolism (24), sterol biosynthesis (2), synthesis and degradation of ketone bodies (3), glycerolipid metabolism (8), inositol phosphate metabolism (2), phospholipid degradation (1), prostaglandin and leukotriene metabolism (1), and sphingoglycolipid metabolism (2). Possibly in the energy metabolism (Supplementary table 9), proteins with potential functions of ATP synthesis (13 proteins), energy production and conversion (50), nitrogen metabolism (9), and oxidative phosphorylation (13) were detected.

Likely, for the cellular processes and signaling (Supplementary table 10), aminoacyl-tRNA biosynthesis (21 proteins), intracellular trafficking, secretion, and vesicular transport (92), posttranslational modification, protein turnover, chaperones (94), replication, recombination and repair (1), RNA processing and modification (46), signal transduction mechanisms (67),

transcription (2), and translation, ribosomal structure and biogenesis (33) were produced by the fungus.

With the potential functions in the biodegradation of xenobiotics (Supplementary table 11), the identified proteins were possibly involved in the following pathways; 1,4-Dichlorobenzene degradation (3 proteins), 2,4-Dichlorobenzoate degradation (5), atrazine degradation (1), benzoate degradation via CoA ligation (7), benzoate degradation via hydroxylation (1), gamma-hexachlorocyclohexane degradation (9), glutathione metabolism (21), nitorobenzene degradation (3), and miscellaneous proteins with different functions (5). In the biosynthesis of secondary metabolites (Supplementary table 12), pathways for betalain biosynthesis (1 protein), flavonoids, stilbene and lignin biosynthesis (6), terpenoid biosynthesis (2), and proteins with other functions (13) were detected.

For metabolism of cofactors and vitamins (Supplementary table 13), possibly active pathways were biotin metabolism (1 protein), folate biosynthesis (1), nicotinate and nicotinamide metabolism (3), pantothenate and CoA biosynthesis (1), riboflavin metabolism (5), thiamine metabolism (3), and proteins with other functions (5). Potentially 13 (chromatin structure and dynamics), and 42 (cytoskeleton) proteins were found as structural proteins (Supplementary table 14). 40S ribosomal (24 proteins), 60S ribosomal (34) proteins were found to probably be involved in protein biosynthesis (Supplementary table 15). Besides these proteins, 9 proteins were identified to likely act in inorganic ion transport and metabolism (Supplementary table 16). Potentially, 55 proteases and peptidases (Supplementary table 17), 240 proteins with other functions (Supplementary table 18), and 80 proteins with unknown function (hypothetical protein - Supplementary table 19) were identified in the samples.

3.5 Secretome of *S. commune* grown on beech wood

Secretomic analysis of *S. commune* grown on beech sapwood particles was performed using nanoLC-MS/MS to understand the decay of different components of wood. 3-partitions Petri dishes filled with beech sapwood particles (as shown in Figure 2-1) and inoculated with the Sc-M1 strain (the strain was selected because of fast growth compared to the dikaryon) were used to determine the *S. commune* secretome from 2 weeks grown samples. To grasp better the *S. commune* wood decay mechanism, the identified proteins in three biological replicates were combined due to variation in numbers of identified proteins. Total proteins 539, 108 and 466, and proteins with signal peptide 177, 60, and 157 were identified in the three replicates R1 to R3, respectively (Supplementary figure 4). This variation in the biological replicates may be due to polysaccharides produced by *S. commune* in substrate, which probably trapped the secreted proteins and made protein isolation difficult. (Own observations: in the process of protein purification of *S. commune* samples grown on wood, a transparent clot has been observed. *S. commune* produces polysaccharides while growing on wood and in liquid cultures. Therefore, this transparent clot is possibly a polysaccharide clot, which can create hurdle in protein isolation. Similar has been described by Fragner et al. (2009), extracellular polysaccharides creates a mucilagous layer around the fungal hyphae).

Potential functions of the identified proteins revealed the extracellular enzymes possibly involved in the degradation of lignocellulose. According to putative function categorization, approximately 8 % (16 proteins) cellulases, 11 % (22) hemicellulases, 17 % (33) pectinases, 7 % (13) auxiliary activities enzymes, 1 % (2) lipases, 5 % (9) chitinases, 1 % (2) amylases, 18 % (35) proteases and peptidases, 24 % (47) others (miscellaneous) proteins, 3 % (6) DUF (proteins with domain of unknown function) proteins, and 6 % (12) uncharacterized proteins were found in the secretome (Figure 3-26).

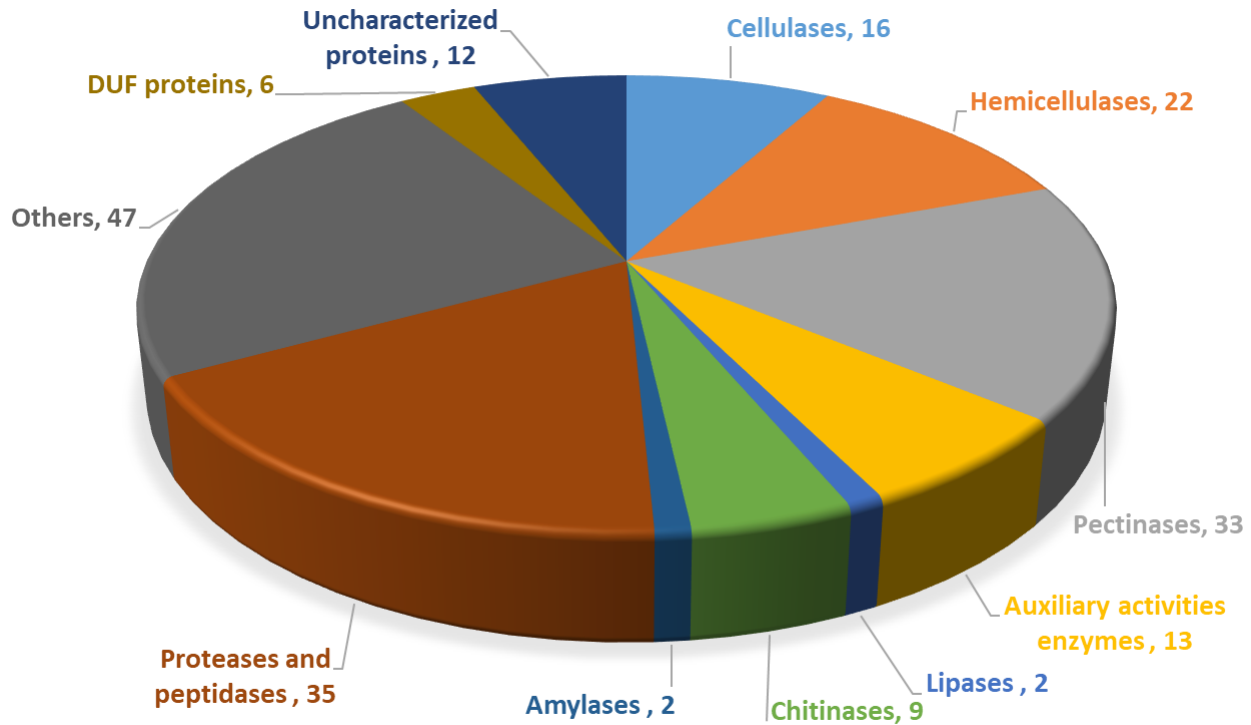


Figure 3-26 Functional distribution of identified proteins from the *S. commune* secretome. Monokaryotic *S. commune* strain (*Sc*-M1) was grown on beech wood particles for 2 weeks at 25 °C in dark. (DUF proteins = proteins with domain of unknown function).

S. commune produced all three types of enzymes necessary for the complete degradation of cellulose to glucose (Table 3-7). *S. commune* secreted four exoglucanases (GH6 - 3.2.1.91, GH7 - 3.2.1.176, and GH131) which possibly cleaved the nonreducing or reducing end of the cellulose chain. Likely to cut randomly internal bonds in the cellulose polymer, processive/non-processive three endoglucanases (endo- β -1,4-glucanase - 3.2.1.4 - GH5) were identified. Finally, nine β -glucosidases (two belongs to GH1 - 3.2.1.21, and seven to GH3 - 3.2.1.21) were released in substrate by *S. commune*, which potentially converted cellobiose and cello-oligosaccharides to glucose.

Table 3-7 Identified enzymes with potential cellulose-degrading activities in the monokaryotic *S. commune* (Sc-M1) secretome on beech sapwood after 2 weeks of incubation

JGI protein ID ^a	SignalP ^b	Putative protein function ^c	Family ^d	EC ^d	UP ^e	<i>pI</i> ^f	<i>Mw</i> ^f
β-glucosidases							
2607228	Y	β-glucosidase	GH1	3.2.1.21	2	8.49	57190.91
2607232	N	β-glucosidase	GH1	3.2.1.21	6	5.79	120983.23
2172097	Y	β-glucosidase	GH3	3.2.1.21	26	9.63	24005.23
2604319	Y	β-glucosidase	GH3	3.2.1.21	10	8.17	63660.94
2629974	Y	β-glucosidase	GH3	3.2.1.21	13	7.87	21162.84
2538080	Y	β-glucosidase	GH3	3.2.1.21	7	8.58	62700.34
13228	N						
[2612856]	[Y]	β-glucosidase	GH3	3.2.1.21	17	6.41	131339.27
2606766	N	β-glucosidase	GH3	3.2.1.21	4	9.89	20068.14
2623407	N	β-glucosidase	GH3	3.2.1.21	7	7.46	75866.47
Endoglucanases							
2502504	Y	Cellulase (endo-β-1,4-glucanase)	GH5	3.2.1.4	4	7.56	23449.17
2635181	Y	Cellulase (endo-β-1,4-glucanase)	GH5	3.2.1.4	8	4.55	44431.77
2637065	N	Cellulase (endo-β-1,4-glucanase)	GH5	3.2.1.4	4	9.26	38311.10
Exoglucanases							
2639534	Y	Cellobiohydrolase	GH6	3.2.1.91	22	11.93	10412.18
2609170	Y	Reducing end-acting cellobiohydrolase	GH7	3.2.1.176	24	7.78	22230.11
2633816	Y	Reducing end-acting cellobiohydrolase	GH7	3.2.1.176	14	10.82	22917.54
2615989	Y	Exoglucanase 1	GH131	-	24	6.76	39826.55

^a [] = alternative model with signal peptide, ^b Signal peptide was predicted with SignalP-5.0 database. ^c Putative function for identified proteins was obtained from the JGI, InterPro, UniProt and NCBI databases. ^d Carbohydrate-active enzymes database (CAZy) was used for the family information and for the enzyme commission number (EC number). ^e Unique peptides. ^f The theoretical *pI* (isoelectric point) and *Mw* (molecular weight) were computed based on protein sequence obtained from the JGI database.

Hemicellulose is the second most common heterogeneous polysaccharides in (beech) wood, is composed of xylans, mannans, β -(1,3;1,4)-glucans, and xyloglucans and jointed by β -(1,4)-linked backbones (Adav and Sze 2014; Scheller and Ulvskov 2010). *S. commune* secreted several enzymes with potential functions for the degradation of backbone and side-groups of these polysaccharides. Six enzymes were identified likely acting on xylan cleavage. Four endo-1,4- β -xylanases (EC 3.2.1.8 – GH10, 11 and 43) released by the *Sc*-M1 strain to possibly endohydrolyze the (1 \rightarrow 4)- β -D-xylosidic linkages in xylans. The fungus produced one xylan 1,4- β -xylosidase (EC 3.2.1.37 - GH43) to probably cleave the successive D-xylose units from the non-reducing ends, and one oligoxyloglucan reducing-end-specific cellobiohydrolase (EC 3.2.1.150 - GH74) with potential function to hydrolyze the cellobiose from the reducing end of xyloglucans (Table 3-8).

Besides these, the fungus produced one β -mannosidase (EC 3.2.1.37 - GH2), one α -mannosidase (EC 3.2.1.24 - GH38), two mannosyl-oligosaccharide 1,2- α -mannosidase (EC 3.2.1.113 - GH47 and 92), one α -1,6-mannanase (EC 3.2.1.101 - GH76), two α -1,2-mannosidase (GH92), and one metal-independent α -mannosidase (GH125) probably for the degradation of mannans. With potential activities in heteroxyylan side chain degradation, one of each, acetyl xylan esterase (EC 3.1.1.72 - CE1), acetyl xylan esterase with fungal cellulose binding domain (EC 3.1.1.72 - CE1, CMB1), 4-O-methyl-glucuronoyl methylesterase domain (CE15), and acetylesterase (EC 3.1.1.6 - CE16) were identified (Table 3-8). Additionally, one α -L-fucosidase (EC 3.2.1.51 - GH29), one glycosyl hydrolase family 79 C-terminal β domain (GH79) and two α -(4-O-methyl)-glucuronidases (GH115) were secreted potentially for side chain hemicellulose degradation (Table 3-8).

Thirty-three enzymes in total were involved with potential functions in the degradation of highly branched heteropolysaccharide, pectin. Due to complex chemical and structural composition, large variety of enzymes were produced by *S. commune* to possibly split pectin in to consumable product (Table 3-9). Likely to cleave backbone, and main- and side-chains, four pectate lyases (EC 4.2.2.2 - PL1 and - PL3), two rhamnogalacturonases B (EC 4.2.2.23 - PL4), two rhamnogalacturonan acetylesterases (EC 3.1.1.86 - CE12), two pectinesterases (EC 3.1.1.11 - CE8), two endo-polygalacturonases (EC 3.2.1.15 - GH28), two d-4,5 unsaturated β -glucuronyl hydrolases (GH88), two endo-1,3(4)- β -glucanases (EC 3.2.1.6 - GH16), one feruloyl esterase (EC 3.1.1.73 - CE1) and one exo- β -1,3-glucanase (EC 3.2.1.58 - GH55) were identified from the secretome (Table 3-9).

Table 3-8 Identified enzymes with potential hemicellulose-degrading activities in the monokaryotic *S. commune* (Sc-M1) secretome on beech sapwood after 2 weeks of incubation

JGI protein ID ^a	SignalP ^b	Putative protein function ^c	Family ^d	EC ^d	UP ^e	pI ^f	Mw ^f
Enzymes degrading xylans							
2625061	Y	Endo-1,4- β -xylanase (Glycoside hydrolase family 10 and carbohydrate-binding module family 1 protein)	GH10, CMB1	3.2.1.8	48	9.41	36388.68
2621717	Y	Endo-1,4- β -xylanase	GH10	3.2.1.8	2	4.43	57193.44
2612719	Y	Endo-1,4- β -xylanase	GH11	3.2.1.8	36	9.37	8449.90
2618973	Y	Xylan 1,4- β -xylosidase	GH43	3.2.1.37	6	10.33	11460.10
2502024	Y	Endo-1,4- β -xylanase	GH43	3.2.1.8	3	11.97	17795.85
2610111	Y	Oligoxyloglucan reducing end-specific cellobiohydrolase	GH74	3.2.1.150	9	9.65	63643.35
Enzymes degrading mannans							
2633317	Y	β -mannosidase	GH2	3.2.1.37	3	7.26	68961.17
2639708	N	α -mannosidase	GH38	3.2.1.24	4	6.78	26123.01
2088105	Y	Mannosyl-oligosaccharide 1,2- α -mannosidase	GH47	3.2.1.113	13	9.02	59191.95
2635219	Y	α -1,6-mannanase	GH76	3.2.1.101	4	9.22	115163.70
2613271	Y	Mannosyl-oligosaccharide 1,2- α -mannosidase	GH92	3.2.1.113	13	7.03	36559.64
64002	Y	α -1,2-mannosidase	GH92	-	5	7.10	83023.010
2495315	Y	α -1,2-mannosidase	GH92	-	4	8.37	93499.66
1185226	Y	Metal-independent α -mannosidase	GH125	-	5	5.17	39946.85
Esterases							
2624486	Y	Acetyl xylan esterase	CE1	3.1.1.72	44	7.73	83466.50
2637585	Y	Acetyl xylan esterase with Fungal cellulose binding domain	CE1, CMB1	3.1.1.72	31	8.15	43961.78
2754043 [2673984]	Y [Y]	4-O-methyl-glucuronoyl methylesterase domain	CE15	3.1.1.-	19	6.18	52215.17
2612695	Y	Acetylesterase	CE16	3.1.1.6	2	7.88	19901.45

Others							
2624823	Y	α -L-fucosidase	GH29	3.2.1.51	3	8.62	77001.26
2615052	Y	Glycosyl hydrolase family 79 C-terminal β domain	GH79	-	7	7.40	25268.21
2643621	Y	α -(4-O-methyl)-glucuronidase	GH115	3.2.1.-	12	5.94	18324.31
2074391	Y	α -(4-O-methyl)-glucuronidase	GH115	3.2.1.-	18	5.22	41923.40

^a [] = alternative model with signal peptide, ^b Signal peptide was predicted with SignalP-5.0 database. ^c Putative function for identified proteins was obtained from the JGI, InterPro, UniProt and NCBI databases. ^d Carbohydrate-active enzymes database (CAZy) was used for the family information and for the enzyme commission number (EC number). ^e Unique peptides. ^f The theoretical *pI* (isoelectric point) and *M_w* (molecular weight) were computed based on protein sequence obtained from the JGI database.

Table 3-9 Identified enzymes with potential pectin-degrading activities in the monokaryotic *S. commune* (Sc-M1) secretome on beech sapwood after 2 weeks of incubation

JGI protein ID ^a	SignalP ^b	Putative protein function ^c	Family ^d	EC ^d	UP ^e	pI ^f	Mw ^f
2602778	Y	Feruloyl esterase	CE1	3.1.1.73	4	5.89	7906.79
2614029	Y	Pectinesterase (pectin methylesterase)	CE8	3.1.1.11	15	9.29	108166.31
2614257	Y	Pectinesterase (pectin methylesterase)	CE8	3.1.1.11	3	8.44	73628.97
2285680	Y	Rhamnogalacturonan acetylerase	CE12	3.1.1.86	2	6.14	58051.41
2529062	Y	Rhamnogalacturonan acetylerase	CE12	3.1.1.86	16	7.67	57400.59
2614994	Y	Endo-1,3(4)- β -glucanase	GH16	3.2.1.6	3	5.50	36097.19
2630028	Y	Endo-1,3(4)- β -glucanase	GH16	3.2.1.6	2	10.38	7275.29
2492671	Y	Endo-polygalacturonase	GH28	3.2.1.15	5	8.32	59227.94
2507164	Y	Endo-polygalacturonase	GH28	3.1.1.15	5	8.23	12358.42
2482998	Y	Exo- β -1,3-glucanase	GH55	3.2.1.58	2	5.06	39638.67
2604720	Y	d-4,5 unsaturated β -glucuronyl hydrolase	GH88	3.2.1.-	10	9.28	23838.77
2642275	Y	d-4,5 unsaturated β -glucuronyl hydrolase	GH88	3.2.1.-	4	10.26	12281.01
2662427	Y	Pectate lyase	PL1	4.2.2.2	47	8.45	60495.10
2499464	N						
[2700502]	[Y]	Pectate lyase	PL1	4.2.2.2	4	6.24	106304.58
2732642	Y	Pectate lyase	PL1	4.2.2.2	2	9.15	10300.23
2639020	Y	Pectate lyase	PL3	4.2.2.2	4	5.61	12027.59
2713063	Y	Rhamnogalacturonase B	PL4	4.2.2.23	13	5.98	70930.88
2637845	Y	Rhamnogalacturonase B	PL4	4.2.2.23	30	8.77	80976.90
Enzymes degrading galactans							
2625740	N	Galactan endo- β -1,3-galactanase	GH16	3.2.1.181	8	7.14	93175.79
2611511	N						
[2611510]	[Y]	α -galactosidase	GH27	3.2.1.22	6	6.06	38456.38
2631687	Y	β -galactosidase	GH35	3.2.1.23	23	6.97	56636.26
2600123	Y	β -galactosidase	GH35	3.2.1.23	20	5.77	37001.06
2610023	Y	β -galactosidase	GH35	3.2.1.23	7	8.64	47428.52
2609013	Y	β -galactosidase	GH35	3.2.1.23	5	7.33	60301.35
2609561	Y	Galactan 1,3- β -galactosidase	GH43	3.2.1.145	11	6.23	32556.14
2541949	Y	Arabinogalactan endo-1,4- β -galactosidase	GH53	3.2.1.89	4	11.72	20899.42

Enzymes degrading arabinans							
2605157	Y	Arabinan endo-1,5- α -L-arabinosidase	GH43	3.2.1.99	6	9.46	16668.85
2614610	Y	Arabinan endo-1,5- α -L-arabinosidase	GH43	3.2.1.99	5	11.74	13750.22
2516245	Y	Non-reducing end α -L-arabinofuranosidase	GH43	3.2.1.55	3	11.71	5416.28
2737804	Y	Non-reducing end α -L-arabinofuranosidase	GH43	3.2.1.55	4	6.61	104662.90
2626905	Y	α -L-arabinofuranosidase	GH51	3.2.1.55	19	8.30	10782.03
2612425	Y	α -L-arabinofuranosidase	GH62	3.2.1.55	8	9.06	5756.74
2616491	Y	β -L-arabinofuranosidase	GH127	3.2.1.185	3	5.73	52388.32

^a [] = alternative model with signal peptide, ^b Signal peptide was predicted with SignalP-5.0 database. ^c Putative function for identified proteins was obtained from the JGI, InterPro, UniProt and NCBI databases. ^d Carbohydrate-active enzymes database (CAZy) was used for the family information and for the enzyme commission number (EC number). ^e Unique peptides. ^f The theoretical *pI* (isoelectric point) and *M_w* (molecular weight) were computed based on protein sequence obtained from the JGI database.

Further eight enzymes such as one α -galactosidase (EC 3.2.1.22 - GH27), four β -galactosidases (EC 3.2.1.23 - GH35), one galactan endo- β -1,3-galactanase (EC 3.2.1.181 - GH16), one galactan 1,3- β -galactosidase (EC 3.2.1.145 - GH43), and one arabinogalactan endo-1,4- β -galactosidase (EC 3.2.1.89 - GH53) were involved probably in degradation of pectic galactans (Table 3-9). Potentially, to breakdown linear and branched arabinans (composed of α -1,5-linked arabinofuranose units), two arabinan endo-1,5- α -L-arabinosidase (EC 3.2.1.99 - GH43), two non-reducing end α -L-arabinofuranosidases (EC 3.2.1.55 - GH43), two α -L-arabinofuranosidase (EC 3.2.1.55 - GH51 and GH62) and one β -L-arabinofuranosidase (EC 3.2.1.185 - GH127) were detected in the secretome (Table 3-9).

Besides the above plethora of enzymes, there were thirteen supporting enzymes from the auxiliary activities (AA) families to possibly depolymerize the reluctant polysaccharides in wood which might involve in the lignin degradation (Table 3-10). From the auxiliary activities families, AA3 (cellobiose dehydrogenase – EC 1.1.99.18), AA9 (lytic polysaccharide monooxygenases), and AA6 (1,4-benzoquinone reductase – EC 1.6.5.6) were present in the *S. commune* secretome.

In addition to the depolymerizing of major polysaccharides (cellulose, hemicellulose, pectin), proteases, peptidases, amylases, chitinases, lipases, other proteins with different functions and uncharacterized proteins were identified from the secretome to likely breakdown other biomolecules, and/or to probably perform various extracellular functions (Supplementary table 21, Supplementary table 22 and Supplementary table 23).

Table 3-10 Auxiliary activities enzymes identified in the monokaryotic *S. commune* (Sc-M1) secretome on beech sapwood after 2 weeks of incubation

JGI protein ID ^a	SignalP ^b	Putative protein function ^c	Family ^d	EC ^d	UP ^e	<i>pI</i> ^f	<i>Mw</i> ^f
2642438	Y	Cellobiose dehydrogenase	AA3	1.1.99.18	16	11.87	15598.05
2607856	Y	Lytic polysaccharide monooxygenases	AA9	-	3	5.66	91348.92
2617723	Y	Lytic polysaccharide monooxygenases	AA9	-	7	7.98	7302.41
2621099	Y	Lytic polysaccharide monooxygenases	AA9	-	16	5.68	106768.47
2627990	Y	Lytic polysaccharide monooxygenases	AA9	-	13	9.45	68017.28
2634027	Y	Lytic polysaccharide monooxygenases	AA9	-	11	6.43	125903.99
2640531	Y	Lytic polysaccharide monooxygenases	AA9	-	6	7.43	53592.51
2640920	Y	Lytic polysaccharide monooxygenases	AA9	-	20	6.39	51273.82
2628203	N						
[16233]	[Y]	Lytic polysaccharide monooxygenases	AA9	-	2	9.40	22678.12
2604326	N	1,4-benzoquinone reductase	AA6	1.6.5.6	12	6.60	38084.77
2611263	Y	1,4-benzoquinone reductase	AA6	1.6.5.6	5	4.51	13529.98
2611287	Y	1,4-benzoquinone reductase	AA6	1.6.5.6	6	9.04	31662.42
2636150	N	1,4-benzoquinone reductase	AA6	1.6.5.6	9	6.36	93604.25

^a [] = alternative model with signal peptide, ^b Signal peptide was predicted with SignalP-5.0 database. ^c Putative function for identified proteins was obtained from the JGI, InterPro, UniProt and NCBI databases. ^d Carbohydrate-active enzymes database (CAZy) was used for the family information and for the enzyme commission number (EC number). ^e Unique peptides. ^f The theoretical *pI* (isoelectric point) and *Mw* (molecular weight) were computed based on protein sequence obtained from the JGI database.

3.6 Secretome analysis of *T. versicolor* and *S. commune* in dual culture

For the dual culture secretome analysis, dikaryotic strains of *T. versicolor* (*Tv-D*) and *S. commune* (*Sc-D*) were opted and inoculated on *S. commune* minimal medium surfaced with glass-fiber filters. The reason of using the dikaryons in this experiment originated from the fact that in nature these fungi are usually the dikaryons which are confronted with each other. Three replicates of each, one, two and three layers (1L, 2L and 3L respectively) of glass-fiber filter were compared with control (no filter) to determine the optimum number of filter layers for the dual interaction (Figure 3-27). It was found that the *Tv-D* strain had grown on all different numbers of glass-fiber filter layers while the *Sc-D* strain couldn't grow on 3L filters. Fungal growth and interaction zone of both fungi on 1L and 2L were comparable with control. However, color in interaction zone was darker in the presence of 1L and 2L glass-fiber filters (Figure 3-27). Color in interaction zone was probably extracellular melanin pigments which were formed due to competitive reactions between both fungi.

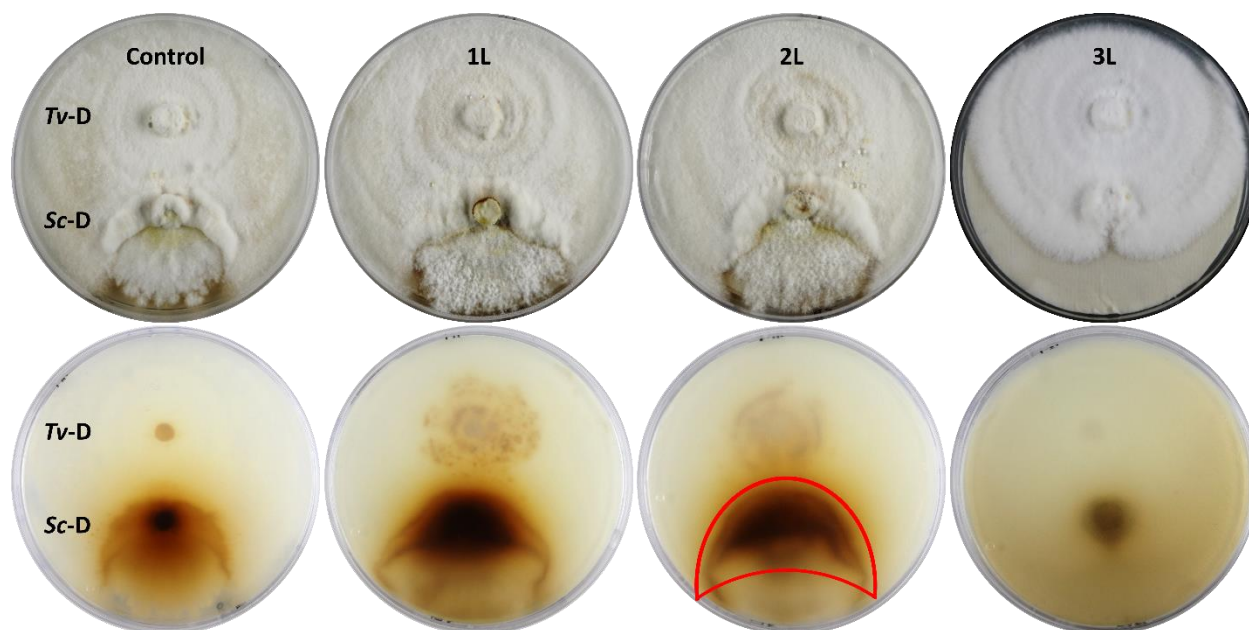


Figure 3-27 Comparison of fungal growth in dual culture (of dikaryotic strains *T. versicolor* - *Tv-D* and *S. commune* - *Sc-D*) on different glass-fiber filter layers (10 days old) with *S. commune* minimal medium. Control is without any glass-fiber filter, whereas 1L, 2L and 3L have one, two and three layers of glass-fiber filter, respectively.

To isolate the secretome from the interaction zone, glass-fiber filters (from 2L, selected based on volume of the extracted protein suspension from the filters which was double than 1L) were cut to separate the interaction region (brown areas of filters) as shown in Figure 3-27. The fungal interaction zone was processed to identify the secreted proteins using nanoLC-MS/MS. For the better description of the results, three biological replicates (Venn diagram - Supplementary figure 5) were merged after the identification of proteins. In this way, 453 secreted proteins in total were identified, from which 284 and 169 proteins were from *T. versicolor* and *S. commune* respectively. The putative function of each protein was assigned using online JGI, NCBI, uniprot, interpro and HMMER databases, and grouped under 10 main categories of likely connection to organismal interactions according to their functions (Figure 3-28). In this experiment, *T. versicolor* had produced comparatively higher number of proteins/ enzymes in all categories except proteins with potential antimicrobial activities compared to *S. commune* (Figure 3-28). Approximately 8% (35 proteins), and 5% (23 proteins) of the total identified proteins were involved in fungal cell wall-degrading enzymes and chitinases. Moreover, 8% (34) antimicrobial proteins, and 2% (9) ribonucleases were found in the secretome. In the interaction zone, 10% (46) proteins were exclusive to oxidases and peroxidases, 17% (77) to proteases and peptidases, and 15% (70) to proteins of other polysaccharides degrading enzymes. Besides these, 4% (19) cell-wall proteins, 17% (76) proteins of other functions and 14 % (64) uncharacterized proteins were identified (Figure 3-28).

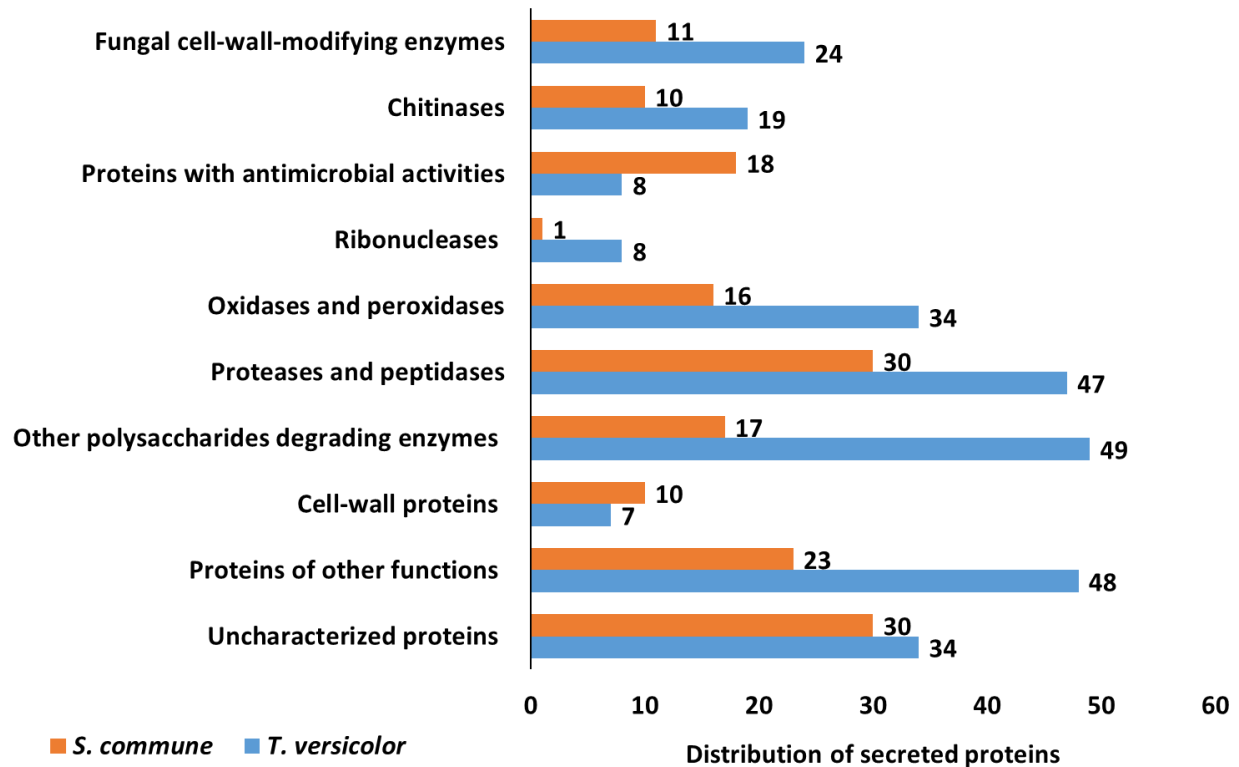


Figure 3-28 Distribution of identified proteins in the secretome of dikaryotic strains *T. versicolor* (Tv-D) and *S. commune* (Sc-D) interaction after 10 days of incubation.

3.6.1 Fungal cell wall-degrading proteins

Principally, fungal cell wall is composed of glucans ($\alpha(1,3)$ -glucans, $\beta(1,3)$ -glucans, $\beta(1,6)$ -glucans, and $\beta(1,3)$ -(1,4)-glucan), chitin, galactomannan, mannans (Gow et al. 2017). To possibly degrade the most abundant fungal cell wall polymer glucan, both fungi secreted different numbers and types of glucanases. *T. versicolor* produced more than double proteins (24) for fungal cell wall degradation, while only 11 proteins were identified from *S. commune* (Figure 3-28). Substantial higher number of glucanases (15) and proteins with other function (4) were detected from *T. versicolor*, contrariwise only 4 glucanases from *S. commune* were identified. In the case of mannanases, *S. commune* secreted 7 proteins, while *T. versicolor* secreted 5 proteins (Figure 3-29).

Table 3-11 Identified enzymes with potential fungal cell wall-degrading activities in the dual-interaction (dikaryotic strains, *Tv*-D and *Sc*-D) secretome on glass-fiber filters after 10 days of inoculation

JGI protein ID	SignalP ^a	Putative protein function ^b	Family ^c	EC ^c	UP ^d	pI ^e	Mw ^e
<i>T. versicolor</i>							
Glucanases							
62730	Y	Exo-1,3- β -glucosidase	GH17	3.2.1.58	14	5.36	40216.33
34683	Y	Exo-1,3- β -glucosidase	GH55	3.2.1.58	7	6.18	81149.78
25402	Y	Exo-1,3- β -glucosidase	GH5_9	3.2.1.58	11	5.42	46753.04
37357	Y	Exo-1,4- α -glucosidase	GH15-CBM20	3.2.1.3	17	4.93	61189.81
54963	Y	Exo-1,4- α -glucosidase	GH15-CBM20	3.2.1.3	10	4.95	61300.74
28580	Y	Exo-1,4- α -glucosidase	GH15-CBM20	3.2.1.3	3	5.43	60938.42
127701	Y	Endo-1,3(4)- β -glucanase	GH16	3.2.1.6	2	4.52	40820.34
29114	Y	Endo-1,3(4)- β -glucanase	GH16	3.2.1.6	2	5.42	35648.60
33707	Y	Endo-1,3(4)- β -glucanase	GH16	3.2.1.6	2	4.93	33869.36
125375	Y	Glucan endo-1,3- α -glucosidase	GH71	3.2.1.59	2	5.15	47982.89
46788	Y	Glucan endo-1,3- α -glucosidase	GH71	3.2.1.59	6	5.16	51765.80
48867	Y	Glucan endo-1,3- α -glucosidase	GH71	3.2.1.59	2	4.55	48359.99
134721	Y	Glucan endo-1,3- β -D-glucosidase	GH16	3.2.1.39	4	6.02	33748.08
27227	Y	Glucan endo-1,3- β -D-glucosidase	GH128	3.2.1.39	2	7.29	39488.44
148125	Y	Glucan endo-1,6- β -glucosidase	GH5_15	3.2.1.75	2	5.25	51527.26
Mannanases							
30268	N	α -mannosidase	GH38	3.2.1.24	3	6.62	128044.88
61724	Y	β -mannosidase	GH2	3.2.1.25	14	4.62	105255.35
26323	Y	β -mannosidase	GH2	3.2.1.25	13	4.76	106684.52
115416	Y	Exo- α -1,6-mannosidase	GH125	3.2.1.-	12	5.37	55880.75
131501	Y	Mannosyl-oligosaccharide 1,2- α -mannosidase	GH47	3.2.1.113	50	4.83	59763.96
Others							

33189	Y	Distantly related to plant expansins	-	-	2	8.57	26283.51
32245	Y	Distantly related to plant expansins	-	-	3	4.72	36376.31
171033	Y	Distantly related to plant expansins	-	-	4	4.76	12861.44
141737	Y	Distantly related to plant expansins	-	-	4	4.76	12866.46
<i>S. commune</i>							
Glucanases							
2631634	Y	Exo-1,4- α -glucosidase	GH15-CBM20	3.2.1.3	3	10.31	21753.97
2614994	Y	Endo-1,3(4)- β -glucanase	GH16	3.2.1.6	19	5.50	36097.19
2630028	Y	Endo-1,3(4)- β -glucanase	GH16	3.2.1.6	10	10.38	7275.29
2518879	Y	Glucan endo-1,3- α -glucosidase	GH71	3.2.1.59	31	4.28	38068.09
Mannanases							
2635216	Y	Mannan endo-1,6- α -mannosidase	GH76	3.2.1.101	7	7.46	73663.61
2624668	Y	Mannan endo-1,6- α -mannosidase	GH76	3.2.1.101	2	5.79	27669.39
2516065	Y	Mannan endo-1,6- α -mannosidase	GH76	3.2.1.101	2	9.34	41365.59
2335629	Y	Mannan endo-1,6- α -mannosidase	GH76	3.2.1.101	4	7.20	16525.73
2635219	Y	Predicted α -1,6-mannanase	GH76	3.2.1.101	2	9.22	115163.70
2088105	Y	Mannosyl-oligosaccharide 1,2- α -mannosidase	GH47	3.2.1.113	23	9.02	59191.95
2497878	Y	Glycosyl hydrolase family 99 domain	GH99	-	2	5.84	32449.89

^a Signal peptide was predicted with SignalP-5.0 database. ^b Putative function for identified proteins was obtained from the JGI, InterPro, UniProt and NCBI databases. ^c Carbohydrate-active enzymes database (CAZy) was used for the family information and for the enzyme commission number (EC number). ^d Unique peptides. ^e The theoretical *pI* (isoelectric point) and *M_w* (molecular weight) were computed based on protein sequence obtained from the JGI database.

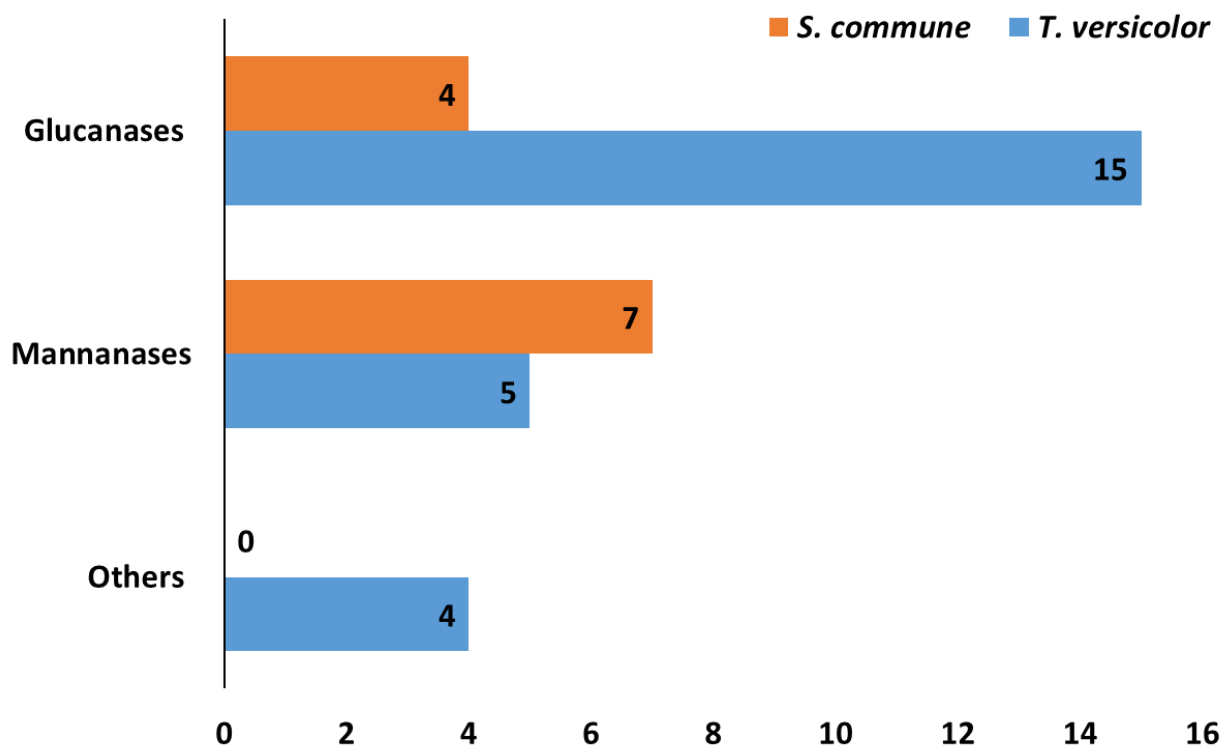


Figure 3-29 Distribution of identified fungal cell wall-degrading proteins in the secretome of dikaryotic strains *T. versicolor* (*Tv-D*) and *S. commune* (*Sc-D*) interaction after 10 days of incubation.

T. versicolor produced 15 proteins to depolymerize the glucan at various positions. To likely cleave the non-reducing ends of (1→3)-β-D-glucans and to probably liberate β-D-glucose, three exo-1,3-β-glucosidases (EC 3.2.1.58, from GH17, GH55 and GH5_9) and three exo-1,4-α-glucosidases (EC 3.2.1.3, from GH15-CBM20) were released by *T. versicolor*. In contrast, *S. commune* only secreted one exo-1,4-α-glucosidase (EC 3.2.1.3, from GH15-CBM20) potentially for the same purpose (Table 3-11 and Figure 3-29). Three and two endo-1,3(4)-β-glucanases (EC 3.2.1.6, GH16) were identified from *T. versicolor* and *S. commune*, respectively with the potential function for the endohydrolysis of (1→3)- or (1→4)-linkages in β-D-glucans. Possibly for the (1→3)-α-D-glucosidic linkages endohydrolysis, three glucan endo-1,3-α-glucosidases (EC 3.2.1.59, GH71) from *T. versicolor* were detected, contrarily only one from *S. commune*. In addition to these, only *T. versicolor* produced two glucan endo-1,3-β-D-glucosidases (EC 3.2.1.39, from GH16 & GH128) to possibly cut (1→3)-β-D-glucans at (1→3)-β-D-glucosidic linkages and

one glucan endo-1,6- β -glucosidase (EC 3.2.1.75, GH5_15) to probably cut (1 \rightarrow 6)- β -D-glucans at (1 \rightarrow 6)- β -D-glucosidic linkages (Table 3-11 and Figure 3-29).

To likely depolymerize the mannanproteins, 5 proteins by *T. versicolor* and 6 proteins by *S. commune* were identified in the secretome. One mannosyl-oligosaccharide 1,2- α -mannosidase (EC 3.2.1.113, GH47) by each fungus was released to possibly slice the oligo-mannose at the terminal (1 \rightarrow 2)- α -D-mannose linkages. Furthermore, one member of GH99 family was also secreted by *S. commune* potentially for the same function. The possible cleavage of unbranched (1 \rightarrow 6)-mannans at (1 \rightarrow 6)- α -D-mannosidic linkages was carried out by the release of five mannan endo-1,6- α -mannosidases (EC 3.2.1.101, GH76) by *S. commune*, while one exo- α -1,6-mannosidase (EC 3.2.1.-, GH125) secreted by *T. versicolor*. Additionally, *T. versicolor* secreted one α -mannosidase (EC 3.2.1.24, GH38) and two β -mannosidases (EC 3.2.1.25, GH2) to probably hydrolyze the non-reducing ends of α -D-mannosides and β -D-mannosides, respectively. In addition to possibly depolymerize glucan and mannan, only *T. versicolor* secreted four expansins (distantly related to plant expansins) for the loosening of plant cell wall (Table 3-11 and Figure 3-29).

3.6.2 Chitinases

In the interaction region, 13 from *T. versicolor* and 10 from *S. commune* potential chitin-degrading enzymes were identified (Figure 3-28) for the extremely recalcitrant and insoluble polymer, chitin. Potentially, the main chitin-degrading enzyme, chitinase (EC 3.2.1.14, GH18) binds to chitin and randomly breaks (1 \rightarrow 4)- β -linkages in chitin (Seidl 2008). Four chitinases from *S. commune* and ten from *T. versicolor* were identified which may be secreted for own hyphal growth for chitin-cell wall expansion or may be for own hyphal recycling in nitrogen-poor environments (such as on wood). Three chitin deacetylases (EC 3.5.1.41, CE4) from *T. versicolor* and 5 from *S. commune* were found in the secretome to possibly hydrolyze chitin. One protein containing chitin-binding type-4 domain was only detected from *S. commune* (Table 3-12 and Figure 3-28).

3.6.3 Proteins with potential antimicrobial activities

To possibly encounter the external stresses and to defend itself, both fungi produced various types and numbers of antimicrobial proteins (14 proteins by *T. versicolor* and 20 proteins

by *S. commune*). Five lactamases by *T. versicolor* and one by *S. commune* were expressed with the potential function to degrade yet unknown xenobiotics, or to combat antibiosis. Ceramidase (EC 3.5.1.23, likely alkaline ceramidase) is known to likely trigger apoptosis, organelle fragmentation and accelerated ageing (as known in yeast, Aerts et al. 2008), which was found (one protein from each fungus) in the secretome of both fungi (Figure 3-28 and Table 3-13).

Table 3-12 Identified chitinases in the dual-interaction (dikaryotic strains, *Tv*-D and *Sc*-D) secretome on glass-fiber filters after 10 days of inoculation

JGI protein ID	SignalP ^a	Putative protein function ^b	Family ^c	EC ^c	UP ^d	pI ^e	Mw ^e
<i>T. versicolor</i>							
72257	Y	Chitinase	GH18	3.2.1.14	10	5.65	36557.28
131793	Y	Chitinase	GH18	3.2.1.14	7	4.68	33022.22
136980	Y	Chitinase	GH18	3.2.1.14	2	4.16	45176.55
18215	Y	Chitinase	GH18	3.2.1.14	6	6.47	60897.00
26449	Y	Chitinase	GH18	3.2.1.14	6	4.96	45551.50
37625	Y	Chitinase	GH18	3.2.1.14	11	4.65	32418.60
47923	Y	Chitinase	GH18	3.2.1.14	6	4.66	34927.34
49346	Y	Chitinase	GH18	3.2.1.14	2	5.06	33059.33
158931	Y	Chitinase	GH18- CBM5	3.2.1.14	4	5.15	51379.75
73594	Y	Chitinase	GH18- CBM5	3.2.1.14	4	5.70	55766.14
144169	Y	Chitin deacetylase	CE4	3.5.1.41	7	4.88	47619.47
68340	Y	Chitin deacetylase	CE4	3.5.1.41	2	4.92	49835.71
138209	Y	Putative catalytic domain of chitin deacetylase-like protein	CE4	3.5.1.41	5	4.71	55288.09
<i>S. commune</i>							
2623305	Y	Chitinase	GH18	3.2.1.14	11	9.30	11418.45
2643740	Y	Chitinase	GH18	3.2.1.14	4	7.94	66479.62
2645822	Y	Chitinase	GH18	3.2.1.14	32	4.95	17074.15
2706631	Y	Chitinase	GH18	3.2.1.14	10	8.85	38530.81
2627742	Y	Chitin-binding type-4 domain-containing protein	-	-	3	6.74	51710.95

2641020	Y	Carbohydrate Esterase Family 4/ Chitin deacetylase	CE4	3.5.1.41	6	7.24	39097.04
2641022	Y	Carbohydrate Esterase Family 4/ Chitin deacetylase	CE4	3.5.1.41	4	5.19	26075.49
2618997	Y	Carbohydrate Esterase Family 4/ Chitin deacetylase	CE4	3.5.1.41	5	4.70	49913.42
2626756	Y	Carbohydrate Esterase Family 4/ Polysaccharide deacetylase	CE4	-	14	5.33	30150.61
2501021	Y	Carbohydrate Esterase Family 4	CE4	-	3	6.99	191537.76

^a Signal peptide was predicted with SignalP-5.0 database. ^b Putative function for identified proteins was obtained from the JGI, InterPro, UniProt and NCBI databases. ^c Carbohydrate-active enzymes database (CAZy) was used for the family information and for the enzyme commission number (EC number). ^d Unique peptides. ^e The theoretical *pI* (isoelectric point) and *M_w* (molecular weight) were computed based on protein sequence obtained from the JGI database.

Table 3-13 Identified proteins with potential antimicrobial activities in the dual-interaction (dikaryotic strains, *Tv-D* and *Sc-D*) secretome on glass-fiber filters after 10 days of inoculation

JGI protein ID	SignalP ^a	Putative protein function ^b	Family ^c	EC ^c	UP ^d	pI ^e	Mw ^e
<i>T. versicolor</i>							
23421	Y	β-lactamase	-	3.5.2.6	2	5.10	62927.81
30240	N	β-lactamase domain	-	3.5.2.6	5	5.50	61194.37
17633	N	β-lactamase domain-containing protein	-	3.5.2.6	2	5.95	31825.16
17636	N	β-lactamase domain-containing protein	-	3.5.2.6	7	5.30	28654.12
68886	N	β-lactamase domain-containing protein	-	3.5.2.6	2	5.92	38878.61
31157	Y	Ceramidases	-	3.5.1.23	33	5.59	77471.70
116268	Y	Cerato-platanin	-	-	6	5.14	14184.94
28335	Y	Cerato-platanin	-	-	8	5.74	13957.72
70402	Y	Cerato-platanin	-	-	5	4.33	14228.86
87426	N	Cerato-platanin domain	-	-	8	4.41	11912.17
23498	Y	Osmotin thaumatin-like protein	-	-	2	4.56	26593.66
20736	Y	Ricin B-like lectins	-	-	7	4.75	16379.61
159352	Y	PR-1-like protein	-	-	2	8.59	39863.77
51381	Y	Lysozyme	GH25	3.2.1.17	5	5.48	24687.38
<i>S. commune</i>							
2646069	Y	β-lactamase domain-containing protein	-	-	5	5.47	30429.60
2635356	Y	Ceramidases	-	3.5.1.23	2	5.83	66465.91
2620687	Y	Cerato-platanin	-	-	7	4.61	15669.78
2619664	Y	Cerato-platanin	-	-	11	6.51	14842.73
2621855	Y	Cerato-platanin	-	-	5	7.71	100897.37
2621834	Y	Cerato-platanin	-	-	4	6.02	25091.18
2608711	Y	Thaumatococcus and allergenic/antifungal thaumatin-like proteins	-	-	8	5.38	19682.36

2591254	Y	Thaumatococcus and allergenic/antifungal thaumatin-like proteins	-	-	2	6.27	38758.29
2637223	Y	Thaumatococcus domain	-	-	11	4.91	17342.58
2489112	Y	Thaumatococcus domain	-	-	9	9.94	15783.45
2637206	Y	Thaumatococcus domain	-	-	3	7.26	108847.07
2628713	Y	Thaumatococcus domain	-	-	4	5.70	47070.45
2488822	N	Thaumatococcus domain	-	-	8	9.15	9421.57
2621085	Y	RICIN domain-containing protein	CBM13	-	20	6.86	58223.04
2607675	Y	RICIN domain-containing protein	CBM13	-	3	6.39	6420.42
2627898	Y	Defense-related protein containing SCP domain (PR1 protein)	-	-	6	7.09	26414.71
2696376	Y	Defense-related protein containing SCP domain (PR1 protein)	-	-	3	4.95	17971.92
2627902	Y	Defense-related protein containing SCP domain (PR1 protein)	-	-	4	11.00	18282.96
2513897	Y	Non-viral sialidases (exo- α -sialidase)	-	3.2.1.18	9	5.93	15559.83
2701331	Y	TAP-like domain containing protein	-	-	3	7.25	29246.99

^a Signal peptide was predicted with SignalP-5.0 database. ^b Putative function for identified proteins was obtained from the JGI, InterPro, UniProt and NCBI databases. ^c Carbohydrate-active enzymes database (CAZy) was used for the family information and for the enzyme commission number (EC number). ^d Unique peptides. ^e The theoretical *pI* (isoelectric point) and *M_w* (molecular weight) were computed based on protein sequence obtained from the JGI database.

Four cerato-platanins from each fungus were probably released for hyphal growth, mycelial development, and/or fungal virulence in the interaction zone. Seven thaumatin-like proteins (TLPs, antifungal proteins) were secreted by *S. commune* to possibly inhibit the growth of *T. versicolor*, while only one TLP was released by *T. versicolor*. This comparison explained that *S. commune* was attempting to likely inhibit the fungal growth strongly compared to *T. versicolor*. Besides it, ricin B-like lectins were expressed by *S. commune* (2 proteins) and *T. versicolor* (1 protein) while the function of these proteins in fungi is unclear, except as homomultimers they have toxic effects (Kim 2020). In response to the enzymatic stress, PR-1 (pathogenesis-related family 1) like proteins, 3 proteins by *S. commune* and 1 protein by *T. versicolor*, were secreted to probably hinder the growth of the opponent (as PR-1 proteins are known for antifungal properties; Ali et al. 2018). Additionally, *S. commune* alone secreted a sialidase (EC 3.2.1.18) with the potential function for pathogenesis and cellular interactions, and a protein containing TAP-like domain for antigen processing. Other hand, alone *T. versicolor* produced a lysozyme (EC 3.2.1.17, GH25) to probably hydrolyze the (1→4)-β-linkages between *N*-acetyl-β-D-glucosamine. This enzyme is already known as an antimicrobial enzyme to have fungistatic (as demonstrated in *Aspergillus fumigatus* by Yudina et al. 2012) or fungicidal (as shown in *Candida albicans* by Wu and Daeschel 2007) activities (Figure 3-28 and Table 3-13).

3.6.4 Ribonucleases

Seven exoribonucleases (three 5' nucleotidase - EC 3.1.3.5, two ribonuclease T2 - EC 4.6.1.19 and two extracellular nucleases) were secreted by *T. versicolor* possibly for RNA and DNA fragmentation. Contrarily only one ribonuclease was secreted by *S. commune* (Figure 3-28 and Table 3-14). One sphingomyelin phosphodiesterase (EC 3.1.4.12) was secreted by *T. versicolor* and belongs to DNase I superfamily of enzymes.

3.6.5 Oxidases and peroxidases

Laccase (4 proteins; TvLac1, 2, 3 & 7; EC 1.10.3.2; AA1_1), manganese peroxidases (7 proteins; MnP1, 2, 3, 4, 6, 10 & 11; EC 1.11.1.13; AA2), versatile peroxidases (3 proteins; VP1, 1at & 2; EC 1.11.1.16; AA2), GMC oxidoreductase (4 proteins; AA3_2), copper radical oxidase (5 proteins; AA5_1), galactose oxidase (1 protein; EC 1.1.3.9; AA5_1), lytic polysaccharide monooxygenase - formerly GH61 (2 proteins; AA9), manganese superoxide dismutase (1 protein; EC 1.15.1.1), prenylcysteine oxidase (1 protein; EC 1.8.3.5), amine oxidase (1 protein), and a

predicted oxidoreductase were released by *T. versicolor* in the interaction zone. On the other hand, laccase (1 protein; Lcc2; EC 1.10.3.2; AA1), multicopper oxidases (2 proteins; AA1), choline dehydrogenase (8 proteins; EC 1.1.99.1; AA3), lytic polysaccharide monooxygenase - formerly GH61 (3 proteins; AA9), catalase (1 protein; EC 1.11.1.6), and oxalate oxidase (1 protein; EC 1.2.3.4) were expressed by *S. commune* (Table 3-15).

Table 3-14 Identified nucleases in the dual-interaction (dikaryotic strains, *Tv*-D and *Sc*-D) secretome on glass-fiber filters after 10 days of inoculation

JGI protein ID	SignalP ^a	Putative protein function ^b	Family ^c	EC ^c	UP ^d	<i>pI</i> ^e	<i>Mw</i> ^e
<i>T. versicolor</i>							
173577	Y	5' nucleotidase	-	3.1.3.5	6	5.80	68956.39
59656	Y	5'-nucleotidase	-	3.1.3.5	2	5.16	31589.53
165641	Y	5'-nucleotidase	-	3.1.3.5	2	5.27	34000.26
149654	Y	Predicted extracellular nuclease	-	-	6	5.38	70249.42
71601	Y	Predicted extracellular nuclease	-	-	15	5.07	65494.71
67924	Y	Ribonuclease, T2 family	-	4.6.1.19	4	5.36	40711.98
55174	Y	Ribonuclease, T2 family	-	4.6.1.19	5	5.77	33808.97
138540	Y	Sphingomyelin phosphodiesterase	-	3.1.4.12	11	5.83	74293.61
<i>S. commune</i>							
2636155	Y	Fungal type ribonuclease	-	-	2	7.76	12922.88

^a Signal peptide was predicted with SignalP-5.0 database. ^b Putative function for identified proteins was obtained from the JGI, InterPro, UniProt and NCBI databases. ^c Carbohydrate-active enzymes database (CAZy) was used for the family information and for the enzyme commission number (EC number). ^d Unique peptides. ^e The theoretical *pI* (isoelectric point) and *Mw* (molecular weight) were computed based on protein sequence obtained from the JGI database.

Table 3-15 Identified oxidases and peroxidases in the dual-interaction (dikaryotic strains, *Tv*-D and *Sc*-D) secretome on glass-fiber filters after 10 days of inoculation

JGI protein ID	SignalP ^a	Putative protein function ^b	Family ^c	EC ^c	UP ^d	pI ^e	Mw ^e
<i>T. versicolor</i>							
68023	Y	Laccase (TvLac1)	AA1_1	1.10.3.2	15	6.44	55796.01
146232	Y	Laccase (TvLac2)	AA1_1	1.10.3.2	13	4.92	56189.77
138261	Y	Laccase (TvLac3)	AA1_1	1.10.3.2	15	5.09	55484.98
47314	Y	Laccase (TvLac7)	AA1_1	1.10.3.2	6	6.04	56751.24
51375	Y	Manganese peroxidase (MnP1s)	AA2	1.11.1.13	10	4.44	37881.43
112835	Y	Manganese peroxidase (MnP2s)	AA2	1.11.1.13	4	4.49	38360.91
131080	Y	Manganese peroxidase (MnP3s)	AA2	1.11.1.13	17	4.93	37879.80
130496	Y	Manganese peroxidase (MnP4s)	AA2	1.11.1.13	19	4.97	37930.90
51455	Y	Manganese peroxidase (MnP6s)	AA2	1.11.1.13	22	5.06	38290.22
44897	Y	Manganese peroxidase (MnP10s)	AA2	1.11.1.13	2	5.21	37983.86
74595	Y	Manganese peroxidase (MnP11s)	AA2	1.11.1.13	2	5.22	38603.57
43289	Y	Versatile peroxidase (VP1)	AA2	1.11.1.16	11	4.93	39301.24
28895	Y	Versatile peroxidase (VP1at)	AA2	1.11.1.16	7	4.44	38129.56
26239	Y	Versatile peroxidase (VP2)	AA2	1.11.1.16	32	4.48	38147.82
133945	Y	GMC oxidoreductase	AA3_2	-	19	5.11	65362.50
122574	Y	GMC oxidoreductase	AA3_2	-	18	5.29	64111.25
57372	Y	GMC oxidoreductase	AA3_2	-	3	5.27	73213.42
176148	Y	GMC oxidoreductase	AA3_2	-	9	6.63	64504.39
118266	Y	Copper radical oxidase	AA5_1	-	19	5.31	59998.30
116129	Y	Copper radical oxidase	AA5_1	-	11	5.69	59108.58
115556	Y	Copper radical oxidase	AA5_1	-	3	4.84	59386.57
130016	Y	Copper radical oxidase	AA5_1	-	24	4.88	81435.55

117805	Y	Copper radical oxidase	AA5_1	-	19	5.48	59963.48
111444	Y	Galactose oxidase	AA5_1	1.1.3.9	3	6.57	41284.96
43058	Y	Lytic polysaccharide monooxygenase (formerly GH61)	AA9	-	2	6.77	25863.05
62497	Y	Lytic polysaccharide monooxygenase (formerly GH61)	AA9	-	3	6.21	34811.57
109828	Y	Manganese superoxide dismutase	-	1.15.1.1	15	8.76	24644.07
143288	Y	Predicted oxidoreductase	-	-	15	7.02	42198.45
172083	Y	Prenylcysteine oxidase	-	1.8.3.5	2	5.09	60521.15
128410	Y	Amine oxidase	-	-	7	4.93	54278.75
<i>S. commune</i>							
1194451	Y	Laccase (lcc 2)	AA1	1.10.3.2	4	6.94	55268.11
2509814	Y	Multicopper oxidases	AA1	-	4	9.02	24030.86
2516955	Y	Multicopper oxidases	AA1	-	2	11.84	22480.98
2642607	Y	Choline dehydrogenase	AA3	1.1.99.1	13	5.24	46946.79
2527132	Y	Choline dehydrogenase	AA3	1.1.99.1	17	10.08	36294.22
2343265	Y	Choline dehydrogenase	AA3	1.1.99.1	36	10.07	36066.78
2343034	Y	Choline dehydrogenase	AA3	1.1.99.1	13	5.89	114025.36
65412	Y	Choline dehydrogenase	AA3	1.1.99.1	4	6.41	54538.61
2666039	Y	Choline dehydrogenase	AA3	1.1.99.1	5	7.71	6716.57
2641528	Y	Choline dehydrogenase	AA3	1.1.99.1	5	6.78	16930.00
2511180	Y	Choline dehydrogenase	AA3	1.1.99.1	5	6.09	45533.23
2693183	Y	Lytic polysaccharide monooxygenase (formerly GH61)	AA9	-	2	11.60	35060.71
2641623	Y	Lytic polysaccharide monooxygenase (formerly GH61)	AA9	-	2	6.37	57351.14
2625035	Y	Lytic polysaccharide monooxygenase (formerly GH61)	AA9	-	3	8.49	74923.96

2620726	Y	Catalase	-	1.11.1.6	8	5.39	63526.97
2626947	Y	Oxalate oxidase	-	1.2.3.4	12	5.68	26913.02

^a Signal peptide was predicted with SignalP-5.0 database. ^b Putative function for identified proteins was obtained from the JGI, InterPro, UniProt and NCBI databases. ^c Carbohydrate-active enzymes database (CAZy) was used for the family information and for the enzyme commission number (EC number). ^d Unique peptides. ^e The theoretical *pI* (isoelectric point) and *M_w* (molecular weight) were computed based on protein sequence obtained from the JGI database.

3.6.6 Proteases and peptidases

For a range of proteolytic activities, 47 from *T. versicolor* and 30 from *S. commune* proteases and peptidases were identified. Serine peptidases were secreted higher in numbers (40 proteins), followed by aspartic (19 proteins), metallo peptidases (17 proteins) and other peptidases (1 protein). All 19 aspartic peptidases were from peptidase family A1. In *T. versicolor*, 9 acid and aspartyl proteases, one aspergillopepsin (EC 3.4.23.18), one pepsin A (EC 3.4.23.1), one polyporopepsin (EC 3.4.23.29), and one saccharopepsin (EC 3.4.23.25) were secreted. On other hand, only 6 acid and aspartyl proteases were secreted by *S. commune*.

Zn-dependent exopeptidase (2 proteins, M28), leucine aminopeptidase-1 (1 protein, EC 3.4.11.1, M28), peptidyl-Lys metalloendopeptidase (2 protein, EC 3.4.24.20, M35), and fungalysin (3 protein, M36) were secreted by *T. versicolor*. In contrast *S. commune*, from metallo peptidases, secreted fungalysin (2 protein, M36), deuterolysin (2 protein, EC 3.4.24.39, M35), aspzincin domain-containing protein (1 protein, M35), Zn-dependent exopeptidase (2 protein, M28), zinc carboxypeptidase domain-containing protein (1 protein, M14), and peptidase domain-containing protein (1 protein, M3) (Figure 3-30 and Supplementary table 24).

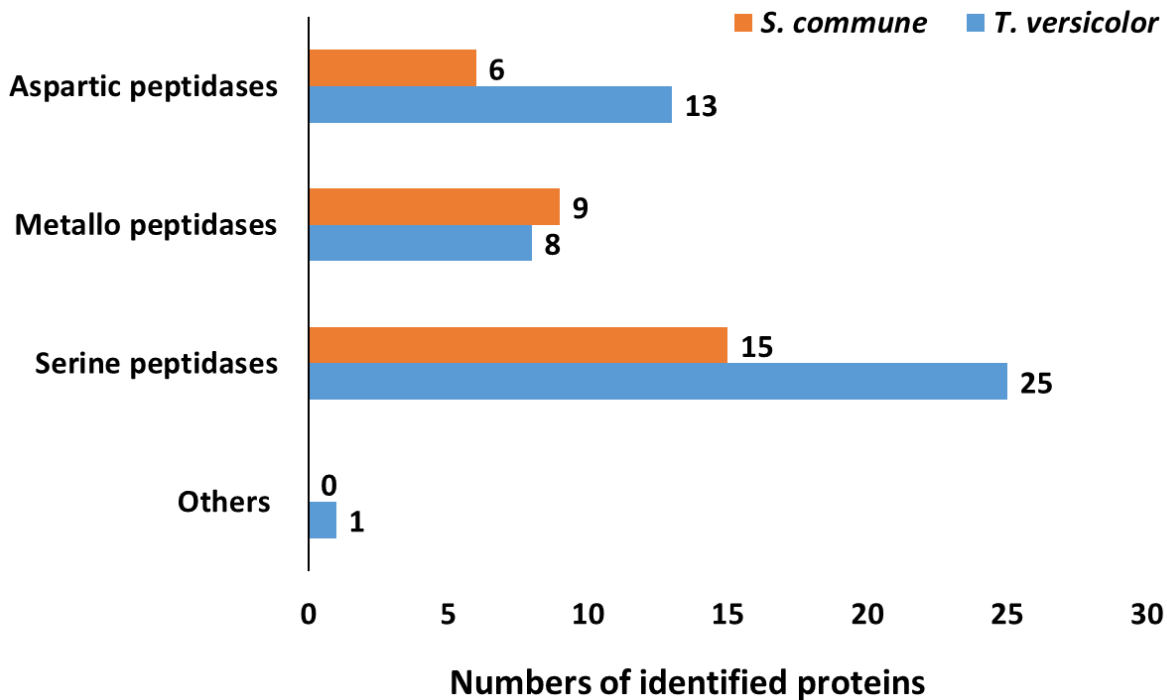


Figure 3-30 Distribution of proteases and peptidases identified in the secretome of dikaryotic strains *T. versicolor* (*Tv-D*) and *S. commune* (*Sc-D*) interaction.

From serine peptidases family, subtilisin-related protease with peptidase inhibitor I9 (1 protein, S8), subtilisin (1 protein, EC 3.4.21.62, S8), serine carboxypeptidase (10 protein, S10), lysosomal pro-xaa carboxypeptidase (2 protein, EC 3.4.16.2, S28), C-terminal processing peptidase-like protein (1 protein, S41A), and tripeptidyl peptidase I (10 protein, EC 3.4.14.9, S53) were identified from *T. versicolor*. While from *S. commune* side, subtilase with Pro-kumamolisin (activation) domain-containing protein (3 protein, EC 3.4.21.62, S8A), subtilisin-related protease with peptidase inhibitor I9 domain-containing protein (1 protein, S8A), dipeptidyl aminopeptidase (1 protein, S9), serine carboxypeptidase (3 protein from S10 and 3 protein from S28), peptidase (2 protein, S41), C-terminal processing peptidase (1 protein, S41A), and sedolisin with pro-kumamolisin (activation) domain-containing protein (1 protein, S53) were identified. In addition to above, one peptide N-acetyl- β -D-glucosaminyl asparaginase amidase A (EC 3.5.1.52) was also detected from *T. versicolor* (Figure 3-30 and Supplementary table 24).

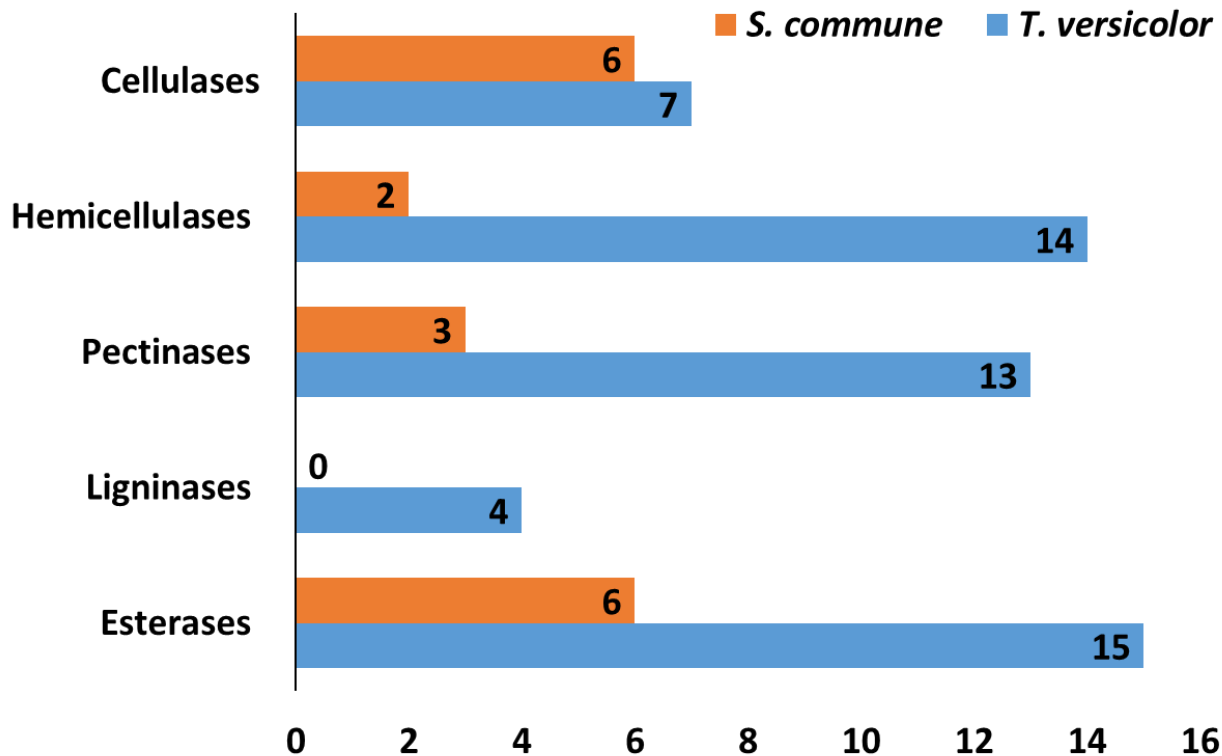


Figure 3-31 Distribution of other polysaccharides degrading enzymes identified in the secretome of dikaryotic strains *T. versicolor* (Tv-D) and *S. commune* (Sc-D) interaction.

3.6.7 Potentially plant cell wall degrading enzymes

Besides chitin and glucan polymers, in total 13 cellulases, 16 hemicellulases, 16 pectinases, and 21 esterases were secreted by both fungi. Four ligninases were only secreted by *T. versicolor* (Figure 3-28, Figure 3-31, and Supplementary table 25).

3.6.8 Miscellaneous identified proteins

Besides all above identified proteins, 8 fungal cell-wall proteins from *T. versicolor* and 11 proteins from *S. commune* were found in the interaction zone (Figure 3-28 and Supplementary table 26). 53 proteins of other functions from *T. versicolor* and 23 proteins from *S. commune* were also detected for various extra/cellular functions (Figure 3-28 and Supplementary table 27). Moreover, proteins of unknown function were identified from *T. versicolor* (34 proteins) and from *S. commune* (30 proteins) (Figure 3-28 and Supplementary table 28).

4 Discussion

4.1 Comparison of beech bark and sapwood weight losses in decay tests

4.1.1 Wood decay by *T. versicolor*

In this study, monokaryotic and dikaryotic strains of *S. commune* and *T. versicolor* were tested and compared for their ability to degrade the beech sapwood particles. Overall, *T. versicolor* strains reduced wood weight considerably higher (up to 53%) than the tested *S. commune* strains (maximum 6%). Similarly to the outcomes of this study, Peddireddi (2008) observed that *S. commune* strains were able to reduce only up to 5% wood weight while *T. versicolor* was able to decay up to 50%. *T. versicolor* is a well-known strong white rot fungus causing massive degradation in non-living wood worldwide (Bari et al. 2015a). According to DIN EN 113 (1997), the fungus should cause the minimum mass loss of 20% (after 16 weeks of exposure) in beech to declare as an aggressive strain (Bari et al. 2015a). Therefore, the *T. versicolor* strains used in this study are aggressive strains and the *S. commune* strains do not comply with the criteria. *T. versicolor* has been reported to reduce wood weight up to 26% in beech after 4 months of exposure (Bari et al. 2015a; 2015b), 36% in Chinese fir in 4.5 months (Chen et al. 2017), about 59% in beech, 46% in birch and 41% in pine after 5 months of incubation (Peddireddi 2008), and 60% in beech after 3 months of incubation (Mohebbi 2003, 2005). The massive degradation by *T. versicolor* is considered that the white-rot fungus attacks simultaneously all wood components at early stages of decay (Cowling 1961; Kirk 1973; Mohebbi 2003; Bari et al. 2015a). In this context, Chen et al. (2017) recorded progressive decay of holocellulose (40%), cellulose (29%), hemicellulose (10%) and acid-insoluble lignin (25%) after 4.5 months of exposure to *T. versicolor* in Chinese fir.

Here in wood decay tests, the monokaryotic *T. versicolor* strain caused a mass loss of 11% in 30 days and 24% in 90 days of incubation. But, the dikaryotic *T. versicolor* strain decayed wood 32% and 53% after 30- and 90-days of incubation, respectively. Similar results were presented by Hiscox et al. (2010b), where 19% decay of beech wood by *T. versicolor* monokaryons and 30% by heterokaryons were noticed after 10 months of exposure. Addleman and Archibald (1993) compared *T. versicolor* monokaryons and dikaryons for delignification and enzyme production but there was no difference except the monokaryons were slow growing. However, dikaryons grew

generally faster than monokaryons e.g., *Pleurotus ostreatus* (Eichlerová and Homolka 1999), *Phellinus weirii* (Hansen 1979) and *Gloeophyllum trabeum* (Bezemer 1973). In *P. weirii*, homokaryons decayed wood slower than heterokaryons (Hansen 1979).

With the prolongation of incubation period, *T. versicolor* showed strong decay effects by reducing wood weight up to 32% and 53% after 30- and 90- days of incubation, respectively. Likewise, the increase in wood decay over time has been detected in beech wood by *T. versicolor* with 18%, 21% and 26% mass losses after the exposure periods of 30, 60 and 120 days (Bari et al. 2015b). An increase was also observed in the mass loss of Chinese fir over 6, 12 and 18 weeks by *T. versicolor* with the values of 15%, 34%, and 36% in sapwood and 15%, 28%, and 35% in heartwood, respectively (Chen et al. 2017).

Under the influence of different light schemes, *T. versicolor* degraded the sapwood with different intensities. The decay was higher in continuous dark condition compared to dark, continuous light, and 12h light/ 12h dark conditions. In dark, the focus of a wood decay fungus is to degrade the wood for nutrient and to gain the territory, but the energies of the fungus in light divide into wood degradation, space capturing and production of the fruiting bodies. Therefore, we have observed the variations in wood decay and fungal growth under continuous light to continuous dark conditions. Pawlik et al. (2019) demonstrated the influence of different light conditions on the metabolic activity of *Cerrena unicolor* (a wood-degrading basidiomycete) which was highest in the dark.

4.1.2 Wood decay by *S. commune*

On the other hand in detailed literature search, surprising reoccurring findings were then that many isolated *S. commune* strains tend not (much) to degrade the wood when it is applied under sterile conditions in specific laboratory wood decay tests with fungal cultures, regardless of classical ratings of wood resistances (e.g. see Abdurachim 1965; Schmidt and Liese 1980; Peddireddi 2008; Takemoto et al. 2010; Lakkireddy et al. 2017; Table 4-1 and our results Figure 3-2 and Figure 3-3). Some of the used test systems are standardized as for applications for the wood industries (EN113/DIN52176, ASTM D2017, AWAP E10, SNI 7207-2014) while others were more individual to a study (Table 4-1). Nevertheless, trends in fungal behavior are recognizable. In many instances (60 % of in total 20 tested temperate wood species; 27.7 % of in total 159 tested tropical wood species; Table 4-1), wood weight loss in decay tests with *S. commune*

strains was low (0-5 %), even after many months of incubation. The decay capacity of this fungus varied from 0 % (with conifer wood of *P. abies* in Slovenia, *Pinus* species; Humar et al. 2001; 2002; Schirp et al. 2003; Ujang et al. 2007) to in best cases 68 % weight loss (wood of broadleaf tree *Cecropia* sp. in Brazil; Reis et al. 2017; Table 4-1).

We have observed a slight change in weight loss over time by all *S. commune* strains (Figure 3-2 and Figure 3-3). In literature, time of incubations varied within and between studies (Table 4-1). Where weight loss by slightly or much better competent *S. commune* strains was measured within a study after different incubation times, noteworthy increases in weight loss (~10 % or more) were observed after about 6 to 8 weeks of incubation (Jurášek et al. 1968; Peters and Allen 1994; Padhiar et al. 2010; Nagadesi and Arya 2014; Koyani et al. 2016; Table 4-1). Timings will relate to first the colonization of the substrate and the possible consumption of easily accessible nutrients in the wood prior to accelerated weight loss by attack of degradable polymers within the wood. Indeed, Indian research groups showed with distinct local fungal isolates specified as *S. commune* that increasing weight loss over the time involved acid-insoluble lignin for *Pinus roxburghii* and *T. grandis* wood (Nagadesi and Arya 2014) and Klason lignin and holocellulose for *M. indica* and *Syzygium cumini* wood (Padhiar et al. 2010), respectively. Further, in various tests, the incubation temperature at 22 °C was sub-optimal for growth and probably also for wood decay (Henningsson 1967) but decay rates as expressed by weight loss were also as poor in tests at better growth temperatures of 25 to 28 °C (Table 4-1). In the study of Henningsson (1967), optimum growth rates and highest decay rates of 10 % (*Populus tremula* wood) correlated at the temperature of 30 °C (Table 4-1).

In this study, there was no significant difference in the weight losses of the mono- and dikaryotic *S. commune* strains (Figure 3-2 and Figure 3-3). However, information on type of tested mycelium (monokaryon or dikaryon) and also respective strain names are often lacking in the available literature (Table 4-1). When isolated as often from fruiting bodies, test strains may likely be dikaryotic but monokaryotic outgrowth from germinating spores cannot be excluded and clear descriptions (clamped mycelium?, fruiting mycelium?) would be preferable. Furthermore, proof of correct species identification of mycelial isolates is often, while not always lacking (confirmation by *ITS* and 26S rDNA D21/D2 sequencing was given for dikaryon MX4 from China and for strain KSR3 from India; Luo et al. 2015; Koyani et al. 2016). This fact should also be kept in mind in the validation of the data in Table 4-1 because mis-identifications as *S. commune* are

not always excluded (see below). At least for broadly used strains with reported good wood decay abilities such as the Indonesian isolate HHBI-204 frequently tested by the group of Djarwanto and Supraptri (see references in Table 4-1) and other more often used Indian isolates (Padhiar et al. 2010; Nagadesi and Arya 2014; Table 4-1), molecular identification data should be provided for species confirmation in order to elucidate the variation in the wood decay potential of the species most properly and reliably. [Fungi can however also later become mixed up as in one study which presented an undoubted *S. commune* ITS sequence (HQ271349) with photos of an apparent conidiogenous ascomycete as *S. commune* culture (Joel and Bhimba 2013).]

A few studies compared mono- and dikaryotic strains (co-isogenic North-American isolates 4-39 and 4-40, monokaryotic and dikaryotic derivatives of these) with each other, with no significantly different results of low weight losses (Peddireddi 2008; Lakkireddy et al. 2017; Table 4-1). Where compact wood blocks and loose wood particles were used from a same tree species with same *S. commune* strains, data of absolute weight losses were also comparable low (Peddireddi 2008; Lakkireddy et al. 2017). In other instances with an Indian isolate, weight loss over time enhanced with the more broken wood presenting a larger surface area for fungal attack and more infection points (Nagadesi and Arya 2014; Table 4-1).

In some studies, slightly higher weight losses were observed with *S. commune* strains in wood samples with extra added nutritional sources. Ca. 3 to 6 % more weight loss of beech wood blocks was recorded with peptone and thiamine added than without, i.e. in average of all tested strains 6.8 % weight loss as compared to 3.8 % (Schmidt and Liese 1980; Table 4-1). Addition of *S. commune* minimal medium to pine, birch or beech saw dust resulted in ca. 10-15 % weight loss (Peddireddi 2008; Table 4-1). When 30 mg glucose or glutamate was added to 3.0 g mixed maple and birch wood chips, wood weight loss was ca 5 % more than without additions. Lignin degradation increased slightly by 2.3 and 2.0 % with glucose or glutamate, respectively, as compared to 0.2 % lignin loss in the control (Boyle 1998; Table 4-1). On the other hand, addition of nitrogen-poor malt extract or minerals made no difference in other studies (Jurášek et al. 1968; Nilsson and Daniel 1983; Wei et al. 2013; Table 4-1). For well-growing within the wood and for usage of the wood for nutrition, *S. commune* might thus regularly miss something, may be sufficient vitamins such as thiamine which the fungus is not producing (see above), or a good nitrogen source which can significantly influence fungal decay rates (Weedon et al. 2009).

Origins of strains have been discussed to play a role in degree of wood decay by *S. commune* (Abdurachim 1965; Schmidt and Liese 1980; Erwin et al. 2008; Koyani et al. 2016). Especially under natural tropical and subtropical climate conditions (ever wet or with rainy seasons; Degreef et al. 1997; Ujang et al. 2002; 2007; Fernando 2009; Seephueak et al. 2011; Andrew et al. 2013; Tapwal et al. 2013; Udochukwu et al. 2014; Lallawmsanga et al. 2016; Shuhada et al. 2017; Singha et al. 2017) infestation of wood and probably also decay of wood by *S. commune* can be very frequent as judged by abundant fruiting body appearances and by observations that wood deterioration in nature appears to be also stronger than in temperate regions. Tropical strains are therefore suspected to be more aggressive than strains which originate from temperate regions (Abdurachim 1965; Erwin et al. 2008; Koyani et al. 2016). While however not all tropical isolates might behave aggressive in wood decay tests (e.g. see Schmidt and Liese 1980; Nsolomo et al. 2000; Erwin et al. 2008; Wei et al. 2013; Table 4-1), others appear to perform much better than any isolates from colder regions (e.g. Abdurachim 1965; Islam et al. 2009; Padhiar et al. 2010; Suprapti 2010; Ashaduzzaman et al. 2011; Nagadesi and Arya 2014; Suprapti and Djarwanto 2014; Koyani et al. 2016; Suprapti et al. 2016; Table 4-1), unless the tested wood species were not instead responsible for the observations.

Only few wood species (*P. sylvestris*, *F. sylvatica*, *Hevea brasiliensis*, *T. grandis*) have been tested in plural by different isolates of different origins (Table 4-1). The only comparative tests between temperate and tropical isolates on the same wood species were so far restricted to pine and beech. Schmidt and colleagues compared 53 different *S. commune* strains of mixed origin from different temperate (9 from Eu, 30 from NA; in total 39) and tropical (3 from Af, 7 from As, 4 from SA; in total 14) geographic areas (Schmidt and Liese 1978; 1980; Schmidt et al. 2011) on *P. sylvestris* and *F. sylvatica* wood blocks. Outcomes of only minimal wood weight loss were however always very similar (Schmidt and Liese 1980; Wei et al. 2013; Table 4-1). Tests with different strains (all tropical or subtropical?) on *H. brasiliensis* wood resulted in weight losses in ranges of 10 to > 40 % (Abdurachim 1965; Hong 1982; Ujang et al. 2007; Suprapti 2010; Jusoh et al. 2014; Cherdchim and Satansat 2016; Table 4-1), with reductions in weight losses after removal of extractives (Hong 1982; Table 4-1). Weight losses in different tests of *T. grandis* wood varied between < 3 and 24 % (Abdurachim 1965; Nagadesi and Arya 2014; Luo et al. 2015; Koyani et al. 2016; Table 4-1), while the two confirmed *S. commune* strains MX4 from China and KSR3

from India caused the lowest and highest weight loss of sapwood, respectively (Luo et al. 2015; Koyani et al. 2016; Table 4-1).

Where higher wood losses were reported in the literature, it was typically with wood species from warmer countries (mainly from India and Indonesia, but also from Bangladesh, Thailand, Malaysia and Brasil) and usually also with fungal isolates from the same countries (Table 4-1). This observation reinforces the question whether local adaptations between the fungi and the wooden hosts might play a role. Total weight losses caused by tropical isolates of the fungus in combination with certain tropical wood species can be as high as >20, >30 or sometimes even more % (Abdurachim 1965; Islam et al. 2009; Suprapti 2010; Koyani et al. 2016; Reis et al. 2017; Table 4-1). Among these cases are Indian reports of specific losses of original lignin by 14.0 % of *T. grandis* and 22.8 % of *P. roxburghii* wood after 20 days of incubation (Nagadesi and Arya 2014), by 10.6 % of *H. brasiliensis* after 50 days of incubation (Hong 1982) and by 20.1 % of *S. cumini* and 20.9 % of *M. indica* wood after 90 days of incubation (Padhiar et al. 2010). In another Indian study with twigs of *Acacia dealbata*, lignin losses by 8.9 % were reported in 90 days incubation as compared to 5.1 % from leaves and 15.5 % from barks (Abubacker and Prince 2013).

The Indonesian isolate HHBI-204 as the most intensively investigated tropical example has been tested on 96 different wood species (compare the extended work by the group of Djarwanto and Suprapti in Table 4-1). The strain caused >25 % weight loss (arbitrarily defined here by us for *S. commune* decay of heartwood as resistance class IV; non-resistant) in 3-month incubation with wood of 2 different plant species [*Altingia (Liquidambar) excelsa*, *H. brasiliensis*; 2.1 % of total species tested with the strain]. Further in 3-month incubation, HHBI-204 showed 15-24.9 % weight loss (*S. commune* resistance class III; moderate resistant) with wood of 29 different species (30.2 % of total), 5-14.9 % weight loss (*S. commune* resistance class II; resistant) with wood of 40 different species (41.7 % of total), and 0-4.9 % weight loss (*S. commune* resistance class I; very resistant) with wood of 25 different species (26.0 % of total). Thus, about 1/3 of tested wood species were considerably decayed by strain HHBI-204, 1/3 suffered from still partial decay and 1/3 was slightly or fully resistant against decay by strain HHBI-204. The Indian isolates mentioned already above behaved in sum similarly variable with different wood species, by decaying some wood species stronger (>25.1 % weight loss; 28.5 % of tested wood species) than others (15 - 24.9 % or 5 - 14.9 % weight loss; both groups represent 28.5 % of tested wood species)

and some (14.3 % of tested species) not (Padhiar et al. 2010; Nagadesi and Arya 2014; Koyani et al. 2016; Table 4-1).

An important reoccurring issue in the data sets in Table 4-1 is the performance of comparative tests on sapwood and heartwood, because sapwood with much living parenchymatous tissue is likely to contain more easily accessible nutrients than heartwood (e.g. Meerts 2002; Vek et al. 2014; Furze et al. 2019). Among the wood species of which both sapwood and heartwood had been tested, weight loss in sapwood was slightly (*S. commune* class III: *Acer niveum*, *Erythrina fusca*, *Sterculia oblongata*; *S. commune* class II: *Gironniera subaequalis*, *Haplolobus* sp., *Tamarindus indica*; *S. commune* class I: *Lindera polyantha*, *Litsea calophylla*, *Turpinia sphaerocarpa*) or considerably higher than in heartwood (*S. commune* class III: *Acacia auriculiformis*, *Ficus vasculosa*, *Neolitsea triplinervia* ; *S. commune* class II: *D. sissoo*, *Hymenaea courbaril*, *Melaleuca cajuputi*, *T. grandis* as tested by different strains, *Tetrameles nudiflora*; *S. commune* class I: *A. indica* as tested by different strains, *Zanthoxylum rhetsa*). In other cases weight losses were comparable (*S. commune* class III: *Castanopsis acuminatissima*, *Cinnamomum iners*, *Horsfieldia glabra*, *Litsea angulata*, *Ficus nervosa*, *Pentaphalangium praviflorum*, *Sloanea sigun*; *S. commune* class II: *Acacia mangium*, *Calophyllum grandiflorum*, *Castanopsis tungurru*, *Diplodiscus* sp., *Ehretia accuminata*, *Gymnacranthera paniculata*, *Ficus variegata*, *Mastixiodendron pachyclados*, *Pimeleodendron amboinicum*, *Pterygota horsfieldii*, *Rhus taitensis*, *Sterculia cordata*, *Temibalia complanata*) and in one case weight loss in heartwood was clearly higher than in softwood (*S. commune* class III: *Sterculia shillinglawii*), (Abdurachim 1965; Suprapti 2002; Suprapti et al. 2007; 2011; 2016; Ashaduzzaman et al. 2011; Suprapti and Djarwanto 2012; 2013, 2014, 2015; Luo et al. 2015; Koyani et al. 2016; Djarwanto et al. 2018; Table 4-1). Thus, the frequent observation of *S. commune* occurrence on sapwood in nature is found back in wood decay tests in the preference of mostly sapwood over heartwood (Table 4-1).

However, not only the respective wood species and whether sapwood or heartwood are tested is of influence on resulting decay but also parameters such as tree wood age and whether tested samples come from the bottom, the middle or the top of a tree. In tests of 9-12 year-old trees of *A. auriculiformis* and *D. sissoo* for instance, weight loss increased with 19.0-21.7-25.8 % and 11.0-13.9-15.9 % for sapwood and with 1.88-2.02-2.10 % and 3.83-4.37-4.89 % for heartwood, respectively, with the wood origin from the bottom over the middle to the top of trees. Along the length of trees, resistance to *S. commune* apparently decreases from bottom to top (Ashaduzzaman

et al. 2011; Table 4-1). Among possible reasons, this might again rely on higher nonstructural carbohydrate contents (starch, easily accessible mono- and disaccharides) in the top stem parts and in branches of trees (e.g. see Furze et al. 2019).

In this connection it is further interesting to note that in one study with *S. commune* fresh sapwood and bark blocks (2 x 2 x 0.4-0.6 cm) of *F. sylvatica* and *P. abies* were compared. After 3 month of incubation, weight losses of pure sapwood of the two temperate species were with 3 and < 1 % negligible unlike the 23 and 25 % weight losses observed in the bark samples, respectively (Wilhelm et al. 1976; Table 4-1). The barks of these trees may thus supply *S. commune* with extras which help the physiological growth activities of the fungus. Depending on the tree species (Dossa et al. 2016), barks of trees, especially the inner bark (living phloem) may contain higher amounts of nutrients than the wood underneath and also better accessible C and N sources (Wetzel et al. 1989; Nordin et al. 2001; Franceschi et al. 2005; Harmon et al. 2013; Martin et al. 2015; Kim and Daniel 2017; 2018; Kim et al. 2017). Presence of bark on dead wood, in particular on branches and twigs, can thus speed up for a range of tree species effectively the natural wood decomposition (Johnson et al. 2014; Dossa et al. 2016; Ulyshen et al. 2016). In nature, barks and thereby especially the outer water-repellent and insulating parts (dead rhytidome) provide additional beneficial features to well adapted fungi, for example by limiting the access of other, competing organisms to the plant substrate and by establishing a specific stable micro-climate with respect to temperature and humidity (Dossa et al. 2016). Because the early sapwood-fungus *S. commune* occurs in nature preferentially on bark-covered substrates, the roles of barks in ecology of *S. commune* certainly deserve more attention than given so far (Thorn et al. 2016). (Note: this text has been written together with Prof. Dr. Ursula Kües.)

Table 4-1 Wood decay tests with *S. commune* isolates

Wood species	Strain origin (name)	Mycelium	Test system	T (°C)	Time (m)	Weight loss (%)	Reference
Temperate Gymnosperms							
<i>Cryptomeria japonica</i>	Japan (Sch2a)	?	Wood blocks (heartwood)	28	2, 4, 8	1.9, 1.8, 1.6	1
<i>Picea abies</i>	Slovenia (ZIM L042)	?	Wood blocks (sapwood) ¹	25	3	0	2,3
	?	?	Wood blocks (sapwood, fresh)	?	3	< 1	4
			Bark blocks (fresh)			25	
<i>Pinus densiflora</i>	Japan (Sch2a)	?	Wood blocks (heartwood)	28	2, 4, 8	2.2, 2.4, 2.2	1
<i>Pinus radiata</i>	New Zealand (3)	?	Wood blocks (sapwood, fresh)	25	4	0	5
	New Zealand (2; 3)	D	Wood blocks (fresh)		4¼	0.5 - 0.7	6
<i>Pinus sylvestris</i>	Variably tested: France (13; 14), Germany (11; 12), Hungary (7; 8), Spain (2; 3), Canada (42 - 47), USA (15 - 37), Cuba (6), Venezuela (38; 39), Indonesia (1), Philippines (4; 5), Thailand (9; 48), Ghana (10), Nigeria (40; 41)	D	Wood blocks (sapwood, stored, on water agar) ¹	22	7	0.4 - 6.2	7
			Wood blocks (sapwood, fresh, on malt agar) ¹		3	0.5	
			Wood blocks (sapwood, stored, on malt agar) ¹		3, 7	0.5, 0.0 - 2.1	
	Germany (12)	D	Wood blocks (sapwood)	?	1½	0.6	8
	Sweden? (A-686)	?	Wood blocks (sapwood on vermiculite with 2 % malt extract)	25	4	3 - 4	9
	USA (4-39; 4-40; others)	M	Wood blocks	25	4, 5	0.2 - 3.0, 1.9 - 2.8	10
	USA (4-39 x 4-40; others)	D				0.1 - 7.0, 1.8 - 3.3	
		USA (4-39; 4-40)	M	Saw dust with minimal medium		4	11.3 - 16.2
	USA (4-39 x 4-40)	D	12.3 - 15.3				
<i>Pinus taeda</i>	USA (not named)	?	Sawdust	?	2	4.7	11
<i>Pseudotsuga menziesii</i>	China (MX4)	D	Wood blocks (sapwood)	25	3	< 3	12
<i>Tsuga heterophylla</i>	USA (SS 3)	?	Wood blocks	26	3	3.2	13
Tropical Gymnosperms							
<i>Agathis borneensis</i>	Indonesia (HHBI-204)	?	Wood blocks (heartwood) ¹	22	3	5.2	14
<i>Agathis dammara</i>	?	?	Wood blocks (heartwood) ¹	?	3	36.3	15
<i>Araucaria cunninghamii</i>	?(6440)	?	Wood blocks (sapwood)	?	1, 2½	2.0, 5.0	16
<i>Pinus kesiya</i>	SC	D	Wood powder		2, 4, 8, 12	< 5	17
<i>Pinus massoniana</i>	China (MX4)	D	Wood blocks (sapwood)	25	3	< 3	12

<i>Pinus merkusii</i>	Indonesia (HHBI-204)	?	Wood blocks (heartwood) ¹	22	3	3.9	14	
<i>Pinus roxburghii</i>	India (not named)	D	Wood chips	27	¾, 1⅓	2.8, 13.0	18	
<i>Pinus</i> sp.	?	?	Wood blocks	?	2½	0	19	
<i>Pinus thunbergii</i>	?	?	Wood blocks (sapwood)	28	3	1.1	20	
Temperate Dicotyledons								
<i>Acer</i> sp. and <i>Betula</i> sp.	Canada (QFB 536)	?	Wood chips	25	1¾	13.4	21	
			Wood chips with glucose			18.3		
			Wood chips with glutamate			18.6		
<i>Betula</i> sp.	USA (SS 3)	?	Wood chips	26	3	2.5	13	
<i>Betula papyrifera</i>	USA (ATCC 18246)	?	Wood blocks (sapwood) ⁴	27	2	< 1	22	
<i>Betula pendula</i>	USA (4-39; 4-40; others)	M	Wood blocks	25	4, 5	2.2 - 4.3, 3.2 - 4.8	10	
	USA (4-39 x 4-40; others)	D				1.6 - 2.4, 2.6 - 2.9		
	USA (4-39, 4-40; others)	M	Saw dust with minimal medium			4		10.2 - 14.9
	USA (4-39 x 4-40; others)	D						10.7 - 12.9
<i>Betula pubescens</i>	Sweden (not named)	D	Wood blocks (sapwood)	22	3	0.9 - 3.9	23	
<i>Fagus crenata</i>	Japan (not named)	D	Wood blocks (sapwood)	?	1⅓, 2¾	1.0, 1.3	24	
	Japan (Sch2a)	?	Wood blocks (heartwood)	28	2, 4, 8	0.7, 0.7, 1.5	1	
<i>Fagus sylvatica</i>	?	?	Wood blocks (sapwood, fresh)	?	3	3	4	
			Bark blocks (fresh)			23		
	Germany (12)	D	Wood blocks (sapwood)	?	2¼	0.8	8	
	Belgium (MUCL31016)	D	Wood blocks (sapwood)	22	3	1.3	25	
	France (13; 14), Germany (11; 12), Hungary (7; 8), Spain (2; 3), Canada (42 - 47), USA (15 - 37), Cuba (6), Venezuela (38; 39), Indonesia (1), Philippines (4; 5), Thailand (9; 48), Ghana (10), Nigeria (40; 41)	D	Wood blocks (sapwood, fresh) ¹	22	5	0.6 - 7.5	7	
			Wood blocks (sapwood, stored) ¹			0.7 - 7.0		
			Wood blocks (sapwood, 1 % peptone-thiamine impregnated) ¹			2		2.9 - 11.7
	USA (26)					10.4, 23.8		
	Costa Rica (87)	?		Wood blocks on vermiculite with malt solution	22	8	0.7 - 2.0	26
	USA (4-39; 4-40; others)	M		Wood blocks	25	4, 5	0.9 - 4.2, 2.1 - 5.2	10
		D					2.0 - 2.4, 1.9 - 4.0	
	Austria (not named)	D?		Wood	28	2½	2	27
USA (4-39; 4-40)	M		Wood chips ≤ 4 mm (sapwood, fresh)	25	1	2.5 - 3.6	28	
	D					2.8		

	USA (4-39; 4-40; others)	M	Saw dust with minimal medium		4	9.4 - 14.8	10	
	USA (4-39 x 4-40; others)	D				10.6 - 12.3		
	Czechoslovakia (not named)	?	Saw dust with mineral elements		2, 4, 6, 8	3.7, 3.3, 5.9, 5.6	29	
<i>Fouquieria splendens</i>	USA (KKN-248)	D	Wood blocks	25	5	12.6 - 29.7	30	
<i>Juglans ailantifolia</i>	USA (4-39; 4-40; others)	M	Wood blocks	25	2, 3, 4, 5	3.6 - 6.5, 3.5 - 5.3, 5.6 - 10.8, 6.4 - 9.0	10	
	USA (4-39 x 4-40; others)	D				3.7 - 8.9, 2.5 - 9.5, 4.7 - 8.9, 5.5 - 10.9		
<i>Populus sp.</i>	?	?	Wood wafers	?	3	7.2	31	
<i>Populus tremula</i>	Sweden (not named)	?	Wood blocks (sapwood)	22	3	22.4 - 24.6	32	
	Sweden (B64105)	D?	Wood blocks (heartwood)			1.1 - 11.8	23	
			Wood blocks	20	2	5.8		
				25		7.0		
				30		8.0		
		35	10.0					
						4.0		
<i>Quercus mongolica</i>	China (MX4)	D	Wood blocks (sapwood)	25	3	< 3	12	
Tropical Dicotyledons, non-durable (over 25.1 % weight loss, 3 months) - <i>S. commune</i> durability class IV								
<i>Ailanthus excelsa</i>	India (KSR3)	D	Wood blocks (sapwood)	27	1, 2, 3, 4	6.7, 18.9, 28.3, 34.4	33	
<i>Albizia saman</i>	Bangladesh (not named)	D?	Wood blocks	25	3	30.5 - 36.4	34	
<i>Altingia excelsa</i>	Indonesia (HHBI-204)	?	Wood blocks (heartwood) ¹	22	3	15.3, 17.1	14,35	
	?			?		27.0		
<i>Cecropia sp.</i>	Brazil (PD21)	D?	Wood blocks ²	27	3	68.0	36	
<i>Hevea brasiliensis</i>	Indonesia (HHBI-204)	?	Wood blocks (heartwood) ¹	22	3	33.6	14	
	?			?	3	40.2	15	
	Thailand (not named)		Wood blocks			1½, 3	9, 12	37
	?		Wood blocks ²			2½	11.3	38
	?		Wood blocks			2½	10.4	19
	?				26	?	16.3	39
						1¾, 2½, 6½	15.5, 20.3, 47.7	
			Wood blocks (water extracted)			1¾, 6½	17.2, 27.2	

			Wood blocks (water and ethanol extracted)		1¾, 6⅓	15.2, 36.4	
<i>Leucaena leucocephala</i>	India (KSR3)	D	Wood blocks (sapwood)	27	1, 2, 3, 4	5.3, 17.6, 26.8, 30.8	33
<i>Mangifera indica</i>	Bangladesh (not named)	D?	Wood blocks	25	3	32.4 - 37.0	34
	India (not named)	D	Wood blocks ²	27	¾, 1½, 3	1.9, 10.5, 26.9	40
<i>Vachellia nilotica</i>	India (not named)	D	Wood chips	27	¾, 1⅓	20.0, 29.1	18
<i>Artocarpus elasticus</i> , <i>Chrysophyllum flexuosum</i> , <i>Cryptocarya integerrima</i> , <i>Ilex pleiobrachiata</i> , <i>Macropanax aromatica</i> , <i>M. dispermus</i> , <i>Schima wallichii</i> , <i>Symplocos fasciculata</i> , <i>Vernonia arborea</i>	?	?	Wood blocks (heartwood) ¹	?	3	26.8 - 55.0	15
Tropical Dicotyledons, moderately durable (15 – 24.9 % weight loss, 3 months) - <i>S. commune</i> durability class III							
<i>Acacia auriculiformis</i>	Bangladesh (WM - 011)	?	Wood blocks (sapwood) ²	25	3	19.0 - 25.8	41
			Wood blocks (heartwood) ²			1.9 - 2.1	
	Indonesia (HHBI-204)	?	Wood blocks (heartwood) ¹	22	3	19.1	14
	?	?	Wood blocks ²	?	2½	1.4	38
<i>Erythrina fusca</i>	Indonesia (HHBI-204)	?	Wood blocks (sapwood) ³	25	3	12.2 - 16.3	42
			Wood blocks (heartwood) ³			10.4 - 13.7	
<i>Eucalyptus</i> sp.	India (KSR3)	D	Wood blocks (sapwood)	27	1, 2, 3, 4	5.7, 13.9, 22.4, 29.7	33
<i>Haldina cordifolia</i>	India (not named)	D	Wood chips	27	¾, 1⅓	7.3 - 15.4	18
<i>Pentaphalangium parviflorum</i>	Indonesia (HHBI-204)	?	Wood blocks (sapwood) ³	25	3	23.8	43
			Wood blocks (heartwood) ³			23.0	
<i>Salmalia insignis</i>	?	?	Wood blocks	25	4	17.0	44
<i>Sterculia shillinglawii</i>	Indonesia (HHBI-204)	?	Wood blocks (sapwood) ³	25	3	10.5	43
			Wood blocks (heartwood) ³			16.1	
<i>Syzygium cumini</i>	India (not named)	D	Wood blocks ²	27	¾, 1½, 3	2.1, 10.5, 23.7	40
<i>Terminalia bellirica</i>	India (not named)	D	Wood chips	27	¾, 1⅓	5.2 - 17.6	18
	?	?	Wood blocks	25	4	8.3	44
<i>Acer niveum</i> , <i>Neolitsea triplinervia</i> , <i>Sloanea sigun</i>	Indonesia (HHBI-204)	?	Wood blocks (sapwood) ¹	?	3	16.1 - 21.7	45
			Wood blocks (heartwood) ¹			14.6 - 15.5	
<i>Acacia crassicarpa</i> , <i>Aleurites moluccanus</i> , <i>Artocarpus gomezianus</i> , <i>Cryptocarya agathophylla</i> , <i>Blumeodendron kurzii</i> , <i>Ceiba pentandra</i> , <i>Colona javanica</i> , <i>Drypetes</i> sp., <i>Glochidion philippicum</i> , <i>Hibiscus</i>	Indonesia (HHBI-204)	?	Wood blocks (heartwood) ¹	22	3	15.2 - 23.0	14

<i>macrophyllus, Hopea odorata, Khaya anthothesca, Koilodepas sp., Mastixia trichotoma, Triomma malaccensis</i>							
<i>Castanopsis acuminatissima, Cinnamomum iners, Ficus nervosa, Horsfieldia glabra, Litsea angulata</i>	Indonesia (HHBI-204)	?	Wood blocks (sapwood, unscrewed) ³	22	3	16.7 - 26.7	14,46,47
			Wood blocks (sapwood, screwed) ³			13.3 - 23.4	
			Wood blocks (heartwood, unscrewed) ^{1,3}			16.3 - 25.2	
			Wood blocks (heartwood, screwed) ³			18.5 - 21.0	
<i>Fagraea sp., Glochidion macrocarpum, Glochidion zeylanicum var. arborescens, Lithocarpus sundaicus, Mitrephora sp., Syzygium glabratum, Weinmannia blumei</i>	?	?	Wood blocks (heartwood) ¹	?	3	15.5 - 23.8	15
<i>Ficus vasculosa, Sterculia oblongata</i>	Indonesia (HHBI-204)	?	Wood blocks (sapwood) ¹	22	3	15.5 - 21.1	14,48
			Wood blocks (heartwood) ¹			12.8 - 16.3	
Tropical Dicotyledons, durable (5 – 14.9 % weight loss, 3 months) - S. commune durability class II							
<i>Acacia mangium</i>	Indonesia (HHBI-204)	?	Wood blocks (sapwood) ¹	22	3	7.1 - 12.6	14,49
			Wood blocks (heartwood) ¹			2.0 - 14.1	
	?	?	Wood blocks ²	?	2½	1.8, 1.4	38
	Indonesia (HHBI-204)	?	Leaves and twigs (particles)	?	1, 2, 3, 4	0.6, 1.6, 2.4, 3.2	50
<i>Castanopsis tungurrut</i>	Indonesia (HHBI-204)	?	Wood blocks (sapwood) ¹	?	3	9.2	45
			Wood blocks (heartwood) ¹			10.5	
	?	?	22	10.5		14	
	?	?	?	9.7		15	
<i>Dalbergia sissoo</i>	Bangladesh (WM - 011)	?	Wood blocks (sapwood) ²	25	3	11.0 - 15.9	41
			Wood blocks (heartwood) ²			3.8 - 4.9	
	India (not named)	D	Wood chips	27	¾, 1½	14.0, 15.2	18
<i>Diplodiscus sp.</i>	Indonesia (HHBI-204)	?	Wood blocks (sapwood) ¹	22	3	8.8	14,51
			Wood blocks (heartwood) ¹			11.1	
<i>Ehretia acuminate</i>	Indonesia (HHBI-204)	?	Wood blocks (sapwood) ¹	22	3	11.2	
			Wood blocks (heartwood) ¹			12.0, 12.2	
<i>Eucalyptus sp.</i>	Brazil (not named)	?	Wood rods	28	2, 4	12.6, 13.2	52
			Wood discs			11.3, 9.1	
<i>Falcataria moluccana</i>	Indonesia (HHBI-204)	?	Wood blocks (heartwood) ¹	22	3	5.4	14
	?	?	Wood blocks (heartwood) ¹	?	3	36.6	15
	?	?	Wood blocks (flakeboard) ²	?	2	5.1 - 6.6	53

	SC	D	Wood powder	27	2, 4, 8	< 5	17
	Indonesia (HHBI-204)	?	Sawdust	?	1	6.7	54
			Leaves and twigs (particles)			1.3	
<i>Ficus variegata</i>	Indonesia (HHBI-204)	?	Wood blocks (sapwood) ¹	22	3	1.9	14,51
			Wood blocks (heartwood) ¹			12.4	
						12.8, 12.9, 22.8	
<i>Hymenaea courbaril</i>	Indonesia (HHBI-204)	?	Wood blocks (sapwood) ¹	22	3	18.8	
			Wood blocks (heartwood) ¹			8.2, 9.0	
<i>Tamarindus indica</i>	Indonesia (HHBI-204)	?	Wood blocks (sapwood) ¹	22	3	14.3	
			Wood blocks (heartwood) ¹			9.9, 10.1	
<i>Tectona grandis</i>	China (MX4)	D	Wood blocks (sapwood)	25	3	< 3	12
	India (KSR3)	D		27	1, 2, 3, 4	3.7, 10.0, 17.9, 24.1	33
	?	?	Wood blocks (heartwood) ¹	?	3	3.1	15
	India (not named)	D	Wood blocks	27	³ / ₄ , 1 ¹ / ₃ , 2	4.1, 4.7, 7.0	18
			Wood chips		³ / ₄ , 1 ¹ / ₃	3.9, 12.9	
<i>Vochysia maxima</i>	Brazil (PD21)	D?	Wood blocks ²	27	3	8.7	36
<i>Acacia aulacocarpa, Acer laurinum, Artocarpus horridus, Diospyros macrophylla, Eucalyptus pellita, Gonystylus macrophyllus</i>	Indonesia (HHBI-204)	?	Wood blocks (heartwood) ¹	22	3	9.2 - 15.0	14
<i>Betula alnoides, Lithocarpus dealbatus</i>	India (MTCC 1096)	D	Wood blocks	25	10	5.5 - 7.4	55
<i>Calophyllum grandiflorum, Gironniera subaequalis</i>	Indonesia (HHBI-204)	?	Wood blocks (sapwood) ¹	22	3	6.6 - 8.7	14,48
			Wood blocks (heartwood) ¹			3.9 - 7.1	
<i>Dipterocarpus pachyphyllus, D. stellatus, D. glabrigemmatum, Vatica nitens</i>	Indonesia (HHBI-204)	?	Wood blocks ³	25	3	5.1 - 14.1	56
<i>Endospermum diadenum, Lansium sp., Mezzettia parviflora, Palaquium gutta, Teijsmanniodendron simplicoides, Trigonopleura malayana, Vitex glabrata, V. pinnata, Xanthophyllum flavescens</i>	Indonesia (HHBI-204)	?	Wood blocks (heartwood) ¹	22	3	5.4 - 9.0	14
<i>Eugenia spp., Protium serratum, Stereospermum personatum, Terminalia tomentosa</i>	?	?	Wood blocks	25	4	5.3 - 5.9	44
<i>Gymnacranthera paniculata, Mastixiodendron pachyclados, Pterygota horsfieldii, Terminalia complanata</i>	Indonesia (HHBI-204)	?	Wood blocks (sapwood) ³	25	3	7.1 - 11.0	43
			Wood blocks (heartwood) ³			7.8 - 12.0	
<i>Haplolobus sp., Pimeleodendron amboinicum, Rhus taitensis, Tetrameles nudiflora</i>	Indonesia (HHBI-204)	?	Wood blocks (sapwood) ³	25	3	5.3 - 13.5	57
			Wood blocks (heartwood) ³			5.7 - 15.0	

<i>Lagerstroemia speciosa, Lannea coromandelica, Mangifera</i> spp.	?	?	Wood blocks	25	4	9.2 - 13.0	44
<i>Melaleuca cajuputi, Sterculia cordata</i>	Indonesia (HHBI-204)	?	Wood blocks (sapwood) ³	25	3	8.1 - 11.9	42
			Wood blocks (heartwood) ³			3.2 - 8.1	
<i>Pternandra azurea, Syzygium acuminatissimum</i>	?	?	Wood blocks (heartwood) ¹	?	3	9.5 - 14.6	15
Tropical Dicotyledones, very durable (0 – 4.9 % weight loss, 3 months) - S. commune durability class I							
<i>Acacia</i> hybrid (<i>A. mangium</i> x <i>A. auriculiformis</i>)	?	?	Wood blocks ²	?	2½	1.5	38
<i>Artocarpus heterophyllus</i>	?	?	Wood blocks (heartwood) ¹	?	3	2.9	15
<i>Azadirachta indica</i>	India (KSR3)	D	Wood blocks (sapwood)	27	1, 2, 3, 4	4.7, 13.4, 21.6, 30.1	33
	Indonesia (HHBI-204)	?	Wood blocks (sapwood) ¹	22	3	8.4	14,45
		Wood blocks (heartwood) ¹	1.3, 1.6				
<i>Chlorocardium rodiei</i>	USA (885)	?	Wood blocks (sapwood)	26	12	1.3	58
<i>Dryobalanops</i> sp.	SC	D	Wood powder	27	2, 4, 8, 12	< 5	17
<i>Eucalyptus grandis</i>	? (UEC-2076)	?	Wood blocks (fresh)	25	2	3.3	59
<i>Eucalyptus</i> sp.	? (SC17/08)	?	Sawdust	27	2	0.8 - 2.6	60
	Indonesia (HHBI-204)	?	Leaves and twigs (particles)	?	1, 2, 3, 4	0.5, 0.9, 1.3, 1.9	50
<i>Lindera polyantha</i>	Indonesia (HHBI-204)	?	Wood blocks (sapwood) ¹	22	3	4.1	14,45
			Wood blocks (heartwood) ¹			0.6, 0.8	
<i>Liquidambar styraciflua</i>	?	?	Wood blocks	?	2½	0.3	19
	USA (Mad. 619)	?	Wood blocks	26	3	1.9	61
	USA (not named)	?	Sawdust	?	1	3.7	11
<i>Ocotea usambarensis</i>	Tanzania (not named)	?	Wood blocks (sapwood)	22	4	2.4	62
<i>Schleichera oleosa</i>	?	?	Wood blocks	25	4	3.7	44
<i>Shorea hopeifolia</i>	Indonesia (HHBI-204)	?	Wood blocks ³	25	3	3.7	56
<i>Shorea smithiana</i>	Japan (not named)	D	Wood blocks	26	3	1.8	63
<i>Terminalia arjuna</i>	India (not named)	D	Wood blocks	27	¾, 1½, 2	1.0, 2.0, 3.9	18
			Wood chips			¾, 1½	
<i>Triplochiton scleroxylon</i>	4 non-specified	D	Wood blocks (sapwood) ¹	22	2	3.7 - 4.5	7
<i>Aglaia rubiginosa, Cananga odorata, Dehaasia firma, Dialium indum, Ganophyllum falcatum, Garcinia nervosa, Kokoona reflexa, Manilkara fasciculata, M. kanosiensis, Parkia javanica, Planchonia grandis, Pterospermum elongatum, Shorea laevifolia, S. platyclados, Tristaniopsis whiteana, Vitex cofassus</i>	Indonesia (HHBI-204)	?	Wood blocks (heartwood) ¹	22	3	1.2 - 4.3	14,35

<i>Apuleia leiocarpa</i> , <i>Bagassa guianensis</i> , <i>Dinizia excelsa</i>	Brazil (PD21)	D?	Wood blocks ²	27	3	0.6 - 3.7	36
<i>Cunninghamia lanceolata</i> , <i>Intsia bijuga</i>	China (MX4)	D	Wood blocks (sapwood)	25	3	< 3	12
<i>Litsea calophylla</i> , <i>Turpinia sphaerocarpa</i> , <i>Zanthoxylum rhetsa</i>	Indonesia (HHBI-204)	?	Wood blocks (sapwood) ^{1,3}	22,	3	4.3 - 7.6	42,48
			Wood blocks (heartwood) ^{1,3}	25		0.7 - 4.0	

Mycelium: M = Monokaryon; D = Dikaryon or assumed to be dikaryon by information of isolation from fruiting bodies or wood in the literature; ? = no further information on type of isolation available

Test system: ¹EN113/DIN 52176 (European Standard, 2000), ²ASTM D2017 (American Society for Testing Materials, 2005), ³SNI 7207-2014 (SNI, 2014), ⁴AWPA E-10 (AWAP Technical Subcommittee P6, 2008), and earlier versions thereof

References: ¹Takahashi 1977; ²Humar et al. 2001; ³Humar et al. 2002; ⁴Wilhelm et al. 1976; ⁵Schirp et al. 2003; ⁶Ah Chee et al. 1998; ⁷Schmidt and Liese 1980; ⁸Hegarty et al. 1987; ⁹Nilsson and Daniel 1983; ¹⁰Peddireddi 2008; ¹¹Koenigs 1974; ¹²Luo et al. 2015; ¹³Safo-Sampah 1975; ¹⁴Suprapti 2010; ¹⁵Abdurachim 1965; ¹⁶Peters and Allen 1994; ¹⁷Priadi 2011; ¹⁸Nagadesi and Arya 2014; ¹⁹Ujang et al. 2007; ²⁰Nagatomo and Akai 1953; ²¹Boyle 1998; ²²Richter et al. 2010; ²³Henningsson 1967; ²⁴Tanesaka et al. 1993; ²⁵Leithoff and Peek 2001; ²⁶Wei et al. 2013; ²⁷Gradinger et al. 2004; ²⁸Lakkireddy et al. 2017; ²⁹Jurášek et al. 1968; ³⁰Nakasone 1977; ³¹Floudas et al. 2015; ³²Henningsson 1965; ³³Koyani et al. 2016; ³⁴Islam et al. 2009; ³⁵Djarwanto and Suprapti 2004; ³⁶Reis et al. 2017; ³⁷Cherdchim and Satansat 2016; ³⁸Jusoh et al. 2014; ³⁹Hong 1982; ⁴⁰Padhiar et al. 2010; ⁴¹Ashaduzzaman et al. 2011; ⁴²Suprapti and Djarwanto 2014; ⁴³Suprapti et al. 2016; ⁴⁴Win et al. 2005; ⁴⁵Suprapti and Djarwanto 2012; ⁴⁶Suprapti and Djarwanto 2013; ⁴⁷Suprapti and Djarwanto 2015; ⁴⁸Suprapti et al. 2011; ⁴⁹Suprapti 2002; ⁵⁰Djarwanto et al. 2009; ⁵¹Suprapti et al. 2007; ⁵²Abreu et al. 2007; ⁵³Hadi et al. 1994; ⁵⁴Djarwanto 2009; ⁵⁵Lyngdoh 2014; ⁵⁶Djarwanto and Suprapti 2014; ⁵⁷Djarwanto et al. 2018; ⁵⁸Humphrey 1915; ⁵⁹Ferraz et al. 1998; ⁶⁰da Silva et al. 2010; ⁶¹Cowling 1961; ⁶²Nsolomo et al. 2000; ⁶³Erwin et al. 2008

4.1.3 Fungal growth on wood wash-out

From many factors responsible for wood resistance, wood extractives are one of the most influential actors to the durability of wood by inhibiting the fungal growth (Chen et al. 2017). In this study, *T. versicolor* couldn't grow on concentrated wood wash-out, although this fungus is a strong wood degrader. In contrast, *S. commune* is a well-known weak wood degrader, but it could grow on the concentrated wood wash-out. It indicates that *S. commune* might take up/ degrade the wood extractive components and let *T. versicolor* grow on wood in nature. Tchinda et al. (2018) reported inhibition of *T. versicolor* growth by the acetone and toluene-ethanol extracts of *Baillonella toxisperma*, *Distemonanthus benthamianus*, *Erythrophleum suaveolens*, *Pterocarpus soyauxii*, and *Triplochiton scleroxylon*, and the inhibition of fungal growth was increased with the increase of extract concentration. In the wood decay tests with *T. versicolor*, *Baillonella toxisperma* (extracted wood 5.6%, and not extracted 3.3%), *Distemonanthus benthamianus* (extracted wood 26%, and not extracted 0.9%), *Pterocarpus soyauxii* (extracted wood 40%, and not extracted 1.9%), and *Erythrophleum suaveolens* (extracted wood 15.9%, and not extracted 1.5%) showed resistance in the presence of wood extractives (Tchinda et al. 2018).

4.2 Fungal interactions between *S. commune* and *T. versicolor* on natural and artificial substrates

Presence of different fungi (in general and two fungal species used in this study) as fruiting bodies and mycelia on decaying wood in nature have been reported by various researchers (Nordin 1954; Rayner and Boddy 1988; Guglielmo et al. 2007; Boddy and Heilmann-Clausen 2008; Peddireddi 2008; Seephueak et al. 2010; 2011; Gonthier et al. 2015; Blinkova and Ivanenko 2016; Lakkireddy et al. 2017; Bhatt et al. 2018; Hagge et al. 2019). By living together, these fungi frequently interact with each other for nutrients and space/territory. These encounters can influence the wood decay processes, synergistically or inversely (Rayner and Boddy 1988; Iakovlev and Stenlid 2000; Schwarze et al. 2012; Burcham et al. 2017). Contrariwise, these encounters are under the influence of the nutrient composition of the substrate. In many instances, the outcomes of using the natural substrates were found to be correlated with the artificial (commonly used, agar-based) substrates (Boddy and Rayner 1983; Holmer and Stenlid 1997; Roy et al. 2003; Woods et al. 2005). However, contrasting outcomes were also found by Nicolotti and Varese (1996), Highley (1997), Lundborg and Unestam (1980), Woods et al. (2005), Peddireddi (2008), and Martínez-Álvarez et

al. (2012). Due to the presence of different assessments, both types of substrates (natural and artificial) were used to investigate the interactions between *S. commune* and *T. versicolor* and, to correlate our observations related to their co-occurrence in nature.

In the current work, after the initial encounter between *S. commune* and *T. versicolor*, *T. versicolor* was able to grow over *S. commune* completely in the presence of wood substrate. On the contrary, on artificial substrate *S. commune* defended itself against *T. versicolor*, stopped the opponent after the infiltration and did not allow it to move further. These contrasting outcomes were previously observed by Peddireddi (2008) where *S. commune* behaved similarly against *Trametes hirsuta*. The increase in strength for combat and defense in *S. commune* is probably due to presence of high sugar (glucose) level in agar medium (Woods et al. 2005) compared to wood. Although, agar-based medium are more common in use and supported for investigations of the competition in wood decay fungi (Henningsson 1967; Boddy and Rayner 1983; Holmer and Stenlid 1997; Tsujiyama and Minami 2005; Woods et al. 2005; Peddireddi 2008; Pasaylyuk 2017). However these contrasting observations (*S. commune* can defend itself against *T. versicolor* on artificial substrate but could not do so on wood substrate) suggest to use natural substrate for the confrontational studies as it is more near natural conditions (Nicolotti and Varese 1996; Highley 1997; Woods et al. 2005; Peddireddi 2008).

In nature, we have observed early emergence of the fruiting bodies of *S. commune* and *T. versicolor* together on freshly fallen deadwood with intact bark and on scorched wood (details published in Lakkireddy et al. 2017). In particularized observations, it is found that the fruiting bodies of *S. commune* appeared first on the decaying wood which were later replaced by the fruiting bodies of *T. versicolor*. As shown in Figure 3-1 (above), *S. commune* is replaced by *T. versicolor* over time in nature. For many instances, *S. commune* has been reported the first appearing mushroom on the decaying wood (Peddireddi 2008; Osemwegie and Okhuoya 2011; Seephueak et al. 2011; Heilmann-Clausen et al. 2014; Lakkireddy et al. 2017; Zia et al. 2018; Khonsuntia et al. unpublished), first on heat-affected wood debris (Carpenter et al. 1987), and even first to fruit after forest fires (Abdulhadi et al. 2000; Sysouphanthong et al. 2010; Kutorga et al. 2012; Lygis et al. 2014; Motiejūnaitė et al. 2014; Greeshma et al. 2016). Besides fruiting bodies of *S. commune*, mushrooms of other coinhabiting fungi like, *Antrodiella fragrans*, *Auricularia auricula-judae*, *Bjerkandera agusta*, *Byssomerulius corium*, *Coprinellus disseminatus*, *Exidia glandulosa*, *Flammulina velutipes*, *Ganoderma lucidum*, *Hypholoma fasciculare*, *Mycena* sp.,

Radulomyces molaris, *Skeletocutis nivea*, *S. subincarnata*, *Trametes* sp., *T. hirsuta*, *T. pubescens*, *T. versicolor* and many others were reported (Seephueak et al. 2011; Bässler et al. 2012; Lakkireddy et al. 2017; Zia et al. 2018). Therefore, the interactions between *S. commune* and other coinhabiting fungi are interesting to study their relationship and impact on wood decay. Here in this study, the confrontational studies were carried out between *S. commune* and *T. versicolor* to understand the sequence of wood colonization. In our laboratory tests, similar pattern as mentioned above was observed where *S. commune* first colonized the sapwood particles which later replaced or colonized by *T. versicolor*. These results are in accordance with the pervious co-culture interaction studies, where *S. commune* was overgrown by strong wood degrading fungi e.g., *T. versicolor* (Gramss 1987; Tsujiyama and Minami 2005; Lakkireddy et al. 2017; Zia et al. 2018) and *T. hirsuta* (Peddireddi 2008).

In this study, a massive production of spicules on surfaces of monokaryotic and dikaryotic hyphae of *S. commune* on beech sapwood, with and without *T. versicolor* as competitor (above, Figure 3-13 and Figure 3-14). Spicules present a unique morphological hyphal character for the discrimination of the *Schizophyllaceae* from other filamentous *Agaricomycetes* (Nobles 1965; Stalpers 1988; Sigler et al. 1999; Romanelli et al. 2010). These spicules might be produced for attachment purposes at solid surfaces as suggested by Kirtzel et al. (2017), or might be correspond to the penetration pegs observed in *S. commune* invasion in mycoparasitism actions (Tzean and Estey 1978). Spicules are nice morphological characters to distinguish *S. commune* (Chowdhary et al. 2013b) from other fungus (like; *T. versicolor*, in this study). Without these spicules, the fungus can be confused with other fungus, like *Irpex lacteus* (Yao et al. 2017) which was first considered as *Schizophyllum* sp. (Cheng et al. 2007; Tang et al. 2011; Yao et al. 2013; Guo et al. 2014; Zhou et al. 2014) but turned out by genome sequencing to be *I. lacteus*.

As found in results of the interaction studies, the combative interactions between *S. commune* and *T. versicolor* were also influenced by the light condition. In dark, mycelial growth of the *S. commune* dikaryotic strain was faster and uniform compared to light conditions where *S. commune* had fruiting bodies (Figure 3-1). Growth of dikaryons is influenced by light, as an adaptation to nature when the mycelium grows vegetatively without light within its plant substrate (the apparently longer period of mycelial growth) and when it appears on substrate surfaces where the fungus fruits under light control. Dikaryotic colonies of *S. commune* in dark conditions grow usually much faster and uniformly than under light when fruiting body formation is initiated by

asymmetrically growing retarded mycelia which are apparently affected by an extracellular antagonistic growth inhibitor of unknown structure (Klein et al. 1997; Ásgeirsdóttir et al. 1995; Schuurs et al. 1998; Ohm et al. 2011). In contrast to dikaryons, the colony growth of monokaryons does not underlie any light-control (Klein et al. 1997; Clark and Anderson 2004) and the same was observed in this study.

In the combative interactions, barrage/barriers formation, deadlocks and pigments production were observed on agar medium with different intensities in the light and dark conditions and the pigmentation differed from monokaryons to dikaryons. In confrontations, the barrage formation is usually considered the resistance response and the production of pigments is a stress response from a fungus to an opponent (Boddy 2000; Iakovlev and Stenlid 2000; Wald et al. 2004; Arun et al. 2015; Menezes et al. 2015; Gmoser et al. 2018; Krause et al. 2020). Gmoser et al. (2018) reported that the pigments production by *Neurospora intermedia* was greatly influenced by light. Although, A range of candidate secondary metabolites have been described from *S. commune* which are of possible origin from indole or tryptophan: the blue water-insoluble pigment indigotin, the red indirubin, the plant hormone indole-3-acetic acid (IAA), the yellow isatin, toxic schizocommunin, tryptanthrin, and the iminolactones schizine A and B (Hosoe et al. 1999; Menezes et al. 2015; Liu et al. 2015) and the melanin production was reported from both fungi in combative interactions (Tudor et al. 2014; Arun et al. 2015; Krause et al. 2020). Deadlock reactions (none of the competing fungi wins territory) with blue pigment (indigo and indirubin) production occurred further in agar cultures in confrontations of *S. commune* with e.g. *F. velutipes*, *Ganoderma lucidum*, *Hypholoma fasciculare*, and *P. ostreatus* (Menezes et al. 2015; Menezes 2014). Similar to our results, deadlock reactions were also observed in combative interactions of *S. commune* strain on agar with *T. hirsuta*, under blue pigment formation by *S. commune*. However, particularly in confrontations on wood, *S. commune* was eventually overgrown by *T. hirsuta* (Peddireddi 2008). In other confrontations, *S. commune* has been overgrown by the strong mycoparasite *Trichoderma viride* and other ascomycetous mycoparasites after a phase of sealing-off, barrage formation and pigment production (Badalyan et al. 2004; Ujor et al. 2012a; 2012b; Hiscox and Boddy 2017). Other studies described *S. commune* isolates to overgrow mycelium of other species, e. g. of the plant pathogens *Gaeumanomyces graminis* var. *tritici*, *Cochliobolus sativus*, *Fusarium culmorum* and *Ceratorhiza cerealis* (Badalyan et al. 2002). On the other hand, *T. versicolor* replaced *Stereum gausapatum* and *Hypholoma fasciculare* while formed a deadlock

with *Bjerkandera adusta* (Eyre et al. 2010). However, the mono- and dikaryotic *S. commune* strains did not grow over the mono- and dikaryotic *T. versicolor* strains while growing on artificial and natural substrate in laboratory tests. These results and observations by Lakkireddy et al. (2017) in nature suggest that *S. commune* colonize wood first and, later *T. versicolor* grows over the wood inhabited by *S. commune*. (Note: partially, this text has been written together with Prof. Dr. Ursula Kües.)

4.3 The *T. versicolor* secretome on beech wood

T. versicolor secreted all four types of the essential lignin-modifying enzymes i.e., lignin peroxidases (LiPs), manganese peroxidases (MnPs), versatile peroxidase (VP) and laccases for the depolymerization of lignin. *T. versicolor* contains genes for 10 LiPs, 13 MnPs, 2 VP, and 7 laccases in its genome (Kersten and Cullen 2014) which have been studied intensively for its various abilities (Rogalski et al. 1991; Marco-Urrea et al. 2009; Carabajal et al. 2012; 2013). *T. versicolor* grown on tomato juice secreted 5 MnPs, 2 Dyp (dye-decolorizing peroxidase), 1 VP, 2 laccases and no LiP (Carabajal et al. 2013). Among all detected lignin-modifying enzymes, the major enzymes were found to be LiPs and MnPs in this study.

T. versicolor degrades simultaneously lignin, cellulose, hemicellulose, pectin, and other wood components. For the depolymerization of cellulose, the required set of enzymes were found in the secretome which includes cellulose 1,4- β -cellobiosidase, glucan 1,4- α -glucosidase, glucan 1,3- β -glucosidase, endo- β -1,4-glucanase, endo-1,3- β -glucanase and β -glucosidase required (Horn et al. 2012; Kostylev and Wilson 2012; Kubicek et al. 2014; Gupta 2016; Ceballos 2018). *T. versicolor* secreted a range of the enzymes acting on hemicellulose main and side chains for degradation. Vasina et al. (2016) identified cellobiohydrolase, exo- β -1,3-glucanase, and members of GH 2, 13, and 51 families in the secretome of *T. hirsuta* for cellulolytic and hemicellulolytic activities. We identified members of GH 2, 5, 10, 12, 27, 30, 43, 51, and 74 families likely for the depolymerization of hemicellulose which are in accordance with Kubicek et al. (2014), and Rytioja et al. (2014). Members of GH 28 family (exopolygalacturonase, endo-polygalacturonase and rhamnogalacturonan hydrolase) and CE 8 family (pectinesterase) were identified for the cleavage of main and side chains of the heteropolysaccharide, pectin (Presley et al. 2018; Stoilova and Krastanov 2008).

Another major group secreted by *T. versicolor* was proteases and peptidases, contained members of aspartic, metallo, and serine peptidases. This group is probably involved in the recycling of its own proteins by the degradation of plant cell wall proteins and lipids (Viterbo et al. 2002; Suárez et al. 2007; Treseder and Lennon 2015; Ramada et al. 2016). Carabajal et al. (2013) found, 13% (22) of the total proteins are proteases in the secretome of *T. versicolor* grown on tomato juice. However, it is also speculated that the secretion of these enzymes is controlled by the ratio of substrate carbon and nitrogen and low level of available nitrogen triggers the secretion (Sato et al. 2007). This low level of proteases and peptidases expression was tested in *T. hirsuta* and only one serine protease (S53) was detected in glucose-peptone medium (Vasina et al. 2016).

4.4 Secretome of *S. commune* on beech wood

The genome analysis of *S. commune* revealed a diverse range of enzymes and the fungus has a distinct mode of biodegradation of wood, diverse from already known white rot and brown rot (Riley et al. 2014). *S. commune* with features in between white and brown rot (a fungus lacks genes for ligninolytic peroxidases but have diverse ranges of enzymes attacking crystalline cellulose) (Riley et al. 2014; Floudas et al. 2015), at the present time is thus distinctively listed as a ‘grey rot’ (Kirker 2018; Krah et al. 2018; Kües et al. 2018). For further clarification of the ambiguity and poorly understood wood decay mechanism, the secretome of *S. commune* was analyzed grown on beech sapwood using modern proteomic approach.

Using nanoLC-MS/MS, a total of 197 secreted proteins were identified in the secretome of *S. commune*, grouped according to their functions (Figure 3-26). *S. commune* has genes for enzymes from the GH5, 10, 11, 27, 28, 29, 31, 35, 43, 51, 53, 62, 78, 93, 88, 105, and 115 families with putative functions in xylan and pectin degradation. Other genes code for enzymes from the GH families 5, 6, 7, 12, 45, 74, and 93 predicted to act on cellulose and *S. commune* has an unusual high number (22 in total) of auxiliary activity genes for AA9 family lytic polysaccharide monooxygenases (LPMOs, formerly classified as GH61 while not being glycoside hydrolases) for cleavage of crystalline cellulose (Ohm et al. 2010; Zhao et al. 2013; Floudas et al. 2015). Accordingly, the highest number of secreted proteins (i.e., cellulases, hemicellulases, and pectinases) were released likely for the degradation of plant cell wall carbohydrates, as the fungus has a full enzymatic collection for it. For the complete degradation of cellulose, three main classes of cellulases (exoglucanases, endoglucanases, and β -glucosidases) were required (Horn et al. 2012;

Kostylev and Wilson 2012; Kubicek et al. 2014; Gupta 2016; Ceballos 2018) and we identified all in the secretome (Table 3-7). Zhu et al. (2016) also found the complete set of cellulases in the secretome of *S. commune* grown on Jerusalem artichoke.

Hemicellulose, a complex and branched heteropolymer is comprised of several polymers like xylan, xyloglucan, arabinoxylan, glucuronoxylan, glucomannan and others. Degradation of this plant cell wall component, *S. commune* produced a repertoire of enzymes (Table 3-8) to act on backbones and side-chains of the polymers. Zhu et al. (2016) reported members of GH families (2, 10, 11, 43, 74, and 115) and EC families (1 and 15) for the cleavage of hemicellulose, which also identified here in the *S. commune* secretome but the members of GH families (27, 31, 35, 51 and 62) could not be detected on beech wood. Additionally, we also identified members of GH families (29, 38, 47, 76, 79, 92 and 125) and EC family (16) from the secretome grown on beech sapwood, which were probably due to different chemical composition of substrate.

On wood of Jerusalem artichoke, *S. commune* secreted members of PL families (1, 3 and 4), GH families (16, 28, 43, 53 and 93) and EC families (8 and 12) to degrade plant cell wall pectin (Zhu et al. 2016). These results partially agree with our results, as the proteins identified for the degradation of pectin in the secretome grown on beech sapwood are members of PL families (1, 3 and 4), GH families (16, 27, 28, 35, 43, 51, 53, 55, 62, 88 and 127) and EC families (1, 8 and 12), as shown in Table 3-9. In non-hydrolytic proteins, *S. commune* produced a similar number (8) of AA9 family members on Jerusalem artichoke (Zhu et al. 2016) and beech.

The most important lignin-degrading enzymes (members of fungal class II peroxidases, i.e., lignin peroxidases, manganese peroxidases, and versatile peroxidases), characteristic feature of white rot fungi, were not secreted by *S. commune*, although the genome has two genes encoding laccases (Ohm et al. 2010; Kersten and Cullen 2014; Zhu et al. 2016). However, some modifications (side-chain oxidation, demethylation, and demethoxylation) of lignin substructure was observed during the degradation of Jerusalem artichoke stalks by *S. commune* (Zhu et al. 2016). These minor alterations of lignin that can resemble chemically-induced modifications of lignin can be provoked by the brown-rot *Gloeophyllum trabeum* (Zhu et al. 2016). These alterations might be for the removal of lignin from polysaccharides. One cellobiose dehydrogenase (CDH), four benzoquinone reductase and six GMC oxidoreductases were secreted by the fungus on beech which might be involved in Fenton chemistry (Zhu et al. 2016). As well, no ligninolytic

activities, neither of laccase nor of peroxidase, were encountered during the growth on Jerusalem artichoke stalks (Zhu et al. 2016). Therefore, it is possible that *S. commune* as early colonizer targets easily accessible compounds, and lignin degrades by other fungi such as *T. versicolor*.

4.5 Secretome analysis of *T. versicolor* and *S. commune* in dual culture

Dual interaction of *T. versicolor* and *S. commune* dikaryotic strains was carried out to isolate secretome and to identify the involved proteins in defense reactions and interaction/competition. In total, 284 and 169 proteins were identified from *T. versicolor* and *S. commune* respectively in the dual culture secretome and grouped according to putative functions (Figure 3-28).

Fungal cell wall composition varies from fungus to fungus but basically consists of chitin, β -1,3-glucan, β -1,6-glucan, and mannan (Gow et al. 2017). Excluding chitin modifying enzymes, *T. versicolor* secreted 24 fungal cell wall degrading enzymes, a higher number compared to its competitor *S. commune*, with only 11 proteins (Table 3-11). For cleavage of basic structure of fungal cell wall, both fungi produced glucanases, mannanases and chitinases in different numbers. In glucanases, 15 enzymes from *T. versicolor* and 4 from *S. commune* were identified in the secretome potentially for the breakdown of glucan polymers. β -1,3-glucanases, and β -1,6-glucanase have been described in mycoparasitic *Trichoderma* spp. (Djonović et al. 2006; Kubicek et al. 2011; Gruber and Seidl-Seiboth 2012) and especially the later one has been identified from numerous filamentous fungi (Djonović et al. 2006). α -1,3-glucanases and α -mannosidases play a role in fungal cell wall cleavage (Gruber and Seidl-Seiboth 2012), and here (in this study) in the secretome three α -1,3-glucanases and one α -mannosidase from *T. versicolor* and only one α -1,3-glucanase from *S. commune* were identified. Endo- β -1,6-glucanase performs synergistically with chitinase and β -1,3-glucanase in fungal cell wall degradation (Ramada et al. 2016). However, exo-1,3- β -glucanases and endo-1,3- β -glucanase were detected in cell wall autolysates of *Aspergillus fumigatus* (Adams 2004). In addition to glucanases and mannanases, *T. versicolor* also secreted four expansin-like proteins but none from *S. commune*, although, it has at least one fully characterized expansin protein (ScExlx1) (Tovar-Herrera et al. 2015). These non-enzymatic proteins have been reported to be involved in liberation of N-acetyl glucosamine (reducing sugar) from chitin, and expansin with chitinase can boost chitin hydrolysis (Tovar-Herrera et al. 2015). These expansins may be involved in loosening of the opponent fungal cell wall and helping the

fungus to penetrate the opponent cell, or possibly these expansins with other fungal cell wall degrading enzymes are altering fungal cell walls for growth of cells with necessary extension of cell walls.

In the dual culture secretome, 13 chitin-modifying enzymes from *T. versicolor* and 10 from *S. commune* were found. Usually, these enzymes are involved in self-degradation for recycling and remodeling of cell wall, for nutritional purpose and for autolysis, but in the event of non-self-degradation, these enzymes are involved in mycoparasitism (Adams 2004; Seidl 2008; Druzhinina et al. 2012; Gruber and Seidl-Seiboth 2012). The highest number of secreted chitinases was from *T. versicolor* (10 enzymes) which possibly contribute to its aggressive behavior in the combat with *S. commune*, where only 4 enzymes were detected. As Druzhinina et al. (2012) described, a higher number of chitinases in the comparison of different *Trichoderma* species is connected to better attack capabilities.

To possibly nullify the effects, to defend itself, and to overcome the opponent, both fungi produced many enzymes. Five lactamases from *T. versicolor* and one from *S. commune* were identified in the secretome. The potential functions of these enzymes are in the detoxification of xenobiotics (Bush 2018; Gao et al. 2017a), as a lactamase from *Fusarium* spp. degraded the benzoxazolinone (Kettle et al. 2015; Glenn et al. 2016). Thaumatin-like proteins have inhibitory effects on fungal growth (Ng 2004; Grenier et al. 2000) known from *Irpex lacteus*, *Lentinus edodes* and *Rhizoctonia solani*. Pathogenesis-related (PR) protein, PR-1 has been reported for its antifungal properties (Selitrennikoff 2001). Ceramides are involved in apoptosis, cell cycle arrest, organelle fragmentation and accelerated ageing (Aerts et al. 2008). Cerato-platanin proteins can set off the loosening of fungal cell wall while binding to it through its carbohydrate-binding feature (Gaderer et al. 2014; Luti et al. 2020). Presence of these proteins in the culture filtrates also suggests the involvement in fungal growth and development (Bacelli 2014).

Besides the other enzymes, 17% of the total *T. versicolor* secreted proteins and 18% of the *S. commune* proteins were identified as proteases and peptidases (Supplementary table 24). According to MEROPS database (<https://www.ebi.ac.uk/merops/index.shtml>), *S. commune* has 192 known and putative peptidases while *T. versicolor* has 175 (Rawlings et al. 2018). All the expressed proteases and peptidases belong to aspartic, metallo and serine peptidases except one. These enzymes are probably participating in recycling of the own proteins of the fungi, in the

enzyme inactivation of proteins released by the opponent during combat, and in host cell lysis by attacking and degrading the cell wall proteins and lipids (Viterbo et al. 2002; Suárez et al. 2007; Ramada et al. 2016). Treseder and Lennon (2015) described the degradation process of proteins by proteases into single amino acids and small peptides, i.e., the long chains of a protein split by metallo- or serine protease into shorter chains which after cleaved by peptidases, and the resulted single amino acids and small peptides can be commenced by fungi. *S. commune* secreted members of M3, M14 and S9 peptidase families in addition to members of A1, M28, M35, M36, S8, S10, S28, S41, and S53 peptidase families which were only expressed by *T. versicolor*. The high heterogeneity of proteases released by mycoparasitic *S. commune* in combat with *T. versicolor*, may reflect the ability to defend itself or indicate the effective system to use of proteins, as suggested by Ramada et al. (2016) in *Trichoderma harzianum*.

Seven ribonucleases from *T. versicolor* and one from *S. commune* were detected in the dual culture secretome. These ribonucleases are probably involved in defense, and in the recycling of extracellular nucleic acids which the fungus can take up as nucleotides (Galiana et al. 1997; Deshpande and Shankar 2002; MacIntosh 2011; Terakawa et al. 2016; Hasunuma and Ishikawa 1977).

In this study, the identified proteins in the combat from *T. versicolor* were higher in number compared to *S. commune*. Production of versatile and comparatively higher numbers of chitinases, cell wall degrading enzymes, oxidases and peroxidases, and proteases were produced by *T. versicolor*. However, *S. commune* secreted comparatively higher numbers of potential antimicrobial proteins compared to the *T. versicolor* which was probably a defensive behavior by *S. commune* on the plate medium.

5 Conclusion and outlook

Some general conclusions drawn from this thesis work are as follows:

1. Early sapwood colonizers *Schizophyllum commune* and *Trametes versicolor* coexist on decaying wood in nature during the early decay stage.
2. *T. versicolor* caused a greater overall mass reduction than *S. commune* in the beech sapwood and bark decay tests under all light and dark conditions. This demonstrates that *T. versicolor* is an aggressive white rot, as opposed to *S. commune*, which is a weak degrader.
3. *T. versicolor* could not grow on concentrated wood wash-out under any of the conditions tested in tests of fungal growth on wood wash-out collected from a European ash tree log. It suggests that *S. commune* may engross or degrade wood extractive components, allowing *T. versicolor* to grow on wood in nature.
4. A dense mycelium appeared in the interaction zone of both early sapwood colonizers on natural (beech sapwood particles) and artificial (*S. commune* minimal medium) substrates. The *T. versicolor* dikaryotic strain then colonized compartments throughout the *S. commune* (all strains) while growing on wood. On *S. commune* minimal medium, however, the *T. versicolor* dikaryotic strain outgrew the *S. commune* strains and formed dense mycelia barriers. It suggests that *T. versicolor* may outgrow *S. commune*, which is what happens in nature, as shown in Figure 3-1.
5. Buffer 1 was the best for isolating the secretome from fungus-wood samples because it extracted the lowest number of contaminating intracellular proteins of the four buffers tested.
6. In a comparison of *T. versicolor* secretomes from early (10 day) and late (28 day) decay stages, the early decay stage has more laccases than the late decay stage, which has more chitinases. However, comparing these secretomes to the secretome of uninoculated wood samples can improve the understanding of these results.
7. Lignin-modifying enzymes (laccases and other multi-copper oxidases) were not expressed in the secretome of *S. commune*, which could be an indication of its grey rot behavior.

The experiments conducted for this PhD project revealed that both early sapwood colonizers (*Schizophyllum commune* and *Trametes versicolor*) coexist and influence wood decay and growth. It is also clear that both fungi compete while growing on wood and artificial medium under the laboratory condition. It is currently unknown how much reduction in wood weight can be caused by the fungi growing together on wood, and whether they have a synergistic effect. Both fungi should grow on the same wood in a wood decay test to understand this effect. The secretomes of *S. commune* and *T. versicolor* were studied on a single time point in this study. However, in order to gain a better understanding of the ecological functions of both fungi's secretomes, it is necessary to conduct experiments on both fungi's secretomes in signal culture on wood at different time intervals. Similarly, studying secretome dynamics over time can provide a better understanding of how the two fungi interact. After biochemical characterization, proteins that have been identified as potential candidates should be studied for their potential applications. The following strategy can be implemented: 1) transformation of a suitable bacteria or fungus with an interested protein's gene; 2) gene regulation optimization for high protein production; 3) fermentation optimization for pilot scale production.

Several proteins/enzymes identified in this study that have not yet been biochemically characterized could be promising candidates for biotechnological applications.

T. versicolor secreted four proteins (32245, 33189, 141737, and 171033; see table 3-11) of expansins (distantly related to plant expansins). These non-enzymatic proteins, known as expansins, have been found in a variety of microorganisms as well as all plants. Because these proteins are required in almost all aspects of plant physiological development phases from germination to fruiting, they can be used for crop improvement, such as enhancing seed germination, increasing plant capacity to withstand biotic and abiotic stresses, and breeding to increase fruit shelf life and reduce post-harvest losses (Sampedro and Cosgrove 2005; Marowa et al. 2016; Cosgrove 2000; Cosgrove 2015; Nikolaidis et al. 2014).

In table 3-12, chitin-binding type-4 domain-containing protein (2627742) and carbohydrate esterase family 4 proteins (2626756 and 2501021) identified in the secretome of *S. commune* can be used as biopesticides to control plant pests and diseases. Chitin-binding proteins are a family of genes associated with pathogenesis that are essential for plant defense mechanisms and

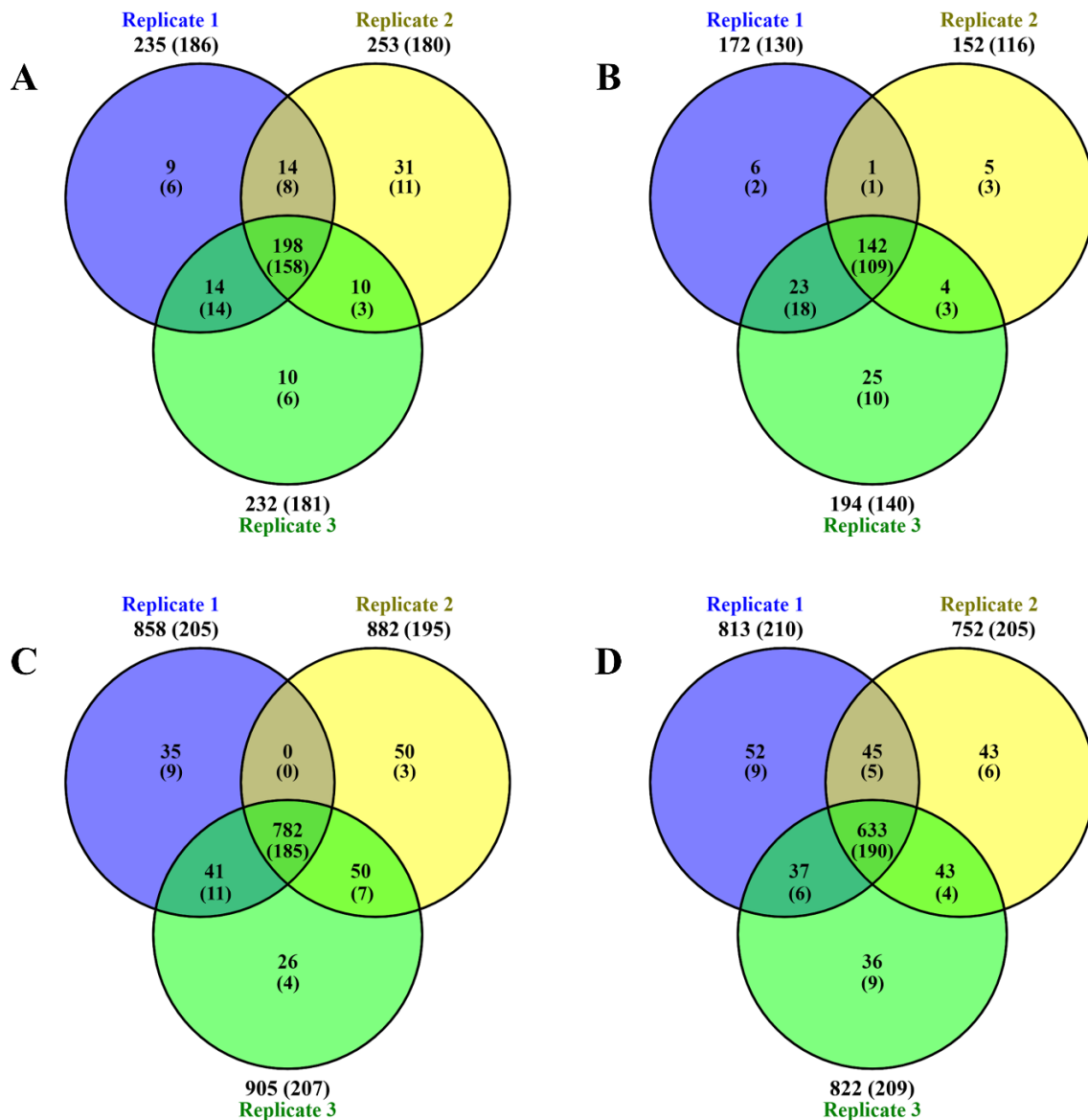
antifungal activity (Ali et al. 2018). Chitinolytic enzymes can also target the peritrophic matrix and the cuticle, which are two distinct insect structures (Berini et al. 2019).

Beta-lactamases were produced by both fungi: four by *T. versicolor* (17633, 17636, 23421, and 30240) and only one by *S. commune* (2646069), see table 3-13. These enzymes can be potentially used for multi-resistance to beta-lactam antibiotics (e.g., carbapenems, cephamycins, and penicillins) as described previously by Bush (2018). Each fungus secreted four cerato-platanin proteins (table 3-13), which can be used as biosurfactants and bioemulsifiers, as demonstrated Pitocchi et al. (2020). Only *S. commune* secreted seven thaumatin-like proteins in total (table 3-13). These proteins have antifungal activity and can provide tolerance to fungal pathogens, making them suitable for biopesticides candidates (Misra et al. 2016).

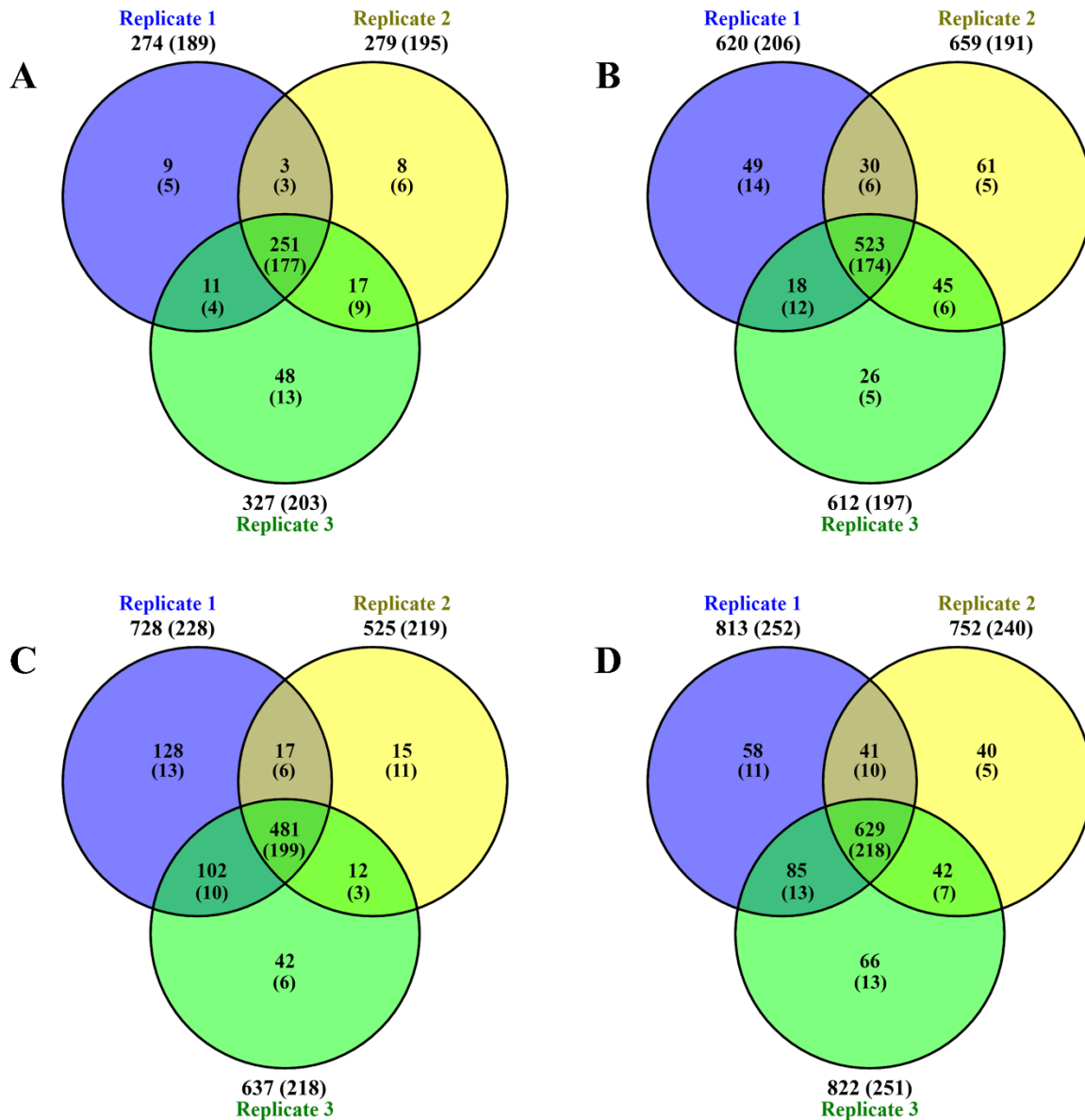
Laccase (EC 1.10.3.2), for example, is a well-studied enzyme released by both fungi in dual interaction, *S. commune* (lcc2-1194451), and *T. versicolor* (TvLac1-68023, TvLac2-146232, TvLac3-138261, and TvLac7-47314). The approach of Zolan and Pukkila (1986) can be used to isolate genomic DNA containing target genes (for example, lcc1 from *Coprinopsis cinerea*). Isolated genomic DNA is used to amplify a target gene (e.g., lcc1) using chosen PCR primers and accessible sequence information to make multiple copies of the specific sequence encoding the target protein (e.g., Kilaru (2006) lists primer pairs for a number of laccases). Isolated genomic DNA is used to perform PCR amplification of a target gene (e.g., lcc 1) using a chosen PCR primer and accessible sequence information to make many copies of the specific sequence encoding the target protein (e.g., listed primer pairs for a number of laccases). The targeted gene's PCR result is then often put into a cloning vector, which makes it easier for it to undergo convenient further amplification. Plasmids are the vectors that are employed with *E. coli* the most frequently (e.g., pYSK2 - *Saccharomyces cerevisiae*). The modified vector is then introduced into *E. coli* cells via a transformation procedure, and in the case of laccase, transformed into the momokaryotic strain FA2222 of *C. cinerea*, as the following step in the cloning process (lcc1). High levels of target gene expression are the next objective once the gene or cDNA encoding a possible target protein has been identified. These expression vectors come in a wide variety and are now readily available commercially. Each is obviously designed to function optimally in a particular host cell type. The transformant (carrying the lcc 1 gene) can be grown a greater quantity of the intended purified protein after a proper system of overexpression of the target gene has been achieved. After the fermentation, the crude protein is isolated by primary purification (e.g., crystallization). Enzymatic

proteolysis is used if the isolated protein needs modification (e.g., in case of insulin purification process, partially purified proinsulin is converted to crude insulin). Ion exchange and gel filtration can be used to purify the protein. To get highly pure protein, if required, the purified protein is processed by HPLC (e.g., PP-HPLC is used to get highly pure insulin) (Walsh 2015). In multicopper oxidases, laccases have potential biotechnological applications in the production of cosmetics, food and beverages, pulp and leather, paper, textiles, and wood products, as well as biosensor development, bioremediation, and textile and wood industries. (Kilaru 2006).

6 Supplementary data



Supplementary figure 1 Venn diagrams for comparison of the identified proteins (in secretome) from three biological replicates of four buffers (A – buffer 1, B – buffer 2, C – buffer 3, and D – buffer 4) from 10 days old *T. versicolor*-beech wood samples. Dikaryotic *T. versicolor* strain (*Tv*-D) was grown on beech wood particles (inoculated with one medium-free pellet) and incubated in dark at 25 °C. Numbers outside brackets are total identified proteins, and numbers in brackets are proteins with signal peptide.



Supplementary figure 2 Venn diagrams for comparison of the identified proteins (in secretome) from three biological replicates of four buffers (A – buffer 1, B – buffer 2, C – buffer 3, and D – buffer 4) from 28 days old *T. versicolor*-beech wood samples. Dikaryotic *T. versicolor* strain (*Tv*-D) was grown on beech wood particles (inoculated with one medium-free pellet), and incubated in dark at 25 °C. Numbers outside brackets are total identified proteins, and numbers in brackets are proteins with signal peptide.

Supplementary table 1: Proteases and peptidases identified in the shared dikaryotic *T. versicolor* strain (Tv-D) secretome between early (10 days) and late (28 days) stages of decay, grown as single culture on beech sapwood

JGI protein ID ^a	Putative protein function ^b	Family ^c	EC ^b	UP ^d	<i>pI</i> ^e	<i>Mw</i> ^e
Aspartic peptidases						
69348	Aspartyl protease; Pepsin A	A1	3.4.23.1	13	5.53	41328.01
40281	Aspergillopepsin	A1	3.4.23.18	9	5.12	27645.42
144202	Saccharopepsin	A1	3.4.23.25	27	4.9	44864.92
40186	Polyporoepsin	A1	3.4.23.29	53	5.07	44403.51
136392	Acid protease	A1	-	10	4.49	43480.83
54018	Acid protease	A1	-	15	4.66	43832.71
56073	Acid protease	A1	-	3	4.7	55558.16
Metallo peptidases						
170685	Zn-dependent exopeptidase	M28	-	20	4.99	50845.3
39578	Zn-dependent exopeptidase	M28	-	42	5.51	50028.63
27233	Leucine aminopeptidase-1	M28	3.4.11.1	6	5	43944.26
175022	Fungalysin	M36	-	89	5.27	64255.09
176097	Fungalysin	M36	-	23	5.48	63963.71
36519	Fungalysin	M36	-	54	5.19	64186.1
Serine peptidases						
57337	Serine carboxypeptidase	S10	-	13	5.29	52549.68
126828	Serine carboxypeptidase	S10	-	18	5.13	72100.51
133452	Serine carboxypeptidase	S10	-	7	5.52	72773.32
148659	Serine carboxypeptidase	S10	-	13	4.98	72850.23
32193	Serine carboxypeptidase	S10	-	9	4.8	53232.59
45058	Serine carboxypeptidase	S10	-	12	5.06	56145.72
70376	Serine carboxypeptidase	S10	-	12	5.14	56559.25
27131	Lysosomal Pro-X carboxypeptidase	S28	3.4.16.2	10	5.62	57650.71
110969	Lysosomal Pro-X carboxypeptidase	S28	3.4.16.2	14	5.59	58338.67
172472	Peptidase family S41	S41	-	23	5.64	73672.03
154838	C-terminal processing peptidase-like protein	S41A	-	55	5.19	72165.32
113847	Tripeptidyl-peptidase I	S53	3.4.14.9	210	4.91	57811.06

126771	Tripeptidyl-peptidase I	S53	3.4.14.9	20	4.95	67210.44
135882	Tripeptidyl-peptidase I	S53	3.4.14.9	20	4.71	68573.7
147958	Tripeptidyl-peptidase I	S53	3.4.14.9	154	5.21	63345.61
166188	Tripeptidyl-peptidase I	S53	3.4.14.9	44	4.8	58463.38
169734	Tripeptidyl-peptidase I	S53	3.4.14.9	5	4.99	67856.08
174508	Tripeptidyl-peptidase I	S53	3.4.14.9	34	5.51	67301.45
69742	Tripeptidyl-peptidase I	S53	3.4.14.9	82	5.25	65727.09
Others						
45345	Peptide N-acetyl- β -D-glucosaminyl asparaginase amidase A (PNGaseA)	-	-	40	5.3	62148.43

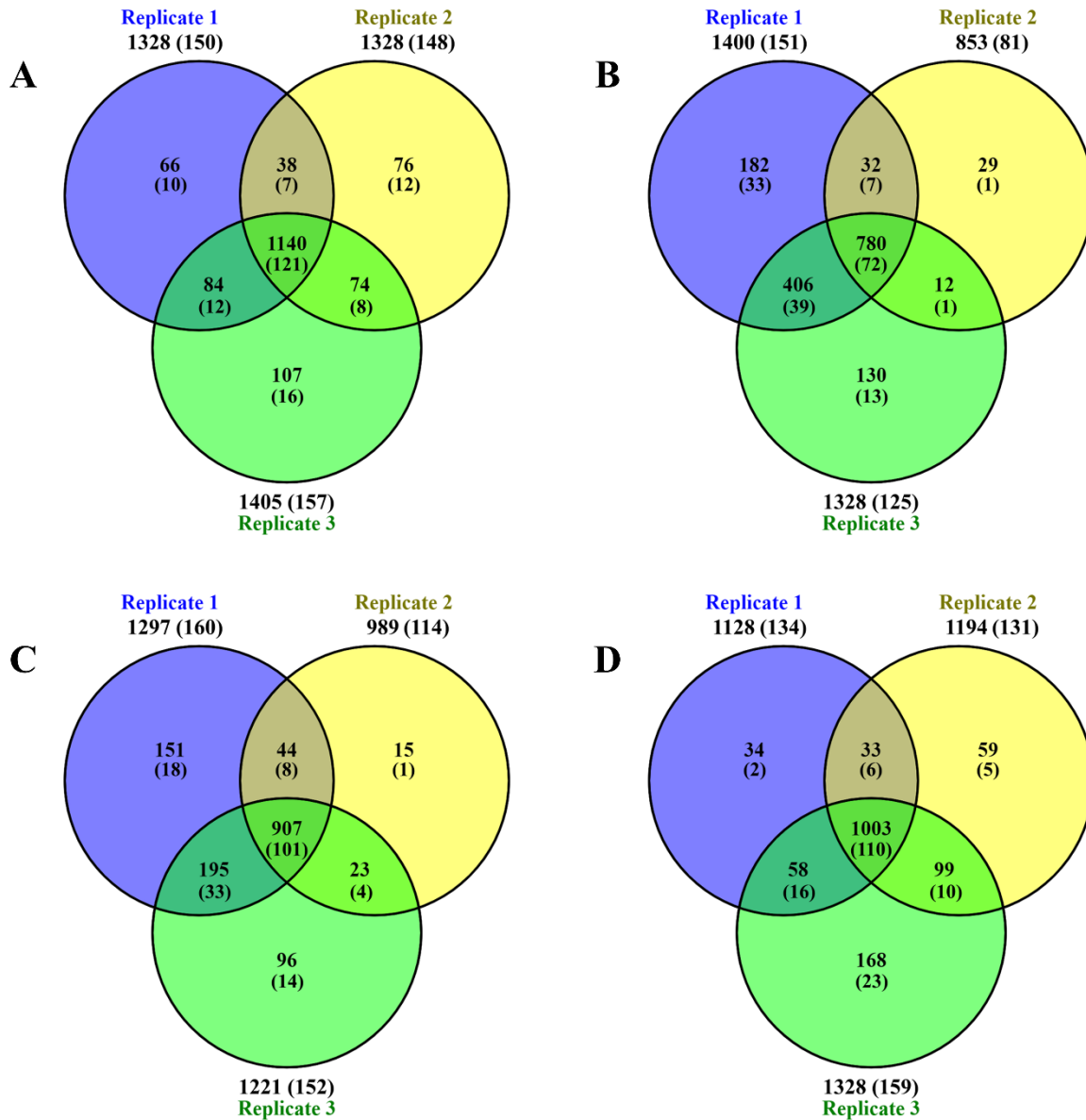
^a with signal peptide (predicted with SignalP-5.0 database). ^b Putative function for identified proteins was obtained from the JGI, InterPro, UniProt and NCBI databases. ^c MEROPS database was used for the family and subfamily information. ^d Unique peptides. ^e The theoretical *pI* (isoelectric point) and *M_w* (molecular weight) were computed based on protein sequence obtained from the JGI database.

Supplementary table 2: Proteins of other functions identified in the shared dikaryotic *T. versicolor* strain (Tv-D) secretome between early (10 days) and late (28 days) stages of decay, grown as single culture on beech sapwood

JGI protein ID ^a	Putative protein function ^b	Family ^c	EC ^c	UP ^d	pI ^e	Mw ^e
145154	Alkaline phosphatase domain	-	-	8	6.16	68306.24
128410	Amine oxidase; Polyamine oxidase	-	-	8	4.93	54278.75
43972	Carbohydrate-binding WSC domain	-	-	4	4.36	23406.38
35444	Domains of unknown function (DUF 5127, 4965, 1793)	-	-	20	5.79	74467.68
71601	Extracellular nuclease	-	-	31	5.07	65494.71
42899	Ferritin-like domain	-	-	42	4.69	31000.96
19890	GPI-anchored domain containing protein	-	-	4	6.11	13819.89
32323	GPI-anchored domain containing protein	-	-	5	6.53	14441.82
47480	Lactonase domain	-	-	8	4.95	42250.92
34378	PLC-like phosphodiesterases domain	-	-	11	4.85	32866.24
159259	Polysaccharide Lyase Family 8 protein	PL8_4	-	5	4.83	93244.28
30590	Predicted DNA repair exonuclease SIA1	-	-	10	5.29	43543.24
173910	Proteins containing the FAD binding domain	-	-	6	4.99	52836.72
52976	Purine nucleoside permease	-	-	35	5.43	44750.66
50621	SMP-30/Gluconolactonase/LRE-like region domain	-	-	24	5.7	44696.53
30524	α -amylase; Glycoside Hydrolase Family 13 / Carbohydrate-Binding Module Family 20 protein	GH13	3.2.1.1	14	5.17	62883.28
75646	Lipase class 3 (Triglyceride lipase)	CE10	3.1.1.3	6	5.81	32302.55
110860	α -glucosidase	GH31	3.2.1.20	38	5.26	105704.5
140830	α -glucosidase	GH31	3.2.1.20	9	5.19	106792.6
175557	α , α -trehalase	GH37	3.2.1.28	4	5	82401.06
68145	Acid phosphatase	-	3.1.3.2	3	5.13	59588.21
144865	β -glucuronidase	GH79	3.2.1.31	14	5.44	56864.74
26555	β -glucuronidase	GH79	3.2.1.31	9	7.72	49293.38

138540	Sphingomyelin phosphodiesterase	-	3.1.4.12	11	5.83	74293.61
170137	Lysophospholipase	-	3.1.1.5	11	4.57	63790.85
147020	Glucosylceramidase	GH30_3	3.2.1.45	4	5.18	59672.36
45289	α -N-acetylglucosaminidase	GH89	3.2.1.50	3	5.13	82239.41
31157	Ceramidases	-	3.5.1.23	27	5.59	77471.7
174308	Acetylcholinesterase	-	3.1.1.7	11	6.47	58355.63
173577	5' nucleotidase	-	3.1.3.5	11	5.8	68956.39
165641	5'-nucleotidase	-	3.1.3.5	6	5.27	34000.26
59656	5'-nucleotidase	-	3.1.3.5	8	5.16	31589.53
133552	Amidases; Carbon--nitrogen ligases with glutamine as amido-N-donor	-	3.5.1.4	87	5.72	58436.47
74521	Amidases	-	3.5.1.4	35	6.9	70635.98
161547	Amidases; Carbon--nitrogen ligases with glutamine as amido-N-donor	-	3.5.1.4	52	5.46	58435.56
125858	Oxalate decarboxylase	-	4.1.1.2	34	5.19	47190.02
55174	Ribonuclease, T2 family	-	4.6.1.19	6	5.77	33808.97
67924	Ribonuclease, T2 family	-	4.6.1.19	6	5.36	40711.98

^a with signal peptide (predicted with SignalP-5.0 database). ^b Putative function for identified proteins was obtained from the JGI, InterPro, UniProt and NCBI databases. ^c Carbohydrate-active enzymes database (CAZy) was used for the family information and for the enzyme commission number (EC number). ^d Unique peptides. ^e The theoretical *pI* (isoelectric point) and *M_w* (molecular weight) were computed based on protein sequence obtained from the JGI database.



Supplementary figure 3 Venn diagrams for comparison of the identified intracellular proteins from three biological replicates of four buffers (A – buffer 1, B – buffer 2, C – buffer 3 and D – buffer 4) from 28 days old *T. versicolor*-beech wood samples. Dikaryotic *T. versicolor* strain (*Tv*-D) was grown on beech wood particles (inoculated with one medium-free pellet) and incubated in dark at 25 °C. Numbers outside brackets are total identified proteins, and numbers in brackets are proteins with signal peptide.

Supplementary table 3: Intracellular proteins identified with potential functions in carbohydrate metabolism of dikaryotic *T. versicolor* strain (*Tv*-D) grown on beech sapwood (28 days old samples)

JGI protein ID	Putative protein function	EC	UP^a	<i>pI</i>^b	<i>Mw</i>^b
Ascorbate and aldarate metabolism					
150625	Monodehydroascorbate/ferredoxin reductase	1.6.5.4	16	7.78	58471.2
Butanoate metabolism					
43893	4-aminobutyrate aminotransferase.	2.6.1.19	7	7.45	48107.72
61639	Proteins containing the FAD binding domain	1.1.1.4	4	6.81	61513.98
Carbohydrate transport and metabolism					
118020	Dimeric dihydrodiol dehydrogenase	1.3.1.20	3	6.85	48764.75
148872	Dimeric dihydrodiol dehydrogenase	1.3.1.20	14	6.67	41156.19
38225	Dimeric dihydrodiol dehydrogenase	1.3.1.20	20	7.25	41955.05
155066	GDP-L-fucose synthetase		6	6.75	36364.5
69087	Glucosamine-6-phosphate isomerase		2	6.91	115222.25
62774	Glucosidase I		2	5.78	126080.85
69032	Glycolipid transfer protein		7	6.58	22027.31
168170	Predicted sugar kinase		7	7.1	36267.81
117268	Ribokinase		2	5.07	38267.39
153104	Trehalose-6-phosphate synthase component TPS1 and related subunits		7	6.62	101271.49
169188	Trehalose-6-phosphate synthase component TPS1 and related subunits		9	6.13	58039.58
Citrate cycle (TCA cycle)					
152358	2-oxoglutarate dehydrogenase; E1 subunit	1.2.4.2	20	7.22	113071.15
170534	Aconitase/homoaconitase (aconitase superfamily)	4.2.1.3	44	6.58	85235.79
55659	Aconitase/homoaconitase (aconitase superfamily)	4.2.1.3	4	6.58	86904.74
144973	Citrate synthase	2.3.3.1	27	8.25	51151.04
48824	Citrate synthase	2.3.3.1	29	8.37	51092.49
127790	Dihydrolipoamide dehydrogenase	1.8.1.4	12	7.62	53628.37
30906	Dihydrolipoamide succinyltransferase (2-oxoglutarate dehydrogenase; E2 subunit)	2.3.1.61	11	5.92	45664.26
110343	Fumarase	4.2.1.2	13	6.99	54367.29

118212	Isocitrate dehydrogenase; alpha subunit	1.1.1.41	17	8.36	39091.03
163469	Isocitrate dehydrogenase; alpha subunit	1.1.1.42	10	6.95	38501.44
27411	Isocitrate dehydrogenase; gamma subunit	1.1.1.41	8	8.7	40582.58
144781	NAD-dependent malate dehydrogenase	1.1.1.37	28	8.96	35513.79
64103	NAD-dependent malate dehydrogenase	1.1.1.37	39	6.56	34579.12
31439	NADP-dependent isocitrate dehydrogenase		29	8.28	49949.34
69281	Phosphoenolpyruvate carboxykinase (ATP)	4.1.1.49	27	6.12	63188.9
72201	Pyruvate carboxylase	6.4.1.1	42	6.75	131640.85
50112	Succinate dehydrogenase membrane anchor subunit and related proteins	1.3.5.1	4	10.07	17919.69
59445	Succinate dehydrogenase; cytochrome b subunit	1.3.5.1	6	10.46	19281.51
66104	Succinate dehydrogenase; Fe-S protein subunit	1.3.5.1	4	8.23	30761.51
28260	Succinate dehydrogenase; flavoprotein subunit	1.3.5.1	27	7.06	70323.85
41748	Succinyl-CoA synthetase; alpha subunit	6.2.1.4	7	9.22	34536.9
158886	Succinyl-CoA synthetase; beta subunit	6.2.1.5	13	6.1	44281.8
Fructose and mannose metabolism					
118839	Cytoskeletal protein Adducin	4.1.2.17	10	7.17	32077.52
27785	Cytoskeletal protein Adducin	4.1.2.17	4	6.58	31507.93
57857	Fructose-6-phosphate 2-kinase/fructose-2;6-biphosphatase	3.1.3.46	2	7.61	60474.69
23861	GDP-mannose 4;6 dehydratase	4.2.1.47	11	7.59	45546.86
69034	Mannose-1-phosphate guanylyltransferase (GDP)	2.7.7.22	13	6.48	52805.71
171697	Mannose-6-phosphate isomerase	5.3.1.8	3	6.33	45211.76
124166	Phosphomannomutase	5.4.2.8	12	6.31	28966.25
144293	Sorbitol dehydrogenase	1.1.1.14	17	6.62	40496.71
153168	Sorbitol dehydrogenase	1.1.1.14	5	7.58	40627.84
30336	Sorbitol dehydrogenase	1.1.1.14	5	6.46	37768.78
73393	Sorbitol dehydrogenase	1.1.1.14	18	6.36	37819.66
Galactose metabolism					
37740	Galactokinase	2.7.1.6	3	5.76	59374.73
153721	Galactonate dehydratase	4.2.1.6	16	5.73	51292.72
30881	Galactonate dehydratase	4.2.1.6	3	5.84	42865.2

146103	Maltase glucoamylase and related hydrolases; glycosyl hydrolase family 31	3.2.1.20	14	6.5	88455.31
Glycolysis / Gluconeogenesis					
146294	3-phosphoglycerate kinase	2.7.2.3	34	6.76	44943.58
67500	Acetate--CoA ligase.	6.2.1.1	23	6.89	73915.24
27966	Alcohol dehydrogenase (NADP+).	1.1.1.2	22	7.64	33488.41
32150	Alcohol dehydrogenase (NADP+).	1.1.1.2	7	8.86	37470
34454	Alcohol dehydrogenase.	1.1.1.1	5	5.52	36623.22
18373	Alcohol dehydrogenase; class III	1.1.1.1	18	6.74	40345.14
69690	Alcohol dehydrogenase; class IV	1.1.1.1	24	7.64	53334.11
131096	Alcohol dehydrogenase; class V	1.1.1.1	10	7.38	37957.03
130913	Aldehyde dehydrogenase	1.2.1.28	9	6.63	52360.09
24751	Aldehyde dehydrogenase	1.2.1.3	2	8.72	57765.48
26150	Aldehyde dehydrogenase	1.2.1.3	58	6.71	55070.8
27280	Aldehyde dehydrogenase	1.2.1.3	21	5.42	54540.39
44528	Aldehyde dehydrogenase	1.2.1.5	2	5.66	56139.77
75105	Aldehyde dehydrogenase	1.2.1.8	9	5.44	52290.77
142659	Aldehyde dehydrogenase	1.2.1.16	17	7.82	55312.6
139210	Dihydrolipoamide acetyltransferase	2.3.1.12	6	7.47	47598.46
165929	Dihydrolipoamide acetyltransferase	2.3.1.12	2	5.23	29968.07
54983	Enolase	4.2.1.11	44	5.76	47080.56
31116	Fructose 1;6-bisphosphate aldolase	4.1.2.13	25	6.1	39145.3
70572	Fructose-1;6-bisphosphatase	3.1.3.11	14	6.44	37001.34
116044	Glucokinase.	2.7.1.2	13	5.29	57278.97
171831	Glucose-6-phosphate isomerase	5.3.1.9	19	6.54	61645.05
30062	Glyceraldehyde 3-phosphate dehydrogenase	1.2.1.12	19	7.81	36532.8
156755	Hexokinase.	2.7.1.1	9	5.48	54657.53
157183	Phosphoglucomutase	5.4.2.2	23	6.49	61134.15
61994	Phosphoglycerate mutase	5.4.2.1	3	6.89	25171.53
25215	Phosphoglycerate mutase	5.4.2.1	12	6	57027
29629	Pyrophosphate-dependent phosphofructo-1-kinase	2.7.1.11	3	7.53	90030.06
147039	Pyruvate decarboxylase.	4.1.1.1	18	5.74	67149.65

27891	Pyruvate dehydrogenase E1; alpha subunit	1.2.4.1	16	7.58	44527.46
116783	Pyruvate dehydrogenase E1; beta subunit	1.2.4.1	13	5.18	35605.93
110904	Pyruvate kinase	2.7.1.40	43	7.99	57885.67
171695	Triosephosphate isomerase	5.3.1.1	18	6.8	26770.77
Glyoxylate and dicarboxylate metabolism					
48950	Formamidase	3.5.1.49	14	5.55	44972.17
53612	Formamidase	3.5.1.49	2	5.38	35032.82
52212	Glyoxylate/hydroxypyruvate reductase (D-isomer-specific 2-hydroxy acid dehydrogenase superfamily)		11	6.95	36365.81
56391	Glyoxylate/hydroxypyruvate reductase (D-isomer-specific 2-hydroxy acid dehydrogenase superfamily)		63	7.51	43382.57
157876	Isocitrate lyase	4.1.3.1	10	6.81	62860.5
166243	Isocitrate lyase	4.1.3.1	13	6.68	59891.86
Others					
156418	Glycoside Hydrolase Family 15 protein		2	6.43	78151.04
127375	Glycoside Hydrolase Family 3 protein		9	5.68	59488.63
146818	Glycoside Hydrolase Family 3 protein		19	6.26	94628.6
151588	Glycoside Hydrolase Family 3 protein		12	4.99	75425.19
71035	Glycoside Hydrolase Family 3 protein		9	5.92	92922.52
155564	Glycoside Hydrolase Family 5 protein		34	6.34	55504.77
173244	Glycoside Hydrolase Family 5 protein		6	4.85	73101.97
40418	Glycoside Hydrolase Family 5 protein		9	6.04	55653.03
116333	Glycoside Hydrolase Family 92 protein		2	5.1	81607.24
39070	Glycoside Hydrolase Family 95 protein		2	4.85	89823.9
142708	Glycoside hydrolase/deacetylase, beta/alpha-barrel domains		24	5.4	35436.3
Pentose and glucuronate interconversions					
141490	2-deoxy-D-gluconate 3-dehydrogenase.	1.1.1.125	5	8.53	32042.28
28675	2-deoxy-D-gluconate 3-dehydrogenase.	1.1.1.125	3	7.46	26516.39
30865	2-deoxy-D-gluconate 3-dehydrogenase.	1.1.1.125	3	7.65	28004.32
122117	Aldehyde reductase.	1.1.1.21	6	6.55	32486.28
158451	D-ribulose-5-phosphate 3-epimerase	5.1.3.1	2	5.42	24171.08
168510	Predicted transporter (major facilitator superfamily)	5.3.1.4	2	7.24	57901.98

72562	Predicted transporter (major facilitator superfamily)	5.3.1.4	2	6.73	60797.77
63604	Ribulose kinase and related carbohydrate kinases	2.7.1.47	13	6.34	63429.47
174648	Sugar (pentulose and hexulose) kinases	2.7.1.17	8	5.71	82369.3
43337	UDP-glucose pyrophosphorylase	2.7.7.9	44	7.45	56941.35
60939	UDP-glucose/GDP-mannose dehydrogenase	1.1.1.22	8	6.45	51324.96
Pentose phosphate pathway					
42264	6-phosphogluconate dehydrogenase	1.1.1.44	42	6.67	53284.23
42276	6-phosphogluconolactonase - like protein	3.1.1.31	6	6.07	28388.49
144139	Glucose-6-phosphate 1-dehydrogenase	1.1.1.49	40	8.11	58576.08
172153	Ribose 5-phosphate isomerase	5.3.1.6	7	6.88	34197.61
111781	Transaldolase	2.2.1.2	5	5.64	36248.47
30435	Transaldolase	2.2.1.2	26	6.11	35645.83
149921	Transketolase	2.2.1.1	45	6.37	69528.4
64053	Transketolase	2.2.1.1	19	6.74	74305.14
Propanoate metabolism					
161508	2-methylcitrate dehydratase	4.2.1.79	15	8.51	59372.94
Pyruvate metabolism					
116179	Acetyl-CoA acetyltransferase	2.3.1.9	22	8.04	43115.51
52138	Glycolate oxidase	1.1.2.3	20	6.59	56972.89
68523	Glycolate oxidase	1.1.2.3	4	6.49	54177.93
114667	Glyoxalase	4.4.1.5	12	6.01	17233.46
145964	Glyoxylase	3.1.2.6	8	5.75	27071.43
56326	Malate synthase	2.3.3.9	36	6.89	60513.39
47905	Sulfite reductase (ferredoxin)	1.2.1.51	3	6.39	155674.71

^a Unique peptides. ^b The theoretical *pI* (isoelectric point) and *M_w* (molecular weight) were computed based on protein sequence obtained from the JGI database.

Supplementary table 4: Intracellular proteins identified with potential functions in metabolism of complex carbohydrates of dikaryotic *T. versicolor* strain (*Tv-D*) grown on beech sapwood (28 days old samples)

JGI protein ID	Putative protein function	EC	UP ^a	<i>pI</i> ^b	<i>Mw</i> ^b
26884	1;4-alpha-glucan branching enzyme/starch branching enzyme II	2.4.1.18	19	6.4	80397.21
164154	Adaptor protein Enigma and related PDZ-LIM proteins	3.2.1.58	3	4.84	80750.88
30268	Alpha-mannosidase	3.2.1.24	24	6.62	128044.88
139454	CCCH-type Zn-finger protein	3.2.1.18	2	8.34	80556.64
27115	Chitin synthase/hyaluronan synthase (glycosyltransferases)	2.4.1.16	2	6.28	220057.95
30462	Dolichol-phosphate mannosyltransferase	2.4.1.83	3	7.93	30364.14
118501	Glycolipid 2-alpha-mannosyltransferase (alpha-1;2-mannosyltransferase)	2.4.1.131	6	5.81	44827.51
155607	Glycosyltransferase Family 3 protein		13	6.27	84090.94
59694	Glycosyltransferase Family 35 protein		58	6.45	98624.29
54992	In phosphorous-containing anhydrides.	3.6.1.-	3	6.1	50756.45
116241	In phosphorous-containing anhydrides.	3.6.1.-	6	6.48	50721.04
150302	Neutral trehalase	3.2.1.28	2	6.2	90749.43
159039	Phosphoglucomutase/phosphomannomutase	5.4.2.3	11	6.41	59248.34
162659	Predicted beta-mannosidase	3.2.1.25	12	5.64	97937.41
30186	Projectin/twitchin and related proteins	3.2.1.3	6	4.36	162795.14
158031	UDP-N-acetylglucosamine pyrophosphorylase	2.7.7.23	11	6.07	54044.21
72126	Alpha amylase	3.2. 1.1	18	6.23	177069.89

^a Unique peptides. ^b The theoretical *pI* (isoelectric point) and *Mw* (molecular weight) were computed based on protein sequence obtained from the JGI database.

Supplementary table 5: Intracellular proteins identified with potential functions in amino acid metabolism of dikaryotic *T. versicolor* strain (*Tv*-D) grown on beech sapwood (28 days old samples)

JGI protein ID	Putative protein function	EC	UP ^a	pI ^b	M _w ^b
Glycine, serine and threonine metabolism					
29244	Alanine-glyoxylate aminotransferase AGT1	2.6.1.44	7	6.8	41855.01
71817	Aminomethyl transferase	2.1.2.10	5	8.24	44457.06
157861	Betaine aldehyde dehydrogenase	-	7	6.24	69297.58
50107	Cystathionine beta synthase (CBS) domain	-	2	8.88	17890.50
124382	Cystathionine beta-synthase and related enzymes	4.2.1.22	2	6.74	41374.08
111474	D-3-phosphoglycerate dehydrogenase; D-isomer-specific 2-hydroxy acid dehydrogenase superfamily	1.1.1.95	6	7.59	35338.77
62115	D-3-phosphoglycerate dehydrogenase; D-isomer-specific 2-hydroxy acid dehydrogenase superfamily	1.1.1.95	10	6.81	50613.97
144610	Glucose dehydrogenase/choline dehydrogenase/mandelonitrile lyase (GMC oxidoreductase family)	1.1.99.1	80	6.61	72238.51
174536	Glucose dehydrogenase/choline dehydrogenase/mandelonitrile lyase (GMC oxidoreductase family)	1.1.99.1	8	6.25	65329.14
43286	Glucose dehydrogenase/choline dehydrogenase/mandelonitrile lyase (GMC oxidoreductase family)	1.1.99.1	8	5.81	66710.39
157272	Glycine/serine hydroxymethyltransferase	2.1.2.1	11	6.99	51882.22
30896	Homoserine dehydrogenase	1.1.1.3	9	6.27	38946.58
64570	NAD dependent epimerase	1.1.1.103	8	5.52	35956.01
132830	Phosphatidylserine decarboxylase	4.1.1.65	3	6.29	43246.33
156844	Phosphoserine aminotransferase	2.6.1.52	4	6.47	44446.67
55693	Threonine aldolase	4.1.2.5	2	6.8	43160.54
Tryptophan metabolism					
49388	3-deoxy-7-phosphoheptulonate synthase	2.5.1.54	8	8.43	43543.97
152599	3-hydroxyanthranilate oxygenase HAAO	1.13.11.6	4	6.04	19944.77
160039	Amidases	3.5.1.4	8	5.78	63308.25
25794	Amidases	3.5.1.4	8	6.25	61534.27
55560	Amidases	3.5.1.4	4	5.88	60595.1
73684	Amidases	3.5.1.5	16	7.76	61089.17

133329	Catalase	1.11.1.6	2	5.97	58544.32
152398	Catalase	1.11.1.6	105	7.3	57074.46
49962	Collagens (type IV and type XIII); and related proteins	6.3.2.-	2	5.88	94752.96
47250	Drebrins and related actin binding proteins	6.3.2.-	5	4.7	66707.4
66590	Extracellular protein SEL-1 and related proteins	6.3.2.-	4	7.83	89844.89
27749	L-kynurenine hydrolase	3.7.1.3	13	5.83	49856.26
116156	Predicted metal-dependent hydrolase of the TIM-barrel fold	4.1.1.45	5	6.25	42618.4
173545	Predicted proline-serine-threonine phosphatase-interacting protein (PSTPIP)	6.3.2.-	2	8.27	105791.84
150046	Protein interacting with poly(A)-binding protein	6.3.2.-	6	9.65	89777.51
118725	SWI-SNF chromatin-remodeling complex protein	6.3.2.-	13	6.97	150807.09
Lysine biosynthesis					
56842	Aromatic amino acid aminotransferase and related proteins	2.6.1.-	9	5.99	59140.34
145691	Dihydrodipicolinate synthetase domain		8	6.8	35446.61
29711	Dihydrodipicolinate synthetase domain		9	6.8	33055.95
150870	Homoaconitate hydratase.	4.2.1.36	3	7.33	77716.57
34780	Kynurenine aminotransferase; glutamine transaminase K	2.6.1.-	4	5.9	48926.53
55646	Lysine-ketoglutarate reductase/saccharopine dehydrogenase	1.5.1.7	5	5.88	40841.59
171224	Non-ribosomal peptide synthetase/alpha-aminoadipate reductase and related enzymes	1.2.1.31	3	5.84	154555.26
109189	Nucleosome remodeling factor; subunit CAF1/NURF55/MSI1	2.3.1.-	4	4.89	51019.61
Lysine degradation					
147704	Fructose 1;6-bisphosphate aldolase	4.1.2.-	5	5.15	31509.15
26793	Signal peptidase complex subunit	3.4.-.-	3	9.15	19906.71
Valine, leucine and isoleucine biosynthesis					
163369	3-isopropylmalate dehydratase (aconitase superfamily)	4.2.1.33	8	6.13	82984.01
39797	3-isopropylmalate dehydratase (aconitase superfamily)	4.2.1.33	12	5.91	82047.93
44509	3-isopropylmalate dehydrogenase	1.1.1.85	29	5.48	40277.5
43512	Acetolactate synthase; small subunit	2.2.1.6	2	6.69	37751.26
108904	Branched chain aminotransferase BCAT1; pyridoxal phosphate enzymes type IV superfamily	2.6.1.42	9	7.32	41510.87
112760	Dihydroxy-acid dehydratase	4.2.1.9	36	6.8	62673.14

71513	Dihydroxy-acid dehydratase	4.2.1.9	4	7.13	64531.08
55496	Ketol-acid reductoisomerase (NADP+)	1.1.1.86	19	5.37	37367.48
Valine, leucine and isoleucine degradation					
61238	3-Methylcrotonyl-CoA carboxylase; biotin-containing subunit/Propionyl-CoA carboxylase; alpha chain/Acetyl-CoA carboxylase; biotin carboxylase subunit	6.4.1.4	6	5.59	132322.2
61659	3-Methylcrotonyl-CoA carboxylase; biotin-containing subunit/Propionyl-CoA carboxylase; alpha chain/Acetyl-CoA carboxylase; biotin carboxylase subunit	6.4.1.4	2	6.34	85379.1
145549	Isovaleryl-CoA dehydrogenase	1.3.99.10	2	8.39	46415.92
61985	Methylmalonate semialdehyde dehydrogenase	1.2.1.27	15	7.8	58696.95
56981	Propionyl-CoA carboxylase	6.4.1.3	4	8.67	59796.54
Phenylalanine, tyrosine and tryptophan biosynthesis					
156387	Anthranilate phosphoribosyltransferase	2.4.2.18	5	6.8	38413.09
46764	Chorismate mutase	5.4.99.5	3	6.26	34460.24
17003	Chorismate synthase	4.2.3.5	7	6.95	43580.42
64032	Isochorismate synthase	4.1.3.27	6	6.77	56677.34
173713	Phenylalanine and histidine ammonia-lyase	4.3.1.5	24	6.47	79084.19
57752	Prephenate dehydrogenase (NADP+)	1.3.1.13	2	6.93	51172.85
61512	Tryptophan synthase beta chain	4.2.1.20	8	6.08	76170.82
Tyrosine metabolism					
124955	Homogentisate 1;2-dioxygenase	1.13.11.5	13	7.16	57455.18
20432	Homogentisate 1;2-dioxygenase	1.13.11.5	3	6.34	52918.69
164961	Kynurenine aminotransferase; glutamine transaminase K	2.6.1.1	10	7.07	57392.2
138052	Phenylpyruvate tautomerase	5.3.2.1	3	5.89	13536.27
36441	Phenylpyruvate tautomerase	5.3.2.1	3	5.41	13327.02
Arginine and proline metabolism					
155351	Copper amine oxidase	1.4.3.6	11	6.24	82319.75
34882	Delta-1-pyrroline-5-carboxylate dehydrogenase	1.5.1.12	18	7.23	59583.85
130721	Diamine acetyltransferase	2.3.1.57	2	5.65	18122.67
59093	Soluble epoxide hydrolase (Prolyl aminopeptidase)	3.4.11.5	8	5.67	35431.98
Histidine metabolism					

117325	Histidinol dehydrogenase	1.1.1.23	10	5.36	90444.26
60950	Metalloexopeptidases	3.4.13.20	31	5.43	52556.97
28029	O-methyltransferase	2.1.1.-	25	5.36	24525.8
62921	Protein arginine N-methyltransferase PRMT1 and related enzymes	2.1.1.-	6	5.39	39893.56
Methionine metabolism					
114509	Homoserine acetyltransferase domain		3	6.67	35912.91
164252	Methionine synthase, vitamin-B12 independent domain		26	6.26	45489.07
151784	S-adenosylhomocysteine hydrolase	3.3.1.1	23	6.24	46931.94
145618	S-adenosylmethionine synthetase	2.5.1.6	26	6.15	42816.49
Alanine and aspartate metabolism					
109115	Aspartate aminotransferase/Glutamic oxaloacetic transaminase AAT1/GOT2	2.6.1.1	10	9.14	46774.53
145091	Aspartate aminotransferase/Glutamic oxaloacetic transaminase AAT2/GOT1	2.6.1.1	16	7.22	45307.63
64917	Carnitine O-acyltransferase CRAT	2.3.1.7	6	7.18	70191.54
Cysteine metabolism					
26407	Cysteine synthase	2.5.1.47	5	8.47	38246.56
Glutamate metabolism					
172749	Glucosamine 6-phosphate synthetases; contain amidotransferase and phosphosugar isomerase domains	2.6.1.16	23	6.66	77207.94
Amino acid transport and metabolism					
50581	Acetylglutamate kinase/acetylglutamate synthase		25	8.6	95730.21
110523	Alpha-isopropylmalate synthase/homocitrate synthase		9	6.32	50401.23
36100	Alpha-isopropylmalate synthase/homocitrate synthase		10	5.56	87905.08
160974	Anthranilate synthase component II		3	6.62	84695.4
161451	Bleomycin hydrolases and aminopeptidases of cysteine protease family	3.4.22.40	9	5.5	55690.05
45346	C1-tetrahydrofolate synthase		35	6.86	100995.1
118736	C-3 sterol dehydrogenase/3-beta-hydroxysteroid dehydrogenase and related dehydrogenases		6	6.71	46715.43
122801	C-3 sterol dehydrogenase/3-beta-hydroxysteroid dehydrogenase and related dehydrogenases		4	6.88	48161.68
28212	Carbon-nitrogen hydrolase		10	5.81	33138.6

142870	Cystathionine beta-lyases/cystathionine gamma-synthases		5	6.89	43768.91
21006	Cystathionine beta-lyases/cystathionine gamma-synthases		5	6.68	99577.86
24316	Cystathionine beta-lyases/cystathionine gamma-synthases		11	6.76	47150.97
62114	Glutamine amidotransferase/cyclase	2.4.2.-	2	5.96	60796.61
45290	M13 family peptidase	3.4.24.71	11	4.96	97303.07
158584	Prephenate dehydratase		2	4.99	34265.71
55832	Proline oxidase	1.5.3.-	4	7.49	40120.96
161325	Puromycin-sensitive aminopeptidase and related aminopeptidases	3.4.11.14	2	5.71	101006.84
148553	Putative glutamate/ornithine acetyltransferase		8	6.05	49850.4
162831	Serine racemase	5.1.1.-	2	6.15	34835.74
119185	Thiamine pyrophosphate-requiring enzyme		6	8	71806.56
40679	Thiamine pyrophosphate-requiring enzyme		4	6.28	63351.39
67419	Thiamine pyrophosphate-requiring enzyme		5	5.56	64394.32
160600	Threonine/serine dehydratases		2	6.25	59831.67
114596	Xaa-Pro aminopeptidase	3.4.11.9	3	8.71	82206.76
176228	Xaa-Pro aminopeptidase	3.4.11.9	5	5.69	68521.63
27763	Xaa-Pro aminopeptidase	3.4.11.9	8	5.9	45621.56
Metabolism of amino groups					
144048	Acetylornithine aminotransferase	2.6.1.11	3	8.12	52638.28
119923	Arginase	3.5.3.1	2	6.01	33745.74
27767	Argininosuccinate lyase	4.3.2.1	8	6.37	51807.41
59636	Argininosuccinate synthase	6.3.4.5	15	5.83	47430.3
53623	Lysine-ketoglutarate reductase/saccharopine dehydrogenase	2.5.1.16	25	5.94	82411.75
155608	Ornithine carbamoyltransferase OTC/ARG3	2.1.3.3	4	7.89	41505.61

^a Unique peptides. ^b The theoretical *pI* (isoelectric point) and *M_w* (molecular weight) were computed based on protein sequence obtained from the JGI database.

Supplementary table 6: Intracellular proteins identified with potential functions in nucleotide metabolism of dikaryotic *T. versicolor* strain (*Tv*-D) grown on beech sapwood (28 days old samples)

JGI protein ID	Putative protein function	EC	UP ^a	pI ^b	M _w ^b
Nucleotide transport and metabolism					
28989	AICAR transformylase/IMP cyclohydrolase/methylglyoxal synthase		10	6.88	58538.71
70332	dTDP-glucose 4-6-dehydratase/UDP-glucuronic acid decarboxylase	4.1.1.35	15	7.1	48832.52
135620	Equilibrative nucleoside transporter protein		2	5.34	17492.85
33049	Glycinamide ribonucleotide synthetase (GARS)/Aminoimidazole ribonucleotide synthetase (AIRS)		5	5.26	81976.2
57263	Methylthioadenosine phosphorylase MTAP	2.4.2.28	8	6.36	34120.9
36446	Pyridine nucleotide-disulphide oxidoreductase		14	6.74	51011.28
120740	Uridylate kinase/adenylate kinase	2.7.4.-	3	5.86	28799.65
Purine metabolism					
35205	Adenine phosphoribosyl transferases	2.4.2.7	8	6.34	20009.4
146611	Adenylate kinase	2.7.4.3	3	9.02	28949.45
170800	Adenylosuccinate lyase	4.3.2.2	7	6.55	54256.06
57620	Adenylosuccinate synthase	6.3.4.4	3	6.94	47351.54
115397	Atrazine chlorohydrolase/guanine deaminase	3.5.4.3	11	6.06	52682.97
121597	Atrazine chlorohydrolase/guanine deaminase	3.5.4.3	2	5.86	51467.66
30298	Dihydroorotase and related enzymes	3.5.2.5	7	5.43	49804.1
31580	Exopolyphosphatases and related proteins	3.6.1.11	3	6.19	46391.52
65411	GMP synthase	6.3.5.2	12	6.41	59903
58836	Guanylate kinase	2.7.4.8	4	6.23	22423.46
144891	IMP dehydrogenase/GMP reductase	1.1.1.205	11	7.7	58487.05
153612	IMP dehydrogenase/GMP reductase	1.1.1.205	4	7.94	35637.32
28124	Nucleoside diphosphate kinase	2.7.4.6	24	8.14	16619.26
165737	Peroxisome assembly factor 2 containing the AAA+-type ATPase domain	3.6.1.3	2	5.17	105502.86
144724	Phosphoribosylamidoimidazole-succinocarboxamide synthase	4.1.1.21	3	7.38	62443.36
20372	Phosphoribosylamidoimidazole-succinocarboxamide synthase	6.3.2.6	3	5.56	33623.44

67804	Possible pfkB family carbohydrate kinase (Adenosine kinase)	2.7.1.20	14	5.32	36685.86
142741	Predicted ATP-dependent RNA helicase FAL1; involved in rRNA maturation; DEAD-box superfamily	3.6.1.3	10	5.56	44694.34
29473	Urease	3.5.1.5	5	6.29	89930.59
156281	Uricase (urate oxidase)	1.7.3.3	16	6.81	36000.98
Pyrimidine metabolism					
156600	Bis(5'-nucleosyl)-tetrphosphatase (asymmetrical).	3.6.1.17	5	6.95	15530.12
151856	CTP synthase (UTP-ammonia lyase)	6.3.4.2	6	6.63	67519.64
140806	Cytosine deaminase FCY1 and related enzymes	3.5.4.1	2	4.89	18266.48
58917	Dihydroorotate dehydrogenase	1.3.98.1	2	7.55	53890.22
143884	dUTP pyrophosphatase.	3.6.1.23	4	5.89	16576.86
173716	Multifunctional pyrimidine synthesis protein CAD (includes carbamoyl-phosphate synthetase; aspartate transcarbamylase; and glutamine amidotransferase)	6.3.5.5	6	5.63	128585.91
39957	Purine nucleoside phosphorylase	2.4.2.1	3	6.89	33750.55
28460	Ribonucleotide reductase; alpha subunit	1.17.4.1	3	7.13	98759.75
144749	Uracil phosphoribosyltransferase.	2.4.2.9	7	5.99	24303.15
162714	Uracil phosphoribosyltransferase.	2.4.2.9	5	6.79	23680.43
128636	Uridine 5'- monophosphate synthase/orotate phosphoribosyltransferase	2.4.2.10	3	7.05	24327.05
70238	Uridine 5'- monophosphate synthase/orotate phosphoribosyltransferase	4.1.1.23	7	5.88	30556.61
169258	Uridine kinase.	2.7.1.48	2	7.6	62657.98

^a Unique peptides. ^b The theoretical *pI* (isoelectric point) and *M_w* (molecular weight) were computed based on protein sequence obtained from the JGI database.

Supplementary table 7: Intracellular proteins identified with potential functions in lipid metabolism of dikaryotic *T. versicolor* strain (Tv-D) grown on beech sapwood (28 days old samples)

JGI protein ID	Putative protein function	EC	UP ^a	pI ^b	Mw ^b
Fatty acid metabolism					
149581	3-oxoacyl-(acyl-carrier-protein) synthase (I and II)	2.3.1.41	20	6.22	426948.81
137226	3-oxoacyl-[acyl-carrier protein] reductase.	1.1.1.100	2	6.07	31359.61
150013	3-oxoacyl-[acyl-carrier protein] reductase.	1.1.1.100	15	7.38	28744.1
172485	3-oxoacyl-[acyl-carrier protein] reductase.	1.1.1.100	12	5.68	33194.82
158338	Acetyl-CoA C-acyltransferase.	2.3.1.16	6	7.62	44262.88
159255	Acetyl-CoA C-acyltransferase.	2.3.1.16	10	7.89	43184.8
58924	Acetyl-CoA C-acyltransferase.	2.3.1.16	10	8.01	42492.8
138410	Enoyl-CoA hydratase	4.2.1.17	7	9.13	30364.76
27849	Enoyl-CoA hydratase	4.2.1.17	18	6.82	54290.07
74886	Enoyl-CoA hydratase	4.2.1.17	17	9.27	32170.02
42724	Enoyl-CoA isomerase	4.2.1.17	3	7.61	32372.15
74291	Glutaryl-CoA dehydrogenase	1.3.8.6	2	7.82	45936.82
149709	Hydroxyacyl-CoA dehydrogenase/enoyl-CoA hydratase	5.3.3.8	2	8.43	30219.06
175503	Hydroxysteroid 17-beta dehydrogenase 11	1.1.1.100	11	6	34923.78
37318	Long chain fatty acid acyl-CoA ligase	6.2.1.3	3	6.73	60799.9
164992	Long-chain acyl-CoA synthetases (AMP-forming)	6.2.1.3	8	6.37	60867.58
28052	Long-chain acyl-CoA synthetases (AMP-forming)	6.2.1.3	4	8.39	75316.22
127107	Long-chain-fatty-acid--CoA ligase.	6.2.1.3	11	8.07	76277.17
159946	Mitochondrial/plastidial beta-ketoacyl-ACP reductase	1.1.1.100	16	9.09	29456.72
59703	Mitochondrial/plastidial beta-ketoacyl-ACP reductase	1.1.1.100	3	7.2	29352.68
68666	Peroxisomal 3-ketoacyl-CoA-thiolase P-44/SCP2	2.3.1.16	9	7.09	49790.39
57215	Predicted acyl-CoA dehydrogenase	1.3.8.7	13	8.78	49779.58
Lipid transport and metabolism					
172598	1-Acyl dihydroxyacetone phosphate reductase and related dehydrogenases	1.1.1.101	6	7.99	31242.03
123703	Acetyl-CoA carboxylase	6.4.1.2	12	6.08	248571.94
60988	Animal-type fatty acid synthase and related proteins		5	5.72	209752.45
64761	Cyclopropane-fatty-acyl-phospholipid synthase.	2.1.1.79	3	6.54	55390.75

74073	Delta(24)-sterol C-methyltransferase.	2.1.1.41	2	6.16	39808.08
136829	Hormone-sensitive lipase HSL		2	7.93	43632.12
167853	Hormone-sensitive lipase HSL		11	7.22	44334.89
148803	Hydroxymethylglutaryl-CoA synthase		2	6.39	51340.46
165799	Isoamyl acetate-hydrolyzing esterase	3.1.-.-	5	5.86	28896.63
112170U	Lipase, class 3 domain		6	6.22	29308.18
109956	Lipocalins domain		3	5.01	22350.95
160610	Low density lipoprotein receptor		2	5.89	100298.96
173225	Lysosomal & prostatic acid phosphatases		28	6.88	50000.66
57474	N-myristoyl transferase (Glycylpeptide N-tetradecanoyltransferase)	2.3.1.97	2	7.1	62812.72
121229	Phosphatidylinositol transfer protein SEC14 and related proteins (Protein-tyrosine-phosphatase)	3.1.3.48	2	7.7	37667.82
148594	Phosphatidylinositol transfer protein SEC14 and related proteins (Protein-tyrosine-phosphatase)	3.1.3.48	7	4.9	41235.8
45106	Phosphatidylinositol transfer protein SEC14 and related proteins (Protein-tyrosine-phosphatase)	3.1.3.48	8	6.4	33012.77
70704	Phospholipase A2-activating protein (contains WD40 repeats)		10	5.56	89250.77
154114	Predicted L-carnitine dehydratase/alpha-methylacyl-CoA racemase	5.1.99.4	5	7.01	52080.88
130612	Soluble epoxide hydrolase		11	5.24	44016.88
172632	Soluble epoxide hydrolase		4	5.03	43776.61
94256E	Soluble epoxide hydrolase		2	5.76	37085.8
118975	Sphingosine kinase; involved in sphingolipid metabolism		2	5.1	43083.6
161541	Vigilin		15	8.06	135771.34
Sterol biosynthesis					
160627	Mevalonate pyrophosphate decarboxylase	4.1.1.33	8	7.8	43639.69
34338	Phosphomevalonate kinase	2.7.4.2	2	6.16	54919.54
Synthesis and degradation of ketone bodies					
40216	Hydroxymethylglutaryl-CoA lyase	4.1.3.4	5	8.6	38868.39
145135	Succinyl-CoA:alpha-ketoacid-CoA transferase	2.8.3.5	18	7.96	57914.71
70557	Succinyl-CoA:alpha-ketoacid-CoA transferase	2.8.3.5	30	7.59	56127.7

^a Unique peptides. ^b The theoretical *pI* (isoelectric point) and *Mw* (molecular weight) were computed based on protein sequence obtained from the JGI database.

Supplementary table 8: Intracellular proteins identified with potential functions in metabolism of complex lipids of dikaryotic *T. versicolor* strain (*Tv-D*) grown on beech sapwood (28 days old samples)

JGI protein ID	Putative protein function	EC	UP ^a	<i>pI</i> ^b	<i>Mw</i> ^b
Glycerolipid metabolism					
118507	2-acetyl-1-alkylglycerophosphocholine esterase.	3.1.1.47	2	5.6	84033.9
168593	Dihydroxyacetone kinase/glycerone kinase	2.7.1.29	20	5.65	62837.45
137276	Glycerol dehydrogenase	1.1.1.6	13	5.46	42121.18
169905	Lysophospholipase	3.1.1.23	6	6.86	34299.38
119326U	Phosphatidylinositol synthase	2.7.8.11	2	7.91	24301.39
72036	Ribulose kinase and related carbohydrate kinases	2.7.1.30	7	5.74	58370.53
176166	Triacylglycerol lipase.	3.1.1.3	17	5.76	156413.77
162460	U5 snRNP-specific protein-like factor and related proteins	3.1.1.47	3	7.13	39407.53
Inositol phosphate metabolism					
32707	Inositol monophosphatase	3.1.3.25	6	5.35	33531.14
154039	Myo-inositol-1-phosphate synthase	5.5.1.4	8	6.44	60243.51
Phospholipid degradation					
75277	Phospholipase D1	3.1.4.4	6	5.98	97593.99
Prostaglandin and leukotriene metabolism					
140546	Bifunctional leukotriene A4 hydrolase/aminopeptidase LTA4H	3.3.2.6	11	6.05	72405.52
Sphingoglycolipid metabolism					
141971	Glutamate decarboxylase/sphingosine phosphate lyase	4.1.2.27	2	8.93	59022.42
144721	Short-chain acyl-CoA dehydrogenase	1.3.99.-	6	6.93	46495.01

^a Unique peptides. ^b The theoretical *pI* (isoelectric point) and *Mw* (molecular weight) were computed based on protein sequence obtained from the JGI database.

Supplementary table 9: Intracellular proteins identified with potential functions in energy metabolism of dikaryotic *T. versicolor* strain (*Tv*-D) grown on beech sapwood (28 days old samples)

JGI protein ID	Putative protein function	EC	UP ^a	<i>pI</i> ^b	<i>Mw</i> ^b
ATP synthesis					
58816	F0F1-type ATP synthase; alpha subunit	3.6.3.14	53	9.16	58794.72
52345	F0F1-type ATP synthase; gamma subunit	3.6.3.14	13	7.37	29389.63
47305	Mitochondrial F1F0-ATP synthase; subunit b/ATP4	3.6.3.14	12	5.32	23180.47
144542	Mitochondrial F1F0-ATP synthase; subunit d/ATP7	3.6.3.14	14	7.61	19055.85
142467	Mitochondrial F1F0-ATP synthase; subunit delta/ATP16	3.6.3.14	3	6.54	17182.52
59461	Mitochondrial F1F0-ATP synthase; subunit g/ATP20	3.6.3.14	11	10.34	19019.89
28333	Vacuolar H ⁺ -ATPase V0 sector; subunit a	3.6.3.14	3	5.3	94767.72
166903	Vacuolar H ⁺ -ATPase V0 sector; subunit d	3.6.3.14	6	4.93	41900.21
64093	Vacuolar H ⁺ -ATPase V1 sector; subunit A	3.6.3.14	17	6.06	68060.86
28619	Vacuolar H ⁺ -ATPase V1 sector; subunit B	3.6.3.14	26	5.6	56919.74
159612	Vacuolar H ⁺ -ATPase V1 sector; subunit C	3.6.3.14	6	5.92	44863.99
152124	Vacuolar H ⁺ -ATPase V1 sector; subunit E	3.6.3.14	7	5.83	25637.19
28145	Vacuolar H ⁺ -ATPase V1 sector; subunit H	3.6.3.14	9	6.64	49409.92
Energy production and conversion					
133775	Alanine aminotransferase	2.6.1.2	11	7.01	52636.64
171840	ATP-citrate lyase		71	7.87	125795.75
28498	Citrate lyase beta subunit	4.1.3.6	3	8.3	38325.95
56508	Electron transfer flavoprotein; alpha subunit		10	7.03	36254.18
156129	Electron transfer flavoprotein; beta subunit		4	8.74	28972.02
160018	NADH:flavin oxidoreductase/12-oxophytodienoate reductase		3	7.01	44490.49
43161	NADH:flavin oxidoreductase/12-oxophytodienoate reductase		2	6.94	55852.94
49236	NADH:flavin oxidoreductase/12-oxophytodienoate reductase		6	5.37	41149.4
56531	NADH:flavin oxidoreductase/12-oxophytodienoate reductase		6	5.92	40664.93
60179	NADH:flavin oxidoreductase/12-oxophytodienoate reductase		4	7.12	44246.2
39181	NADH:ubiquinone oxidoreductase NDUFA2/B8 subunit		6	9.5	10331.88
139828	NADH:ubiquinone oxidoreductase; NDUFA5/B13 subunit		3	5.53	15027.03
73095	NADH:ubiquinone oxidoreductase; NDUFA6/B14 subunit		3	9.66	15838.3

96002	NADH:ubiquinone oxidoreductase; NDUFA8/PGIV/19 kDa subunit		2	7.88	17095.6
146897	NADH:ubiquinone oxidoreductase; NDUFA9/39kDa subunit		15	7.95	40987.86
117214	NADH:ubiquinone oxidoreductase; NDUFB9/B22 subunit		5	9.18	13759.47
67970	NADH:ubiquinone oxidoreductase; NDUFS2/49 kDa subunit		16	6.84	53932.94
163087	NADH:ubiquinone oxidoreductase; NDUFS8/23 kDa subunit		3	6.53	27242.03
156371	NADH:ubiquinone oxidoreductase; NDUFV1/51kDa subunit		5	8.43	54334.35
120720	NADH:ubiquinone oxidoreductase; NDUFV2/24 kD subunit		3	8.23	27462.47
47809	NADH:ubiquinone reductase (H ⁺ -translocating)		2	8.4	18977.47
137938	NADH-cytochrome b-5 reductase		2	9.23	35835.41
154794	NADH-ubiquinone oxidoreductase; NDUFS1/75 kDa subunit		21	6.84	80426.41
108885	NADH-ubiquinone oxidoreductase; NDUFS3/30 kDa subunit		9	8.23	31162.46
161867	NADH-ubiquinone oxidoreductase; NUFS7/PSST/20 kDa subunit		3	9.95	25043.12
61356	NADP/FAD dependent oxidoreductase		24	6.56	116752.12
138083	NADP ⁺ -dependent malic enzyme		4	6.21	64269.8
172494	NADP ⁺ -dependent malic enzyme		10	6.81	59947.23
32715	NADP ⁺ -dependent malic enzyme		12	5.48	63439.78
33277	Predicted quinone oxidoreductase	1.6.5.5	13	7.71	36836.54
73456	Predicted quinone oxidoreductase	1.6.5.5	9	7.61	36913.52
34877	Prohibitins and stomatins of the PID superfamily		13	6.4	39270.9
159410	Proteins containing the FAD binding domain		9	6.43	55104.1
54353	Proteins containing the FAD binding domain		5	5.78	50047.98
63977	Sulfide:quinone oxidoreductase/flavo-binding protein	1.-.-.-	10	9.11	48382.04
124364	Trans-2-enoyl-CoA reductase (NADPH).	1.3.1.38	2	8.64	40690.38
110377	Voltage-gated shaker-like K ⁺ channel; subunit beta/KCNAB		24	6.87	40197.13
127395	Voltage-gated shaker-like K ⁺ channel; subunit beta/KCNAB		21	7.19	38805.03
145012	Voltage-gated shaker-like K ⁺ channel; subunit beta/KCNAB		9	6.55	37660.32
145839	Voltage-gated shaker-like K ⁺ channel; subunit beta/KCNAB		28	7.15	35729.23
28405	Voltage-gated shaker-like K ⁺ channel; subunit beta/KCNAB		8	7.21	39018.15
28406	Voltage-gated shaker-like K ⁺ channel; subunit beta/KCNAB		30	6.95	38457.34
31310	Voltage-gated shaker-like K ⁺ channel; subunit beta/KCNAB		17	7.15	38304.33

46289	Voltage-gated shaker-like K ⁺ channel; subunit beta/KCNAB		16	7.61	39031.04
46294	Voltage-gated shaker-like K ⁺ channel; subunit beta/KCNAB		5	6.54	38271.19
46312	Voltage-gated shaker-like K ⁺ channel; subunit beta/KCNAB		15	6.91	39118.87
52551	Voltage-gated shaker-like K ⁺ channel; subunit beta/KCNAB		9	6.41	135615.11
52556	Voltage-gated shaker-like K ⁺ channel; subunit beta/KCNAB		19	7.51	43474.82
61602	Voltage-gated shaker-like K ⁺ channel; subunit beta/KCNAB		12	6.15	37174.64
71966	Voltage-gated shaker-like K ⁺ channel; subunit beta/KCNAB		11	6.7	41553.48
Nitrogen metabolism					
161766	Asparaginase	3.5.1.1	2	7.89	39793.07
63732	Asparagine synthase (glutamine-hydrolyzing)	6.3.5.4	8	6.36	65970.08
139011	Carbon-nitrogen hydrolase	3.5.5.1	9	5.43	34910.78
27775	Glutamate synthase	1.4.1.13	6	6.74	236187.66
156153	Glutamate/leucine/phenylalanine/valine dehydrogenases	1.4.1.2	3	6.75	118302.53
116287	Glutamine synthetase	6.3.1.2	25	6.84	39357.47
127334	Glutamine synthetase	6.3.1.2	4	5.7	46263.77
164678	Glutamine synthetase	6.3.1.2	5	5.94	54824.42
168197	Nitronate monooxygenase	1.13.12.16	6	8.27	36983.04
Oxidative phosphorylation					
37723	Cytochrome c		4	9.35	11714.36
33262	Cytochrome c oxidase; subunit Va/COX6	1.9.3.1	5	7.35	15135.06
125834	Cytochrome c oxidase; subunit Vb/COX4	1.9.3.1	2	7.1	16695.95
138997	Cytochrome c oxidase; subunit VIa/COX13	1.9.3.1	2	8.5	14317.35
29759	Cytochrome c oxidase; subunit VIb/COX12	1.9.3.1	2	6.01	9913.99
168516	Cytochrome c1	1.10.2.2	12	7.28	36064.84
26601	Cytochrome-c peroxidase (CCP1)	1.11.1.5	6	8.72	41680.85
111649	Inorganic pyrophosphatase/Nucleosome remodeling factor; subunit NURF38	3.6.1.1	12	6.06	33581.03
69482	NADH dehydrogenase 21 kDa subunit	1.6.5.3	2	9.46	19853.58
152955	Plasma membrane H ⁺ -transporting ATPase	3.6.3.6	30	5.72	109169.57
44704	Ubiquinol cytochrome c oxidoreductase; subunit QCR9	1.10.2.2	2	9.25	7083.1
128283	Ubiquinol cytochrome c reductase; subunit QCR2	1.10.2.2	16	7.64	43647.36
159748	Ubiquinol cytochrome c reductase; subunit RIP1	1.10.2.2	4	8.43	30058.37

^a Unique peptides. ^b The theoretical *pI* (isoelectric point) and *M_w* (molecular weight) were computed based on protein sequence obtained from the JGI database.

Supplementary table 10: Intracellular proteins identified with potential functions in cellular processes and signaling of dikaryotic *T. versicolor* strain (Tv-D) grown on beech sapwood (28 days old samples)

JGI protein ID	Putative protein function	EC	UP ^a	<i>pI</i> ^b	<i>Mw</i> ^b
Aminoacyl-tRNA biosynthesis					
21080	Alanyl-tRNA synthetase	6.1.1.7	29	6.03	108161.73
152999	Arginyl-tRNA synthetase	6.1.1.19	13	6.61	69205.26
31222	Asparaginyl-tRNA synthetase	6.1.1.22	15	5.88	63692.5
159304	Aspartyl-tRNA synthetase	6.1.1.12	18	6.45	61692.49
26341	Cysteinyl-tRNA synthetase	6.1.1.16	9	6.35	87635.15
28297	Cytoplasmic tryptophanyl-tRNA synthetase	6.1.1.2	6	7.15	50125
143272	Glutaminyl-tRNA synthetase	6.1.1.18	12	6.72	93741.45
140508	Glutamyl-tRNA synthetase (mitochondrial)	6.1.1.17	2	8.13	56125.27
30509	Glycyl-tRNA synthetase and related class II tRNA synthetase	6.1.1.14	11	6.38	73029.05
41333	Histidyl-tRNA synthetase	6.1.1.21	9	6.83	66976.85
161079	Isoleucyl-tRNA synthetase	6.1.1.5	17	6.45	124758.29
151266	Leucyl-tRNA synthetase	6.1.1.4	12	6.39	122830.43
56549	Lysyl-tRNA synthetase (class II)	6.1.1.6	8	6.54	66215.46
149996	Methionyl-tRNA synthetase	6.1.1.10	8	6.77	77636.64
116804	Phenylalanyl-tRNA synthetase beta subunit	6.1.1.20	16	5.59	70350.79
163523	Phenylalanyl-tRNA synthetase; beta subunit	6.1.1.20	10	7.46	59195.5
30355	Prolyl-tRNA synthetase	6.1.1.15	25	6.63	79042.3
134279	Seryl-tRNA synthetase	6.1.1.11	11	6.25	51197.58
174356	Threonyl-tRNA synthetase	6.1.1.3	19	6.78	83014.76
61159	Tyrosyl-tRNA synthetase; cytoplasmic	6.1.1.1	5	6.68	47660.5
40422	Valyl-tRNA synthetase	6.1.1.9	11	6.35	117984.21
Intracellular trafficking, secretion, and vesicular transport					
161675	Amphiphysin		5	5.28	29653.63
140401	Armadillo repeat protein VAC8 required for vacuole fusion; inheritance and cytosol-to-vacuole protein targeting		3	5.51	67604.59
67937	ATP synthase E chain domain		2	8.44	9993.35
147339	COPII vesicle protein		5	8.07	46701.97
29867	COPII vesicle protein		2	8.92	57826.34

152121	Cytosolic sorting protein GGA2/TOM1	5	6.08	57348.78
173529	ER-Golgi vesicle-tethering protein p115	8	4.78	91794.3
157296	Golgi protein	3	5.91	42157.94
68910	Golgi SNAP receptor complex member	2	8.99	27524.03
36458	GTPase Rab11/YPT3; small G protein superfamily	10	6.21	23118.03
139953	GTPase Rab5/YPT51 and related small G protein superfamily GTPases	10	4.94	26959.04
41455	GTPase Rab5/YPT51 and related small G protein superfamily GTPases	2	7.71	22713.68
57563	GTPase Rab6/YPT6/Ryh1; small G protein superfamily	8	5.49	23862.15
27977	GTPase Ran/TC4/GSP1 (nuclear protein transport pathway); small G protein superfamily	8	6.55	24224.74
116906	GTP-binding ADP-ribosylation factor Arf1	10	7.34	20517.7
63207	Guanine nucleotide exchange factor	4	6.05	211837.01
139002	Karyopherin (importin) alpha	14	5.11	57820.65
158750	Medium subunit of clathrin adaptor complex	10	5.36	57763.38
31604	Membrane coat complex Retromer; subunit VPS26	2	6.96	34730.78
171110	Membrane coat complex Retromer; subunit VPS29/PEP11	2	6.08	23305.59
160026	Membrane coat complex Retromer; subunit VPS35	9	5.63	108489.56
138784	Membrane coat complex Retromer; subunit VPS5/SNX1; Sorting nexins; and related PX domain-containing proteins	2	5.66	53262.74
41997	Mitochondrial ADP/ATP carrier proteins	31	9.75	33631.97
109478	Mitochondrial aspartate/glutamate carrier protein Aralar/Citrin (contains EF-hand Ca ²⁺ -binding domains)	2	8.98	76196.27
63578	Mitochondrial associated endoribonuclease MAR1 (isochorismatase superfamily)	2	8.31	22942.76
159017	Mitochondrial import inner membrane translocase; subunit TIM22	2	7.13	17241.48
174772	Mitochondrial oxodicarboxylate carrier protein	2	9.56	37852.07
50673	Mitochondrial oxoglutarate/malate carrier proteins	18	9.75	33822.48
20755	Mitochondrial phosphate carrier protein	11	9.16	33840.6
139175	Mitochondrial translation elongation factor Tu	23	7.33	50540

139094	Mitochondrial tricarboxylate/dicarboxylate carrier proteins	2	9.74	32011.37
150398	Nuclear export receptor CSE1/CAS (importin beta superfamily)	12	5.32	109035.02
169469	Nuclear mRNA export factor receptor LOS1/Exportin-t (importin beta superfamily)	2	5.1	119558.81
136690	Nuclear pore complex; Nup133 component (sc Nup133)	2	5.63	132846.35
159402	Nuclear pore complex; Nup155 component (D Nup154; sc Nup157/Nup170)	2	5.6	152121.59
144551	Nuclear pore complex; Nup160 component	2	6.07	152700.14
27006	Nuclear pore complex; Nup98 component (sc Nup145/Nup100/Nup116)	2	9.33	102865.87
72848	Nuclear pore complex; Nup98 component (sc Nup145/Nup100/Nup116)	5	6.34	70359.45
146525	Nuclear transport factor 2	4	4.7	13736.62
165456	Nuclear transport receptor CRM1/MSN5 (importin beta superfamily)	12	5.25	122249.97
66788	Nuclear transport receptor Karyopherin-beta2/Transportin (importin beta superfamily)	6	4.94	104798.02
147211	Nuclear transport receptor RANBP7/RANBP8 (importin beta superfamily)	10	4.82	116165.1
25539	Nuclear transport regulator	6	5.17	103650.88
140844	Nucleosome assembly protein NAP-1	9	4.51	46810.64
145396	Pattern-formation protein/guanine nucleotide exchange factor	6	5.56	167039.58
25862	Peroxisomal biogenesis protein (peroxin)	2	10.39	27621.35
54946	Predicted importin 9	5	4.73	113613.74
44269	Protein involved in glucose derepression and pre-vacuolar endosome protein sorting	2	4.94	25735.99
33785	Protein involved in membrane traffic (YOP1/TB2/DP1/HVA22 family)	8	8.88	21700.92
18509	Protein involved in vacuole import and degradation	3	5.17	87750.68
159041	Protein required for fusion of vesicles in vesicular transport; alpha-SNAP	6	5.47	32207.14
59839	Putative cargo transport protein ERV29	2	9.78	34887.88

115259	Ran-binding protein RANBP1 and related RanBD domain proteins		3	4.97	23315.8
110699	Septin family protein (P-loop GTPase)		21	5.12	42617.98
174957	Septin family protein (P-loop GTPase)		23	7.12	44548.74
33124	Septin family protein (P-loop GTPase)		18	6.29	51054.1
160134	Signal recognition particle; subunit Srp68		2	8.99	71669.5
138352	SNARE protein GS28		2	6.8	25172.46
145085	SNARE protein Syntaxin 1 and related proteins		2	7.9	37335.88
45271	SNARE protein Syntaxin 1 and related proteins		3	5.98	32649.4
69583	Sorting nexin SNX11		2	7.39	18112.63
146188	Synaptic vesicle protein EHS-1 and related EH domain proteins	3.1.13.4	4	5.08	145407.22
50414	Synaptic vesicle transporter SVOP and related transporters (major facilitator superfamily)		6	7.87	59999.98
73532	Synaptobrevin/VAMP-like protein		3	8.44	24638.2
121877	Translation elongation factor 2/ribosome biogenesis protein RIA1 and related proteins		3	6.01	120112.4
110730	Translation elongation factor EF-1 alpha/Tu		35	9.08	50089.84
57449	Translocase of outer mitochondrial membrane complex; subunit TOM40		3	6.65	38384.23
155503	Translocase of outer mitochondrial membrane complex; subunit TOM70/TOM72		11	5.66	66143.06
165161	Transport protein particle (TRAPP) complex subunit		2	4.6	23087.2
175632	Transport protein Sec61; alpha subunit		2	7.41	52183.67
163153	Vacuolar assembly/sorting protein DID2		2	6.11	22536.58
150323	Vacuolar sorting protein VPS1; dynamin; and related proteins		3	8.44	104418.52
165834	Vacuolar sorting protein VPS1; dynamin; and related proteins		22	7.92	77028.47
71799	Vacuolar sorting protein VPS1; dynamin; and related proteins		11	6.51	87192.29
158094	Vacuolar sorting protein VPS33/slp1 (Sec1 family)		2	6.39	74990.38
166729	Vacuolar sorting protein VPS45/Stt10 (Sec1 family)		4	6.9	70660.97
122609	VAMP-associated protein involved in inositol metabolism		5	5.02	37013.65
30209	Vesicle coat complex AP-1/AP-2/AP-4; beta subunit		8	5.11	79217.16
168213	Vesicle coat complex AP-1; gamma subunit		10	6.36	91405.86

159181	Vesicle coat complex AP-2; alpha subunit	3	7.23	104363.35
172870	Vesicle coat complex COPI; alpha subunit	15	6.48	133961.64
31022	Vesicle coat complex COPI; alpha subunit	16	6.63	133958.74
138513	Vesicle coat complex COPI; beta subunit	10	5.68	106391.16
44357	Vesicle coat complex COPI; beta' subunit	5	5.07	95337.39
55151	Vesicle coat complex COPI; gamma subunit	11	5.43	101280.96
154229	Vesicle coat complex COPI; zeta subunit	2	6.42	20870
145251	Vesicle coat complex COPII; GTPase subunit SAR1	10	6.03	21456.77
40529	Vesicle coat complex COPII; subunit SEC13	3	6.61	34850.28
153111	Vesicle coat complex COPII; subunit SEC23	11	6.59	84862.28
153406	Vesicle coat complex COPII; subunit SEC24/subunit SFB2	17	6.16	102844.47
168399	Vesicle coat protein clathrin; heavy chain	37	5.92	191112.7
158232	Vesicle trafficking protein Sly1 (Sec1 family)	10	5.81	75536.8
Posttranslational modification, protein turnover, chaperones				
115541	AAA+-type ATPase	10	6.7	86263.98
154509	AAA+-type ATPase	7	6.1	76509.8
156194	AAA+-type ATPase	2	5.99	38268.21
26086	AAA+-type ATPase	4	6.05	48281.72
69811	AAA+-type ATPase	8	6.03	60714.89
71710	AAA+-type ATPase	34	5.1	89907.18
74607	AAA+-type ATPase	4	7.27	85576.1
130108	Alkyl hydroperoxide reductase/peroxiredoxin	5	5.9	18621.43
60144	Alkyl hydroperoxide reductase/peroxiredoxin	29	5.89	18157.98
130067	Alkyl hydroperoxide reductase; thiol specific antioxidant and related enzymes	2	8.82	25319.88
135477	Alkyl hydroperoxide reductase; thiol specific antioxidant and related enzymes	2	5.94	23066.33
143925	Alkyl hydroperoxide reductase; thiol specific antioxidant and related enzymes	11	6.15	24405.76
28493	Alkyl hydroperoxide reductase; thiol specific antioxidant and related enzymes	10	6.35	20514.26
171293	Anaphase-promoting complex (APC); Cdc23 subunit	4	5.34	83702.98

56085	beta-1;6-N-acetylglucosaminyltransferase; contains WSC domain		2	5.42	73121.87
61229	beta-1;6-N-acetylglucosaminyltransferase; contains WSC domain		14	4.34	99854.9
64710	Chaperone HSP104 and related ATP-dependent Clp proteases		3	5.98	82497.09
165469	Chaperonin complex component; TCP-1 alpha subunit (CCT1)		10	7.18	59485.74
144774	Chaperonin complex component; TCP-1 beta subunit (CCT2)		16	5.5	56501.76
164623	Chaperonin complex component; TCP-1 delta subunit (CCT4)		10	7.86	57445.76
29433	Chaperonin complex component; TCP-1 epsilon subunit (CCT5)		10	5.65	59697.59
67874	Chaperonin complex component; TCP-1 eta subunit (CCT7)		13	6.57	60948.26
138012	Chaperonin complex component; TCP-1 gamma subunit (CCT3)		17	6.75	60494.75
154033	Chaperonin complex component; TCP-1 theta subunit (CCT8)		13	5.71	60239.04
56149	Chaperonin complex component; TCP-1 zeta subunit (CCT6)		6	7.06	59852.95
120446	Cyclophilin type peptidyl-prolyl cis-trans isomerase	5.2.1.8	2	7.51	17144.44
134604	Cyclophilin type peptidyl-prolyl cis-trans isomerase	5.2.1.8	13	8.94	17440.65
22021	Cyclophilin type peptidyl-prolyl cis-trans isomerase	5.2.1.8	22	8.37	17511.77
168556	Dolichyl-phosphate-mannose:protein O-mannosyl transferase	2.4.1.109	6	6.95	86862.65
148682	E3 ubiquitin protein ligase	6.3.2.19	2	5.15	190414.54
69070	E3 ubiquitin-protein ligase/Putative upstream regulatory element binding protein	6.3.2.19	13	4.98	405804.25
29198	ER membrane protein SH3_chaperone		2	5.02	20235.42
113328	FKBP-type peptidyl-prolyl cis-trans isomerase	5.2.1.8	2	5.53	13990.99
171918	FKBP-type peptidyl-prolyl cis-trans isomerase	5.2.1.8	14	7.26	11754.48
125655	Fungal transcriptional regulatory protein, N-terminal		6	8.07	71907.94
68200	Fungal transcriptional regulatory protein, N-terminal domains		2	7.18	80607.74
75707	Fungal transcriptional regulatory protein, N-terminal domains		2	7.26	78009.46
66902	HSP90 co-chaperone CPR7/Cyclophilin	5.2.1.8	6	5.89	40800.38
68660	HSP90 co-chaperone p23		4	4.48	24970.19
29660	Mitochondrial ATP-dependent protease PIM1/LON	3.4.21.-	8	5.63	115552.39
29896	Mitochondrial chaperonin		5	9.13	11435.2
61252	Mitochondrial chaperonin; Cpn60/Hsp60p	3.6.4.9	29	5.82	62393.25

167240	Mitochondrial processing peptidase; beta subunit; and related enzymes (insulinase superfamily)	3.4.24.64	19	6.7	52381.36
146311	Molecular chaperone (DnaJ superfamily)		2	6.31	44115.08
136662	Molecular chaperone (HSP90 family)		26	5.04	79624.36
21807	Molecular chaperone Prefoldin; subunit 3		2	5.01	26246.5
142636	Molecular chaperones HSP105/HSP110/SSE1; HSP70 superfamily		28	5.59	85489.93
119097	Molecular chaperones HSP70/HSC70; HSP70 superfamily		42	5.57	67178.03
140838	Molecular chaperones HSP70/HSC70; HSP70 superfamily		9	4.92	66996.58
27783	Molecular chaperones HSP70/HSC70; HSP70 superfamily		42	5.24	70581.25
173663	Molecular chaperones mortalin/PBP74/GRP75; HSP70 superfamily		16	5.76	71760.51
162598	Multifunctional chaperone (14-3-3 family)		2	6.1	28050.15
27130	Multifunctional chaperone (14-3-3 family)		24	4.9	28956.55
40757	N-6 adenine-specific DNA methylase, conserved site domain		2	5.55	26505.81
70638	N-arginine dibasic convertase NRD1 and related Zn ²⁺ -dependent endopeptidases; insulinase superfamily		2	6.53	128084.14
152658	NEDD8-activating complex; APP-BP1/UBA5 component		6	5.27	58182.62
164597	NEDD8-activating complex; catalytic component UBA3		5	5.29	47995.91
70779	OTU-like cysteine protease		3	6.14	37874.8
154958	Predicted dinucleotide-utilizing enzyme involved in molybdopterin and thiamine biosynthesis (Ubiquitin--protein ligase)	6.3.2.19	3	7.75	53009.93
172972	Predicted E3 ubiquitin ligase		2	5.75	62027.32
69060	Predicted pyroglutamyl peptidase	3.4.19.3	2	5.78	36150.41
25565	Predicted Zn ²⁺ -dependent endopeptidase; insulinase superfamily		16	5.43	116488.77
167189	Prohibitin-like protein		7	9.5	33833.82
142800	Proteasome formation inhibitor PI31		4	6.04	36048.6
30914	Protein farnesyltransferase; alpha subunit/protein geranylgeranyltransferase type I; alpha subunit		3	5.62	38672.73
26718	Protein involved in autophagy and nutrient starvation		3	6.53	38632.12

36361	Puromycin-sensitive aminopeptidase and related aminopeptidases	3.4.11.-	7	5.64	99791.29
67848	RAB proteins geranylgeranyltransferase component A (RAB escort protein)		38	5.6	50004.97
75537	Renal dipeptidase	3.4.13.19	11	6.13	47454.02
118908	SCF ubiquitin ligase; Skp1 component		3	4.61	18445.91
159926	Serine carboxypeptidases (lysosomal cathepsin A)	3.4.16.6	7	5.17	56122.01
157308	SMT3/SUMO-activating complex; AOS1/RAD31 component	6.3.2.19	3	5.08	36813.05
141168	Subtilisin-related protease/Vacuolar protease B		22	4.88	85169.94
25315	Thioredoxin		4	8.87	17607.2
32746	Thioredoxin		7	4.76	11396.2
156571	Thioredoxin reductase		10	5.89	36343.29
115468	Transferrin receptor and related proteins containing the protease-associated (PA) domain	3.4.17.21	13	7.2	91712.4
24665	Ubiquitin activating E1 enzyme-like protein		13	6.03	75642.53
163768	Ubiquitin activating enzyme UBA1		27	5.28	112484.83
144972	Ubiquitin carboxyl-terminal hydrolase		16	6.13	127445.67
147426	Ubiquitin fusion degradation protein-2		6	5.7	123197.8
146382	Ubiquitin protein ligase RSP5/NEDD4		3	6.55	94532.08
72002	Ubiquitin-conjugating enzyme E2		2	6.52	15585.64
31378	Ubiquitin-like protein		2	7.43	8407.75
67745	Ubiquitin-like protein		3	5.29	43405.13
175464	Ubiquitin-protein ligase	6.3.2.19	3	6.24	24472.81
30096	Ubiquitin-protein ligase	6.3.2.19	2	5.12	20205.88
30645	Ubiquitin-protein ligase	6.3.2.19	6	6.33	16924.39
39399	Ubiquitin-protein ligase	6.3.2.19	4	7.24	16398.86
170451	Ubiquitin-specific protease	3.1.2.15	4	5.69	59491.91
26176	Ubiquitin-specific protease UBP14	3.1.2.15	4	5.95	88510.92
54920	UDP-glucose 4-epimerase/UDP-sulfoquinovose synthase		12	7.88	121212.04
31785	U-snRNP-associated cyclophilin type peptidyl-prolyl cis-trans isomerase	5.2.1.8	4	8.45	19262.07

155203	Zuotin and related molecular chaperones (DnaJ superfamily); contains DNA-binding domains	2	8.71	43990.17	
Replication, recombination and repair					
148714	DNA repair/transcription protein Mms19	2	6.17	114443.43	
RNA processing and modification					
27854	Alternative splicing factor SRp55/B52/SRp75 (RRM superfamily)	3	8.93	34135.14	
125432	ATP-dependent RNA helicase	5	9.13	54142.61	
140419	ATP-dependent RNA helicase	12	6.09	48974.09	
167369	ATP-dependent RNA helicase	3	9.07	67999.15	
72423	ATP-dependent RNA helicase	12	6.82	52401.06	
74021	ATP-dependent RNA helicase	5	8.56	56007.08	
165188	Fibrillarin and related nucleolar RNA-binding proteins	4	10.35	33831.51	
165582	mRNA cleavage and polyadenylation factor I complex; subunit RNA15	9	9.47	57981.89	
60908	mRNA cleavage and polyadenylation factor I complex; subunit RNA15	2	6.86	43040.35	
58071	mRNA deadenylase subunit	3	4.98	38182.4	
65239	mRNA export protein (contains WD40 repeats)	3	7.96	39228.06	
68627	mRNA splicing factor	6	6.33	54026.88	
155656	mRNA splicing factor ATP-dependent RNA helicase	3	7.31	85303.01	
64114	mRNA splicing protein CDC5 (Myb superfamily)	2	6.42	93088.26	
57273	Nuclear cap-binding complex; subunit NCBP1/CBP80	8	5.76	97203.69	
31389	Oligoribonuclease (3'->5' exoribonuclease)	3.1.-.-	2	7.83	26128.11
136559	Polyadenylate-binding protein (RRM superfamily)	21	8.07	68774.24	
153466	Polyadenylate-binding protein (RRM superfamily)	8	7.68	85294.69	
51265U	Polyadenylate-binding protein (RRM superfamily)	3	10.59	18123.39	
59063	Polyadenylation factor I complex; subunit; Yth1 (CPSF subunit)	3	5.84	37175.48	
17567	Predicted ribosomal RNA adenine dimethylase	2	8.49	42735.32	
25803	Predicted RNA-binding protein	3	9.08	35946.02	
129197	Predicted RNA-binding protein; contains KH domains	5	6.39	36494.19	
33947	Predicted snRNP core protein	5	8.84	10995.76	

36780	Ran GTPase-activating protein	6	4.63	42801.21
75637	RNA helicase BRR2; DEAD-box superfamily	2	5.39	245206.41
171608	RNA polymerase I-associated factor - PAF67	10	5.14	69245.77
60398	RNA polymerase II general transcription factor BTF3 and related proteins	6	5.1	19476.8
59082	RNA polymerase; 25-kDa subunit (common to polymerases I; II and III)	2	8.85	24052.5
46948	RNA recognition motif, RNP-1	8	6.1	28595.81
70736	RNA-binding protein (contains RRM and Pumilio-like repeats)	10	8.11	138277.4
55734	RNA-binding protein LARK; contains RRM and retroviral-type Zn-finger domains	2	8.62	53492.98
172622	RNAse L inhibitor; ABC superfamily	2	8.31	67571.64
31401	RRM motif-containing protein	2	10.35	27949.6
51115	RRM motif-containing protein	3	10.27	14399.25
55600	Small nuclear ribonucleoprotein (snRNP) Sm core protein	3	9.99	12821.97
27310	Small nuclear ribonucleoprotein (snRNP) SMF	2	6.61	8961.28
25956	Small nuclear ribonucleoprotein E	3	8.53	10145.95
69671	Small Nuclear ribonucleoprotein G	2	9.18	8569.96
115078	Small nuclear ribonucleoprotein Sm D3	3	11.55	14370.94
153771	Small nuclear ribonucleoprotein SMD1 and related snRNPs	3	11.4	13471.56
138080	Spliceosomal protein snRNP-U1A/U2B	3	9.57	31059.17
175011	Splicing coactivator SRm160/300; subunit SRm300	2	6.64	129722.92
168211	Splicing factor 3b; subunit 1	2	6.12	128668.39
158956	U2-associated snRNP A' protein	3	9.18	27867.07
71259	U5 snRNP spliceosome subunit	2	8.8	274077.49
Signal transduction mechanisms				
165892	Adenylate cyclase-associated protein (CAP/Srv2p)	5	6.47	55894.86
163103	ADP-ribosylation factor GTPase activator	3	6.74	45770.35
23626	Ca ²⁺ /calmodulin-dependent protein kinase; EF-Hand protein superfamily	12	6.14	44647.93
31295	Ca ²⁺ -binding protein; EF-Hand protein superfamily	10	5.36	24651.4
30695	Calmodulin and related proteins (EF-Hand superfamily)	2	4.62	15390.26

66035	Calmodulin and related proteins (EF-Hand superfamily)	4	4.28	16783.64
31211	cAMP-dependent protein kinase catalytic subunit (PKA)	2	8.04	45866.17
55442	Casein kinase II; alpha subunit	6	8.38	40261.14
31518	COP9 signalosome; subunit CSN1	7	6.86	56653.43
111734	COP9 signalosome; subunit CSN2	9	5.28	53990.89
127525	COP9 signalosome; subunit CSN3	4	6.8	45464.97
27385	COP9 signalosome; subunit CSN4	10	5.18	50410.06
171197	COP9 signalosome; subunit CSN5	9	6.26	39929.22
55452	COP9 signalosome; subunit CSN6	5	5.82	35940.88
109231	COP9 signalosome; subunit CSN7	2	5.78	32902.36
31114	Dehydrogenase kinase	2	7.47	51274.74
142154	G protein beta subunit-like protein	13	6.38	34760.25
112226	G-protein alpha subunit (small G protein superfamily)	2	5.64	40794.42
141528	G-protein alpha subunit (small G protein superfamily)	5	5.91	40488.24
29511	G-protein alpha subunit (small G protein superfamily)	7	8	59039.48
32890	G-protein beta subunit	2	7	38316.26
119425	GTPase Rab1/YPT1; small G protein superfamily; and related GTP-binding proteins	13	6.04	22500.45
69660	GTP-binding protein DRG1 (ODN superfamily)	2	8.54	40148.47
55422	GTP-binding protein DRG2 (ODN superfamily)	3	8.36	40830.27
33861	GTP-binding protein SEC4; small G protein superfamily; and related Ras family GTP-binding proteins	7	5.68	23025.16
64856	Invasion-inducing protein TIAM1/CDC24 and related RhoGEF GTPases	2	6.8	117130.45
174906	Lysophosphatidic acid acyltransferase endophilin/SH3GL; involved in synaptic vesicle formation	10	5.45	33620.82
172826	Mitogen-activated protein kinase	4	7.03	44081.83
173791	Mitogen-activated protein kinase	8	6.83	48988.67
61654	Mitogen-activated protein kinase	6	5.48	41832.13
30040	Neurotransmitter release regulator; UNC-13	4	6.25	153142.26
109425	Oxysterol-binding protein	2	6.48	46919.28
59645	Oxysterol-binding protein	3	6.82	44029.44

133664	Predicted signal transduction protein	3.1.3.48	4	6.32	114446.37
16673	Protein phosphatase 2A regulatory subunit A and related proteins	3.1.3.16	20	4.96	67548.74
115392	Protein phosphatase 2C/pyruvate dehydrogenase (lipoamide) phosphatase	3.1.3.16	2	6.87	58935.58
162184	Rho GDP-dissociation inhibitor		9	5.66	22306.11
29646	Ribosomal protein RPL1/RPL2/RL4L4		14	11.11	41041.64
43358	Ribosomal protein S18		4	10.84	17961.88
61738	Ribosomal protein S4		8	10.61	22364.03
73549	Ribosomal protein S6 kinase and related proteins		6	7.2	61512.15
56182	Ribosomal protein S7		10	9.84	22585.19
63396	Ribosome biogenesis protein - Nop58p/Nop5p		2	9.04	62060.41
156983	Septin CDC10 and related P-loop GTPases		24	6.67	36357.35
146826	Serine/threonine protein kinase	2.7.1.37	2	6.47	71678.59
147078	Serine/threonine protein kinase		5	7.75	125924.15
155735	Serine/threonine protein kinase		2	5.66	29554.57
158819	Serine/threonine protein kinase		3	5.41	55674.43
29154	Serine/threonine protein kinase	6.3.2.-	6	6.7	125297.3
169208	Serine/threonine protein kinase/TGF-beta stimulated factor	2.7.1.37	3	6.05	47599.42
28625	Serine/threonine protein phosphatase	3.1.3.16	7	4.62	58730.65
34622	Serine/threonine protein phosphatase	3.1.3.16	3	5.13	35389.54
168876	Serine/threonine protein phosphatase 2A; catalytic subunit	3.1.3.16	4	5.23	34802.3
148355	Serine/threonine protein phosphatase 2A; regulatory subunit	3.1.3.16	6	6.1	51299.09
70499	Serine/threonine protein phosphatase 2A; regulatory subunit	3.1.2.16	5	6.47	78449.76
172672	Serine/threonine specific protein phosphatase PP1; catalytic subunit	3.1.3.16	5	6.13	38153.03
55512	Serine/threonine specific protein phosphatase PP1; catalytic subunit	3.1.3.16	2	5.99	52691.77
32380	Serine-threonine phosphatase 2B; catalytic subunit	3.1.3.16	9	5.57	72158.73
119985	Sexual differentiation process protein ISP4		2	5.98	84981.43
68913	Sexual differentiation process protein ISP4		3	7.96	87422.46
58676	Signal transducing adaptor protein STAM/STAM2		3	5.37	92441.11
69252	Signaling protein DOCK180		2	6.57	243380.53

31426	Sorbin and SH3 domain-containing protein		3	5.36	59444.61
147688	Sterol reductase/lamin B receptor		4	8	48889.43
42032	Suppressor of G2 allele of skp1		3	5.51	21884.45
146732	Synaptic vesicle protein EHS-1 and related EH domain proteins	3.1.13.4	2	5.8	215181.48
116115	WW domain binding protein WBP-2; contains GRAM domain		4	5.42	20567.16
Transcription					
29992	Elongation factor 1 beta/delta chain		11	4.61	23587.29
138745	Elongation factor 2		46	6.57	93322.65
Translation, ribosomal structure and biogenesis					
142047	ATPase component of ABC transporters with duplicated ATPase domains/Translation elongation factor EF-3b		2	8.1	118411
57970	ATPase component of ABC transporters with duplicated ATPase domains/Translation elongation factor EF-3b		26	6.32	116146.93
73375	ATPase component of ABC transporters with duplicated ATPase domains/Translation elongation factor EF-3b		7	9.41	94544.78
54102	ATPase family associated with various cellular activities (AAA) domains		4	6.3	82460.87
27392	Exosomal 3'-5' exoribonuclease complex; subunit Rrp44/Dis3	3.1.13.1	7	6.51	139143.36
51720	Protein containing adaptin N-terminal region		11	5.96	278185.16
175840	Translation initiation factor 1 (eIF-1/SUI1)		2	7.34	12610.27
113520	Translation initiation factor 2; alpha subunit (eIF-2alpha)		6	5.1	36305.42
154566	Translation initiation factor 2; beta subunit (eIF-2beta)		2	5.86	39872.85
49432	Translation initiation factor 2; gamma subunit (eIF-2gamma; GTPase)		5	8.52	54406.03
145904	Translation initiation factor 2B; alpha subunit (eIF-2Balpha/GCN3)		2	5.67	37365.56
174368	Translation initiation factor 2C (eIF-2C) and related proteins		2	9.46	118071.99
70213	Translation initiation factor 2C (eIF-2C) and related proteins		7	9.57	100717.78
175066	Translation initiation factor 3; subunit a (eIF-3a)		9	8.72	114885.22
143044	Translation initiation factor 3; subunit b (eIF-3b)		5	5.53	85902.38
26379	Translation initiation factor 3; subunit c (eIF-3c)		13	6.46	98565.53
56875	Translation initiation factor 3; subunit d (eIF-3d)		3	5.39	63883.99

157392	Translation initiation factor 3; subunit e (eIF-3e)	8	5.2	52431.15	
56907	Translation initiation factor 3; subunit f (eIF-3f)	5	5.14	32750.89	
39027	Translation initiation factor 3; subunit g (eIF-3g)	4	7.83	31231.75	
166416	Translation initiation factor 3; subunit i (eIF-3i)/TGF-beta receptor-interacting protein (TRIP-1)	6	6.27	39561.27	
139190	Translation initiation factor 4F; cap-binding subunit (eIF-4E) and related cap-binding proteins	6	5.58	33594.02	
157249	Translation initiation factor 4F; cap-binding subunit (eIF-4E) and related cap-binding proteins	3	6.02	45762.49	
45669	Translation initiation factor 4F; helicase subunit (eIF-4A) and related helicases	18	5.31	45281.17	
173662	Translation initiation factor 4F; ribosome/mRNA-bridging subunit (eIF-4G)	4	8.98	161487.07	
30057	Translation initiation factor 5A (eIF-5A)	4	5.74	17568.78	
144706	Translation initiation factor 5B (eIF-5B)	3	5.86	133313.76	
168964	Translation initiation factor 6 (eIF-6)	7	4.7	26257.58	
26016	Translational repressor MPT5/PUF4 and related RNA-binding proteins (Puf superfamily)	3	7.27	108068.85	
109774	tRNA nucleotidyltransferase/poly(A) polymerase	2.7.7.25	2	5.55	61013.76
64507	tRNA-binding protein	6	7.86	43211.27	
67940	U5 snRNP-specific protein	6	5.15	109660.41	
47672	Ubiquitin/40S ribosomal protein S27a fusion	10	9.9	18143.35	

^a Unique peptides. ^b The theoretical *pI* (isoelectric point) and *Mw* (molecular weight) were computed based on protein sequence obtained from the JGI database.

Supplementary table 11: Intracellular proteins identified with potential functions in biodegradation of xenobiotics of dikaryotic *T. versicolor* strain (Tv-D) grown on beech sapwood (28 days old samples)

JGI protein ID	Putative protein function	EC	UP ^a	pI ^b	Mw ^b
1,4-Dichlorobenzene degradation					
42128	Carboxymethylenebutenolidase	3.1.1.45	12	6.24	27315.01
28066	hydroxyquinol 1,2-dioxygenase	1.13.11.37	3	5.66	32809.91
62764	Hydroxyquinol 1,2-dioxygenase	1.13.11.37	6	5.65	38010.68
121361	Arylacetamide deacetylase	3.1.1.-	8	6.37	39987.67
139611	Arylacetamide deacetylase	3.1.1.-	7	6.04	35931.08
155533	Arylacetamide deacetylase	3.1.1.-	4	5.65	34263.29
52953	Arylacetamide deacetylase	3.1.1.-	5	5.41	36721.09
126181	Predicted acetyltransferases and hydrolases with the alpha/beta hydrolase fold (Carboxylic ester hydrolases)	3.1.1.-	2	5.53	40768.4
Atrazine degradation					
150975	Cyanamide_fam: HD domain protein, cyanamide hydratase family domain	4.2.1.69	5	6.11	28607.63
Benzoate degradation via CoA ligation					
31193	3-hydroxyacyl-CoA dehydrogenase	1.1.1.157	6	7.88	32365.45
143313	cAMP-dependent protein kinase types I and II; regulatory subunit	2.7.1.-	10	5.48	55141.94
25423	Casein kinase (serine/threonine/tyrosine protein kinase)	2.7.1.-	4	9.31	38616.34
142070	Dehydrogenases with different specificities (related to short-chain alcohol dehydrogenases)	1.1.-.-	2	8.24	33629.52
113884	Fumarate reductase; flavoprotein subunit	1.3.99.1	30	7.61	62920.78
176367	Fumarate reductase; flavoprotein subunit	1.3.99.1	6	6.63	55645.16
162152	Hydroxysteroid 17-beta dehydrogenase 11	1.1.-.-	2	6.8	42355.1
Benzoate degradation via hydroxylation					
26871	Predicted fumarylacetoacetate hydrolase	5.3.3.10	21	7.56	32672.69
gamma-Hexachlorocyclohexane degradation					
30566	1;4-benzoquinone reductase-like; Trp repressor binding protein-like/protoplast-secreted protein	1.6.5.7	15	7.06	21353.42
149846	Cytochrome P450		5	6.77	61874.9

21513	Cytochrome P450 CYP2 subfamily		5	6.42	55679.78
175371	Cytochrome P450 CYP3/CYP5/CYP6/CYP9 subfamilies		6	6.95	53261.47
53859	Cytochrome P450 CYP3/CYP5/CYP6/CYP9 subfamilies		25	6.3	54356.6
67999	Cytochrome P450 CYP3/CYP5/CYP6/CYP9 subfamilies		2	6.49	56641.26
55960	Cytochrome P450 CYP4/CYP19/CYP26 subfamilies		2	7.3	61063.3
68000	Cytochrome P450 CYP4/CYP19/CYP26 subfamilies		2	6.61	57414.04
68720	Multiple inositol polyphosphate phosphatase	3.1.3.2	3	5.4	66917.13
Nitorobenzene degradation					
16216	Kynurenine 3-monooxygenase and related flavoprotein monooxygenases	1.14.13.1	4	6.07	45864.97
47635	Monooxygenase involved in coenzyme Q (ubiquinone) biosynthesis	1.14.13.7	12	6.68	66159.64
58730	Monooxygenase involved in coenzyme Q (ubiquinone) biosynthesis	1.14.13.7	2	6.16	66573.61
Glutathione metabolism					
158425	Gamma-glutamyltransferase	2.3.2.2	16	6.07	62031.05
124939	Glutathione peroxidase	1.11.1.9	8	7.85	18152.85
117926	Glutathione S-transferase	2.5.1.18	8	7.54	25379.91
157166	Glutathione S-transferase	2.5.1.18	2	5.34	25811.42
168632	Glutathione S-transferase	2.5.1.18	14	7.05	23348.84
22196	Glutathione S-transferase	2.5.1.18	2	9.07	24921.76
33495	Glutathione S-transferase	2.5.1.18	11	5.63	29890.84
54358	Glutathione S-transferase	2.5.1.18	5	6.41	27049
60698	Glutathione S-transferase	2.5.1.18	5	6.8	29435.47
62807	Glutathione S-transferase	2.5.1.18	33	7.64	25326.75
67635	Glutathione S-transferase	2.5.1.18	27	7.3	26563.34
73357	Glutathione S-transferase	2.5.1.18	5	7.58	26369.51
75639	Glutathione S-transferase	2.5.1.18	7	5.75	28298.62
73974	Glutathione S-transferase C-terminal-like protein	2.5.1.18	6	6.92	31264.42
42031	Glutathione S-transferase, N-terminal domain	2.5.1.18	15	6.56	38825.87

64328	Glutathione S-transferase, N-terminal domain	2.5.1.18	6	6.02	29187.31
175838	Glutathione synthetase	6.3.2.3	2	6.48	56026.69
162670	Glutathione-S-Trfase_C-like, Thioredoxin-like_fold domains	2.5.1.18	6	9.14	37556.36
171539	Oxoprolinase /5-oxoprolinase (ATP-hydrolysing)	3.5.2.9	8	6.07	63341.58
31931	Oxoprolinase /5-oxoprolinase (ATP-hydrolysing)	3.5.2.9	14	5.91	83461.86
72991	Translation elongation factor EF-1 gamma	2.5.1.18	42	6.24	46787.05
Others					
30240	Beta-lactamase domain		2	5.5	61194.37
68942	Beta-lactamase-like domain		5	6.28	32082.4
48870	Dye-decolorizing peroxidase 1 (DyP1)	1.11.1.19	18	5.66	52171.73
48874	Dye-decolorizing peroxidase 2 (DyP2)	1.11.1.19	12	5.8	52634.32
73942	Predicted glutathione S-transferase		2	6.66	36290.43

^a Unique peptides. ^b The theoretical *pI* (isoelectric point) and *M_w* (molecular weight) were computed based on protein sequence obtained from the JGI database.

Supplementary table 12: Intracellular proteins identified with potential functions in biosynthesis of secondary metabolites of dikaryotic *T. versicolor* strain (Tv-D) grown on beech sapwood (28 days old samples)

JGI protein ID	Putative protein function	EC	UP ^a	pI ^b	Mw ^b
Flavonoids, stilbene and lignin biosynthesis					
154843	4-coumarate--CoA ligase.	6.2.1.12	4	7.62	63139.1
74713	4-coumarate--CoA ligase.	6.2.1.12	5	8.12	63350.77
74714	4-coumarate--CoA ligase.	6.2.1.12	2	7.83	64804.96
136252	Beta-glucosidase; lactase phlorizinhydrolase; and related proteins	3.2.1.21	3	5.52	60199.5
171192	Beta-glucosidase; lactase phlorizinhydrolase; and related proteins	3.2.1.21	11	5.82	52140.26
69327	UDP-glucuronosyl and UDP-glucosyl transferase	2.4.1.91	2	6.3	56063.52
Betalain biosynthesis					
19453	Dopa 4,5-dioxygenase domain		2	6.8	20567.35
Terpenoid biosynthesis					
55519	Isopentenyl pyrophosphate:dimethylallyl pyrophosphate isomerase	5.3.3.2	2	5.42	28591.5
148221	Squalene synthetase	2.5.1.21	3	5.96	57044.5
Miscellaneous proteins					
55899	Flavin-containing monooxygenase	1.14.13.8	4	6.5	67524.73
55900	Flavin-containing monooxygenase	1.14.13.8	2	6.24	67728.13
130004	Flavonol reductase/cinnamoyl-CoA reductase		15	5.57	37182.1
168897	Flavonol reductase/cinnamoyl-CoA reductase		11	6.31	38242.22
171842	Flavonol reductase/cinnamoyl-CoA reductase		9	7.09	37162.1
175251	Flavonol reductase/cinnamoyl-CoA reductase		2	5.21	39606.22
31564	Flavonol reductase/cinnamoyl-CoA reductase		14	5.83	37149.07
50399	Flavonol reductase/cinnamoyl-CoA reductase		3	6.56	38333.6
52513	Flavonol reductase/cinnamoyl-CoA reductase		15	7.64	38869.33
172511	Multidrug resistance-associated protein/mitoxantrone resistance protein; ABC superfamily		2	6.48	174541.55
31517	Multidrug resistance-associated protein/mitoxantrone resistance protein; ABC superfamily		6	6.32	185141.05
147761	Multidrug/pheromone exporter; ABC superfamily		4	6.21	145303.82
166013	Transporter; ABC superfamily (Breast cancer resistance protein)		2	6.74	101407.22

^a Unique peptides. ^b The theoretical pI (isoelectric point) and Mw (molecular weight) were computed based on protein sequence obtained from the JGI database.

Supplementary table 13: Intracellular proteins identified with potential functions in metabolism of cofactors and vitamins of dikaryotic *T. versicolor* strain (*Tv-D*) grown on beech sapwood (28 days old samples)

JGI protein ID	Putative protein function	EC	UP ^a	pI ^b	Mw ^b
Biotin metabolism					
47642	Alanine-glyoxylate aminotransferase AGT2	2.6.1.62	10	6.48	49988.86
Folate biosynthesis					
34829	Folypolyglutamate synthase	6.3.2.17	4	6.32	54575.24
Nicotinate and nicotinamide metabolism					
27969	NAD(P)+ transhydrogenase	1.6.1.2	22	8.38	112337.95
26348	NADH pyrophosphatase I of the Nudix family of hydrolases	3.6.1.22	7	6.08	50046.35
65474	Nicotinic acid phosphoribosyltransferase	2.4.2.11	4	6.08	49301.94
Pantothenate and CoA biosynthesis					
39401	Phosphopantothenate--cysteine ligase.	6.3.2.5	3	6.41	39129.15
Riboflavin metabolism					
155092	3'-phosphoadenosine 5'-phosphosulfate sulfotransferase (PAPS reductase)/FAD synthetase and related enzymes	2.7.7.2	2	5.71	40849.01
23676	3'-phosphoadenosine 5'-phosphosulfate sulfotransferase (PAPS reductase)/FAD synthetase and related enzymes	2.7.7.2	6	5.37	33210.12
28907	5;10-methylenetetrahydrofolate reductase	1.5.1.20	6	6.11	69113.76
145512	6;7-dimethyl-8-ribityllumazine synthase	2.5.1.9	3	7.18	21771.03
32938	Riboflavin synthase alpha chain	2.5.1.9	4	5.77	25286.15
Thiamine metabolism					
132179	Cysteine desulfurase NFS1	2.8.1.7	13	6.19	45770.22
149895	Cysteine desulfurase NFS1	2.8.1.8	6	6.44	51906.82
57523	Cysteine desulfurase NFS1	2.8.1.9	5	8.13	53111.46
Proteins with other functions					
163388	Uroporphyrinogen decarboxylase	4.1.1.37	7	6.25	39656.83
156126	Coproporphyrinogen III oxidase CPO/HEM13	1.3.3.3	6	6.34	39320.81
141446	Delta-aminolevulinic acid dehydratase	4.2.1.24	10	7.03	36030.66
53347	Ferredoxin/adrenodoxin reductase	1.18.1.2	2	6.71	54140.58
34375	Protoheme ferro-lyase (ferrochelatase)	4.99.1.1	11	7.57	39099.71

^a Unique peptides. ^b The theoretical *pI* (isoelectric point) and *Mw* (molecular weight) were computed based on protein sequence obtained from the JGI database.

Supplementary table 14: Intracellular proteins identified with potential functions as structural proteins of dikaryotic *T. versicolor* strain (*Tv*-D) grown on beech sapwood (28 days old samples)

JGI protein ID	Putative protein function	EC	UP ^a	<i>pI</i> ^b	<i>M_w</i> ^b
Chromatin structure and dynamics					
29408	Hismacro and SEC14 domain-containing proteins		7	5.58	23413.46
151476	Histone 2A		3	10.57	15658.21
168287	Histone 2A		6	10.09	14711.92
172565	Histone 2A		6	10.14	14917.09
28287	Histone H1		2	10.91	25762.3
60297	Histone H2B		9	10.22	15574.86
29136	Histone H4		10	11.36	11366.34
89142E	Histones H3 and H4		3	11.52	15247.87
171322	N-terminal acetyltransferase (Peptide alpha-N-acetyltransferase)	2.3.1.88	6	6.84	98580.47
56675	Predicted component of NuA3 histone acetyltransferase complex		2	4.98	71779.78
161748	Sister chromatid cohesion complex Cohesin; subunit RAD21/SCC1		2	4.92	76330.28
138897	SWI-SNF chromatin-remodeling complex protein		3	7.73	99025.85
66022	SWI-SNF chromatin-remodeling complex protein		4	6.03	98621.34
Cytoskeleton					
149162	Actin and related proteins		3	5.92	53215.8
18717	Actin and related proteins		49	5.68	41674.64
25778	Actin and related proteins		2	6.6	42224.37
28597	Actin depolymerizing factor		8	5.4	15491.5
37525	Actin filament-coating protein tropomyosin		7	4.89	18719.78
47258	Actin-binding protein Coronin; contains WD40 repeats		9	6.33	56079.86
55210	Actin-binding protein SLA2/Huntingtin-interacting protein Hip1		13	6	121491.53
31405	Actin-like ATPase domain		3	5.68	38035.46
57190	Actin-related protein - Arp4p/Act3p		2	6.29	47464.78
167567	Actin-related protein Arp2/3 complex; subunit Arp2		12	5.94	44508.24
169020	Actin-related protein Arp2/3 complex; subunit Arp3		6	6.34	47950.21
27913	Actin-related protein Arp2/3 complex; subunit ARPC1/p41-ARC		4	6.8	43970.35
169800	Actin-related protein Arp2/3 complex; subunit ARPC2		8	7.63	34913.02

35159	Actin-related protein Arp2/3 complex; subunit ARPC3		5	8.65	20254.19
34212	Actin-related protein Arp2/3 complex; subunit ARPC4		4	9.02	20249.71
151515	Actin-related protein Arp2/3 complex; subunit ARPC5		4	4.79	16823.14
171395	Acyl-CoA N-acyltransferases (Nat) domain		2	7.6	50351.48
168936	Acyl-CoA-binding protein		2	6.13	11801.37
134202	Adaptor complexes medium subunit family		3	7.54	50223.98
116814	Alpha tubulin		18	5.42	49427.7
69843	Alpha tubulin		19	5.12	49356.53
24301	Beta tubulin		55	4.88	49919.35
59312	Beta tubulin		8	4.7	52149.28
171916	Ca ²⁺ -binding actin-bundling protein (fimbrin/plastin); EF-Hand protein superfamily		17	5.99	72427.8
29343	Dynein light chain type 1	3.6.4.2	3	6.68	12120.76
62339	Dyneins; heavy chain (Dynein ATPase)	3.6.4.2	3	5.67	392528.51
68194	Dystonin; GAS (Growth-arrest-specific protein); and related proteins		5	4.97	106956.55
121593	F-actin capping protein; alpha subunit		5	5.14	32675.12
126825	F-actin capping protein; beta subunit		3	4.91	31887.92
153101	Flotillins		7	7.7	60758.26
64071	Gamma tubulin		2	5.75	50792.64
27730	Kinesin (SMY1 subfamily)	3.6.4.4	16	6.01	107657.18
146085	Microtubule-associated anchor protein involved in autophagy and membrane trafficking		2	8.56	13742.88
35395	Microtubule-binding protein (translationally controlled tumor protein)		8	4.68	18902.36
175445	Microtubule-binding protein involved in cell cycle control		5	5.4	27889.55
45594	Mitochondrial inheritance and actin cytoskeleton organization protein		2	6.18	106429.44
70168	Myosin class II heavy chain		2	8.6	59374.65
71028	Myosin class V heavy chain		8	8.83	184012.74
50307	Profilin		3	6.63	13284.12
161761	Putative dynamitin		2	5.92	47837.52

136599	WASP-interacting protein VRP1/WIP; contains WH2 domain	3	9.15	32169.36
172835	WD40 repeat stress protein/actin interacting protein	6	7.27	62989.67

^a Unique peptides. ^b The theoretical *pI* (isoelectric point) and *Mw* (molecular weight) were computed based on protein sequence obtained from the JGI database.

Supplementary table 15: Intracellular proteins identified with potential functions in protein biosynthesis of dikaryotic *T. versicolor* strain (Tv-D) grown on beech sapwood (28 days old samples)

JGI protein ID	Putative protein function	UP^a	pI^b	Mw^b
72344	40s ribosomal protein s10	4	8.83	35899.81
159130	40S ribosomal protein S11	5	10.49	17620.7
129558	40S ribosomal protein S12	5	5.59	15982.55
152971	40S ribosomal protein S13	3	10.54	17056.01
50212	40S ribosomal protein S14	3	10.53	16447.89
47782	40S ribosomal protein S15	5	11	21228.82
160126	40S ribosomal protein S15/S22	5	10.21	14638.1
33356	40S ribosomal protein S16	7	10.37	15833.49
26112	40S ribosomal protein S17	6	10.43	16841.32
147007	40S ribosomal protein S19	8	4.98	17877.72
34281	40S ribosomal protein S2	3	8.92	17567.27
112869	40S ribosomal protein S2/30S ribosomal protein S5	12	10.18	28397.25
150437	40S ribosomal protein S20	3	9.77	13799.05
175850	40S ribosomal protein S21	6	7.18	9284.48
25777	40S ribosomal protein S24	5	11.45	15680.36
35560	40S ribosomal protein S25	3	10.62	11504.5
130225	40s ribosomal protein S26	4	10.28	13536.7
109668	40S ribosomal protein S28	4	10.56	13005.44
25792	40S ribosomal protein S3	13	8.98	28995.52
143816	40S ribosomal protein S3A	10	9.87	29318.15
168053	40S ribosomal protein S4	8	10.41	29529.31
60198	40S ribosomal protein S6	7	10.39	27772.37
63130	40S ribosomal protein S7	9	8.49	66395.74
34201	40S ribosomal protein S8	6	10.65	24085.39
149851	60S acidic ribosomal protein P0	9	5.28	33378.37
124797	60S acidic ribosomal protein P2	4	4.48	11227.5

31118	60s ribosomal protein L10	5	10.31	25044.09
43986	60S ribosomal protein L10A	9	9.94	24539.03
142588	60S ribosomal protein L11	5	10.33	20192.47
41978	60S Ribosomal protein L13	6	11.06	24241.93
25566	60S ribosomal protein L13a	7	10.69	22881.04
26446	60S ribosomal protein L14	7	10.95	15438.96
73600	60S ribosomal protein L14/L17/L23	4	10.12	14734.17
33449	60s ribosomal protein L15	5	11.46	23845.78
172975	60s ribosomal protein L15/L27	7	11.06	16446.1
45000	60s ribosomal protein L18	5	11.25	23739
111807	60s ribosomal protein L19	6	11.58	22592.55
111858	60S ribosomal protein L21	2	10.43	18302.26
166840	60S ribosomal protein L22	5	10.47	21655.88
25859	60S ribosomal protein L22	5	9.4	13569.45
51824	60s ribosomal protein L23	6	10.53	17558.56
30458	60s ribosomal protein L24	4	11.52	17125.93
36111	60S ribosomal protein L26	4	10.81	15874.42
173909	60S ribosomal protein L27	3	10.31	15679.55
32741	60S ribosomal protein L28	4	10.86	15565.21
26940	60S ribosomal protein L3 and related proteins	14	10.26	43820.97
149158	60S ribosomal protein L30	4	9.95	12057.11
154749	60S ribosomal protein L31	5	10.13	14383.62
139836	60S ribosomal protein L32	6	11.5	14639.33
174021	60s ribosomal protein L34	2	11.21	12761.16
47564	60S ribosomal protein L35A/L37	4	11.69	11935.9
144269	60S ribosomal protein L36	5	11.91	11561.55
171991	60S ribosomal protein L38	2	10	9623.39
70197	60S ribosomal protein L5	5	8.74	34478.99
144284	60s ribosomal protein L6	12	10.27	26022.19
27958	60S ribosomal protein L7	9	10.18	28774.54

60172	60S ribosomal protein L7A	10	10.27	30761.04
35434	60S ribosomal protein L9	5	9.31	21474.03

^a Unique peptides. ^b The theoretical *pI* (isoelectric point) and *Mw* (molecular weight) were computed based on protein sequence obtained from the JGI database.

Supplementary table 16: Intracellular proteins identified with potential functions in inorganic ion transport and metabolism of dikaryotic *T. versicolor* strain (Tv-D) grown on beech sapwood (28 days old samples)

JGI protein ID	Putative protein function	EC	UP ^a	<i>pI</i> ^b	<i>M_w</i> ^b
28094	Ca ²⁺ transporting ATPase	3.6.3.8	2	5.54	108633.83
164339	Copper chaperone		4	7.28	7904.14
62820	Heavy metal exporter HMT1; ABC superfamily		5	6.01	123420.3
144526	Manganese superoxide dismutase	1.15.1.1	2	8.66	37241.37
175708	Manganese superoxide dismutase	1.15.1.1	17	7.27	22531.53
150713	Protein involved in inorganic phosphate transport		4	9.25	20363.95
33838	Putative arsenite-translocating ATPase	3.6.3.16	3	5.1	36177.76
25905	Rhodanese-related sulfurtransferase		2	9.44	19698.38
134691	Salt-sensitive 3'-phosphoadenosine-5'-phosphatase HAL2/SAL1		2	5.15	37839.85

^a Unique peptides. ^b The theoretical *pI* (isoelectric point) and *M_w* (molecular weight) were computed based on protein sequence obtained from the JGI database.

Supplementary table 17: Proteins identified with potential functions of proteases and peptidases, dikaryotic *T. versicolor* strain (*Tv*-D) grown on beech sapwood (28 days old samples)

JGI protein ID	Putative protein function	UP^a	pI^b	Mw^b
35262	20S proteasome; regulatory subunit alpha type PSMA1/PRE5	11	5.79	30087.81
143930	20S proteasome; regulatory subunit alpha type PSMA2/PRE8	6	6.93	27433.47
162206	20S proteasome; regulatory subunit alpha type PSMA3/PRE10	13	6.16	27279.92
160573	20S proteasome; regulatory subunit alpha type PSMA4/PRE9	9	5.88	28871.69
111373	20S proteasome; regulatory subunit alpha type PSMA5/PUP2	13	5.25	26827.59
144814	20S proteasome; regulatory subunit alpha type PSMA6/SCL1	10	6.81	29113.2
27866	20S proteasome; regulatory subunit alpha type PSMA7/PRE6	12	7.89	29189.39
67483	20S proteasome; regulatory subunit beta type PSMB1/PRE7	10	7.59	27913.58
40225	20S proteasome; regulatory subunit beta type PSMB2/PRE1	5	7.54	21829.05
152169	20S proteasome; regulatory subunit beta type PSMB3/PUP3	7	5.17	23053.6
67268	20S proteasome; regulatory subunit beta type PSMB4/PRE4	5	6.34	29261.05
164705	20S proteasome; regulatory subunit beta type PSMB5/PSMB8/PRE2	4	6.54	33593.56
162201	20S proteasome; regulatory subunit beta type PSMB6/PSMB9/PRE3	8	5.41	25749
155593	20S proteasome; regulatory subunit beta type PSMB7/PSMB10/PUP1	4	6.78	29226.53
19290	26S proteasome regulatory complex; ATPase RPT1	14	6.76	98214.32
72656	26S proteasome regulatory complex; ATPase RPT2	7	6.17	50022.49
175824	26S proteasome regulatory complex; ATPase RPT3	18	5.44	46745.52
58745	26S proteasome regulatory complex; ATPase RPT4	12	6.63	44779.54
122728	26S proteasome regulatory complex; ATPase RPT5	9	5.24	47346.5
54381	26S proteasome regulatory complex; ATPase RPT6	7	8.8	44593.8
73466	26S proteasome regulatory complex; subunit RPN1/PSMD2	25	4.94	103483.99
144763	26S proteasome regulatory complex; subunit RPN10/PSMD4	6	4.7	35656.83
116190	26S proteasome regulatory complex; subunit RPN11	8	7.2	33408.38
163820	26S proteasome regulatory complex; subunit RPN11	8	9.53	33933.75
69637	26S proteasome regulatory complex; subunit RPN12/PSMD8	7	5.35	29844.34
68159	26S proteasome regulatory complex; subunit RPN2/PSMD1	13	5.26	108475.17

74103	26S proteasome regulatory complex; subunit RPN3/PSMD3	6	7.69	56274.29
109996	26S proteasome regulatory complex; subunit RPN5/PSMD12	9	7.36	54474.47
156931	26S proteasome regulatory complex; subunit RPN6/PSMD11	12	6.81	47528.59
75560	26S proteasome regulatory complex; subunit RPN7/PSMD6	15	6.07	43574.02
145790	26S proteasome regulatory complex; subunit RPN8/PSMD7	6	5.39	36400.13
128001	26S proteasome regulatory complex; subunit RPN9/PSMD13	13	6	44232.81
45634	AAA+-type ATPase containing the peptidase M41 domain	6	7.54	86535.01
124091	Aminoacylase ACY1 and related metalloexopeptidases	10	6.56	67934.7
124267	Aminoacylase ACY1 and related metalloexopeptidases	6	5.87	65360.26
64964	Aminoacylase ACY1 and related metalloexopeptidases	9	6.37	64762.4
26923	Aminopeptidase I zinc metalloprotease (M18)	12	6.77	50953.67
27303	Aspartyl protease	13	5.37	41763.45
64339	Aspartyl protease	5	5.15	44321.57
167196	Dipeptidyl aminopeptidase	28	6.47	81347.69
31466	Dipeptidyl aminopeptidase	6	5.85	71572.82
56726	Dipeptidyl peptidase III	18	5.45	77125.28
46542	Metalloendopeptidase family - saccharolysin & thimet oligopeptidase	2	5.85	76757.85
46546	Metalloendopeptidase family - saccharolysin & thimet oligopeptidase	21	5.79	77043.66
150124	Metallopeptidase	12	7.8	42548.57
61072	Metalloprotease	2	8.72	53745.91
60604	Peptidase C45, acyl-coenzyme A:6-aminopenicillanic acid acyl-transferase domains	3	5.67	40444.28
68383	Peptidase M14 domain	15	6.49	49161.05
174361	Peptidase M20A, amidohydrolase, predicted domains	2	5.94	43772.84
29674	Peptidase S33, tricorn interacting factor 1, prolyl aminopeptidase domains	4	5.47	36513.75
119907	Peptide chain release factor 1 (eRF1)	7	5.72	49043.83
25194	Peptidyl-prolyl cis-trans isomerase (Peptidylprolyl isomerase)	2	6.89	18836.04
42757	Predicted aminopeptidase of the M17 family	2	6.07	52930.21
114132	Tripeptidyl-peptidase I.	10	4.7	56038.7

^a Unique peptides. ^b The theoretical *pI* (isoelectric point) and *Mw* (molecular weight) were computed based on protein sequence obtained from the JGI database.

Supplementary table 18: Miscellaneous intracellular proteins for various potential functions, dikaryotic *T. versicolor* strain (Tv-D) grown on beech sapwood (28 days old samples)

JGI protein ID	Putative protein function	EC	UP ^a	pI ^b	Mw ^b
160508	17 beta-hydroxysteroid dehydrogenase type 3; HSD17B3	1.1.1.62	2	9.87	37822.05
169846	17 beta-hydroxysteroid dehydrogenase type 3; HSD17B3	1.1.1.62	4	9.49	35283.83
38101	17 beta-hydroxysteroid dehydrogenase type 3; HSD17B3	1.1.1.62	2	6.41	27607.29
61044	17 beta-hydroxysteroid dehydrogenase type 3; HSD17B3	1.1.1.62	6	8.77	27833.34
53118	Acetyltransferase (GNAT) family domain		2	4.87	24727.55
53125	Acetyltransferase (GNAT) family domain		2	5.24	23937.21
57951	Acetyltransferase (GNAT) family domain		7	5.87	141089.15
115387	Aldo/keto reductase family proteins	1.1.1.-	17	6.19	34831.55
30772	Aldo/keto reductase family proteins	1.1.1.-	14	6.89	34529.46
31299	Aldo/keto reductase family proteins	1.1.1.-	21	6.14	36772.08
33990	Aldo/keto reductase family proteins	1.1.-.-	5	6.88	30968.36
38959	Aldo/keto reductase family proteins	1.1.1.-	13	6.65	32404.42
60268	Aldo/keto reductase family proteins	1.1.1.-	9	6.06	32809.26
66860	Aldo/keto reductase family proteins	1.1.1.-	13	6.4	35584.71
160585	alpha/beta-Hydrolases domain		6	5.4	38411.62
168559	alpha/beta-Hydrolases domain		3	6.46	45403.98
27033	alpha/beta-Hydrolases domain		2	5.76	45532.06
45221	alpha/beta-Hydrolases domain		8	5.42	37623.5
59416	alpha/beta-Hydrolases domain		4	7	37630.16
36295	alpha/beta-Hydrolases domain and Lipase, active site		3	5.74	97233.5
56488	alpha/beta-Hydrolases fold-1, 4 domains		11	6.1	65370.36
74763	alpha/beta-Hydrolases fold-1, 4 domains		3	5.76	65348.01
25850	Amidohydrolase 1, Metal-dependent hydrolase, composite, DNA-directed RNA polymerase, RBP11-like domains		8	6.2	102250.17
51482	AMP-binding enzyme domain		4	5.85	59739.04
164679	Bet v1-like domain		6	5.7	29735.53
122910	Bifunctional GTP cyclohydrolase II/3;4-dihydroxy-2butanone-4-phosphate synthase		13	6.31	58011.4
74836	Biotin holocarboxylase synthetase/biotin-protein ligase		3	6.36	70987.42

155340	BTB/POZ fold domains		4	5.11	36472.57
165804	BTB/POZ fold domains		2	6.64	37549.09
168351	C4-type Zn-finger protein		3	4.77	57209.56
146511	Ca ²⁺ -binding transmembrane protein LETM1/MRS7		2	5.79	71587.75
112899U	Carbohydrate Esterase Family 15 protein		4	5.92	40415.33
33056	Carbohydrate-Binding Module Family 1 / Glycoside Hydrolase Family 5 protein		10	4.72	38149.41
28558	Carbohydrate-Binding Module Family 12 protein		17	6.4	35875.16
56579	Carbonic anhydrase		6	6.89	70402.31
172435	Carboxylesterase and related proteins	3.1.1.1	15	5.81	57800.66
73449	Cell cycle-associated protein		2	4.28	63257.02
28442	Cell division cycle 37 protein; CDC37		3	4.95	56216.14
87426UE	Cerato-platanin domain		2	4.41	11912.17
172999	Chromatin remodeling factor subunit and related transcription factors		5	4.98	77610.27
73434	Chromatin-associated protein Dek and related proteins; contains SAP DNA binding domain		2	5.56	45515.21
27040	Class I glutamine amidotransferase-like domain		6	5.6	23931.23
30469	Conserved protein Mo25		5	9	38289.28
114559	Conserved WD40 repeat-containing protein AN11		2	5.97	46029.57
161174	Conserved Zn-finger protein		8	5.57	63020.18
122257	Cullins		18	7.43	87671.81
140673	Cullins		6	7.46	96470.55
176118	Cupin 2 domain		8	6.34	21396.14
38130	Cyanase	4.2.1.104	11	5.92	18197.14
167065	Damage-specific DNA binding complex; subunit DDB1		2	6.6	135691.08
27917	D-arabinitol 2-dehydrogenase.	1.1.1.250	15	8.31	34255.46
54414	D-arabinitol 2-dehydrogenase.	1.1.1.250	7	6.77	31677.17
156078	Dehydrogenases with different specificities (related to short-chain alcohol dehydrogenases)		22	8.09	34976.09
156395	Dehydrogenases with different specificities (related to short-chain alcohol dehydrogenases)		2	8.38	35093.28

121918	DHAP synthase, class 1 domain		8	7.3	41865.72
52553	Dihydropteroate synthase/7;8-dihydro-6-hydroxymethylpterin-pyrophosphokinase/Dihydroneopterin aldolase		2	6.63	92182.51
67321	Dimeric alpha-beta barrel domain		6	5.3	23497.12
32869	Dopey and related predicted leucine zipper transcription factors		2	6.22	209656.97
149868	DSBA oxidoreductase, Thioredoxin-related domains		3	5.69	27358.32
46345	DUF1688 domain		10	6.4	47017.85
68124	D-xylose 1-dehydrogenase (NADP+).	1.1.1.179	27	6.37	35694.87
59789	Dynein-associated protein Roadblock		2	6.89	13494.37
25474	Esterase D	3.1.1.1	17	6.53	31881.9
155619	Exon-exon junction complex; Magoh component		4	6.64	17503.88
138138	extracellular GDSL-like lipase/acylhydrolase		12	5.49	42575.71
42584	Ferritin-like_SF domain		11	6	44435.3
153802	FOG: Low-complexity		4	4.9	52380.81
115488U	FOG: RRM domain		2	10.17	24686.72
118093	FOG: RRM domain		7	8.95	36372.75
161318	FOG: RRM domain		18	8.44	12684.58
30828	FOG: RRM domain		2	5.99	44545.75
31332	FOG: RRM domain		2	6.95	71663.3
33581	FOG: RRM domain		14	6.35	46087.53
38170	FOG: RRM domain		2	6.27	51561.72
108496	FOG: TPR repeat		5	9.33	126927.14
43453	Formate/nitrite transporter domains		3	7.76	33984.72
125187	Fungal protein of unknown function		2	8.57	8313.42
28241	Glycosyltransferase		42	6.62	81622.05
174721	GMC oxidoreductase		27	5.84	69437.32
60196	Haloacid dehalogenase-like hydrolase domain		2	5.8	29543.25
68853	Haloacid dehalogenase-like hydrolase domain		9	5.98	26737.51
147439	HGG motif-containing thioesterase		3	7.5	17794.2
23785	HTP3, Chloroperoxidase domains		4	7.39	33793.8
67715	Huntingtin interacting protein HYPE		3	6.57	51048.47
171425	Hydantoinase/oxoprolinase domain		2	5.16	105560.77

131840	Hydroxyindole-O-methyltransferase and related SAM-dependent methyltransferases	22	5.69	55431.05
34708	Hydroxyindole-O-methyltransferase and related SAM-dependent methyltransferases	15	6.43	52171.68
133803	Iron/ascorbate family oxidoreductases	3	6.8	41216.53
175496	Iron/ascorbate family oxidoreductases	3	5.21	37189.91
175745	Iron/ascorbate family oxidoreductases	2	6.44	41719.09
18767	Iron/ascorbate family oxidoreductases	4	6.54	40125.63
54030	Iron/ascorbate family oxidoreductases	31	6.54	42160.91
54032	Iron/ascorbate family oxidoreductases	22	6.6	41647.36
63355	Iron/ascorbate family oxidoreductases	4	7.34	42345.94
71567	Iron/ascorbate family oxidoreductases	3	5.5	37359.63
70135	KEKE-like motif-containing transcription regulator (Rlr1)/suppressor of sin4	2	9.43	78532.66
53509	LamB/YcsF family domain	4	6.27	26994.21
66353	MAM33; mitochondrial matrix glycoprotein	2	4.71	29543.89
47799	Membrane protein involved in organellar division	3	7.43	17504.03
65740	Metal-dep hydrolase, composite, Amidohydrolase 3 domains	2	5.43	68483.22
59269	Metal-dependent hydrolase, composite domain	2	5.34	23464.59
114585	Metal-dependent hydrolase, composite, Amidohydrolase 1 domains	3	6.6	103626.96
152882	Metal-dependent hydrolase, composite, Amidohydrolase 1 domains	11	6.71	104482.88
173657	Metal-dependent hydrolase, composite, Amidohydrolase 1 domains	3	6.42	49136.6
152837	Metal-dependent hydrolase, composite, Amidohydrolase 3 domains	5	6.51	97508
160326	Metal-dependent hydrolase, composite, Amidohydrolase 3 domains	5	6.04	67535.6
171365	Metallo-hydrolase/oxidoreductase domain	2	8.11	27111.14
32219	Methyltransferase	19	5.86	31088.08
50314	Methyltransferase	7	6.07	34845.44

27150	Molybdopterin biosynthesis protein	4	6.67	70954.86
155672	Multifunctional pyrimidine synthesis protein CAD (includes carbamoyl-phosphate synthetase; aspartate transcarbamylase; and glutamine amidotransferase)	22	6.25	247228.33
40856	NAD(P)-binding domains	11	5.93	50172.2
17353	NAD-P-binding protein	2	6.11	15024.35
176079	NAD-P-binding protein	3	7.6	34347.39
25971	NAD-P-binding protein	3	8.4	23909.01
48305	NAD-P-binding protein	8	5.81	37936.6
51650	NAD-P-binding protein	8	6.31	36505.83
111418	NDR and related serine/threonine kinases	3	8.74	57334.35
117484	NDR and related serine/threonine kinases	2	7.2	56713.33
45904	Negative regulator of transcription	5	5.97	237449.41
138381	NIPSNAP1 protein	10	8.73	30813.99
73826	NMD protein affecting ribosome stability and mRNA decay	2	5.71	61526.3
56121	Nucleotide excision repair factor NEF2; RAD23 component	6	4.62	39897.92
29538	Oxidative stress survival Svf1-like protein	3	5.53	45952.76
25917	PB1, CBS domains	3	6.35	74584.86
172173	Pentafunctional AROM protein	8	6.5	173393.93
29638	Periplasmic binding protein-like II domain	9	5.01	31567.75
133003	Permease of the major facilitator superfamily	2	9.16	56218.85
157667	Peroxidase/oxygenase	41	6.53	121411.58
64780	Peroxidase/oxygenase	45	6.49	117038.74
125356	Peroxisomal multifunctional beta-oxidation protein and related enzymes	11	6.51	91649.12
175775	Peroxisomal multifunctional beta-oxidation protein and related enzymes	12	9.18	33678.47
28225	Pkinase-domain-containing protein	8	8.44	45450.97
49555	Pleckstrin homology (PH) domain	3	10.93	16770.89
156921	PolyC-binding proteins alphaCP-1 and related KH domain proteins	4	8.36	39346.28

41802	PolyC-binding proteins alphaCP-1 and related KH domain proteins	9	9.03	34740.15
162590	Polypeptide release factor 3	6	8.09	64165.82
134579	Polyprenyl synthetase	12	5.77	41221.4
46679	Porin/voltage-dependent anion-selective channel protein	19	9.18	31150.24
160163	Porphobilinogen deaminase	3	5.73	37152.65
73756	Predicted alpha/beta hydrolase BEM46	2	6.4	38640.44
26778	Predicted cell growth/differentiation regulator; contains RA domain	4	7.34	84308.47
119195	Predicted dehydrogenase	18	7.44	28569.96
164790	Predicted dehydrogenase	5	5.95	35814.12
25627	Predicted dehydrogenase	16	6.85	39682.43
33208	Predicted dehydrogenase	3	6.16	29603.2
69261	Predicted dehydrogenase	2	6.35	32088.66
159290	Predicted dioxygenase	2	6.35	35972.68
164019	Predicted glycosylhydrolase	3	5.8	83081.08
156449	Predicted GTPase-activating protein	4	8.99	50608.66
150496	Predicted GTP-binding protein (ODN superfamily)	15	7.4	43494.83
159764	Predicted hydrolase related to diene lactone hydrolase	16	5.47	27954.7
167313	Predicted hydrolase related to diene lactone hydrolase	9	5.16	27161.89
28810	Predicted hydrolase related to diene lactone hydrolase	7	5.63	26790.64
41188	Predicted hydrolase related to diene lactone hydrolase	10	5.97	28354.32
41189	Predicted hydrolase related to diene lactone hydrolase	3	6.37	27714.58
33477	Predicted hydrolase/acyltransferase (alpha/beta hydrolase superfamily)	7	6.62	30964.68
44116	Predicted hydrolase/acyltransferase (alpha/beta hydrolase superfamily)	3	6.07	35012.87
28400	Predicted membrane protein	2	8.98	33256.92
29086	Predicted membrane protein	2	9.83	10345.09
25788	Predicted metal-binding protein	4	6.21	38278.39
115122	Predicted N-acetyltransferase	3	8.53	19344.23
154739	Predicted NAD-dependent oxidoreductase	3	6.9	37302.53

29635	Predicted NAD-dependent oxidoreductase	1.6.5.5	3	8.88	37193.86
57498	Predicted nucleotidyltransferase		2	6.12	37794.15
117372	Predicted oxidoreductase		2	6.33	42779.77
156677	Predicted oxidoreductase		10	5.6	39459.81
68497	Predicted oxidoreductase		23	6.9	46708.78
112540U	Predicted phosphatase		3	6.14	37826.03
130683	Predicted short chain-type dehydrogenase		12	6.79	25351.13
164738	Predicted short chain-type dehydrogenase		3	7.37	25251.38
172257	Predicted short chain-type dehydrogenase		5	5.06	25558.15
47088	Predicted short chain-type dehydrogenase		7	5.69	25920.9
150386	Predicted steroid reductase		2	9.38	41150.06
56486	Predicted translation factor; contains W2 domain		8	6.32	47823.65
142126	Predicted translation initiation factor related to eIF-2B alpha/beta/delta subunits (CIG2/IDI2)		11	5.94	41217.04
64264	Predicted translation initiation factor related to eIF-3a		2	9.41	70560.72
162097	Predicted transporter (ABC superfamily)		7	6.98	70434.34
26292	Protein involved in autophagocytosis during starvation		4	4.75	40657.26
163609	Protein involved in sister chromatid separation and/or segregation		2	5.99	31075.71
71517	Protein involved in thiamine biosynthesis and DNA damage tolerance		10	5.91	34445.91
55768	Protein kinase PCTAIRE and related kinases		4	8.56	42958.18
145138	Protein tyrosine kinase 9/actin monomer-binding protein		2	5.31	37734.36
31967	Protein tyrosine phosphatase SHP1/Cofactor for p97 ATPase-mediated vesicle membrane fusion		5	4.93	35112.47
161863	Proteinase inhibitor I9, subtilisin propeptide domains		2	4.58	8404.28
37495	PRTase-like domain		2	5.86	23631
19528	Putative cyclase domain		12	6.26	35838.68
46261	Putative cyclase domain		6	6.07	36740.67
66045	putative isomerase YbhE domain		7	6.27	37049.1
174863	Putative metallopeptidase	3.4.13.9	12	6.34	59670.13
141524	Putative steroid membrane receptor Hpr6.6/25-Dx		3	5.07	13402.05

155527	Putative steroid membrane receptor Hpr6.6/25-Dx		3	6.56	18567.33
171260	Putative transcriptional regulator DJ-1		3	5.38	21421.39
110875	Putative translation initiation inhibitor UK114/IBM1		4	7.41	13689.79
166451	Putative translation initiation inhibitor UK114/IBM1		5	5.14	14086.58
159079	Pyrazinamidase/nicotinamidase PNC1		5	5.34	31855.14
20234	Pyridoxal/pyridoxine/pyridoxamine kinase	2.7.1.35	2	6.3	39037.66
143047	Ras GTPase activating protein RasGAP/neurofibromin		2	6.27	304939.53
169528	Ras GTPase-activating protein family - IQGAP		3	7.25	87909.15
159540	Ras-related GTPase		6	4.96	23027.06
29729	Ras-related GTPase		5	5.22	24061.03
146571	Ras-related small GTPase; Rho type		4	6.03	21268.64
41792	Ras-related small GTPase; Rho type		8	7.7	21305.58
53698	Ras-related small GTPase; Rho type		7	7.06	21852.33
142202	Recombination signal binding protein-J kappa(CBF1; Su(H); HS2NF5)		2	8.27	97753.6
68154	Recombination signal binding protein-J kappa(CBF1; Su(H); HS2NF5)		3	7.27	77175.07
117470	Reductases with broad range of substrate specificities		6	7.03	30095.94
159063	Reductases with broad range of substrate specificities		2	6.21	27700.88
165519	Reductases with broad range of substrate specificities	1.1.1.250	16	8.34	36397.37
159805	S-adenosyl-L-methionine-dependent methyltransferases domain		2	6.46	33804.77
25964	S-adenosyl-L-methionine-dependent methyltransferases domain		6	6.27	35650.97
134437	Sensory transduction histidine kinase	2.7.3.-	8	5.68	126946.06
145952	Stationary phase-induced protein; SOR/SNZ family		9	7.27	36046.51
176082	Structural maintenance of chromosome protein 1 (sister chromatid cohesion complex Cohesin; subunit SMC1)		2	5.61	141422.4
164008	Structural maintenance of chromosome protein 2 (chromosome condensation complex Condensin; subunit E)		6	10.83	27569.86
140584	TATA-binding protein-interacting protein		26	5.39	133639.13
160050	TATA-binding protein-interacting protein		14	5.38	94560.38

159706	Taurine catabolism dioxygenase TauD/TfdA domain		19	7.09	41514.49
169625	Taurine catabolism dioxygenase TauD/TfdA domain		11	6.6	45129.57
67834	Taurine catabolism dioxygenase TauD/TfdA domains		3	6.61	44219.57
47002	Terpenoid synthases domains		2	6.23	36348.2
35090	Thioredoxin-like domain		4	6.21	22909.21
40829	Transcription factor containing NAC and TS-N domains		3	4.86	21677.81
25901	Transcription initiation factor TFIID; subunit BDF1 and related bromodomain proteins		2	6.43	81640.39
65907	Transcription regulator dachshund; contains SKI/SNO domain		3	4.61	39766.47
43313	Transcriptional coactivator p100		7	7.48	99716.61
69990	Transferrin receptor and related proteins containing the protease-associated (PA) domain	3.4.17.21	7	5.37	91286.91
149048	U1 snRNP component		2	10.32	18689.07
146160	Uroporphyrin III methyltransferase		2	7.01	30054.65
139192	von Willebrand factor and related coagulation proteins		6	6.09	59398.95
23069	WD40 repeat-containing protein		6	7.22	90236.75
49118	WD40 repeat-containing protein		2	5.1	92919.71
127067	Zinc-binding oxidoreductase		4	6.96	36541.93
145817	Zinc-binding oxidoreductase		6	6.39	37073.34
16631	Zinc-binding oxidoreductase		2	9.37	39715.88
26383	Zinc-binding oxidoreductase		2	8.9	36474.12
37734	Zinc-binding oxidoreductase		15	5.74	37638.15
37737	Zinc-binding oxidoreductase		5	6.57	36810.08
49307	Zinc-binding oxidoreductase		2	7.63	37428.98
72371	Zinc-binding oxidoreductase		14	5.2	37913.75

^a Unique peptides. ^b The theoretical *pI* (isoelectric point) and *M_w* (molecular weight) were computed based on protein sequence obtained from the JGI database.

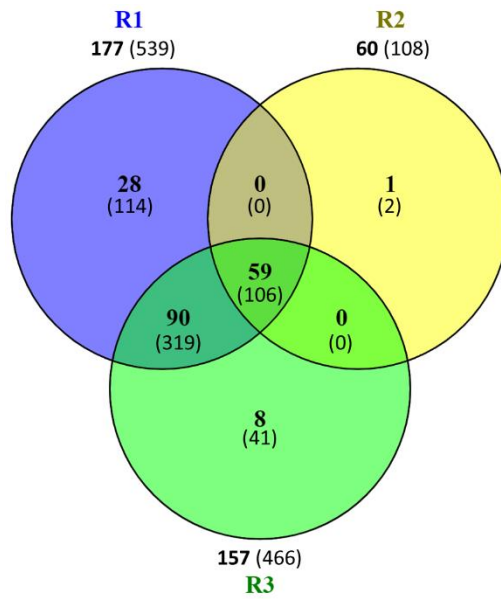
Supplementary table 19: Identified hypothetical proteins, dikaryotic *T. versicolor* strain (*Tv*-D) grown on beech sapwood (28 days old samples)

JGI protein ID	UP^a	<i>pI</i>^b	<i>Mw</i>^b	TMHMM^c	Protein type^d	Localization^d
109967	3	8.22	54606.72	0	Soluble	Nucleus
110515	3	5	46946.43	0	Soluble	Cytoplasm
120108	4	7.38	21923.07	0	Soluble	Plastid
121374	5	5.34	215028.8	0	Soluble	Cytoplasm
122086	3	5.99	32280	0	Soluble	Cytoplasm
123437	2	4.9	13252.25	0	Soluble	Cytoplasm
123989	3	7.14	96659.86	0	Membrane	Nucleus
126359	4	7.34	21312.95	0	Soluble	Cytoplasm
128689	2	6.39	92227.54	0	Membrane	Nucleus
132042	2	6.6	39686.97	0	Soluble	Nucleus
135274	3	5.76	192274.2	0	Soluble	Golgi apparatus
136827	9	5.41	34608.81	0	Soluble	Cytoplasm
138389	2	6.42	55854.09	0	Soluble	Cytoplasm
138946	5	5.77	21160.21	0	Soluble	Lysosome/Vacuole
141453	6	6.36	70767.61	0	Soluble	Peroxisome
141706	5	7.44	18101.49	0	Membrane	Mitochondrion
142067	4	5.25	17280.18	0	Soluble	Cytoplasm
143401	2	5.75	223859.8	0	Membrane	Nucleus
143777	3	8.93	20835.42	0	Soluble	Plastid
144905	3	7.34	39442.36	0	Soluble	Peroxisome
145562	2	6.96	73353.39	0	Soluble	Nucleus
146378	5	5.22	76996.79	0	Membrane	Endoplasmic reticulum
147114	4	8.17	43708.5	6	Membrane	Golgi apparatus
147129	3	6.25	55369.86	0	Membrane	Plastid
154946	2	5.11	40235.79	0	Soluble	Extracellular
155352	2	8.71	24310.47	3	Membrane	Endoplasmic reticulum
158287	2	6.26	90161.94	0	Soluble	Cytoplasm
158912	2	6.84	216609.1	0	Soluble	Cytoplasm
159203	13	6.45	32070.2	0	Soluble	Cytoplasm

159386	2	4.74	27862.78	0	Soluble	Cytoplasm
160067	22	6.45	75491.14	0	Soluble	Cytoplasm
162584	2	8.61	18079.09	0	Soluble	Cytoplasm
163607	7	5.28	11659.83	0	Soluble	Mitochondrion
164125	10	8.74	76240.61	0	Soluble	Nucleus
165288	12	5.29	79588.86	0	Soluble	Cytoplasm
16534	4	5.69	144253.4	0	Soluble	Plastid
165674	3	8.26	44436.11	2	Membrane	Lysosome/Vacuole
165861	17	5.99	23093.29	0	Soluble	Plastid
165979	3	7.75	32820.42	3	Membrane	Endoplasmic reticulum
166737	5	5.83	28817.7	0	Membrane	Mitochondrion
166830	4	9.26	56927.47	7	Membrane	Cell membrane
166999	2	4.64	15792.67	0	Soluble	Cytoplasm
168314	2	5.08	59262.78	0	Soluble	Cytoplasm
170065	4	6.02	64521.85	0	Soluble	Cytoplasm
170539	16	4.79	94791.79	0	Soluble	Cytoplasm
170736	2	5.24	40301.06	1	Soluble	Peroxisome
171239	2	5.25	50352.96	1	Soluble	Cytoplasm
171478	2	6.02	32245.28	0	Soluble	Cytoplasm
175105	7	6.56	58638.4	0	Membrane	Peroxisome
175111	6	6.57	54925.24	0	Membrane	Plastid
26273	4	5.3	39333.48	0	Soluble	Plastid
26989	7	8.54	9649.88	0	Soluble	Nucleus
27229	16	8.54	31089.81	0	Soluble	Cytoplasm
29283	29	4.77	118767.3	0	Soluble	Cytoplasm
29572	4	9.21	37695.12	0	Soluble	Cytoplasm
30821	15	6.29	37813.12	0	Soluble	Cytoplasm
31128	11	5.01	100243.3	0	Soluble	Cytoplasm
34613	2	6.48	77006.49	0	Soluble	Nucleus
35113	3	6.36	33681.33	0	Soluble	Cytoplasm
36289	5	5.28	96004.21	0	Soluble	Cytoplasm
36792	3	6.16	31509.26	0	Soluble	Cytoplasm

38129	7	5.95	48909.2	0	Soluble	Cytoplasm
38438	4	4.96	30391.01	0	Soluble	Cytoplasm
39857	16	5.4	27154.43	0	Soluble	Cytoplasm
39965	8	5.63	34519.62	0	Soluble	Cytoplasm
44482	4	6.1	13075.66	0	Soluble	Cytoplasm
45147	6	7.51	18535.24	0	Soluble	Cytoplasm
49942	4	6.94	11455.14	0	Membrane	Mitochondrion
50918	5	6	27322.42	0	Soluble	Mitochondrion
54997	2	4.85	112739.6	0	Soluble	Golgi apparatus
57526	6	4.83	29871.94	0	Soluble	Nucleus
60396	7	5.65	59616.41	0	Membrane	Mitochondrion
65852	4	6.48	77350.9	6	Membrane	Golgi apparatus
67857	10	7.36	59610.38	0	Soluble	Peroxisome
68765	2	9.2	19693.25	3	Membrane	Endoplasmic reticulum
71750	2	5.16	47849.95	0	Soluble	Cytoplasm
73122	4	5.22	55344.91	0	Soluble	Cytoplasm
73474	12	5.52	47688.77	0	Membrane	Plastid
74254	3	6.09	30224.43	0	Soluble	Cytoplasm
74775	4	6.97	20970.63	0	Soluble	Cytoplasm

^a Unique peptides. ^b The theoretical *pI* (isoelectric point) and *M_w* (molecular weight) were computed based on protein sequence obtained from the JGI database. ^c TMHMM Server v. 2.0 was used for prediction of transmembrane helices in proteins. ^d Protein type and localization were obtained using the DeepLoc-1.0 server.



Supplementary figure 4: Secretome of *S. commune* monokaryotic strain (*Sc-M1*) grown on beech wood particles after 2 weeks of incubation in three partition Petri dish (numbers in brackets: total identified proteins; numbers outside brackets: proteins identified with signal peptide). R1 – replicate 1, R2 – replicate 2, R3 – replicate 3.

Supplementary table 20: Details of uncharacterized proteins with signal peptide identified in the *S. commune* secretome, Sc-M1 (monokaryotic strain) grown as single culture on beech sapwood after 2 weeks of incubation

JGI protein ID	UP ^a	<i>pI</i> ^b	<i>Mw</i> ^b	TMHMM ^c	Protein type ^d	Localization ^d
56791	3	4.49	19783.80	0	Cell membrane	Membrane
75025	3	5.32	12551.00	0	Extracellular	Soluble
150955	25	5.05	59342.61	0	Extracellular	Soluble
129575	29	5.97	98176.34	0	Extracellular	Soluble
174832	2	4.96	53015.76	0	Extracellular	Soluble
161917	2	7.09	47308.20	5	Cell membrane	Membrane

^a Unique peptides. ^b The theoretical *pI* (isoelectric point) and *Mw* (molecular weight) were computed based on protein sequence obtained from the JGI database. ^c TMHMM Server v. 2.0 was used for prediction of transmembrane helices in proteins. ^d Protein type and localization were obtained using the DeepLoc-1.0 server.

Supplementary table 21: Proteins of other functions identified in the *S. commune* secretome, *Sc*-M1 (monokaryotic strain) grown as single culture on beech sapwood after 2 weeks of incubation

JGI protein ID ^a	SignalP ^b	Putative protein function ^c	Family ^d	EC ^d	UP ^e	pI ^f	Mw ^f
Amylases							
2509139	Y	α -amylase	GH13	3.2.1.1	7	6.84	57119.96
85278	Y	α -amylase	GH13	3.2.1.1	2	6.29	46007.61
Chitinases							
2627742	Y	Chitin binding protein-domain	-	-	3	6.74	51710.95
2641020	Y	Chitin deacetylase	CE4	3.5.1.41	2	7.24	39097.04
2623305	Y	Chitinase	GH18	3.2.1.14	5	9.30	11418.45
2643740	Y	Chitinase	GH18	3.2.1.14	8	7.94	66479.62
2645822	Y	Chitinase	GH18	3.2.1.14	14	4.95	17074.15
2706631	Y	Chitinase	GH18	3.2.1.14	6	8.85	38530.81
2486953	N						
[2697104]	[Y]	Chitinase	GH18	3.2.1.14	6	8.82	59744.77
2635003	N	Chitinase	GH18	3.2.1.14	3	7.24	27810.80
234329	Y	Chitinase	GH18	3.2.1.14	3	5.50	57544.54
Lipases							
1211776	Y	Lipase class 3 (Triglyceride lipase)	CE10	3.1.1.3	2	8.86	24914.09
2641616	Y	Lipase class 3 (Triglyceride lipase)	CE10	3.1.1.3	4	8.70	58471.96
Proteins with domain of unknown function							
2326475	Y	Protein of unknown function (DUF1524)	-	-	5	8.31	54817.31
2609957	Y	Protein with different domains (DUF1996, WSC, CMB1)			4	8.42	119375.74
2503541	Y	Fungal protein of unknown function (DUF1748)	-	-	2	9.99	34188.66
2628937	Y	Domain of unknown function (DUF2183)	-	-	5	8.71	59944.78
237513	Y	Domains of D-arabinono-1, 4-lactone oxidase and FAD binding	-	-	4	4.95	60740.24
1184723	Y	Domains of unknown function (DUF5127, DUF4965, DUF1793, DUF4964)	-	-	9	9.31	14348.32
Miscellaneous proteins							

2619208	Y	Acyl-CoA oxidase-domain	-	1.3.3.6	2	10.01	11124.00
1188538	Y	Agmatinase	-	3.5.3.11	2	8.77	17613.48
2604109	Y	α -glucosidase	GH31	3.2.1.20	9	5.31	54011.42
2543909	Y	α -glucosidase	GH31	3.2.1.20	15	10.84	20127.61
2603998	Y	Arylsulfotransferase (ASST)	-	2.8.2.1	7	11.16	12131.16
2630008	N	β -1,3-glucan recognition protein	GH16	-	3	4.94	10570.42
2678335	N	β -N-acetylhexosaminidase	GH3	3.2.1.52	4	5.14	113942.62
257097	Y	Bicupin, oxalate decarboxylase/oxidase	-	-	39	11.9	13840.23
2604351	Y	BNR repeat-containing family member	-	-	5	8.81	7621.94
2495926	Y	BNR/Asp-box repeat domain-containing protein	-	-	4	7.38	11767.53
2670422	Y	Carboxylesterase, type B	-	3.1.1.-	4	6.69	81737.34
2614261	Y	Carboxylesterase, type B	-	3.1.1.-	16	5.97	41807.85
2620726	Y	Catalase	-	1.11.1.6	17	4.92	13127.17
2517462	Y	Cephalosporin-C deacetylase domain-containing protein	-	-	4	5.52	59345.52
2620687	Y	Cerato-platanin	-	-	4	11.71	17220.80
2619664	Y	Cerato-platanin	-	-	2	9.57	15417.82
2642607	Y	Choline dehydrogenase	-	1.1.99.1	15	5.24	46946.79
2343034	Y	Choline dehydrogenase	-	1.1.99.1	3	5.89	114025.36
2343265	Y	Choline dehydrogenase	-	1.1.99.1	4	10.07	36066.78
2527132	Y	Choline dehydrogenase	-	1.1.99.1	5	10.08	36294.22
2609112	Y	Choline dehydrogenase	-	1.1.99.1	8	6.27	133490.53
2717674	N	Choline dehydrogenase	-	1.1.99.1	2	6.27	44159.88
2620755	Y	EEP and Jacalin_EEP domain-containing protein	-	-	8	5.29	17312.37
2615368	Y	Endonuclease/Exonuclease/phosphatase family	-	-	8	8.86	23884.45
2637358	Y	Endonuclease/Exonuclease/phosphatase family	-	-	4	10.39	6519.77
2632136	Y	FMN-dependent dehydrogenase	-	-	2	7.88	54678.79
2636155	Y	Fungal type ribonuclease	-	-	6	7.76	12922.88

2498491	Y	Galactose oxidase, central domain	-	1.1.3.9	3	8.17	145727.73
2518879	Y	Glucan endo-1,3- α -glucosidase	GH71	3.2.1.59	3	4.28	38068.09
2638893	Y	Glucooligosaccharide oxidase	-	-	23	8.34	20021.97
2635920	Y	Glycerophosphoryl diester phosphodiesterase family	-	3.1.4.46	3	6.77	69568.27
2606260	Y	GPI (glycophosphatidylinositol)-anchored domain	-	-	2	7.91	46736.94
2613571	Y	Heterokaryon incompatibility protein Het-C	-	-	2	9.21	94356.18
1191999	Y	Intradiol dioxygenase like (domain)	-	-	20	8.87	91556.39
2524400	Y	Intradiol dioxygenase like (domain)	-	-	2	6.53	63229.62
2629356	Y	Major royal jelly protein	-	-	15	6.25	73569.34
2624887	Y	Mannoprotein	-	-	2	10.65	17209.34
2749855	Y	Metallophosphatase domain (5'-nucleotidases)	-	3.1.3.5	3	11.52	19340.36
2626947	Y	Oxalate oxidase	-	1.2.3.4	16	5.68	26913.02
2607781	Y	Peptide N-acetyl- β -D-glucosaminyl asparaginase amidase A (PNGase)	-	3.5.1.52	7	11.13	21528.08
2668795	Y	Ricin B-like lectins	CBM13	-	4	9.62	35511.51
2621085	Y	Ricin B-like lectins	CBM13	-	2	6.86	58223.04
2645530	Y						
[2673839]		Six-hairpin glycosidase-like domain	-	-	4	9.84	27206.67
2634437	Y	TAP-like protein with α/β hydrolase fold	-	-	2	5.05	26903.82
2489112	Y	Thaumatococcus domain	-	-	2	9.94	15783.45
2637223	Y	Thaumatococcus domain	-	-	2	4.91	17342.58
1158444	Y	Trans-glycosidases superfamily domain	-	-	5	8.81	20385.62
1086210	Y	Vacuolar protein sorting-associated protein 62- domain	-	-	3	8.50	90339.56

^a [] = alternative model with signal peptide, ^b Signal peptide was predicted with SignalP-5.0 database. ^c Putative function for identified proteins was obtained from the JGI, InterPro, UniProt and NCBI databases. ^d Carbohydrate-active enzymes database (CAZy) was used for the family information and for the enzyme commission number (EC number). ^e Unique peptides. ^f The theoretical *pI* (isoelectric point) and *M_w* (molecular weight) were computed based on protein sequence obtained from the JGI database.

Supplementary table 22: Proteases and peptidases identified in the *S. commune* secretome, Sc-M1 (monokaryotic strain) grown as single culture on beech sapwood after 2 weeks of incubation

JGI protein ID	SignalP ^a	UP	Pi	Mw	Putative protein function ^b	Family ^c	Family ^c
2622148	Y	12	8.01	109367.83	Aspartyl protease	A1	Aspartic peptidases
2703034	Y	9	6.67	7753.98	Aspartyl protease	A1	
2619343	Y	2	8.85	13498.8	Pepsin-like aspartic proteases	A1A	
2610732	Y	9	6.15	9203.48	Peptidase family M14 (Zinc carboxypeptidase)	M14	Metallo peptidases
2499312	Y	2	6.3	33127.5	Aminopeptidase I (aspartyl aminopeptidase)	M18	
1176082	Y	5	8.57	7533.85	Peptidase family M28	M28	
2268565	Y	6	10.96	8039.48	Peptidase family M28	M28	
2619224	Y	20	6.53	36266.64	Peptidase family M28	M28	
2699165	Y	20	6.18	28024.58	Peptidase family M28	M28	
2662991	Y	7	5.38	44078.73	Deuterolysin metalloprotease (M35) family	M35	
2604352	Y	18	5.21	22705.27	Lysine-specific metallo-endopeptidase	M35	
2628084	Y	34	11.15	23029.76	Lysine-specific metallo-endopeptidase (Peptidase M35)	M35	
2009250	Y	37	8.85	45867.32	Peptidase M35 (deuterolysin)	M35	
2620813	Y	14	9.09	48586.13	Peptidase M35 (deuterolysin)	M35	
2597255	Y	48	9.11	72871.85	Fungalysin metallopeptidase	M36	
2636955	Y	23	10.68	5545.59	Peptidase M36, fungalysin	M36	
2535918	Y	5	5.24	147235.53	Peptidase M64, IgA	M64	
2499350	Y	8	7.93	106789.15	Subtilase with Pro-kumamolisin (activation) domain	S8A	Serine peptidases
2618632	Y	5	10.94	76196.67	Subtilase with Pro-kumamolisin (activation) domain	S8A	
2622814	Y	21	5.91	25097.49	Subtilase with Pro-kumamolisin (activation) domain	S8A	
2630790	Y	8	9.37	57554	Subtilisin-related protease with Peptidase inhibitor I9 (activation domain)	S8A	
2616249	Y	19	9.47	171527.74	Dipeptidyl aminopeptidase/acylaminoacyl peptidase	S9	
2521311	Y	3	5.94	39689.26	Peptidase S10, serine carboxypeptidase	S10	
2547616	Y	4	6.92	103285.03	Peptidase S10, serine carboxypeptidase	S10	
2631590	Y	6	6.99	65777.59	Peptidase S10, serine carboxypeptidase	S10	
2682108	Y	6	9.34	29539.94	Peptidase S10, serine carboxypeptidase	S10	

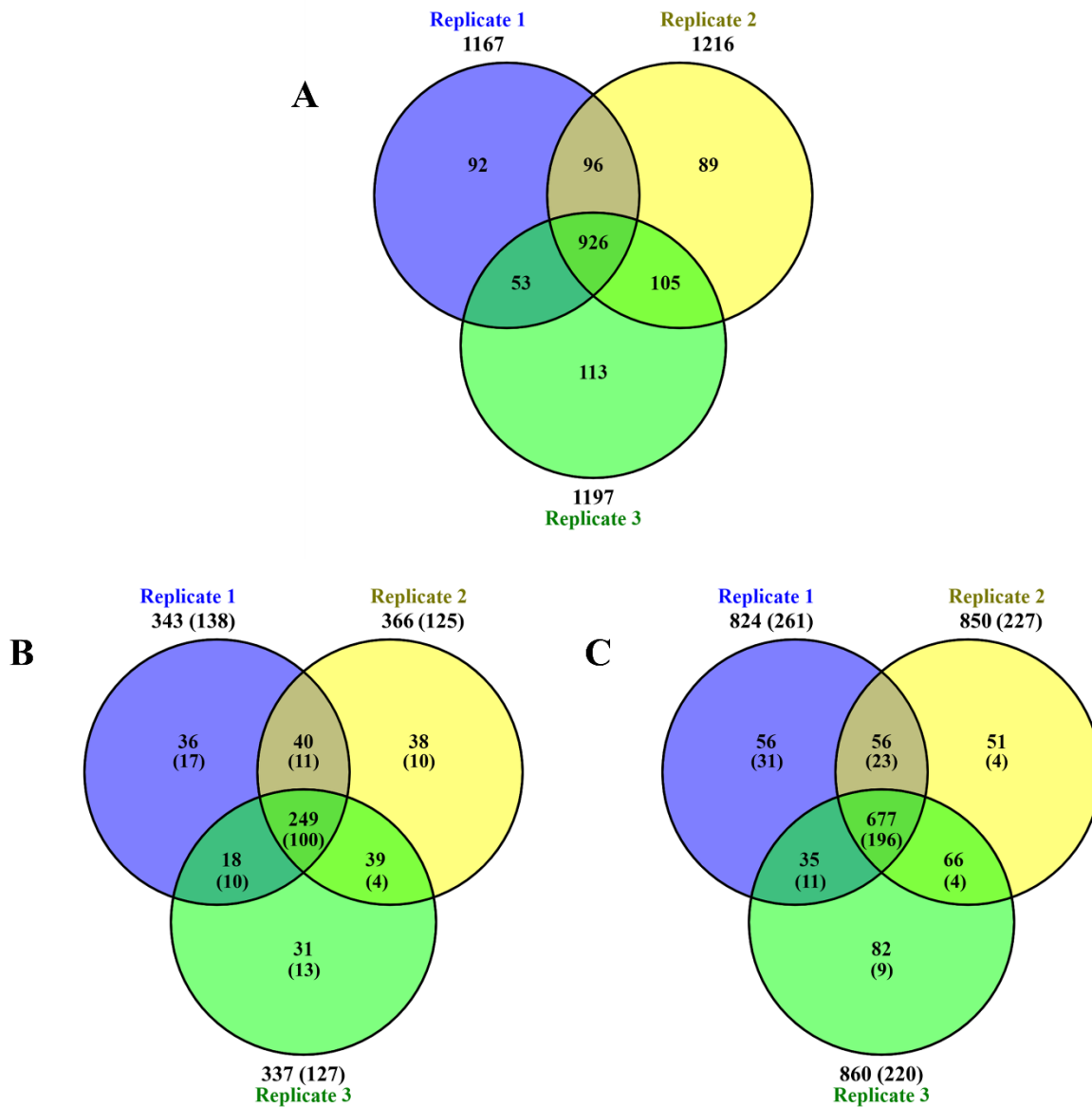
2616087	Y	10	8.83	37259.81	Peptidase S28 (serine carboxypeptidase)	S28	
2616091	Y	4	5.89	52381.06	Peptidase S28 (serine carboxypeptidase)	S28	
2618087	Y	5	10.98	9999.37	Peptidase S28 (serine carboxypeptidase)	S28	
2622534	Y	13	5.24	33633.51	Peptidase S28 (serine carboxypeptidase)	S28	
2622822	Y	7	5.36	21946.74	Peptidase S28 (serine carboxypeptidase)	S28	
1176926	Y	17	7.32	102288.75	Peptidase family S41, Tail-specific protease	S41	
2639849	Y	18	6.55	87055.58	C-terminal processing peptidase-1 domain	S41A	
2627185	Y	4	6.24	36975.18	Sedolisin with Pro-kumamolisin (activation domain)	S53	
2565008	Y	4	5.77	52038.35	Gamma-glutamyltranspeptidase	T3	Threonine peptidases

^a Signal peptide was predicted with SignalP-5.0 database. ^b Putative function for identified proteins was obtained from the JGI, InterPro, UniProt, NCBI and MEROPS databases. ^c MEROPS database was used for the family and subfamily information.

Supplementary table 23: Details of uncharacterized proteins with signal peptide identified in the *S. commune* secretome, Sc-M1 (monokaryotic strain) grown as single culture on beech sapwood after 2 weeks of incubation

JGI protein ID	SignalP ^a	UP ^b	<i>pI</i> ^c	<i>Mw</i> ^c	TMHMM ^d	Protein type ^e	Localization ^e
2626267	Y	3	8.58	20372.48	0	Membrane	Cell membrane
1215107	Y	15	5.87	71531.38	0	Soluble	Cytoplasm
2642232	Y	5	10.33	12251.93	0	Soluble	Cytoplasm
2665837	Y	43	8.20	22504.52	0	Soluble	Cytoplasm
2665838	Y	10	5.78	52236.13	0	Soluble	Cytoplasm
2627148	Y	2	7.57	111642.02	1	Membrane	Endoplasmic reticulum
2615819	Y	5	8.20	12334.08	0	Soluble	Extracellular
2619440	Y	7	9.82	19180.28	1	Soluble	Extracellular
2487644	Y	33	6.63	88356.24	0	Soluble	Extracellular
2618900	Y	10	8.43	16962.11	0	Soluble	Extracellular
2606604	Y	2	5.32	19360.85	0	Soluble	Extracellular
2636264	Y	2	6.05	86817.79	0	Soluble	Extracellular

^a Signal peptide was predicted with SignalP-5.0 database. ^b Unique peptides. ^c The theoretical *pI* (isoelectric point) and *Mw* (molecular weight) were computed based on protein sequence obtained from the JGI database. ^d TMHMM Server v. 2.0 was used for prediction of transmembrane helices in proteins. ^e Protein type and localization were obtained using the DeepLoc-1.0 server.



Supplementary figure 5 Venn diagrams for comparison of the identified proteins from three biological replicates in dual interaction of dikaryotic strains *T. versicolor* (Tv-D) and *S. commune* (Sc-D) on glass-fiber filters (A – total identified proteins, B – proteins identified from *S. commune*, and C – proteins identified from *T. versicolor*). The interaction was carried out on glass-fiber flitters having on *S. commune* minimal medium and incubated in dark at 25 °C for 10 days. Numbers outside brackets are total identified proteins, and numbers in brackets are proteins with signal peptide.

Supplementary table 24: Proteases and peptidases identified in the dual-interaction (dikaryotic strains, *Tv*-D and *Sc*-D) secretome on glass-fiber filters after 10 days of inoculation

JGI protein ID ^a	Putative protein function ^b	Family ^c	EC ^b	UP ^d	pI ^e	Mw ^e
<i>T. versicolor</i>						
Aspartic peptidases						
166665	Acid protease	A1	-	4	4.62	59364.21
167393	Acid protease	A1	-	3	4.40	49979.30
169073	Acid protease	A1	-	4	4.87	54907.94
175792	Acid protease	A1	-	3	4.58	57107.62
27566	Acid protease	A1	-	3	5.98	44026.27
32136	Acid protease	A1	-	6	4.40	36512.71
56073	Acid protease	A1	-	3	4.70	55558.16
56366	Acid protease	A1	-	5	5.54	55474.35
69055	Aspartyl protease	A1	-	2	5.28	43708.79
40281	Aspergillopepsin	A1	3.4.23.18	2	5.12	27645.42
69348	Pepsin A	A1	3.4.23.1	14	5.53	41328.01
40186	Polyporopepsin	A1	3.4.23.29	16	5.07	44403.51
144202	Saccharopepsin	A1	3.4.23.25	19	4.90	44864.92
Metallo peptidases						
39578	Zn-dependent exopeptidase	M28	-	20	5.51	50028.63
170685	Zn-dependent exopeptidase	M28	-	6	4.99	50845.30
27233	Leucine aminopeptidase-1	M28	3.4.11.1	6	5.00	43944.26
158002	Peptidyl-Lys metalloendopeptidase	M35	3.4.24.20	8	5.75	36650.47
164045	Peptidyl-Lys metalloendopeptidase	M35	3.4.24.20	4	5.28	37985.41
176097	Fungalysin	M36	-	28	5.48	63963.71
36519	Fungalysin	M36	-	10	5.19	64186.10
175022	Fungalysin	M36	-	14	5.27	64255.09
Serine peptidases						
153966	Subtilisin-related protease with peptidase inhibitor I9	S8	-	12	6.13	53021.11
147958	Subtilisin	S8	3.4.21.62	31	5.21	63345.61

70376	Serine carboxypeptidase	S10	-	8	5.14	56559.25
45058	Serine carboxypeptidase	S10	-	5	5.06	56145.72
32193	Serine carboxypeptidase	S10	-	3	4.80	53232.59
148659	Serine carboxypeptidase	S10	-	5	4.98	72850.23
57337	Serine carboxypeptidase	S10	-	13	5.29	52549.68
133452	Serine carboxypeptidase	S10	-	2	5.52	72773.32
126828	Serine carboxypeptidase	S10	-	8	5.13	72100.51
163322	Serine carboxypeptidase	S10	-	2	5.42	55401.37
60064	Serine carboxypeptidase	S10	-	6	5.11	58282.22
29080	Serine carboxypeptidase	S10	-	3	4.87	74757.94
27131	Lysosomal Pro-Xaa carboxypeptidase	S28	3.4.16.2	9	5.62	57650.71
110969	Lysosomal Pro-Xaa carboxypeptidase	S28	3.4.16.2	14	5.59	58338.67
154838	C-terminal processing peptidase-like protein	S41A	-	49	5.19	72165.32
172472	Tripeptidyl-peptidase I	S53	3.4.14.9	17	5.64	73672.03
113847	Tripeptidyl-peptidase I	S53	3.4.14.9	26	4.91	57811.06
69742	Tripeptidyl-peptidase I	S53	3.4.14.9	32	5.25	65727.09
174508	Tripeptidyl-peptidase I	S53	3.4.14.9	17	5.51	67301.45
169734	Tripeptidyl-peptidase I	S53	3.4.14.9	4	4.99	67856.08
126771	Tripeptidyl-peptidase I	S53	3.4.14.9	8	4.95	67210.44
50694	Tripeptidyl-peptidase I	S53	3.4.14.9	2	4.80	62136.61
166188	Tripeptidyl-peptidase I	S53	3.4.14.9	54	4.80	58463.38
129797	Tripeptidyl-peptidase I	S53	3.4.14.9	2	4.54	60221.99
129640	Tripeptidyl-peptidase I	S53	3.4.14.9	8	4.90	59152.52
Others						
45345	Peptide N-acetyl- β -D-glucosaminyl asparaginase amidase A	-	3.5.1.52	5	5.30	62148.43
<i>S. commune</i>						
Aspartic peptidases						
2619343	Aspartyl protease	A1	-	2	8.85	13498.80
2634024	Aspartyl protease	A1	-	2	10.19	34010.91
2619340	Aspartyl protease	A1	-	2	4.57	49556.93
2483927	Aspartyl protease	A1	-	10	5.57	25287.80

2622148	Aspartyl protease	A1	-	11	8.01	109367.83
2616983	Acid protease	A1	-	2	6.71	38229.44
Metallo peptidases						
2615329	Peptidase_M3 domain-containing protein	M3	-	10	11.50	27268.96
2610732	Zinc carboxypeptidase domain containing protein	M14	-	4	4.57	47698.81
2619224	Zn-dependent exopeptidase	M28	-	8	6.53	36266.64
2268565	Zn-dependent exopeptidase	M28	-	7	10.96	8039.48
2628084	Aspzincin_M35 domain-containing protein	M35	-	6	11.15	23029.76
2620813	Deuterolysin	M35	3.4.24.39	2	9.09	48586.13
2009250	Deuterolysin	M35	3.4.24.39	3	8.85	45867.32
2636955	Fungalysin	M36	-	4	10.68	5545.59
2702318	Fungalysin	M36	-	3	6.31	35169.50
Serine peptidases						
2622814	Subtilase with Pro-kumamolisin (activation) domain	S8A	3.4.21.62	11	5.91	25097.49
2618632	Subtilase with Pro-kumamolisin (activation) domain	S8A	3.4.21.62	10	10.94	76196.67
2499350	Subtilase with Pro-kumamolisin (activation) domain	S8A	3.4.21.62	5	7.93	106789.15
2630790	Subtilisin-related protease with peptidase inhibitor I9 domain	S8A	-	7	9.37	57554.00
2616249	Dipeptidyl aminopeptidase	S9	-	18	9.47	171527.74
2682108	Serine carboxypeptidase	S10	-	2	9.34	29539.94
2631590	Serine carboxypeptidase	S10	-	6	6.99	65777.59
2547616	Serine carboxypeptidase	S10	-	5	6.92	103285.03
2622822	Serine carboxypeptidase	S28	-	5	5.36	21946.74
2622534	Serine carboxypeptidase	S28	-	12	5.24	33633.51
2616087	Serine carboxypeptidase	S28	-	11	8.83	37259.81
2632551	Peptidase family S41 protein	S41	-	2	8.28	86647.15
1176926	Peptidase family S41 protein	S41	-	15	7.32	102288.75
2639849	C-terminal processing peptidase	S41A	-	6	6.55	87055.58
2627185	Sedolisin with Pro-kumamolisin (activation) domain	S53	-	5	6.24	36975.18

^a with signal peptide (predicted with SignalP-5.0 database). ^b Putative function for identified proteins was obtained from the JGI, InterPro, UniProt and NCBI databases. ^c MEROPS database was used for the family and subfamily information, and carbohydrate-active enzymes database (CAZy) was used for the family information and for the enzyme commission number (EC number). ^d Unique peptides.

^e The theoretical *pI* (isoelectric point) and *M_w* (molecular weight) were computed based on protein sequence obtained from the JGI database.

Supplementary table 25: Other potentially plant polysaccharides (plant cell wall) degrading enzymes de identified in the dual-interaction (dikaryotic strains, *Tv*-D and *Sc*-D) secretome on glass-fiber filters after 10 days of inoculation

JGI protein ID ^a	Putative protein function ^b	Family ^c	EC ^b	UP ^d	<i>pI</i> ^e	<i>Mw</i> ^e
<i>T. versicolor</i>						
Cellulases						
49760	β -glucosidase	GH3	3.2.1.21	12	5.27	94577.86
170938	β -glucosidase	GH3	3.2.1.21	42	5.16	95750.90
67879	β -glucosidase	GH3	3.2.1.21	25	6.13	83898.58
55634	β -glucosidase	GH3	3.2.1.21	8	5.86	76588.16
70471	β -glucosidase	GH3	3.2.1.21	8	5.20	86982.53
63826	Carbohydrate-Binding Module Family 1 / Glycoside Hydrolase Family 6 protein	CBM1-GH6	-	6	5.12	47341.99
175614	Glycoside Hydrolase Family 131 protein	GH131	3.2.1.-	2	5.12	33680.76
Hemicellulases						
60477	α -D-galactosidase (melibiase)	GH27	3.2.1.22	20	5.06	48191.45
159574	α -D-galactosidase (melibiase)	GH27	3.2.1.22	15	5.01	47537.33
75316	β -galactosidase	GH35	3.2.1.23	7	5.82	110304.60
37024	β -galactosidase	GH35	3.2.1.23	17	5.63	109089.91
43877	Carbohydrate-Binding Module Family 1 / Carbohydrate Esterase Family 1 protein	CBM1-CE1	-	7	7.03	37537.74
144893	Carbohydrate-Binding Module Family 1 / Glycoside Hydrolase Family 10 protein	CBM1-GH10	-	16	6.99	39805.73
48717	Carbohydrate-Binding Module Family 1 / Glycoside Hydrolase Family 10 protein	GH10-CBM1	3.2.1.8	2	4.92	43305.60
33948	Endo-1,4- β -xylanase	GH10	3.2.1.8	8	6.08	37673.81
154147	Endo-1,4- β -xylanase	GH10	3.2.1.8	6	5.20	38764.96
49304	Glycoside Hydrolase Family 115 protein	GH115	-	18	5.40	110788.05
75494	Glycoside Hydrolase Family 92 protein	GH92	-	48	5.02	89434.49
43566	Glycoside Hydrolase Family 92 protein	GH92	-	15	5.25	90600.50
40820	Glycoside Hydrolase Family 92 protein	GH92	-	39	5.37	90473.76
132011	Xylan 1,4- β -xylosidase	GH3	3.2.1.37	12	5.89	83851.56

Ligninases						
134657	Lignin peroxidase (LiP10)	AA2	1.11.1.14	7	4.89	38878.82
52333	Lignin peroxidase (LiP2s)	AA2	1.11.1.14	5	4.69	39547.28
134250	Lignin peroxidase (LiP5)	AA2	1.11.1.14	11	4.94	39367.28
134226	Lignin peroxidase (LiP9)	AA2	1.11.1.14	8	5.14	38866.76
Pectinases						
55703	α -L-rhamnosidase	GH78	3.2.1.40	10	5.83	71346.05
151427	α -L-rhamnosidase	GH78	3.2.1.40	9	6.09	70505.32
58222	Arabinan endo-1,5- α -L-arabinosidase	GH43	3.2.1.99	4	5.51	35135.29
143650	Arabinogalactan endo- β -1,4-galactanase	GH53	3.2.1.89	3	6.04	36495.45
52416	Endo-polygalacturonase	GH28	3.2.1.15	12	5.90	37582.77
171861	Endo-polygalacturonase	GH28	3.2.1.15	3	8.48	37250.84
74031	Endo-polygalacturonase	GH28	3.2.1.15	2	4.84	43801.88
145953	Galactan 1,3- β -galactosidase	GH43- CBM35	3.2.1.145	3	5.66	47141.49
66957	Galactan endo-1,6- β -galactosidase	GH30	3.2.1.164	3	6.04	51572.55
59914	Non-reducing end α -L-arabinofuranosidase	GH51	3.2.1.55	22	5.43	68935.97
28809	Non-reducing end β -L-arabinofuranosidase	GH127	3.2.1.185	11	5.49	72304.78
68175	Pectinesterase	CE8	3.1.1.11	2	7.32	32614.40
175476	Pectinesterase	CE8	3.1.1.11	4	4.99	42034.25
Esterases						
174308	Acetylcholinesterase	CE10	3.1.1.7	11	6.47	58355.63
68896	Acetylcholinesterase/Butyrylcholinesterase	CE1	3.1.1.1	12	4.82	57630.98
48030	Acetylcholinesterase/Butyrylcholinesterase	CE1	3.1.1.1	16	5.30	58130.20
41392	Acetylcholinesterase/Butyrylcholinesterase	CE1	3.1.1.1	9	6.56	59200.19
109109	Acetylcholinesterase/Butyrylcholinesterase	CE1	3.1.1.1	6	5.35	53375.75
70662	Acetylesterase	CE16	3.1.1.6	2	5.75	32924.23
168624	Acetylesterase	CE16	3.1.1.6	16	5.42	34478.06
40812	Acetylesterase	CE16	3.1.1.6	14	4.68	38507.84
130597	Carboxylesterase and related proteins	-	-	5	6.11	73329.11
164970	Carboxylesterase and related proteins	CE1	3.1.1.1	8	4.94	58449.99

113190	Carboxylic-ester hydrolase	CE1	3.1.1.1	8	4.64	58145.96
53846	Carotenoid ester lipase precursor	-	-	14	5.21	58445.71
168678	Carotenoid ester lipase precursor	-	-	3	4.69	58409.07
114756	Carotenoid ester lipase precursor	-	-	6	4.85	58373.47
175517	Esterase 1	-	-	7	4.59	56009.38
<i>S. commune</i>						
Cellulases						
2629974	β -glucosidase	GH3	3.2.1.21	3	4.31	80685.84
2604319	β -glucosidase	GH3	3.2.1.21	6	8.17	63660.94
2172097	β -glucosidase	GH3	3.2.1.21	3	9.63	24005.23
2538080	β -glucosidase	GH3	3.2.1.21	9	8.58	62700.34
2615989	Broad specificity exo- β -1,3/1,6-glucanase with endo- β -1,4-glucanase activity	GH131	3.2.1.-	4	6.76	39826.55
2639534	Cellobiohydrolase	GH6	3.2.1.91	2	11.93	10412.18
Hemicellulases						
2502024	Endo-1,4- β -xylanase	GH43	3.2.1.8	5	11.97	17795.85
2615052	Glycosyl hydrolase family 79 C-terminal β domain	GH79	-	4	7.40	25268.21
Pectinases						
2605157	Arabinan endo-1,5- α -L-arabinosidase	GH43	3.2.1.99	4	4.60	34463.35
2662427	Pectate lyase	PL-	4.2.2.2	2	8.45	60495.10
2614257	Pectinesterase (pectin methylesterase)	CE8	3.1.1.11	2	8.44	73628.97
Esterases						
2623577	Acetylcholinesterase	CE10	3.1.1.7	5	7.94	38228.35
2612695	Acylesterase	CE16	3.1.1.6	3	7.88	19901.45
2641780	Acylesterase	CE16	3.1.1.6	3	5.93	23281.47
2614261	Carboxylesterase type B	CE1	3.1.1.1	4	5.97	41807.85
2670422	Carboxylesterase, type B	CE1	3.1.1.1	13	6.69	81737.34
2526695	Carboxylesterase, type B	CE1	3.1.1.1	3	6.06	38357.21

^a with signal peptide (predicted with SignalP-5.0 database). ^b Putative function for identified proteins was obtained from the JGI, InterPro, UniProt and NCBI databases. ^c Carbohydrate-active enzymes database (CAZy) was used for the family information and for the enzyme commission number (EC number). ^d Unique peptides. ^e The theoretical *pI* (isoelectric point) and *M_w* (molecular weight) were computed based on protein sequence obtained from the JGI database.

Supplementary table 26: Identified fungal cell-wall proteins in the dual-interaction (dikaryotic strains, *Tv*-D and *Sc*-D) secretome on glass-fiber filters after 10 days of inoculation

JGI protein ID ^a	Putative protein function ^b	Family ^c	EC ^b	UP ^d	<i>pI</i> ^e	<i>Mw</i> ^e
<i>T. versicolor</i>						
32323	GPI-anchored domain	-	-	13	6.53	14441.82
19890	GPI-anchored domain (membrane-anchored proteins)	-	-	2	6.11	13819.89
99151	GPI-anchored domain (membrane-anchored proteins)	-	-	13	4.53	13016.67
88818	GPI-anchored domain (membrane-anchored proteins)	-	-	6	5.38	13391.45
52018	GPI-anchored domain (membrane-anchored proteins)	-	-	6	5.34	14235.38
173513	GPI-anchored domain (membrane-anchored proteins)	-	-	6	5.83	14321.48
68341	β -1,3-glucanosyltransglycosylase	GH72- CBM43	2.4.1.-	12	4.56	82932.29
34378	PLC (Phospholipase C)-like phosphodiesterase	-	-	19	4.85	32866.24
<i>S. commune</i>						
2606260	GPI (glycophosphatidylinositol)-anchored domain	-	-	2	7.91	46736.94
2628870	GPI-anchored	-	-	3	6.06	100785.35
2614981	GPI-anchored	-	-	3	6.96	57918.33
2627223	GPI-anchored domain	-	-	3	6.53	17432.85
2603309	GPI-anchored domain	-	-	5	11.27	6752.92
2483770	GPI-anchored domain	-	-	7	4.66	25563.30
2752351	Lytic transglycolase domain (Rare lipoprotein A)	-	-	2	5.08	47577.05
2608547	Lytic transglycolase domain (Rare lipoprotein A)	-	-	10	6.49	70924.48
2605437	Lytic transglycolase domain (Rare lipoprotein A)	-	-	3	5.25	12530.23
2612452	β -1,3-glucanosyltransglycosylase	GH72- CBM43	2.4.1.-	2	7.14	62709.82
2628532	PLC (Phospholipase C)-like phosphodiesterases superfamily domain	-	-	3	9.82	8573.78

^a with signal peptide (predicted with SignalP-5.0 database). ^b Putative function for identified proteins was obtained from the JGI, InterPro, UniProt and NCBI databases. ^c Carbohydrate-active enzymes database (CAZy) was used for the family information and for the enzyme commission number (EC number). ^d Unique peptides. ^e The theoretical *pI* (isoelectric point) and *Mw* (molecular weight) were computed based on protein sequence obtained from the JGI database.

Supplementary table 27: Proteins of other functions identified in the dual-interaction (dikaryotic strains, *Tv*-D and *Sc*-D) secretome on glass-fiber filters after 10 days of inoculation

JGI protein ID ^a	Putative protein function ^b	Family ^c	EC ^b	UP ^d	<i>pI</i> ^e	<i>Mw</i> ^e
<i>T. versicolor</i>						
68145	Acid phosphatase	-	3.1.3.2	4	5.13	59588.21
157325	Agmatinase	-	3.5.3.11	10	5.73	43331.16
17281	Alcohol dehydrogenase, class V	-	1.1.1.1	11	4.62	37441.65
30524	α -amylase	GH13	3.2.1.1	10	5.17	62883.28
30260	α -amylase	GH13	3.2.1.1	2	4.77	56912.54
140830	α -glucosidase	GH31	3.2.1.20	13	5.19	106792.59
110860	α -glucosidase	GH31	3.2.1.20	41	5.26	105704.47
58033	α -glucosidase	GH31	3.2.1.20	26	6.26	98939.63
161547	Amidases	-	3.5.1.4	18	5.46	58435.56
133552	Amidases	-	3.5.1.4	25	5.72	58436.47
138755	Arginase	-	3.5.3.1	2	5.30	44388.07
61500	ATP synthase F1 β subunit	-	-	13	5.99	57897.09
68104	β -N-acetylhexosaminidase	GH20	3.2.1.52	6	5.20	77083.52
60488	β -N-acetylhexosaminidase	GH20	3.2.1.52	9	5.37	61531.79
175547	β -N-acetylhexosaminidase	GH20	3.2.1.52	13	5.78	59281.88
135976	β -N-acetylhexosaminidase	GH20	3.2.1.52	9	5.48	59409.98
45289	α -N-acetylglucosaminidase	GH89	3.2.1.50	2	5.13	82239.41
47996	β -fructofuranosidase (invertase)	GH32	3.2.1.26	3	4.70	57281.36
141481	β -fructofuranosidase (invertase)	GH32	3.2.1.26	4	4.79	58563.31
147020	β -glucocerebrosidase	GH30_3	3.2.1.45	15	5.18	59672.36
26555	β -glucuronidase	GH79	3.2.1.31	2	7.72	49293.38
144865	β -glucuronidase	GH79	3.2.1.31	11	5.44	56864.74
128509	Bicupin oxalate decarboxylase/oxidase	-	-	25	5.76	51640.02
110458	Calnexin	-	-	5	4.80	60890.35
159259	Chondroitin AC lyase	PL8_4	4.2.2.5	8	4.83	93244.28
59069	FAD-binding domain-containing protein	-	-	3	4.98	62016.17
48384	FAD-binding domain-containing protein	-	-	2	5.02	62105.48

173910	FAD-binding oxidoreductase	-	-	16	4.99	52836.72
71225	Fungal hydrophobin	-	-	2	4.29	10966.72
50621	Gluconolactonase	-	3.1.1.17	19	5.70	44696.53
70818	Glutamyl-tRNA synthetase	-	6.1.1.17	5	6.56	86934.89
27059	Glycoside Hydrolase Family 79 domain-containing protein	GH79	-	2	4.98	61224.61
111717	Heterokaryon incompatibility protein Het-C	-	-	11	5.03	100337.03
126792	Ketol-acid reductoisomerase (NADP+)	-	1.1.1.86	3	8.96	44049.84
47480	Lactonase, 7-bladed β -propeller domain	-	-	6	4.95	42250.92
170137	Lysophospholipase	-	3.1.1.5	5	4.57	63790.85
30590	Metallo-dependent phosphatase	-	-	5	5.29	43543.24
29616	Metallo-dependent phosphatase	-	-	3	6.45	48079.41
170635	Molecular chaperones GRP78/BiP/KAR2, HSP70 superfamily	-	-	9	5.12	73482.96
74027	NAD-P-binding protein	-	-	9	5.95	33125.51
153876	NAD-P-binding protein	-	-	2	5.97	35684.04
175557	Neutral trehalase	GH37	3.2.1.28	18	5.00	82401.06
144227	Protein disulfide isomerase (prolyl 4-hydroxylase β subunit)	-	5.3.4.1	20	4.82	56437.44
52976	Purine nucleoside permease	-	-	9	5.43	44750.66
171483	SdiA-regulated and Phytase-like domain-containing protein	-	-	2	4.56	54272.49
171987	SNARE protein YKT6, synaptobrevin/VAMP superfamily	-	-	5	8.53	22234.51
126658	Tannase and feruloyl esterase	-	-	5	4.75	58603.07
51358	Tannase and feruloyl esterase domain	-	-	11	5.64	58439.67
131278	Tannase and feruloyl esterase domain	-	-	2	5.94	57082.15
152993	Thioredoxin/protein disulfide isomerase	-	5.3.4.1	5	5.32	41779.47
75646	Triacylglycerol lipase	CE10	3.1.1.3	9	5.81	32302.55
29781	Triacylglycerol lipase	CE10	3.1.1.3	2	5.47	31787.99
47228	Zinc finger MYND domain-containing protein	-	-	2	5.92	122972.09

S. commune

2509139	α -amylase	GH13	3.2.1.1	24	6.84	57119.96
2604109	α -glucosidase	GH31	3.2.1.20	6	5.31	54011.42
1078237	Amidohydrolase	-	-	2	6.61	36127.31
2613191	Calnexin	-	-	3	11.21	10300.82
2604720	d-4,5 unsaturated β -glucuronyl hydrolase	GH88	3.2.1.-	5	5.38	43337.19
2637980	Esterase-like activity of phytase domain	-	-	2	8.51	20918.68
2627923	Fruiting body protein SC7	-	-	2	8.67	17289.08
2635107	Fungal calcium binding protein	-	-	2	8.09	171620.28
2546744	Glycoside Hydrolase Family 26 protein	GH26	-	9	6.36	69297.08
2667132	Glycosyl hydrolase catalytic core	-	-	3	11.88	6996.21
2664319	Glycosyl hydrolase catalytic core	-	-	13	4.84	57394.19
1211776	Lipase class 3 (Triglyceride lipase)	PL3	3.1.1.3	4	8.86	24914.09
2608631	Non-Catalytic module family EXPN protein	-	-	7	9.63	34332.32
2610739	Non-specific serine/threonine protein kinase	-	2.7.11.1	2	9.97	26339.44
2606754	Phosphatidylethanolamine binding protein	-	-	4	9.29	50378.31
2611192	Phosphatidylinositol/phosphatidylglycerol transfer protein (PG/PI-TP)	-	-	2	5.62	38170.47
2619796	Poly(3-hydroxybutyrate) depolymerase	-	3.1.1.75	2	5.67	36546.66
2628008	Polysaccharide Lyase Family 8 / Subf 4	-	-	6	6.56	20558.55
2638893	Proteins containing the FAD (flavin-adenine dinucleotide) binding domain	-	-	21	8.34	20021.97
2615375	Putative transcriptional regulator DJ-1	-	-	2	6.45	16449.54
2625127	SC15 protein	-	-	6	7.97	63835.01
2542878	Thioredoxin/protein disulfide isomerase	-	5.3.4.1	2	10.11	51254.65
1158444	Trans-glycosidases superfamily domain	-	-	16	8.81	20385.62

^a with signal peptide (predicted with SignalP-5.0 database). ^b Putative function for identified proteins was obtained from the JGI, InterPro, UniProt and NCBI databases. ^c Carbohydrate-active enzymes database (CAZy) was used for the family information and for the enzyme commission number (EC number). ^d Unique peptides. ^e The theoretical *pI* (isoelectric point) and *Mw* (molecular weight) were computed based on protein sequence obtained from the JGI database.

Supplementary table 28: Details of uncharacterized proteins identified in the dual-interaction (dikaryotic strains, *Tv*-D and *Sc*-D) secretome on glass-fiber filters after 10 days of inoculation

JGI protein ID	SignalP ^a	UP ^b	<i>pI</i> ^c	<i>Mw</i> ^c	TMHMM ^d	Protein type ^e	Localization ^e
<i>T. versicolor</i>							
119225	Y	3	4.64	23171.86	0	Soluble	Extracellular
129575	Y	7	5.97	98176.34	0	Soluble	Extracellular
129957	Y	3	4.74	19270.87	0	Soluble	Extracellular
142961	Y	4	5.11	25317.93	1	Soluble	Extracellular
147588	Y	3	4.94	28215.47	0	Soluble	Extracellular
148335	Y	3	5.24	42207.64	0	Soluble	Extracellular
149253	Y	6	5.18	43168.62	0	Soluble	Extracellular
149403	N	2	7.33	30948.37	0	Soluble	Cytoplasm
150955	Y	15	5.05	59342.61	0	Soluble	Extracellular
159607	Y	3	4.51	22629.13	0	Membrane	Cell membrane
159796	Y	4	6.40	40052.67	0	Soluble	Extracellular
161917	Y	3	7.09	47308.20	5	Membrane	Cell membrane
163366	Y	3	4.96	46486.50	0	Soluble	Extracellular
170658	Y	3	9.95	41594.22	0	Soluble	Extracellular
171442	Y	4	4.60	40226.43	1	Soluble	Extracellular
174832	Y	5	4.96	53015.76	0	Soluble	Extracellular
175079	Y	14	5.07	91982.31	0	Soluble	Extracellular
22538	Y	4	4.49	40878.23	0	Soluble	Extracellular
25580	Y	4	4.85	19571.41	0	Soluble	Extracellular
26090	Y	7	6.63	26785.11	0	Soluble	Extracellular
28514	Y	2	4.53	17248.27	0	Soluble	Extracellular
29347	Y	8	4.64	38417.24	1	Soluble	Extracellular
30879	Y	3	4.72	39182.72	0	Membrane	Cell membrane
35444	Y	19	5.79	74467.68	1	Soluble	Extracellular
41806	Y	6	4.74	33344.29	0	Soluble	Extracellular
44621	Y	3	4.38	42779.67	0	Soluble	Extracellular
51486	Y	10	7.61	12255.65	0	Soluble	Extracellular
56242	Y	2	4.51	22721.32	0	Soluble	Extracellular

56791	Y	7	4.49	19783.80	0	Membrane	Cell membrane
58442	Y	2	6.15	45073.29	0	Soluble	Endoplasmic reticulum
73850	Y	7	4.95	49075.66	1	Soluble	Extracellular
73953	Y	2	4.72	35009.36	0	Membrane	Cell membrane
74601	Y	12	4.75	96604.69	0	Soluble	Extracellular
75025	Y	3	5.32	12551.00	0	Soluble	Extracellular
<i>S. commune</i>							
1176499	Y	2	5.78	72834.65	3	Soluble	Extracellular
1184723	Y	9	9.31	14348.32	0	Soluble	Extracellular
2081077	Y	3	10.39	53630.48	0	Soluble	Extracellular
2086990	Y	3	9.69	86912.48	0	Soluble	Extracellular
2104468	Y	2	8.10	53322.09	0	Soluble	Extracellular
2503433	Y	3	4.96	72543.31	0	Soluble	Extracellular
2514199	Y	8	6.02	51843.16	0	Soluble	Extracellular
2542478	Y	3	8.48	59561.81	0	Soluble	Extracellular
2601653	Y	6	8.71	10781.10	1	Membrane	Cell membrane
2604063	Y	2	8.38	60968.12	0	Soluble	Extracellular
2605742	Y	2	3.99	37163.00	1	Membrane	Cell membrane
2606604	Y	25	5.32	19360.85	0	Soluble	Extracellular
2608085	Y	3	11.68	34206.45	1	Soluble	Extracellular
2611300	Y	3	11.01	16130.26	0	Soluble	Extracellular
2611921	Y	2	9.00	13682.42	0	Soluble	Extracellular
2613526	Y	2	8.33	15075.49	0	Soluble	Extracellular
2615607	Y	4	10.06	144981.80	0	Soluble	Extracellular
2615819	Y	7	5.36	19048.44	0	Soluble	Extracellular
2619440	Y	4	9.04	25443.55	1	Soluble	Extracellular
2620308	Y	3	4.18	18400.35	0	Soluble	Extracellular
2624887	Y	7	10.65	17209.34	1	Membrane	Cell membrane
2624913	Y	7	8.02	39470.61	1	Membrane	Cell membrane
2626239	Y	2	10.37	9391.50	0	Soluble	Extracellular
2626267	Y	4	4.58	18089.75	0	Membrane	Cell membrane
2628937	Y	21	8.71	59944.78	0	Soluble	Mitochondrion

2635740	Y	3	12.27	11049.72	0	Soluble	Extracellular
2638591	Y	6	8.07	14918.26	0	Soluble	Extracellular
2644458	Y	4	11.03	14984.60	0	Soluble	Cell membrane
2676007	Y	2	7.61	52652.33	0	Soluble	Extracellular
2706276	Y	5	6.02	34069.32	0	Soluble	Extracellular

^a Signal peptide was predicted with SignalP-5.0 database. ^b Unique peptides. ^c The theoretical *pI* (isoelectric point) and *M_w* (molecular weight) were computed based on protein sequence obtained from the JGI database. ^d TMHMM Server v. 2.0 was used for prediction of transmembrane helices in proteins. ^e Protein type and localization were obtained using the DeepLoc-1.0 server.

7 Literature Cited

- Abdulahadi, R., Adhikerana, A. S., Ubaidillah, R., and Suharna, N. 2000. Preliminary study of the ecological impact of forest fires in G. Massigit, G. Gede-Pangrango national park, West Java. *The Korean Journal of Ecology* 23(2):125-129.
- Abdullah, F., and Rusea, G. 2009. Documentation of inherited knowledge on wild edible fungi from Malaysia. *Blumea - Biodiversity, Evolution and Biogeography of Plants* 54(1-3):35-38. <https://doi.org/10.3767/000651909X475996>.
- Abdurachim, M. R. A. 1965. Laboratory tests with *Schizophyllum commune* Fr. *Rimba Indonesia* 10(1):34-46.
- Abreu, L. D., Marino, R. H., Mesquita, J. B., and Ribeiro, G. T. 2007. Degradação da madeira de *Eucalyptus* sp. por basidiomicetos de podridão branca (Degradation of the *Eucalyptus* sp. wood by white-rot basidiomycetes fungi). *Arquivos do Instituto Biológico* 74(4):321–328 (in Portuguese).
- Abubacker, M. N., and Prince, M. 2013. Decomposition of lignin and holocellulose of *Acacia dealbata* Link (Mimosoideae) leaves, twigs and barks by fungal isolates from Virgin forest ecosystem of Doddabetta belt of Nilgiris. *Biosciences Biotechnology Research Asia* 10(2):719-726. <https://doi.org/10.13005/bbra/1187>.
- Adams, D. J. 2004. Fungal cell wall chitinases and glucanases. *Microbiology* 150(7):2029-2035. <https://doi.org/10.1099/mic.0.26980-0>.
- Adav, S. S., and Sze, S. K. 2014. *Trichoderma Secretome*. Pages 103–114 in: *Biotechnology and Biology of Trichoderma*. Elsevier.
- Addleman, K., and Archibald, F. 1993. Kraft pulp bleaching and delignification by dikaryons and monokaryons of *Trametes versicolor*. *Applied and Environmental Microbiology* 59(1):266-273.
- Aerts, A. M., Zabrocki, P., François, I. E. J. A., Carmona-Gutierrez, D., Govaert, G., Mao, C., Smets, B., Madeo, F., Winderickx, J., Cammue, B. P. A., and Thevissen, K. 2008. Ydc1p

- ceramidase triggers organelle fragmentation, apoptosis and accelerated ageing in yeast. *Cellular and molecular life sciences CMLS* 65(12):1933-1942.
<https://doi.org/10.1007/s00018-008-8129-8>.
- Aguilar-Pontes, M. V., de Vries, R. P., and Zhou, M. 2014. (Post-)genomics approaches in fungal research. *Briefings in Functional Genomics* 13(6):424-439.
<https://doi.org/10.1093/bfpg/elu028>.
- Agusta, A., Ohashi, K., and Shibuya, H. 2006. Composition of the endophytic filamentous fungi isolated from the tea plant *Camellia sinensis*. *Journal of Natural Medicines* 60(3):268-272.
<https://doi.org/10.1007/s11418-006-0038-2>.
- Ah Chee, A., Farrell, R. L., Stewart, A., and Hill, R. A. 1998. Decay potential of basidiomycete fungi from *Pinus radiata*. *Proceedings of the New Zealand Plant Protection Conference* 51:235-240.
- Ali, S., Ganai, B. A., Kamili, A. N., Bhat, A. A., Mir, Z. A., Bhat, J. A., Tyagi, A., Islam, S. T., Mushtaq, M., Yadav, P., Rawat, S., and Grover, A. 2018. Pathogenesis-related proteins and peptides as promising tools for engineering plants with multiple stress tolerance. *Microbiological research* 212-213:29-37. <https://doi.org/10.1016/j.micres.2018.04.008>.
- Almási, É., Sahu, N., Krizsán, K., Bálint, B., Kovács, G. M., Kiss, B., Cseklye, J., Drula, E., Henrissat, B., Nagy, I., Chovatia, M., Adam, C., LaButti, K., Lipzen, A., Riley, R., Grigoriev, I. V., and Nagy, L. G. 2019. The genome of *Auriculariopsis ampla* sheds light on fruiting body development and wood-decay of bark-inhabiting fungi. *bioRxiv*.
<https://doi.org/10.1101/550103>.
- Andrew, E. E., Kinge, T. R., Tabi, E. M., Thiobaland, N., and Mih, A. M. 2013. Diversity and distribution of macrofungi (mushrooms) in the Mount Cameroon region. *Journal of Ecology and The Natural Environment* 5(10):318-334. <https://doi.org/10.5897/JENE2013.0397>.
- Arfi, Y., Levasseur, A., and Record, E. 2013. Differential gene expression in *Pycnoporus coccineus* during interspecific mycelial interactions with different competitors. *Applied and Environmental Microbiology* 79(21):6626-6636. <https://doi.org/10.1128/AEM.02316-13>.

- Armenteros, J. J. A., Sønderby, C. K., Sønderby, S. K., Nielsen, H., and Winther, O. 2017. DeepLoc: prediction of protein subcellular localization using deep learning. *Bioinformatics* (Oxford, England) 33(21):3387-3395. <https://doi.org/10.1093/bioinformatics/btx431>.
- Arun, G., Eyini, M., and Gunasekaran, P. 2015. Characterization and biological activities of extracellular melanin produced by *Schizophyllum commune* (Fries). *Indian Journal of Experimental Biology* 53(6):380-387.
- Ásgeirsdóttir, S. A., van Wetter, M. A., and Wessels, J. G. H. 1995. Differential expression of genes under control of the mating-type genes in the secondary mycelium of *Schizophyllum commune*. *Microbiology* 141(6):1281-1288. <https://doi.org/10.1099/13500872-141-6-1281>.
- Ashaduzzaman, M., Das, A. K., Kayes, I., and Shams, M. I. 2011. Natural decay resistance of *Acacia auriculiformis* Cunn. ex. Benth and *Dalbergia sissoo* Roxb. *Bangladesh Journal of Scientific and Industrial Research* 46(2):225-230.
- ASTM D2017-05. 2005. Test method of accelerated laboratory test of natural decay resistance of woods (withdrawn 2014). American Society for Testing Materials. <https://doi.org/10.1520/D2017-05>.
- Bacelli, I. 2014. Cerato-platanin family proteins: one function for multiple biological roles? *Frontiers in plant science* 5:769. <https://doi.org/10.3389/fpls.2014.00769>.
- Badalyan, S. M., Innocenti, G., and Garibyan, N. G. 2002. Antagonistic activity of xylotrophic mushrooms against pathogenic fungi of cereals in dual culture. *Phytopathologia Mediterranea* 41:200-225.
- Badalyan, S. M., Innocenti, G., and Garibyan, N. G. 2004. Interactions between xylotrophic mushrooms and mycoparasitic fungi in dual-culture experiments. *Phytopathologia Mediterranea* 43(1):44-48.
- Baldrian, P. 2004. Increase of laccase activity during interspecific interactions of white-rot fungi. *FEMS Microbiology Ecology* 50(3):245-253. <https://doi.org/10.1016/j.femsec.2004.07.005>.
- Bari, E., Nazarnezhad, N., Kazemi, S. M., Ghanbary, M. A. T., Mohebbi, B., Schmidt, O., and Clausen, C. A. 2015a. Comparison between degradation capabilities of the white rot fungi *Pleurotus ostreatus* and *Trametes versicolor* in beech wood. *International Biodeterioration & Biodegradation* 104:231-237. <https://doi.org/10.1016/j.ibiod.2015.03.033>.

- Bari, E., Schmidt, O., and Oladi, R. 2015b. A histological investigation of Oriental beech wood decayed by *Pleurotus ostreatus* and *Trametes versicolor*. *Forest Pathology* 45(5):349-357. <https://doi.org/10.1111/efp.12174>.
- Bässler, C., Müller, J., Svoboda, M., Lepšová, A., Hahn, C., Holzer, H., and Pouska, V. 2012. Diversity of wood-decaying fungi under different disturbance regimes - a case study from spruce mountain forests. *Biodiversity and Conservation* 21(1):33-49. <https://doi.org/10.1007/s10531-011-0159-0>.
- Berini, F., Casartelli, M., Montali, A., Reguzzoni, M., Tettamanti, G., and Marinelli, F. 2019. Metagenome-Sourced Microbial Chitinases as Potential Insecticide Proteins. *Frontiers in Microbiology* 10:1358. <https://doi.org/10.3389/fmicb.2019.01358>.
- Bezemer, L. D. 1973. Variability in mating behaviour and culture appearance of *Lenzites trabea*. *Annals of Botany* 37(3):661-671. <https://doi.org/10.1093/oxfordjournals.aob.a084733>.
- Bhatt, R. P., Singh, U., and Uniyal, P. 2018. Healing mushrooms of Uttarakhand Himalaya, India. *Current Research in Environmental & Applied Mycology* 8(1):1-23. <https://doi.org/10.5943/cream/8/1/1>.
- Blinkova, O., and Ivanenko, O. 2016. Communities of tree vegetation and wood-destroying fungi in parks of the Kyiv city, Ukraine. *Forestry Journal (Lesnícky časopis)* 62(2):110-122. <https://doi.org/10.1515/forj-2016-0012>.
- Boddy, L. 2000. Interspecific combative interactions between wood-decaying basidiomycetes. *FEMS Microbiology Ecology* 31(3):185-194. [https://doi.org/10.1016/S0168-6496\(99\)00093-8](https://doi.org/10.1016/S0168-6496(99)00093-8).
- Boddy, L., and Heilmann-Clausen, J. 2008. Chapter 12 Basidiomycete community development in temperate angiosperm wood. Pages 211–237 in: *Ecology of Saprotrophic Basidiomycetes*. J. Frankland, L. Boddy, and P. van West, eds. Elsevier.
- Boddy, L., and Rayner, A. D. M. 1983. Ecological roles of basidiomycetes forming decay communities in attached oak branches. *The New Phytologist* 93(1):77-88. <https://doi.org/10.1111/j.1469-8137.1983.tb02694.x>.
- Boerjan, W., Ralph, J., and Baucher, M. 2003. Lignin biosynthesis. *Annual Review of Plant Biology* 54:519-546. <https://doi.org/10.1146/annurev.arplant.54.031902.134938>.

- Bourdel, G., Roy-Bolduc, A., St-Arnaud, M., and Hijri, M. 2016. Concentration of petroleum-hydrocarbon contamination shapes fungal endophytic community structure in plant roots. *Frontiers in Microbiology* 7:685. <https://doi.org/10.3389/fmicb.2016.00685>.
- Boyle, D. 1998. Nutritional factors limiting the growth of *Lentinula edodes* and other white-rot fungi in wood. *Soil Biology and Biochemistry* 30(6):817-823.
- Burcham, D. C., Abarrientos, N. V., Wong, J. Y., Ali, M. I. M., Fong, Y. K., and Schwarze, F. W. 2017. Field evaluation of *Trichoderma* spp. as a biological control agent to prevent wood decay on Benin mahogany (*Khaya grandifoliola*) and rain tree (*Samanea saman*) in Singapore. *Biological Control* 114:114-124. <https://doi.org/10.1016/j.biocontrol.2017.08.004>.
- Bush, K. 2018. Past and present perspectives on β -Lactamases. *Antimicrobial Agents and Chemotherapy* 62(10):1-20. <https://doi.org/10.1128/AAC.01076-18>.
- Carabajal, M., Kellner, H., Levin, L., Jehmlich, N., Hofrichter, M., and Ullrich, R. 2013. The secretome of *Trametes versicolor* grown on tomato juice medium and purification of the secreted oxidoreductases including a versatile peroxidase. *Journal of Biotechnology* 168(1):15-23. <https://doi.org/10.1016/j.jbiotec.2013.08.007>.
- Carabajal, M., Ullrich, R., Levin, L., Kluge, M., and Hofrichter, M. 2012. Degradation of phenol and p-nitrophenol by the white-rot polypore *Trametes versicolor*. Pages 69–72 in: *Proceedings book of the 5th international symposium on biosorption and bioremediation*, Prague, Czech Republic, June 24 – 28. P. Lovecká, M. Nováková, P. Prouzová, and O. Uhlík, eds., Prague, Czech Republic.
- Carpenter, S. E., Trappe, J. M., and Ammirati Jr., J. 1987. Observations of fungal succession in the Mount St. Helens devastation zone, 1980–1983. *Canadian Journal of Botany* 65(4):716-728. <https://doi.org/10.1139/b87-096>.
- Carreño-Ruiz, S. D., Lázaro, A. A. á., García, S. C., Hernández, R. G., Chen, J., Navarro, G. K. g., Fajardo, L. V. G., Pérez, N. D. C. J., De La Cruz, M. T., Blanco, J. C., and Cappello, R. E. 2019. New record of *Schizophyllum* (Schizophyllaceae) from Mexico and the confirmation of its edibility in the humid tropics. *Phytotaxa* 413(2):137-148. <https://doi.org/10.11646/phytotaxa.413.2.3>.

- Cavanna, C., Pagella, F., Esposito, M. C., Tamarozzi, F., Clemente, L., Marone, P., Matti, E., and Lallitto, F. 2019. Human infections due to *Schizophyllum commune*: Case report and review of the literature. *Journal de Mycologie Médicale* 29(4):365-371.
<https://doi.org/10.1016/j.mycmed.2019.100897>.
- Ceballos, R. M. 2018. Bioethanol and natural resources: Substrates, chemistry and engineered systems. CRC Press, Boca Raton, London, New York.
- Chang, Y., Zhang, M., Jiang, Y., Liu, Y., Luo, H., Hao, C., Zeng, P., and Zhang, L. 2017. Preclinical and clinical studies of *Coriolus versicolor* polysaccharopeptide as an immunotherapeutic in China. *Discovery Medicine* 23(127):207-219.
- Chen, H., Li, S., Wang, P., Yan, S., Hu, L., Pan, X., Yang, C., and Leung, G. P. 2014. Endothelium-dependent and -independent relaxation of rat aorta induced by extract of *Schizophyllum commune*. *Phytomedicine* 21(11):1230-1236.
<https://doi.org/10.1016/j.phymed.2014.06.008>.
- Chen, M., Wang, C., Fei, B., Ma, X., Zhang, B., Zhang, S., and Huang, A. 2017. Biological degradation of Chinese fir with *Trametes versicolor* (L.) Lloyd. *Materials* 10(7):834.
<https://doi.org/10.3390/ma10070834>.
- Chen, Y., Huang, J., Li, Y., Zeng, G., Zhang, J., Huang, A., Zhang, J., Ma, S., Tan, X., Xu, W., and Zhou, W. 2015. Study of the rice straw biodegradation in mixed culture of *Trichoderma viride* and *Aspergillus niger* by GC-MS and FTIR. *Environmental Science and Pollution Research International* 22(13):9807-9815. <https://doi.org/10.1007/s11356-015-4149-8>.
- Cheng, X., Jia, R., Li, P., Tu, S., Zhu, Q., Tang, W., and Li, X. 2007. Purification of a new manganese peroxidase of the white-rot fungus *Schizophyllum* sp. F17, and decolorization of azo dyes by the enzyme. *Enzyme and Microbial Technology* 41(3):258-264.
<https://doi.org/10.1016/j.enzmictec.2007.01.020>.
- Cherdchim, B., and Satansat, J. 2016. Influences of ethylene stimulation of rubber trees (*Hevea brasiliensis*) on the extractives and fungal resistance of lumber. *CERNE* 22(3):223-232.
<https://doi.org/10.1590/01047760201622032183>.

- Chi, Y., Hatakka, A., and Maijala, P. 2007. Can co-culturing of two white-rot fungi increase lignin degradation and the production of lignin-degrading enzymes? *International Biodeterioration & Biodegradation* 59(1):32-39. <https://doi.org/10.1016/j.ibiod.2006.06.025>.
- Choudhary, M., Devi, R., Datta, A., Kumar, A., and Jat, H. S. 2015. Diversity of wild edible mushrooms in Indian subcontinent and its neighboring countries. *Recent Advances in Biology and Medicine* 01:69-76. <https://doi.org/10.18639/RABM.2015.01.200317>.
- Chowdhary, A., Kathuria, S., Singh, P. K., Agarwal, K., Gaur, S. N., Roy, P., Randhawa, H. S., and Meis, J. F. 2013a. Molecular characterization and *in vitro* antifungal susceptibility profile of *Schizophyllum commune*, an emerging basidiomycete in bronchopulmonary mycoses. *Antimicrobial Agents and Chemotherapy* 57(6):2845-2848. <https://doi.org/10.1128/AAC.02619-12>.
- Chowdhary, A., Randhawa, H. S., Gaur, S. N., Agarwal, K., Kathuria, S., Roy, P., Klaassen, C. H., and Meis, J. F. 2013b. *Schizophyllum commune* as an emerging fungal pathogen: a review and report of two cases. *Mycoses* 56(1):1-10. <https://doi.org/10.1111/j.1439-0507.2012.02190.x>.
- Christopher, L. P., Yao, B., and Ji, Y. 2014. Lignin Biodegradation with Laccase-Mediator Systems. *Front. Energy Res.* 2. <https://doi.org/10.3389/fenrg.2014.00012>.
- Clark, T. A., and Anderson, J. B. 2004. Dikaryons of the basidiomycete fungus *Schizophyllum commune*: evolution in long-term culture. *Genetics* 167(4):1663-1675. <https://doi.org/10.1534/genetics.104.027235>.
- Cole, J. L., Clark, P. A., and Solomon, E. I. 1990. Spectroscopic and chemical studies of the laccase trinuclear copper active site: geometric and electronic structure. *J. Am. Chem. Soc.* 112(26):9534-9548. <https://doi.org/10.1021/ja00182a013>.
- Cooke, W. B. 1961. The Genus *Schizophyllum*. *Mycologia* 53(6):575-599. <https://doi.org/10.2307/3756459>.
- Cosgrove, D. J. 2000. Loosening of plant cell walls by expansins. *Nature* 407(6802):321-326. <https://doi.org/10.1038/35030000>.
- Cosgrove, D. J. 2015. Plant expansins: diversity and interactions with plant cell walls. *Current Opinion in Plant Biology* 25:162-172. <https://doi.org/10.1016/j.pbi.2015.05.014>.

- Cowling, E. B. 1961. Comparative biochemistry of the decay of sweetgum sapwood by white-rot and brown-rot fungi. Technical Bulletin 1258:1-79. <https://doi.org/10.22004/ag.econ.170882>.
- Curling, S. F., Clausen, C. A., and Winandy, J. E. 2002. Relationships between mechanical properties, weight loss, and chemical composition of wood during incipient brown-rot decay. *Forest Products Journal* 52(7/8):34-39.
- da Silva, G. A., Marino, R. H., Lopes, M. E. G., Almeida, T. Á., Costa, Â. C. F., and Martins, M. V. G. 2010. Avaliação do potencial de degradação de fungos causadores de podridão branca (Evaluating the degradation potential of white-rot fungi). *Agraria* 5(2):225–231 (in Portuguese). <https://doi.org/10.5039/agraria.v5i2a683>.
- Dai, W., Chen, X., Wang, X., Xu, Z., Gao, X., Jiang, C., Deng, R., and Han, G. 2018. The Algicidal fungus *Trametes versicolor* F21a eliminating blue algae via genes encoding degradation enzymes and metabolic pathways revealed by transcriptomic analysis. *Frontiers in Microbiology* 9:826. <https://doi.org/10.3389/fmicb.2018.00826>.
- Dashtban, M., Schraft, H., Syed, T. A., and Qin, W. 2010. Fungal biodegradation and enzymatic modification of lignin. *International Journal of Biochemistry and Molecular Biology* 1(1):36-50.
- de León, R. 2003. Cultivation of edible and medicinal mushrooms in Guatemala, Central America. *Micología Aplicada International* 15(1):31-35.
- de Vries, R. P., and Visser, J. 2001. *Aspergillus* enzymes involved in degradation of plant cell wall polysaccharides. *Microbiology and Molecular Biology Reviews* 65(4):497-522, table of contents. <https://doi.org/10.1128/MMBR.65.4.497-522.2001>.
- Deacon, J. W. 2013. *Fungal Biology*. 4., Auflage. John Wiley & Sons, New York, NY.
- Degreef, J., Malaisse, F., Rammeloo, J., and Baudart, É. 1997. Edible mushrooms of the Zambebian woodland area: A nutritional and ecological approach. *Biotechnology, Agronomy, Society and Environment* 1(3):221-231.
- Deshpande, R. A., and Shankar, V. 2002. Ribonucleases from T2 family. *Critical reviews in microbiology* 28(2):79-122. <https://doi.org/10.1080/1040-840291046704>.

- Dhyani, V., and Bhaskar, T. 2018. A comprehensive review on the pyrolysis of lignocellulosic biomass. *Renewable Energy* 129:695-716. <https://doi.org/10.1016/j.renene.2017.04.035>.
- Dhyani, V., and Bhaskar, T. 2019. Pyrolysis of Biomass. Pages 217–244 in: *Biofuels: alternative feedstocks and conversion processes for the production of liquid and gaseous biofuels*. A. Pandey, C. Larroche, E. Gnansounou, S. K. Khanal, C.-G. Dussap, and S. Ricke, eds. Elsevier.
- Dickie, I. A., Fukami, T., Wilkie, J. P., Allen, R. B., and Buchanan, P. K. 2012. Do assembly history effects attenuate from species to ecosystem properties? A field test with wood-inhabiting fungi. *Ecology Letters* 15(2):133-141. <https://doi.org/10.1111/j.1461-0248.2011.01722.x>.
- DIN EN 113. Wood preservatives - Method of test for determining the protective effectiveness against wood destroying basidiomycetes - Determination of the toxic values. German version EN 113:1996: 1996:105-122.
- Djarwanto. 2009. Studi pemanfaatan tiga jenis fungi pada pelapukan daun dan ranting mangium di tempat terbuka (Study on the utilization of three fungi species for *Mangium* leaf and twig decomposition in the open site). *Jurnal Penelitian Hasil Hutan* 27(4):314–322 (In Indonesien). <https://doi.org/10.1001/jama.2014.14950>.
- Djarwanto, and Suprapti, S. 2004. Ketahanan tiga jenis kayu untuk bantalan rel kereta api terhadap jamur perusak kayu secara laboratoris (The resistance of three wood species for railway sleeper against wood destroying fungi in a laboratory experiment). *Jurnal Penelitian Hasil Hutan* 22(4):215–221 (In Indonesien).
- Djarwanto, and Suprapti, S. 2014. Kemampuan 10 strain jamur dalam melapukkan lima jenis kayu asal Kalimantan Timur (Decay capability of ten fungus strains to five wood species from east kalimantan). *Jurnal Penelitian Hasil Hutan* 32(4):263–270 (In Indonesien).
- Djarwanto, Suprapti, S., and Hutapea, F. J. 2018. Kemampuan sepuluh strain jamur melapukkan empat jenis kayu asal Manokwari (The capability of ten fungus strains in decaying four wood species from Manokwari). *Jurnal Penelitian Hasil Hutan* 36(2):129–138 (In Indonesien).
- Djarwanto, Suprapti, S., and Pasaribu, R. A. 2009. Dekomposisi daun dan ranting *Mangium* dan *Ekaliptus* oleh delapan isolat fungi pelapuk (Decomposition of *Mangium* and *Eucalypt* leaves

- and twigs by eight decaying fungi isolates). *Jurnal Penelitian Hasil Hutan* 27(4):303–313 (In Indonesien).
- Djonović, S., Pozo, M. J., and Kenerley, C. M. 2006. Tvbn3, a β -1,6-glucanase from the biocontrol fungus *Trichoderma virens*, is involved in mycoparasitism and control of *Pythium ultimum*. *Applied and Environmental Microbiology* 72(12):7661-7670.
<https://doi.org/10.1128/AEM.01607-06>.
- Dons, J. J. M., de Vries, O. M. H., and Wessels, J. G. H. 1979. Characterization of the genome of the basidiomycete *Schizophyllum commune*. *Biochimica et Biophysica Acta* 563:100-112.
[https://doi.org/10.1016/0005-2787\(79\)90011-X](https://doi.org/10.1016/0005-2787(79)90011-X).
- Dossa, G. G. O., Paudel, E., Cao, K., Schaefer, D., and Harrison, R. D. 2016. Factors controlling bark decomposition and its role in wood decomposition in five tropical tree species. *Scientific Reports* 6:34153. <https://doi.org/10.1038/srep34153>.
- Dou, H., Chang, Y., and Zhang, L. 2019. *Coriolus versicolor* polysaccharopeptide as an immunotherapeutic in China. Pages 361–381 in: *Progress in Molecular Biology and Translational Science*. L. Zhang, ed.
- Druzhinina, I. S., Shelest, E., and Kubicek, C. P. 2012. Novel traits of *Trichoderma* predicted through the analysis of its secretome. *FEMS Microbiology Letters* 337(1):1-9.
<https://doi.org/10.1111/j.1574-6968.2012.02665.x>.
- Durán, N., Rosa, M. A., D’Annibale, A., and Gianfreda, L. 2002. Applications of laccases and tyrosinases (phenoloxidases) immobilized on different supports: a review. *Enzyme and Microbial Technology* 31(7):907-931. [https://doi.org/10.1016/S0141-0229\(02\)00214-4](https://doi.org/10.1016/S0141-0229(02)00214-4).
- Eastwood, D. C., Floudas, D., Binder, M., Majcherczyk, A., Schneider, P., Aerts, A., Asiegbu, F. O., Baker, S. E., Barry, K., Bendiksby, M., Blumentritt, M., Coutinho, P. M., Cullen, D., Vries, R. P. de, Gathman, A., Goodell, B., Henrissat, B., Ihrmark, K., Kauserud, H., Kohler, A., LaButti, K., Lapidus, A., Lavin, J. L., Lee, Y.-H., Lindquist, E., Lilly, W., Lucas, S., Morin, E., Murat, C., Oguiza, J. A., Park, J., Pisabarro, A. G., Riley, R., Rosling, A., Salamov, A., Schmidt, O., Schmutz, J., Skrede, I., Stenlid, J., Wiebenga, A., Xie, X., Kües, U., Hibbett, D. S., Hoffmeister, D., Högborg, N., Martin, F., Grigoriev, I. V., and Watkinson,

- S. C. 2011. The plant cell wall-decomposing machinery underlies the functional diversity of forest fungi. *Science* 333(6043):762-765. <https://doi.org/10.1126/science.1205411>.
- Eichlerová, I., and Homolka, L. 1999. Preparation and crossing of basidiospore-derived monokaryons-a useful tool for obtaining laccase and other ligninolytic enzyme higher-producing dikaryotic strains of *Pleurotus ostreatus*. *Antonie van Leeuwenhoek* 75(4):321-327. <https://doi.org/10.1023/A:1001813603115>.
- Ek, M., Gellerstedt, G., and Henriksson, G. 2009. Pulp and paper chemistry and technology: Wood chemistry and biotechnology 1. De Gruyter, Berlin.
- El-Gebali, S., Mistry, J., Bateman, A., Eddy, S. R., Luciani, A., Potter, S. C., Qureshi, M., Richardson, L. J., Salazar, G. A., Smart, A., Sonnhammer, E. L. L., Hirsh, L., Paladin, L., Piovesan, D., Tosatto, S. C. E., and Finn, R. D. 2019. The Pfam protein families database in 2019. *Nucleic Acids Research* 47(D1):D427-D432. <https://doi.org/10.1093/nar/gky995>.
- Erwin, Takemoto, S., Hwang, W.-J., Takeuchi, M., Itoh, T., and Imamura, Y. 2008. Anatomical characterization of decayed wood in standing light red meranti and identification of the fungi isolated from the decayed area. *Journal of Wood Science* 54(3):233-241. <https://doi.org/10.1007/s10086-008-0947-7>.
- Essig, F. M. 1922. The morphology, development, and economic aspects of *Schizophyllum commune* fries. University of California Publications in Botany 7(14):447-498.
- Eyre, C., Muftah, W., Hiscox, J., Hunt, J., Kille, P., Boddy, L., and Rogers, H. J. 2010. Microarray analysis of differential gene expression elicited in *Trametes versicolor* during interspecific mycelial interactions. *Fungal Biology* 114(8):646-660. <https://doi.org/10.1016/j.funbio.2010.05.006>.
- Fakoussa, R. M., and Hofrichter, M. 1999. Biotechnology and microbiology of coal degradation. *Applied Microbiology and Biotechnology* 52(1):25-40. <https://doi.org/10.1007/s002530051483>.
- Falade, A. O., Nwodo, U. U., Iweriebor, B. C., Green, E., Mabinya, L. V., and Okoh, A. I. 2017. Lignin peroxidase functionalities and prospective applications. *MicrobiologyOpen* 6(1):1-14. <https://doi.org/10.1002/mbo3.394>.

- Farr, D. F., and Rossman, A. Y. 2017. Fungal Databases, U.S. National Fungus Collections. <https://nt.ars-grin.gov/fungaldatabases/>.
- Farr, D. F., and Rossman, A. Y. 2020. Fungal Databases, U.S. National Fungus Collections. Accessed May 13, 2020. <https://nt.ars-grin.gov/fungaldatabases/>.
- Fernández-Acero, F. J., Jorge, I., Calvo, E., Vallejo, I., Carbú, M., Camafeita, E., López, J. A., Cantoral, J. M., and Jorrín, J. 2006. Two-dimensional electrophoresis protein profile of the phytopathogenic fungus *Botrytis cinerea*. *Proteomics* 6(S1):S88-S96. <https://doi.org/10.1002/pmic.200500436>.
- Fernando, K. M. E. P. 2009. Species richness and ecological characterization of wood-inhabiting agaric fungi on home-garden logs in semi-urbanized areas in Colombo suburbs. *Vidyodaya Journal of Science* 14(1):177-187.
- Ferraz, A., Esposito, E., Bruns, R. E., and Durán, N. 1998. The use of principal component analysis (PCA) for pattern recognition in *Eucalyptus grandis* wood biodegradation experiments. *World Journal of Microbiology and Biotechnology* 14(4):487-490. <https://doi.org/10.1023/A:1008875730177>.
- Ferreira, V., Gonçalves, A. L., Pratas, J., and Canhoto, C. 2010. Contamination by uranium mine drainages affects fungal growth and interactions between fungal species and strains. *Mycologia* 102(5):1004-1011. <https://doi.org/10.3852/09-248>.
- Floudas, D., Binder, M., Riley, R., Barry, K., Blanchette, R. A., Henrissat, B., Martínez, A. T., Otiillar, R., Spatafora, J. W., Yadav, J. S., Aerts, A., Benoit, I., Boyd, A., Carlson, A., Copeland, A., Coutinho, P. M., Vries, R. P. de, Ferreira, P., Findley, K., Foster, B., Gaskell, J., Glotzer, D., Górecki, P., Heitman, J., Hesse, C., Hori, C., Igarashi, K., Jurgens, J. A., Kallen, N., Kersten, P., Kohler, A., Kües, U., Kumar, T. K. A., Kuo, A., LaButti, K., Larrondo, L. F., Lindquist, E., Ling, A., Lombard, V., Lucas, S., Lundell, T., Martin, R., McLaughlin, D. J., Morgenstern, I., Morin, E., Murat, C., Nagy, L. G., Nolan, M., Ohm, R. A., Patyshakuliyeva, A., Rokas, A., Ruiz-Dueñas, F. J., Sabat, G., Salamov, A., Samejima, M., Schmutz, J., Slot, J. C., St John, F., Stenlid, J., Sun, H., Sun, S., Syed, K., Tsang, A., Wiebenga, A., Young, D., Pisabarro, A., Eastwood, D. C., Martin, F., Cullen, D., Grigoriev, I. V., and Hibbett, D. S. 2012. The Paleozoic origin of enzymatic lignin decomposition

- reconstructed from 31 fungal genomes. *Science* 336(6089):1715-1719.
<https://doi.org/10.1126/science.1221748>.
- Floudas, D., Held, B. W., Riley, R., Nagy, L. G., Koehler, G., Ransdell, A. S., Younus, H., Chow, J., Chiniquy, J., Lipzen, A., Tritt, A., Sun, H., Haridas, S., LaButti, K., Ohm, R. A., Kües, U., Blanchette, R. A., Grigoriev, I. V., Minto, R. E., and Hibbett, D. S. 2015. Evolution of novel wood decay mechanisms in Agaricales revealed by the genome sequences of *Fistulina hepatica* and *Cylindrobasidium torrendii*. *Fungal Genetics and Biology* 76:78-92.
<https://doi.org/10.1016/j.fgb.2015.02.002>.
- Fraaije, M. W., and van Bloois, E. 2012. DyP-type peroxidases: a promising and versatile class of enzymes. *Enzyme Engineering* 1(2):1-3. <https://doi.org/10.4172/2329-6674.1000e105>.
- Fragner, D., Zomorodi, M., Kües, U., and Majcherczyk, A. 2009. Optimized protocol for the 2-DE of extracellular proteins from higher basidiomycetes inhabiting lignocellulose. *ELECTROPHORESIS* 30(14):2431-2441. <https://doi.org/10.1002/elps.200800770>.
- Franceschi, V. R., Krokene, P., Christiansen, E., and Krekling, T. 2005. Anatomical and chemical defenses of conifer bark against bark beetles and other pests. *The New Phytologist* 167(2):353-375. <https://doi.org/10.1111/j.1469-8137.2005.01436.x>.
- French, J. R. J., and Keirle, R. M. 1969. Studies in fire-damaged Radiata pine plantations. *Australian Forestry* 33(3):175-180. <https://doi.org/10.1080/00049158.1969.10675490>.
- Furze, M. E., Huggett, B. A., Aubrecht, D. M., Stolz, C. D., Carbone, M. S., and Richardson, A. D. 2019. Whole-tree nonstructural carbohydrate storage and seasonal dynamics in five temperate species. *The New Phytologist* 221(3):1466-1477.
<https://doi.org/10.1111/nph.15462>.
- Gadd, G. M. 2001. Fungi in bioremediation. British Mycological Society symposium series v. 23. Cambridge University Press, Cambridge.
- Gadd, G. M. 2007. Geomycology: biogeochemical transformations of rocks, minerals, metals and radionuclides by fungi, bioweathering and bioremediation. *Mycological Research* 111(Pt 1):3-49. <https://doi.org/10.1016/j.mycres.2006.12.001>.

- Gaderer, R., Bonazza, K., and Seidl-Seiboth, V. 2014. Cerato-platanins: a fungal protein family with intriguing properties and application potential. *Applied Microbiology and Biotechnology* 98(11):4795-4803. <https://doi.org/10.1007/s00253-014-5690-y>.
- Galiana, E., Philippe Bonnet, Sandrine Conrod, Keller, H., Franck Panabières, Ponchet, M., Poupet, A., and Ricci, P. 1997. RNase Activity Prevents the Growth of a Fungal Pathogen in Tobacco Leaves and Increases upon Induction of Systemic Acquired Resistance with Elicitin. *Plant physiology* 115(4):1557-1567.
- Gao, M., Glenn, A. E., Blacutt, A. A., and Gold, S. E. 2017a. Fungal lactamases: their occurrence and function. *Frontiers in Microbiology* 8(1775):1-17. <https://doi.org/10.3389/fmicb.2017.01775>.
- Gao, X., Wang, C., Dai, W., Ren, S., Tao, F., He, X., Han, G., and Wang, W. 2017b. Proteomic analysis reveals large amounts of decomposition enzymes and major metabolic pathways involved in algicidal process of *Trametes versicolor* F21a. *Scientific Reports* 7(3907):1-10. <https://doi.org/10.1038/s41598-017-04251-1>.
- GINNS, J. H. 1986. Compendium of plant disease and decay fungi in Canada 1960-1980. Canadian Government Publishing Centre, Canada.
- Glenn, A. E., Davis, C. B., Gao, M., Gold, S. E., Mitchell, T. R., Proctor, R. H., Stewart, J. E., and Snook, M. E. 2016. Two Horizontally Transferred Xenobiotic Resistance Gene Clusters Associated with Detoxification of Benzoxazolinones by *Fusarium* Species. *PloS One* 11(1):e0147486. <https://doi.org/10.1371/journal.pone.0147486>.
- GLTMS. 2015. Note on Common Wood Decay Fungi on Urban Trees of Hong Kong. Greening Landscape and Tree Management Section, Hong Kong.
- Gmoser, R., Ferreira, J. A., Lundin, M., Taherzadeh, M. J., and Lennartsson, P. R. 2018. Pigment production by the edible filamentous fungus *Neurospora intermedia*. *Fermentation* 4(11):1-15. <https://doi.org/10.3390/fermentation4010011>.
- Gonçalves, V. N., Carvalho, C. R., Johann, S., Mendes, G., Alves, T. M. A., Zani, C. L., Junior, P. A. S., Murta, S. M. F., Romanha, A. J., Cantrell, C. L., Rosa, C. A., and Rosa, L. H. 2015. Antibacterial, antifungal and antiprotozoal activities of fungal communities present in

- different substrates from Antarctica. *Polar Biology* 38(8):1143-1152.
<https://doi.org/10.1007/s00300-015-1672-5>.
- Gonthier, P., Guglielmo, F., Sillo, F., Giordano, L., and Garbelotto, M. 2015. A molecular diagnostic assay for the detection and identification of wood decay fungi of conifers. *Forest Pathology* 45(2):89-101. <https://doi.org/10.1111/efp.12132>.
- Gow, N. A. R., Latge, J.-P., and Munro, C. A. 2017. The fungal cell wall: structure, biosynthesis, and function. *Microbiology Spectrum* 5(3):FUNK-0035-2016.
<https://doi.org/10.1128/microbiolspec.FUNK-0035-2016>.
- Gradinger, C., Promberger, A., Schwanninger, M., Messner, K., and Sixta, H. 2004. Characterization of fungal growth on lenzing beech logs. *Lenzinger Berichte* 83:1-5.
- Gramss, G. 1987. Invasion of wood by basidiomycetous fungi. IV. Microbiological approach to the role of kratovirulence in the expression of pathovirulence. *Journal of Basic Microbiology* 27(5):241-251. <https://doi.org/10.1002/jobm.3620270503>.
- Greeshma, A. A., Sridhar, K. R., Pavithra, M., and Ghate, S. D. 2016. Impact of fire on the macrofungal diversity in scrub jungles of south-west India. *Mycology* 7(1):15-28.
<https://doi.org/10.1080/21501203.2016.1147090>.
- Grenier, J., Potvin, C., and Asselin, A. 2000. Some fungi express β -1,3-glucanases similar to thaumatin-like proteins. *Mycologia* 92(5):841-848.
<https://doi.org/10.1080/00275514.2000.12061228>.
- Grigoriev, I. V., Nikitin, R., Haridas, S., Kuo, A., Ohm, R., Otilar, R., Riley, R., Salamov, A., Zhao, X., Korzeniewski, F., Smirnova, T., Nordberg, H., Dubchak, I., and Shabalov, I. 2014. MycoCosm portal: gearing up for 1000 fungal genomes. *Nucleic Acids Research* 42(Database issue):D699-D704. <https://doi.org/10.1093/nar/gkt1183>.
- Gruber, S., and Seidl-Seiboth, V. 2012. Self versus non-self: fungal cell wall degradation in *Trichoderma*. *Microbiology* 158:26-34. <https://doi.org/10.1099/mic.0.052613-0>.
- Guglielmo, F., Bergemann, S. E., Gonthier, P., Nicolotti, G., and Garbelotto, M. 2007. A multiplex PCR-based method for the detection and early identification of wood rotting fungi in standing trees. *Journal of Applied Microbiology* 103(5):1490-1507.
<https://doi.org/10.1111/j.1365-2672.2007.03378.x>.

- Guo, M., Jia, R., and Yang, X. 2014. Decolorization of the azo dye Acid Red 18 by crude manganese peroxidase: Effect of system parameters and kinetic study. *Biocatalysis and Biotransformation* 32(5-6):276-284. <https://doi.org/10.3109/10242422.2014.974575>.
- Gupta, V. K. 2016. Microbial enzymes in bioconversions of biomass. *Biofuel and Biorefinery Technologies* v.3. Springer International Publishing, Cham.
- Hadi, Y. S., Rosyadi, A., and Darma, I. G. K. T. 1994. Acetylated flakeboard resistance to *Schizophyllum commune* fungus attack. *Folia Forestalia Polonica. Series B* 25:13-17.
- Hagge, J., Bässler, C., Gruppe, A., Hoppe, B., Kellner, H., Krah, F.-S., Müller, J., Seibold, S., Stengel, E., and Thorn, S. 2019. Bark coverage shifts assembly processes of microbial decomposer communities in dead wood. *Proceedings of The Royal Society B: Biological Sciences* 286(1912):20191744. <https://doi.org/10.1098/rspb.2019.1744>.
- Hamidi, N. H. 2013. Enzymatic depolymerization of lignin by laccases, Nottingham, United Kingdom.
- Hammel, K. E., and Cullen, D. 2008. Role of fungal peroxidases in biological ligninolysis. *Current Opinion in Plant Biology* 11(3):349-355. <https://doi.org/10.1016/j.pbi.2008.02.003>.
- Hanafusa, Y., Hirano, Y., Watabe, H., Hosaka, K., Ikezawa, M., and Shibahara, T. 2016. First isolation of *Schizophyllum commune* in a harbor seal (*Phoca vitulina*). *Medical Mycology* 54(5):492-499. <https://doi.org/10.1093/mmy/myw008>.
- Hansen, E. M. 1979. Nuclear condition and vegetative characteristics of homokaryotic and heterokaryotic isolates of *Phellinus weirii*. *Canadian Journal of Botany* 57(15):1579-1582. <https://doi.org/10.1139/b79-196>.
- Harholt, J., Suttangkakul, A., and Vibe Scheller, H. 2010. Biosynthesis of pectin. *Plant physiology* 153(2):384-395. <https://doi.org/10.1104/pp.110.156588>.
- Harmon, M. E., Fasth, B., Woodall, C. W., and Sexton, J. 2013. Carbon concentration of standing and downed woody detritus: Effects of tree taxa, decay class, position, and tissue type. *Forest Ecology and Management* 291:259-267. <https://doi.org/10.1016/j.foreco.2012.11.046>.

- Hasunuma, K., and Ishikawa, T. 1977. Control of the production and partial characterization of repressible extracellular 5'-nucleotidase and alkaline phosphatase in *Neurospora crassa*. *Biochimica et Biophysica Acta (BBA) - Enzymology* 480(1):178-193.
[https://doi.org/10.1016/0005-2744\(77\)90332-1](https://doi.org/10.1016/0005-2744(77)90332-1).
- Hegarty, B., Steinfurth, A., Liese, W., and Schmidt, O. 1987. Comparative investigations on wood decay and cellulolytic and xylanolytic activity of some basidiomycete fungi. *Holzforschung* 41(5):265-270. <https://doi.org/10.1515/hfsg.1987.41.5.265>.
- Heilmann-Clausen, J., Aude, E., van Dort, K., Christensen, M., Piltaver, A., Veerkamp, M., Walley, R., Siller, I., Standovár, T., and Ódor, P. 2014. Communities of wood-inhabiting bryophytes and fungi on dead beech logs in Europe - reflecting substrate quality or shaped by climate and forest conditions? *Journal of Biogeography* 41(12):2269-2282.
<https://doi.org/10.1111/jbi.12388>.
- Henningsson, B. 1965. Physiology and decay activity of the birch conk fungus *Polyporus betulinus* (Bull.) Fr. *Studia Forestalia Suecica* 34:1-77.
- Henningsson, B. 1967. Physiology of fungi attacking birch and aspen pulpwood. *Studia Forestalia Suecica* 52:1-55.
- Herz, F. M. 2015. Saccharification of lignocellulosic biomass for bioethanol production with special emphasis on short rotation trees, forest hardwoods, and cascade used wood panels. Dissertation. 1. Auflage, Goettingen, Germany.
- Highley, T. L. 1997. Control of wood decay by *Trichoderma (Gliocladium) virens*. II. Antibiosis. *Material und Organismen* 31(3):157-166.
- Highley, T. L., and Murmanis, L. L. 1987. Micromorphology of degradation in western hemlock and sweetgum by the white-rot fungus *Coriolus versicolor*. *Holzforschung* 41(2):67-71.
<https://doi.org/10.1515/hfsg.1987.41.2.67>.
- Hiscox, J., Baldrian, P., Rogers, H. J., and Boddy, L. 2010a. Changes in oxidative enzyme activity during interspecific mycelial interactions involving the white-rot fungus *Trametes versicolor*. *Fungal Genetics and Biology* 47(6):562-571.
<https://doi.org/10.1016/j.fgb.2010.03.007>.

- Hiscox, J., and Boddy, L. 2017. Armed and dangerous – Chemical warfare in wood decay communities. *Fungal Biology Reviews* 31(4):169-184.
<https://doi.org/10.1016/j.fbr.2017.07.001>.
- Hiscox, J., Clarkson, G., Savoury, M., Powell, G., Savva, I., Lloyd, M., Shipcott, J., Choimes, A., Amargant Cumbriu, X., and Boddy, L. 2016. Effects of pre-colonisation and temperature on interspecific fungal interactions in wood. *Fungal Ecology* 21:32-42.
<https://doi.org/10.1016/j.funeco.2016.01.011>.
- Hiscox, J., Hibbert, C., Rogers, H. J., and Boddy, L. 2010b. Monokaryons and dikaryons of *Trametes versicolor* have similar combative, enzyme and decay ability. *Fungal Ecology* 3(4):347-356. <https://doi.org/10.1016/j.funeco.2010.02.003>.
- Hiscox, J., O'Leary, J., and Boddy, L. 2018. Fungus wars: basidiomycete battles in wood decay. *Studies in Mycology* 89:117-124. <https://doi.org/10.1016/j.simyco.2018.02.003>.
- Hiscox, J., Savoury, M., Müller, C. T., Lindahl, B. D., Rogers, H. J., and Boddy, L. 2015. Priority effects during fungal community establishment in beech wood. *The ISME Journal* 9(10):2246-2260. <https://doi.org/10.1038/ismej.2015.38>.
- Hofrichter, M. 2010. *Industrial Applications*. 2nd ed. The Mycota 10. Springer-Verlag Berlin Heidelberg, Berlin, Heidelberg.
- Holmer, L., and Stenlid, J. 1997. Competitive hierarchies of wood decomposing basidiomycetes in artificial systems based on variable inoculum sizes. *Oikos* 79(1):77-84.
<https://doi.org/10.2307/3546092>.
- Hong, L. T. 1982. The decay of tropical hardwood. II. Mass loss and degradation of cell-wall components of *Hevea brasiliensis* caused by *Ganoderma applanatum*, *Poria* sp., *Schizophyllum commune* and *Trametes corrugata*. *The Malaysian Forester* 45:124-126.
- Horn, S. J., Vaaje-Kolstad, G., Westereng, B., and Eijsink, V. G. 2012. Novel enzymes for the degradation of cellulose. *Biotechnology for Biofuels* 5(45):1-12.
<https://doi.org/10.1186/1754-6834-5-45>.
- Hosoe, T., Nozawa, K., Kawahara, N., Fukushima, K., Nishimura, K., Miyaji, M., and Kawai, K. 1999. Isolation of a new potent cytotoxic pigment along with indigotin from the pathogenic

- basidiomycetous fungus *Schizophyllum commune*. *Mycopathologia* 146(1):9-12.
<https://doi.org/10.1023/A:1007082619328>.
- Humar, M., Petric, M., and Pohleven, F. 2001. Changes of the pH value of impregnated wood during exposure to wood-rotting fungi. *Holz als Roh- und Werkstoff* 59(4):288-293.
<https://doi.org/10.1007/s001070100207>.
- Humar, M., Petrič, M., Pohleven, F., Šentjurc, M., and Kalan, P. 2002. Changes in EPR spectra of wood impregnated with copper-based preservatives during exposure to several wood-rotting fungi. *Holzforschung* 56(3):229-238. <https://doi.org/10.1515/HF.2002.038>.
- Humphrey, C. J. 1915. Tests on the durability of greenheart (*Nectandra rodiaei* Schomb.). *Mycologia* 7:204-209.
- Iakovlev, A., and Stenlid, J. 2000. Spatiotemporal patterns of laccase activity in interacting mycelia of wood-decaying basidiomycete fungi. *Microbial Ecology* 39(3):236-245.
<https://doi.org/10.1007/s002480000022>.
- Islam, M. M., Shams, M. I., Ilias, G., and Hannan, M. O. 2009. Protective antifungal effect of neem (*Azadirachta indica*) extracts on mango (*Mangifera indica*) and rain tree (*Albizia saman*) wood. *International Biodeterioration & Biodegradation* 63(2):241-243.
<https://doi.org/10.1016/j.ibiod.2008.07.010>.
- Jang, Y., Jang, S., Min, M., Hong, J.-H., Lee, H., Lee, H., Lim, Y. W., and Kim, J.-J. 2015. Comparison of the diversity of basidiomycetes from dead wood of the Manchurian fir (*Abies holophylla*) as evaluated by fruiting body collection, mycelial isolation, and 454 sequencing. *Microbial Ecology* 70(3):634-645. <https://doi.org/10.1007/s00248-015-0616-5>.
- Janjušević, L., Karaman, M., Šibul, F., Tommonaro, G., Iodice, C., Jakovljević, D., and Pejin, B. 2017. The lignicolous fungus *Trametes versicolor* (L.) Lloyd (1920): a promising natural source of antiradical and AChE inhibitory agents. *Journal of Enzyme Inhibition and Medicinal Chemistry* 32(1):355-362. <https://doi.org/10.1080/14756366.2016.1252759>.
- Jeffries, P. 1995. Biology and ecology of mycoparasitism. *Canadian Journal of Botany* 73(S1):1284-1290. <https://doi.org/10.1139/b95-389>.

- Jeyaprakasam, N. K., Razak, M. F. A., Ahmad, N. A. B., and Santhanam, J. 2016. Determining the pathogenic potential of non-sporulating molds isolated from cutaneous specimens. *Mycopathologia* 181(5-6):397-403. <https://doi.org/10.1007/s11046-016-9984-8>.
- Jin, H., Yan, Z., Liu, Q., Yang, X., Chen, J., and Qin, B. 2013. Diversity and dynamics of fungal endophytes in leaves, stems and roots of *Stellera chamaejasme* L. in northwestern China. *Antonie van Leeuwenhoek* 104(6):949-963. <https://doi.org/10.1007/s10482-013-0014-2>.
- Joel, E. L., and Bhimba, B. V. 2013. A secondary metabolite with antibacterial activity produced by mangrove foliar fungus *Schizophyllum commune*. *International Journal of Chemical, Environmental & Biological Sciences* 1(1):165-168.
- Johnson, C. E., Siccama, T. G., Denny, E. G., Koppers, M. M., and Vogt, D. J. 2014. In situ decomposition of northern hardwood tree boles: decay rates and nutrient dynamics in wood and bark. *Canadian Journal of Forest Research* 44(12):1515-1524. <https://doi.org/10.1139/cjfr-2014-0221>.
- Jonathan, S., and Fasidi, I. 2001. Studies on phytohormones, vitamins and mineral element requirements of *Lentinus subnudus* (Berk) and *schizophyllum commune* (Fr. Ex. Fr) from Nigeria. *Food Chemistry* 75(3):303-307. [https://doi.org/10.1016/S0308-8146\(01\)00154-6](https://doi.org/10.1016/S0308-8146(01)00154-6).
- Jurášek, L., Sopko, R., and Váradi, J. 1968. Decomposition of beech wood and holocellulose by supernatants of stationary cultures of wood — destroying fungi. *Česká Mykologie* 22(1):43-49.
- Jusoh, I., Zaharin, F. A., and Adam, N. S. 2014. Wood quality of *Acacia* hybrid and second-generation *Acacia mangium*. *BioResources* 9(1):150-160. <https://doi.org/10.15376/biores.9.1.150-160>.
- Kamalebo, H. M., Malale, H. N. S. W., Ndabaga, C. M., Degreef, J., and Kesel, A. d. 2018. Uses and importance of wild fungi: traditional knowledge from the Tshopo province in the democratic republic of the Congo. *Journal of Ethnobiology and Ethnomedicine* 14(13):1-12. <https://doi.org/10.1186/s13002-017-0203-6>.
- Kamei, K., Unno, H., Ito, J., Nishimura, K., and Miyaji, M. 1999. 臨床検体より *Schizophyllum commune* が分離された症例の検討 (Analysis of the cases in

- which *Schizophyllum commune* was isolated). Japanese Journal of Medical Mycology (Nihon Ishinkin Gakkai zasshi) 40(3):175-181 (in Japanese).
<https://doi.org/10.3314/jjmm.40.175>.
- Kano, R., Oomae, S., Nakano, Y., Minami, T., Sukikara, M., Nakayama, T., and Hasegawa, A. 2002. First report on *Schizophyllum commune* from a dog. Journal of Clinical Microbiology 40(9):3535-3537. <https://doi.org/10.1128/jcm.40.9.3535-3537.2002>.
- Kersten, P., and Cullen, D. 2014. Copper radical oxidases and related extracellular oxidoreductases of wood-decay Agaricomycetes. Fungal Genetics and Biology 72:124-130. <https://doi.org/10.1016/j.fgb.2014.05.011>.
- Kettle, A. J., Carere, J., Batley, J., Benfield, A. H., Manners, J. M., Kazan, K., and Gardiner, D. M. 2015. A γ -lactamase from cereal infecting *Fusarium* spp. catalyses the first step in the degradation of the benzoxazolinone class of phytoalexins. Fungal Genetics and Biology 83:1-9. <https://doi.org/10.1016/j.fgb.2015.08.005>.
- Khonsuntia, W., Zia, A., Cherdchim, B., Lakkireddy, K., and Kües, U. unpublished.
Schizophyllum commune – a fungus with a Janus face?
- Kilaru, S. 2006. Identification of fungal multi-copper oxidase gene families: Overexpression and characterization of *Coprinopsis cinerea* laccases for applications in biotechnology. Zugl.: Göttingen, Univ., Diss., 2006. 1. Aufl. Cuvillier, Göttingen.
- Kim, C., Yoo, B. O., Jung, S. Y., and Lee, K. S. 2017. Allometric equations to assess biomass, carbon and nitrogen content of black pine and red pine trees in southern Korea. iForest - Biogeosciences and Forestry 10(2):483-490. <https://doi.org/10.3832/ifor2164-010>.
- Kim, D.-H., Kim, S.-H., Kwon, S.-W., Lee, J.-K., and Hong, S.-B. 2015. The mycobiota of air inside and outside the *Meju* fermentation room and the origin of *Meju* fungi. Mycobiology 43(3):258-265. <https://doi.org/10.5941/MYCO.2015.43.3.258>.
- Kim, J. S., and Daniel, G. 2017. Immunolocalization of pectin and hemicellulose epitopes in the phloem of Norway spruce and Scots pine. Trees 31(4):1335-1353.
<https://doi.org/10.1007/s00468-017-1552-4>.

- Kim, J. S., and Daniel, G. 2018. Heterogeneous distribution of pectin and hemicellulose epitopes in the phloem of four hardwood species. *Trees* 32(2):393-414. <https://doi.org/10.1007/s00468-017-1638-z>.
- Kim, M.-J., Shin, H.-K., Choi, Y.-S., Kim, G.-C., and Kim, G.-H. 2016. An aeromycological study of various wooden cultural heritages in Korea. *Journal of Cultural Heritage* 17:123-130. <https://doi.org/10.1016/j.culher.2015.05.001>.
- Kim, S. 2020. Ricin B-like lectin orthologues from two mushrooms, *Hericium erinaceus* and *Stereum hirsutum*, enable recognition of highly fucosylated N-glycans. *International Journal of Biological Macromolecules* 147:560-568. <https://doi.org/10.1016/j.ijbiomac.2020.01.097>.
- Kirk, T. K. 1973. The chemistry and biochemistry of decay. Pages 149–181 in: *Wood Deterioration and its Prevention by Preservative Treatments*, Vol. 1, Degradation and Protection of Wood. D. D. Nicholas, ed. Syracuse Univ. Press.
- Kirker, G. T. 2018. Wood Decay Fungi. Pages 1–6 in: *Encyclopedia of life sciences*. J. W. & S. Ltd, ed. Nature Pub. Group; Wiley, London, New York, Vols. 21-32, Chichester, West Sussex, U.K.
- Kirtzel, J., Madhavan, S., Wielsch, N., Blinne, A., Hupfer, Y., Linde, J., Krause, K., Svatoš, A., and Kothe, E. 2018. Enzymatic bioweathering and metal mobilization from black slate by the basidiomycete *Schizophyllum commune*. *Frontiers in Microbiology* 9:2545. <https://doi.org/10.3389/fmicb.2018.02545>.
- Kirtzel, J., Siegel, D., Krause, K., and Kothe, E. 2017. Stone-eating fungi: Mechanisms in bioweathering and the potential role of laccases in black slate degradation with the basidiomycete *Schizophyllum commune*. *Advances in Applied Microbiology* 99:83-101. <https://doi.org/10.1016/bs.aambs.2017.01.002>.
- Klein, K. K., Landry, J., Friesen, T., and Larimer, T. 1997. Kinetics of asymmetric mycelial growth and control by dikaryosis and light in *Schizophyllum commune*. *Mycologia* 89(6):916-923. <https://doi.org/10.2307/3761112>.
- Klemm, D., Heublein, B., Fink, H.-P., and Bohn, A. 2005. Cellulose: fascinating biopolymer and sustainable raw material. *Angewandte Chemie (International ed. in English)* 44(22):3358-3393. <https://doi.org/10.1002/anie.200460587>.

- Kligman, A. M. 1950. A basidiomycete probably causing onychomycosis. *The Journal of Investigative Dermatology* 14(1):67-70. <https://doi.org/10.1038/jid.1950.10>.
- Knežević, A., Stajić, M., Sofrenić, I., Stanojković, T., Milovanović, I., Tešević, V., and Vukojević, J. 2018. Antioxidative, antifungal, cytotoxic and antineurodegenerative activity of selected *Trametes* species from Serbia. *PloS One* 13(8):e0203064. <https://doi.org/10.1371/journal.pone.0203064>.
- Koenigs, J. W. 1974. Production of hydrogen peroxide by wood-rotting fungi in wood and its correlation with weight loss, depolymerization, and pH changes. *Archives of Microbiology* 99(1):129-145. <https://doi.org/10.1007/BF00696229>.
- Kostylev, M., and Wilson, D. 2012. Synergistic interactions in cellulose hydrolysis. *Biofuels* 3(1):61-70. <https://doi.org/10.4155/bfs.11.150>.
- Koyani, R. D., Bhatt, I. M., Patel, H. R., Vasava, A. M., and Rajput, K. S. 2016. Evaluation of *Schizophyllum commune* Fr. potential for biodegradation of lignin: A light microscopic analysis. *Wood Material Science & Engineering* 11(1):46-56. <https://doi.org/10.1080/17480272.2014.945957>.
- Krah, F.-S., Bässler, C., Heibl, C., Soghigian, J., Schaefer, H., and Hibbett, D. S. 2018. Evolutionary dynamics of host specialization in wood-decay fungi. *BMC Evolutionary Biology* 18(1):119. <https://doi.org/10.1186/s12862-018-1229-7>.
- Krause, K., Jung, E.-M., Lindner, J., Hardiman, I., Poetschner, J., Madhavan, S., Matthäus, C., Kai, M., Menezes, R. C., Popp, J., Svatoš, A., and Kothe, E. 2020. Response of the wood-decay fungus *Schizophyllum commune* to co-occurring microorganisms. *PloS One* 15(4):e0232145. <https://doi.org/10.1371/journal.pone.0232145>.
- Krogh, A., Larsson, B., Heijne, G. von, and Sonnhammer, E. L. 2001. Predicting transmembrane protein topology with a hidden Markov model: application to complete genomes. *Journal of molecular biology* 305(3):567-580. <https://doi.org/10.1006/jmbi.2000.4315>.
- Kubicek, C. P., Herrera-Estrella, A., Seidl-Seiboth, V., Martinez, D. A., Druzhinina, I. S., Thon, M., Zeilinger, S., Casas-Flores, S., Horwitz, B. A., Mukherjee, P. K., Mukherjee, M., Kredics, L., Alcaraz, L. D., Aerts, A., Antal, Z., Atanasova, L., Cervantes-Badillo, M. G., Challacombe, J., Chertkov, O., McCluskey, K., Couplier, F., Deshpande, N., Döhren, H. von,

- Ebbole, D. J., Esquivel-Naranjo, E. U., Fekete, E., Flipphi, M., Glaser, F., Gómez-Rodríguez, E. Y., Gruber, S., Han, C., Henrissat, B., Hermosa, R., Hernández-Oñate, M., Karaffa, L., Kosti, I., Le Crom, S., Lindquist, E., Lucas, S., Lübeck, M., Lübeck, P. S., Margeot, A., Metz, B., Misra, M., Nevalainen, H., Omann, M., Packer, N., Perrone, G., Uresti-Rivera, E. E., Salamov, A., Schmoll, M., Seiboth, B., Shapiro, H., Sukno, S., Tamayo-Ramos, J. A., Tisch, D., Wiest, A., Wilkinson, H. H., Zhang, M., Coutinho, P. M., Kenerley, C. M., Monte, E., Baker, S. E., and Grigoriev, I. V. 2011. Comparative genome sequence analysis underscores mycoparasitism as the ancestral life style of *Trichoderma*. *Genome Biology* 12(4):R40. <https://doi.org/10.1186/gb-2011-12-4-r40>.
- Kubicek, C. P., Starr, T. L., and Glass, N. L. 2014. Plant cell wall-degrading enzymes and their secretion in plant-pathogenic fungi. *Annual Review of Phytopathology* 52:427-451. <https://doi.org/10.1146/annurev-phyto-102313-045831>.
- Kudanga, T. 2012. Versatility of oxidoreductases in the remediation of environmental pollutants. *Front Biosci* E4(3):1127-1149. <https://doi.org/10.2741/E446>.
- Kües, U., Khonsuntia, W., and Subba, S. 2018. Complex fungi. *Fungal Biology Reviews* 32(4):205-218. <https://doi.org/10.1016/j.fbr.2018.08.001>.
- Kutorga, E., Adamonytė, G., Iršėnaitė, R., Kasparavičius, J., Markovskaja, S., Motiejūnaitė, J., and Treigienė, A. 2012. A checklist of mycobiota recorded in burnt and unburnt *Pinus mugo* plantations in the Curonian spit (Lithuania). *Botanica Lithuanica* 18(1):66-79. <https://doi.org/10.2478/v10279-012-0009-3>.
- Laemmli, U. K. 1970. Cleavage of structural proteins during the assembly of the head of bacteriophage T4. *Nature* 227(5259):680-685. <https://doi.org/10.1038/227680a0>.
- Lakkireddy, K., Zia, A., Khonsuntia, W., and Kües, U. 2017. *Schizophyllum commune* as an early sapwood colonizing fungus. 171-176 in: The 3rd Asia Pacific APRC 2017 Rubber Conference. Prince of Songla University, Surat Thani Campus,, Surat Thani, Thailand.
- Lallawmsanga, Passari, A. K., Mishra, V. K., Leo, V. V., Singh, B. P., Meyyappan, G. V., Gupta, V. K., Uthandi, S., and Upadhyay, R. C. 2016. Antimicrobial potential, identification and phylogenetic affiliation of wild mushrooms from two sub-tropical semi-evergreen Indian forest ecosystems. *PloS One* 11(11):e0166368. <https://doi.org/10.1371/journal.pone.0166368>.

- Lara-Espinoza, C., Carvajal-Millán, E., Balandrán-Quintana, R., López-Franco, Y., and Rascón-Chu, A. 2018. Pectin and pectin-based composite materials: beyond food texture. *Molecules* 23(4):942. <https://doi.org/10.3390/molecules23040942>.
- Ledeboer, M. S. J. 1946. *Schizophyllum commune* as a wound parasite: a warning to wattle growers. *Journal of the South African Forestry Association* 13(1):39-40. <https://doi.org/10.1080/03759873.1946.9631042>.
- Leithoff, H., and Peek, R.-D. 2001. Heat treatment of bamboo. Pages 1–11 in: IRG Scientific Conferences, Nara, Japan.
- Leonhardt, S., Hoppe, B., Stengel, E., Noll, L., Moll, J., Bässler, C., Dahl, A., Buscot, F., Hofrichter, M., and Kellner, H. 2019. Molecular fungal community and its decomposition activity in sapwood and heartwood of 13 temperate European tree species. *PloS One* 14(2):e0212120. <https://doi.org/10.1371/journal.pone.0212120>.
- Lindahl, B. D., and Finlay, R. D. 2006. Activities of chitinolytic enzymes during primary and secondary colonization of wood by basidiomycetous fungi. *The New Phytologist* 169(2):389-397. <https://doi.org/10.1111/j.1469-8137.2005.01581.x>.
- Lipp, F. J. 1971. Ethnobotany of the Chinantec Indians, Oaxaca, Mexico. *Economic Botany* 25(3):234-244. <https://doi.org/10.1007/BF02860760>.
- Liu, X., Frydenvang, K., Liu, H., Zhai, L., Chen, M., Olsen, C. E., and Christensen, S. B. 2015. Iminolactones from *Schizophyllum commune*. *Journal of Natural Products* 78(5):1165-1168. <https://doi.org/10.1021/np500836y>.
- Liu, Y., Srivilai, P., Loos, S., Aebi, M., and Kües, U. 2006. An essential gene for fruiting body initiation in the basidiomycete *Coprinopsis cinerea* is homologous to bacterial cyclopropane fatty acid synthase genes. *Genetics* 172(2):873-884. <https://doi.org/10.1534/genetics.105.045542>.
- Lombard, V., Golaconda Ramulu, H., Drula, E., Coutinho, P. M., and Henrissat, B. 2014. The carbohydrate-active enzymes database (CAZy) in 2013. *Nucleic Acids Research* 42(Database issue):D490-5. <https://doi.org/10.1093/nar/gkt1178>.

- Lundborg, A., and Unestam, T. 1980. Antagonism against *Fomes annosus*. Comparison between different test methods in vitro and in vivo. *Mycopathologia* 70(2):107-115.
<https://doi.org/10.1007/BF00443076>.
- Luo, J., Fu, W., and Pan, C. 2015. Identification of wood-rotting fungi and their decay capability in six wood species. *Journal of Zhejiang A & F University* 32(1):1–10 (In Chinese).
- Luti, S., Sella, L., Quarantin, A., Pazzagli, L., and Baccelli, I. 2020. Twenty years of research on cerato-platanin family proteins: clues, conclusions, and unsolved issues. *Fungal Biology Reviews* 34(1):13-24. <https://doi.org/10.1016/j.fbr.2019.10.001>.
- Lygis, V., Vasiliauskaite, I., Matelis, A., Pliūra, A., Vasaitis, R., Lygis, V., Vasiliauskaite, I., Matelis, A., Pliūra, A., and Vasaitis, R. 2014. Fungi in living and dead stems and stumps of *Pinus mugo* on coastal dunes of the Baltic Sea. *Plant Protection Science* 50(4):221-226.
<https://doi.org/10.17221/25/2014-PPS>.
- Lyngdoh, A. 2014. Diversity of wood-rotting macrofungi of east Khasi hills and decay potential of selected fungal species. Doctor of Philosophy in Botany, Shillong, India.
- MacIntosh, G. C. 2011. RNase T2 Family: Enzymatic Properties, Functional Diversity, and Evolution of Ancient Ribonucleases. Pages 89–114 in: *Ribonucleases*. A. W. Nicholson, ed. Springer Berlin Heidelberg, Berlin, Heidelberg.
- Maduranga, K., Attanayake, R. N., Santhirasegaram, S., Weerakoon, G., and Paranagama, P. A. 2018. Molecular phylogeny and bioprospecting of Endolichenic Fungi (ELF) inhabiting in the lichens collected from a mangrove ecosystem in Sri Lanka. *PloS One* 13(8):e0200711.
<https://doi.org/10.1371/journal.pone.0200711>.
- Marco-Urrea, E., Pérez-Trujillo, M., Caminal, G., and Vicent, T. 2009. Dechlorination of 1,2,3- and 1,2,4-trichlorobenzene by the white-rot fungus *Trametes versicolor*. *Journal of Hazardous Materials* 166(2-3):1141-1147. <https://doi.org/10.1016/j.jhazmat.2008.12.076>.
- Marowa, P., Ding, A., and Kong, Y. 2016. Expansins: roles in plant growth and potential applications in crop improvement. *Plant cell reports* 35(5):949-965.
<https://doi.org/10.1007/s00299-016-1948-4>.

- Martin, A. R., Gezahegn, S., and Thomas, S. C. 2015. Variation in carbon and nitrogen concentration among major woody tissue types in temperate trees. *Canadian Journal of Forest Research* 45(6):744-757. <https://doi.org/10.1139/cjfr-2015-0024>.
- Martínez-Álvarez, P., Alves-Santos, F., and Diez, J. 2012. In vitro and in vivo interactions between *Trichoderma viride* and *Fusarium circinatum*. *Silva Fennica* 46(3). <https://doi.org/10.14214/sf.42>.
- McDonald, A. G., Boyce, S., and Tipton, K. F. 2009. ExplorEnz: the primary source of the IUBMB enzyme list. *Nucleic Acids Research* 37(Database issue):D593-7. <https://doi.org/10.1093/nar/gkn582>.
- Meerts, P. 2002. Mineral nutrient concentrations in sapwood and heartwood: a literature review. *Annals of Forest Science* 59(7):713-722. <https://doi.org/10.1051/forest:2002059>.
- Mellinas, C., Ramos, M., Jiménez, A., and Garrigós, M. C. 2020. Recent trends in the use of pectin from agro-waste residues as a natural-based biopolymer for food packaging applications. *Materials* 13(673):1-17. <https://doi.org/10.3390/ma13030673>.
- Mendiburu, F. de, and Simon, R. 2015. *Agricolae* - Ten years of an open source statistical tool for experiments in breeding, agriculture and biology.
- Menezes, R. C. 2014. Application of raman spectroscopy and mass spectrometry to study growth and interaction processes of the white-rot fungus *Schizophyllum commune*. PhD. Thüringer Universitäts- und Landesbibliothek, Jena, Germany.
- Menezes, R. C., Kai, M., Krause, K., Matthäus, C., Svatoš, A., Popp, J., and Kothe, E. 2015. Monitoring metabolites from *Schizophyllum commune* interacting with *Hypholoma fasciculare* combining LESA-HR mass spectrometry and Raman microscopy. *Analytical and Bioanalytical Chemistry* 407(8):2273-2282. <https://doi.org/10.1007/s00216-014-8383-6>.
- Miles, P. G., Lund, H., and Raper, J. R. 1956. The identification of indigo as a pigment produced by a mutant culture of *Schizophyllum commune*. *Archives of Biochemistry and Biophysics* 62(1):1-5. [https://doi.org/10.1016/0003-9861\(56\)90081-9](https://doi.org/10.1016/0003-9861(56)90081-9).
- Misra, R. C., Sandeep, Kamthan, M., Kumar, S., and Ghosh, S. 2016. A thaumatin-like protein of *Ocimum basilicum* confers tolerance to fungal pathogen and abiotic stress in transgenic *Arabidopsis*. *Scientific Reports* 6:25340. <https://doi.org/10.1038/srep25340>.

- Mitchell, A. L., Attwood, T. K., Babbitt, P. C., Blum, M., Bork, P., Bridge, A., Brown, S. D., Chang, H.-Y., El-Gebali, S., Fraser, M. I., Gough, J., Haft, D. R., Huang, H., Letunic, I., Lopez, R., Luciani, A., Madeira, F., Marchler-Bauer, A., Mi, H., Natale, D. A., Necci, M., Nuka, G., Orengo, C., Pandurangan, A. P., Paysan-Lafosse, T., Pesseat, S., Potter, S. C., Qureshi, M. A., Rawlings, N. D., Redaschi, N., Richardson, L. J., Rivoire, C., Salazar, G. A., Sangrador-Vegas, A., Sigrist, C. J. A., Sillitoe, I., Sutton, G. G., Thanki, N., Thomas, P. D., Tosatto, S. C. E., Yong, S.-Y., and Finn, R. D. 2019. InterPro in 2019: improving coverage, classification and access to protein sequence annotations. *Nucleic Acids Research* 47(D1):D351-D360. <https://doi.org/10.1093/nar/gky1100>.
- Mohebbly, B. 2003. Biological attack of acetylated wood. Ph.D., Göttingen, Germany.
- Mohebbly, B. 2005. Attenuated total reflection infrared spectroscopy of white-rot decayed beech wood. *International Biodeterioration & Biodegradation* 55(4):247-251. <https://doi.org/10.1016/j.ibiod.2005.01.003>.
- Mori, T., Seki, A., Kano, R., Sakai, H., Nakagawa, M., Hasegawa, A., and Maruo, K. 2009. Mycotic osteomyelitis caused by *Schizophyllum commune* in a dog. *The Veterinary Record* 165(12):350-351. <https://doi.org/10.1136/vr.165.12.350>.
- Morón-Ríos, A., Gómez-Cornelio, S., Ortega-Morales, B. O., La Rosa-García, S. de, Partida-Martínez, L. P., Quintana, P., Alayón-Gamboa, J. A., Cappello-García, S., and González-Gómez, S. 2017. Interactions between abundant fungal species influence the fungal community assemblage on limestone. *PloS One* 12(12):e0188443. <https://doi.org/10.1371/journal.pone.0188443>.
- Motiejūnaitė, J., Adamonytė, G., Iršėnaitė, R., Juzėnas, S., Kasparavičius, J., Kutorga, E., and Markovskaja, S. 2014. Early fungal community succession following crown fire in *Pinus mugo* stands and surface fire in *Pinus sylvestris* stands. *European Journal of Forest Research* 133(4):745-756. <https://doi.org/10.1007/s10342-013-0738-6>.
- Nagadesi, P. K., and Arya, A. 2014. Delignification of valuable timbers decayed by India lignicolous fungi. *International Letters of Natural Sciences* 16:101-120. <https://doi.org/10.18052/www.scipress.com/ILNS.16.101>.

- Nagatomo, I., and Akai, S. 1953. Studies on wood-decay. VII. On the relative resistance of black pine sap wood (*Pinus thunbergii* Parl.) to decay. *Journal of The Japanese Forestry* 35:19-21 (In Japanese).
- Nagy, L. G., Riley, R., Bergmann, P. J., Krizsán, K., Martin, F. M., Grigoriev, I. V., Cullen, D., and Hibbett, D. S. 2017. Genetic bases of fungal white rot wood decay predicted by phylogenomic analysis of correlated gene-phenotype evolution. *Molecular Biology and Evolution* 34(1):35-44. <https://doi.org/10.1093/molbev/msw238>.
- Nair, R. B., Lennartsson, P. R., and Taherzadeh, M. J. 2016. Mycelial pellet formation by edible ascomycete filamentous fungi, *Neurospora intermedia*. *AMB Express* 6(31):1-10. <https://doi.org/10.1186/s13568-016-0203-2>.
- Nakasone, K. K. 1977. Fungi that decay ocotillo in Arizona. Master of Science, Tucson, United States.
- Nevalainen, H., Kautto, L., and Te'o, J. 2014. Methods for isolation and cultivation of filamentous fungi. Pages 3–16 in: *Environmental microbiology: Methods and protocols*. I. T. Paulsen, and A. J. Holmes, eds. Humana Press, New York, NY.
- Ng, T. B. 2004. Peptides and proteins from fungi. *Peptides* 25(6):1055-1073. <https://doi.org/10.1016/j.peptides.2004.03.013>.
- Nicolotti, G., and Varese, G. 1996. Screening of antagonistic fungi against air-borne infection by *Heterobasidion annosum* on Norway spruce. *Forest Ecology and Management* 88(3):249-257. [https://doi.org/10.1016/S0378-1127\(96\)03844-3](https://doi.org/10.1016/S0378-1127(96)03844-3).
- Nielsen, H. 2017. Predicting Secretory Proteins with SignalP. *Methods in molecular biology* (Clifton, N.J.) 1611:59-73. https://doi.org/10.1007/978-1-4939-7015-5_6.
- Nikolaidis, N., Doran, N., and Cosgrove, D. J. 2014. Plant expansins in bacteria and fungi: evolution by horizontal gene transfer and independent domain fusion. *Molecular Biology and Evolution* 31(2):376-386. <https://doi.org/10.1093/molbev/mst206>.
- Nilsson, T., and Daniel, G. F. 1983. Micromorphology of *Schizophyllum commune* attack in pine (*Pinus sylvestris*) wood, Stockholm, Sweden.

- Nobles, M. K. 1965. Identification of cultures of wood-inhabiting hymenomycetes. *Canadian Journal of Botany* 43(9):1097-1139. <https://doi.org/10.1139/b65-126>.
- Nordin, A., Uggla, C., and Näsholm, T. 2001. Nitrogen forms in bark, wood and foliage of nitrogen-fertilized *Pinus sylvestris*. *Tree Physiology* 21(1):59-64. <https://doi.org/10.1093/treephys/21.1.59>.
- Nordin, V. J. 1954. Studies in forest pathology: XIII. Decay in sugar maple in the Ottawa–Huron and Algoma extension forest region of Ontario. *Canadian Journal of Botany* 32(1):221-258. <https://doi.org/10.1139/b54-021>.
- Nsolomo, V. R., Venn, K., and Solheim, H. 2000. The ability of some fungi to cause decay in the East African camphor tree, *Ocotea usambarensis*. *Mycological Research* 104(12):1473-1479. <https://doi.org/10.1017/S0953756200003579>.
- Oguma, T., Taniguchi, M., Shimoda, T., Kamei, K., Matsuse, H., Hebisawa, A., Takayanagi, N., Konno, S., Fukunaga, K., Harada, K., Tanaka, J., Tomomatsu, K., and Asano, K. 2018. Allergic bronchopulmonary aspergillosis in Japan: A nationwide survey. *Allergy International* 67(1):79-84. <https://doi.org/10.1016/j.alit.2017.04.011>.
- Ohm, R. A., Jong, J. F. de, Bekker, C. de, Wösten, H. A. B., and Lugones, L. G. 2011. Transcription factor genes of *Schizophyllum commune* involved in regulation of mushroom formation. *Molecular Microbiology* 81(6):1433-1445. <https://doi.org/10.1111/j.1365-2958.2011.07776.x>.
- Ohm, R. A., Jong, J. F. de, Lugones, L. G., Aerts, A., Kothe, E., Stajich, J. E., Vries, R. P. de, Record, E., Levasseur, A., Baker, S. E., Bartholomew, K. A., Coutinho, P. M., Erdmann, S., Fowler, T. J., Gathman, A. C., Lombard, V., Henrissat, B., Knabe, N., Kües, U., Lilly, W. W., Lindquist, E., Lucas, S., Magnuson, J. K., Piumi, F., Raudaskoski, M., Salamov, A., Schmutz, J., Schwarze, F. W. M. R., vanKuyk, P. A., Horton, J. S., Grigoriev, I. V., and Wösten, H. A. B. 2010. Genome sequence of the model mushroom *Schizophyllum commune*. *Nature Biotechnology* 28(9):957-963. <https://doi.org/10.1038/nbt.1643>.
- Ohm, R. A., Riley, R., Salamov, A., Min, B., Choi, I.-G., and Grigoriev, I. V. 2014. Genomics of wood-degrading fungi. *Fungal Genetics and Biology* 72:82-90. <https://doi.org/10.1016/j.fgb.2014.05.001>.

- Okhuoya, J., Akpaja, E., Osemwegie, O., Oghenekaro, A., and Ihayere, C. 2010. Nigerian mushrooms: Underutilized non-wood forest resources. *Journal of Applied Sciences and Environmental Management* 14(1):43-54. <https://doi.org/10.4314/jasem.v14i1.56488>.
- Oliveros, J. C. 2007-2015. Venny. An interactive tool for comparing lists with Venn's diagrams. Oliveros, J.C.
- Olsson, C., and Westm, G. 2013. Direct Dissolution of Cellulose: Background, Means and Applications in: *Cellulose - Fundamental Aspects*. T. G. van de Ven, ed. InTech.
- Osemwegie, O. O., and Okhuoya, J. A. 2011. Diversity and abundance of macrofungi in rubber agroforests in southwestern Nigeria. *Nordic Journal of Botany* 29(1):119-128. <https://doi.org/10.1111/j.1756-1051.2010.00717.x>.
- Padhiar, A., and Albert, S. 2011. Anatomical changes in *Syzygium cumuini* Linn. wood decayed by two white rot fungi *Schizophyllum commune* Fries. and *Flavodon flavus* (Klotzsch) Ryvarden. *J Indian Acad Wood Sci* 8(1):11-20. <https://doi.org/10.1007/s13196-011-0017-4>.
- Padhiar, A., Albert, S., Nagadesi, P. K., and Arya, A. 2010. Lignin degradation by *Flavodon flavus* (Klotzsch.) Ryv. and *Schizophyllum commune* Fr. on *Mangifera indica* and *Syzygium cumini* woods. *Journal of Wood Chemistry and Technology* 30(2):129-139. <https://doi.org/10.1080/02773810903207770>.
- Panno, L., Bruno, M., Voyron, S., Anastasi, A., Gnavi, G., Miserere, L., and Varese, G. C. 2013. Diversity, ecological role and potential biotechnological applications of marine fungi associated to the seagrass *Posidonia oceanica*. *New Biotechnology* 30(6):685-694. <https://doi.org/10.1016/j.nbt.2013.01.010>.
- Parfitt, D., Hunt, J., Dockrell, D., Rogers, H. J., and Boddy, L. 2010. Do all trees carry the seeds of their own destruction? PCR reveals numerous wood decay fungi latently present in sapwood of a wide range of angiosperm trees. *Fungal Ecology* 3(4):338-346. <https://doi.org/10.1016/j.funeco.2010.02.001>.
- Pasaylyuk, M. V. 2017. Xylotrophic agaricomycetes – antagonists of rare mushroom *Hericium coralloides* (Scop.) Pers. (Hericiaceae) in the pure culture [Ксилотрофні агарикоміцети – антагоністи рідкісного гриба *Hericium coralloides* (Scop.) Pers. (Hericiaceae) в культурі].

- Ukrainian Journal of Ecology 7(3):225–233 (in Ukrainian).
https://doi.org/10.15421/2017_72.
- Pawlik, A., Ruminowicz-Stefaniuk, M., Frąc, M., Mazur, A., Wielbo, J., and Janusz, G. 2019. The wood decay fungus *Cerrena unicolor* adjusts its metabolism to grow on various types of wood and light conditions. *PloS One* 14(2):e0211744.
<https://doi.org/10.1371/journal.pone.0211744>.
- Peddireddi, S. 2008. Hydrophobins in wood biology and biotechnology. PhD, Göttingen, Germany.
- Peiris, D., Dunn, W. B., Brown, M., Kell, D. B., Roy, I., and Hedger, J. N. 2008. Metabolite profiles of interacting mycelial fronts differ for pairings of the wood decay basidiomycete fungus, *Stereum hirsutum* with its competitors *Coprinus micaceus* and *Coprinus disseminatus*. *Metabolomics* 4(1):52-62. <https://doi.org/10.1007/s11306-007-0100-4>.
- Perkins, J. H. 1969. Morphogenesis in *Schizophyllum commune*. I. Effects of White Light. *Plant physiology* 44(12):1706-1711.
- Peters, B. C., and Allen, P. J. 1994. Susceptibility of conditioned softwood baits to *Coptotermes* spp. (Isoptera: Rhinotermitidae). *Material und Organismen* 29:47-65.
- Pirt, S. J. 1966. A theory of the mode of growth of fungi in the form of pellets in submerged culture. *Proceedings of The Royal Society B: Biological Sciences* 166(1004):369-373.
<https://doi.org/10.1098/rspb.1966.0105>.
- Pitocchi, R., Cicatiello, P., Birolo, L., Piscitelli, A., Bovio, E., Varese, G. C., and Giardina, P. 2020. Cerato-Platanins from Marine Fungi as Effective Protein Biosurfactants and Bioemulsifiers. *International journal of molecular sciences* 21(8).
<https://doi.org/10.3390/ijms21082913>.
- Pollegioni, L., Tonin, F., and Rosini, E. 2015. Lignin-degrading enzymes. *The FEBS Journal* 282(7):1190-1213. <https://doi.org/10.1111/febs.13224>.
- Poole, R. F. 1929. Sweet potatoes infected by *Schizophyllum commune*. *Journal of the Elisha Mitchell Scientific Society* 45(1):137-139.

- Potter, S. C., Luciani, A., Eddy, S. R., Park, Y., Lopez, R., and Finn, R. D. 2018. HMMER web server: 2018 update. *Nucleic Acids Research* 46(W1):W200-W204.
<https://doi.org/10.1093/nar/gky448>.
- Preecha, C., Wisutthiphaet, W., Seephueak, P., and Thongliumnak, S. 2016. Bag cultivation of split mushroom (*Schizophyllum commune*) by application coconut meal substitute rice bran. *International Journal of Agricultural Technology* 12(7.2):2073-2077.
- Presley, G. N., Panisko, E., Purvine, S. O., and Schilling, J. S. 2018. Coupling Secretomics with Enzyme Activities To Compare the Temporal Processes of Wood Metabolism among White and Brown Rot Fungi. *Applied and Environmental Microbiology* 84(16).
<https://doi.org/10.1128/AEM.00159-18>.
- Priadi, T. 2011. Analisis bahaya pelapukan kayu pada perumahan di Pulau Jawa (Wood decay hazard analyses of residential buildings in Java island), Bogor, Indonesia.
- Qadri, M., Johri, S., Shah, B. A., Khajuria, A., Sidiq, T., Lattoo, S. K., Abdin, M. Z., and Riyaz-Ul-Hassan, S. 2013. Identification and bioactive potential of endophytic fungi isolated from selected plants of the western Himalayas. *SpringerPlus* 2(8):1-14.
<https://doi.org/10.1186/2193-1801-2-8>.
- R Core Team. 2020. R: A language and environment for statistical computing. R Foundation for Statistical Computing, Vienna, Austria.
- Ramada, M. H. S., Steindorff, A. S., Bloch, C., and Ulhoa, C. J. 2016. Secretome analysis of the mycoparasitic fungus *Trichoderma harzianum* ALL 42 cultivated in different media supplemented with *Fusarium solani* cell wall or glucose. *Proteomics* 16(3):477-490.
<https://doi.org/10.1002/pmic.201400546>.
- Rappsilber, J., Mann, M., and Ishihama, Y. 2007. Protocol for micro-purification, enrichment, pre-fractionation and storage of peptides for proteomics using StageTips. *Nature protocols* 2(8):1896-1906. <https://doi.org/10.1038/nprot.2007.261>.
- Raudaskoski, M., and Viitanen, H. 1982. Effect of aeration and light on fruit body induction in *Schizophyllum commune*. *Transactions of the British Mycological Society* 78(1):89-96.
[https://doi.org/10.1016/S0007-1536\(82\)80080-6](https://doi.org/10.1016/S0007-1536(82)80080-6).

- Rawlings, N. D., Barrett, A. J., Thomas, P. D., Huang, X., Bateman, A., and Finn, R. D. 2018. The MEROPS database of proteolytic enzymes, their substrates and inhibitors in 2017 and a comparison with peptidases in the PANTHER database. *Nucleic Acids Research* 46(D1):D624-D632. <https://doi.org/10.1093/nar/gkx1134>.
- Rayner, A. D., Griffith, G. S., and Wildman, H. G. 1994. Induction of metabolic and morphogenetic changes during mycelial interactions among species of higher fungi. *Biochemical Society Transactions* 22(2):389-394. <https://doi.org/10.1042/bst0220389>.
- Rayner, A. D. M., and Boddy, L. 1988. Fungal communities in the decay of wood. Pages 115–166 in: *Advances in Microbial Ecology*. K. C. Marshall, ed. Springer US, Boston, MA.
- Rayner, A. D. M., Griffith, G. S., and Ainsworth, A. M. 1996. Mycelial Interconnectedness. Pages 21–40 in: *Growing Fungus*. N. A. Gow, G. M. Gadd, and G. M. Gadd, eds. Springer Netherlands, London.
- Reis, A. R. S., Reis, L. P., Alves Júnior, M., Carvalho, J. C. d., and Silva, J. R. d. 2017. Natural resistance of four Amazon woods submitted to xylophagous fungal infection under laboratory conditions. *Madera y Bosques* 23(2):155-162. <https://doi.org/10.21829/myb.2017.232968>.
- Richter, D. L., Kangas, L. C., Smith, J. K., and Laks, P. E. 2010. Comparison of effectiveness of wood decay fungi maintained by annual subculture on agar and stored in sterile water for 18 years. *Canadian Journal of Microbiology* 56(3):268-271. <https://doi.org/10.1139/w10-001>.
- Riley, R., Salamov, A. A., Brown, D. W., Nagy, L. G., Floudas, D., Held, B. W., Levasseur, A., Lombard, V., Morin, E., Otilar, R., Lindquist, E. A., Sun, H., LaButti, K. M., Schmutz, J., Jabbour, D., Luo, H., Baker, S. E., Pisabarro, A. G., Walton, J. D., Blanchette, R. A., Henrissat, B., Martin, F., Cullen, D., Hibbett, D. S., and Grigoriev, I. V. 2014. Extensive sampling of basidiomycete genomes demonstrates inadequacy of the white-rot/brown-rot paradigm for wood decay fungi. *Proceedings of the National Academy of Sciences of the United States of America* 111(27):9923-9928. <https://doi.org/10.1073/pnas.1400592111>.
- Rogalski, J., Lundell, T., and Hatakka, A. 1991. Production of laccase, lignin peroxidase and manganese-dependent peroxidase by various strains of *Trametes versicolor* depending on culture conditions. *Acta Microbiologica Polonica* 43(3/4):221-234.

- Romanelli, A. M., Sutton, D. A., Thompson, E. H., Rinaldi, M. G., and Wickes, B. L. 2010. Sequence-based identification of filamentous basidiomycetous fungi from clinical specimens: a cautionary note. *Journal of Clinical Microbiology* 48(3):741-752. <https://doi.org/10.1128/jcm.01948-09>.
- Rowell, R., Pettersen, R., and Tshabalala, M. 2012. Cell wall chemistry. Pages 33–72 in: *Handbook of Wood Chemistry and Wood Composites, Second Edition*. R. Rowell, ed. CRC Press.
- Roy, G., Laflamme, G., Bussieres, G., and Dessureault, M. 2003. Field tests on biological control of *Heterobasidion annosum* by *Phaeotheca dimorphospora* in comparison with *Phlebiopsis gigantea*. *Forest Pathology* 33(2):127-140. <https://doi.org/10.1046/j.1439-0329.2003.00319.x>.
- Rytioja, J., Hildén, K., Yuzon, J., Hatakka, A., de Vries, R. P., and Mäkelä, M. R. 2014. Plant-polysaccharide-degrading enzymes from Basidiomycetes. *Microbiology and Molecular Biology Reviews* 78(4):614-649. <https://doi.org/10.1128/MMBR.00035-14>.
- Safo-Sampah, S. 1975. Ability of selected fungi from Douglas-Fir poles to degrade wood and their tolerance to wood-preserving chemicals. Master of Science, Corvallis, United States.
- Sampedro, J., and Cosgrove, D. J. 2005. The expansin superfamily. *Genome Biology* 6(12):242. <https://doi.org/10.1186/gb-2005-6-12-242>.
- Sánchez-Fernández, R. E., Diaz, D., Duarte, G., Lappe-Oliveras, P., Sánchez, S., and Macías-Rubalcava, M. L. 2016. Antifungal volatile organic compounds from the endophyte *Nodulisporium* sp. strain GS4d2II1a: a qualitative change in the intraspecific and interspecific interactions with *Pythium aphanidermatum*. *Microbial Ecology* 71(2):347-364. <https://doi.org/10.1007/s00248-015-0679-3>.
- Sato, S., Liu, F., Koc, H., and Tien, M. 2007. Expression analysis of extracellular proteins from *Phanerochaete chrysosporium* grown on different liquid and solid substrates. *Microbiology* 153:3023-3033. <https://doi.org/10.1099/mic.0.2006/000513-0>.
- Scheller, H. V., and Ulvskov, P. 2010. Hemicelluloses. *Annual Review of Plant Biology* 61:263-289. <https://doi.org/10.1146/annurev-arplant-042809-112315>.

- Schirp, A., Farrell, R. L., and Kreber, B. 2003. Effects of New Zealand sapstaining fungi on structural integrity of unseasoned radiata pine. *Holz als Roh- und Werkstoff* 61(5):369-376. <https://doi.org/10.1007/s00107-003-0402-9>.
- Schmidt, O., and Czeschlik, D. 2006. Wood and tree fungi: Biology, damage, protection, and use. Springer, Berlin.
- Schmidt, O., and Liese, W. 1978. Biological variations within *Schizophyllum commune*. *Material und Organismen* 13(3):169-185.
- Schmidt, O., and Liese, W. 1980. Variability of wood degrading enzymes of *Schizophyllum commune*. *Holzforschung* 34(2):67-72.
- Schmidt, O., Sheng Wei, D., Liese, W., and Wollenberg, E. 2011. Fungal degradation of bamboo samples. *Holzforschung* 65(6):883-888. <https://doi.org/10.1515/HF.2011.084>.
- Schöneberg, A., Musa, T., Voegele, R. T., and Vogelgsang, S. 2015. The potential of antagonistic fungi for control of *Fusarium graminearum* and *Fusarium crookwellense* varies depending on the experimental approach. *Journal of Applied Microbiology* 118(5):1165-1179. <https://doi.org/10.1111/jam.12775>.
- Schuurs, T. A., Dalstra, H. J., Scheer, J. M., and Wessels, J. G. 1998. Positioning of nuclei in the secondary mycelium of *Schizophyllum commune* in relation to differential gene expression. *Fungal Genetics and Biology* 23(2):150-161. <https://doi.org/10.1006/fgbi.1997.1028>.
- Schwarze, F. W., Jauss, F., Spencer, C., Hallam, C., and Schubert, M. 2012. Evaluation of an antagonistic *Trichoderma* strain for reducing the rate of wood decomposition by the white rot fungus *Phellinus noxius*. *Biological Control* 61(2):160-168. <https://doi.org/10.1016/j.biocontrol.2012.01.016>.
- Schwarze, F. W. M. R., Engels, J., Mattheck, C., and Linnard, W. 2000. Fungal strategies of wood decay in trees: German edition: "*Holzzersetzende Pilze in Bäumen - Strategien der Holzzersetzung*". Springer Verlag, Berlin, Heidelberg.
- Seephueak, P., Petcharat, V., and Phongpaichit, S. 2010. Fungi associated with leaf litter of para rubber (*Hevea brasiliensis*). *Mycology* 1(4):213-227. <https://doi.org/10.1080/21501203.2010.536594>.

- Seephueak, P., Phongpaichit, S., Hyde, K. D., and Petcharat, V. 2011. Diversity of saprobic fungi on decaying branch litter of the rubber tree (*Hevea brasiliensis*). *Mycosphere* 2(4):307-330.
- Sefidi, K., and Etemad, V. 2015. Dead wood characteristics influencing macrofungi species abundance and diversity in Caspian natural beech (*Fagus orientalis* Lipsky) forests. *Forest Systems* 24(2):eSC03. <https://doi.org/10.5424/fs/2015242-06039>.
- Seidl, V. 2008. Chitinases of filamentous fungi: a large group of diverse proteins with multiple physiological functions. *Fungal Biology Reviews* 22(1):36-42. <https://doi.org/10.1016/j.fbr.2008.03.002>.
- Selitrennikoff, C. P. 2001. Antifungal proteins. *Applied and Environmental Microbiology* 67(7):2883-2894. <https://doi.org/10.1128/AEM.67.7.2883-2894.2001>.
- Shams-Ghahfarokhi, M., Aghaei-Gharehbolagh, S., Aslani, N., and Razzaghi-Abyaneh, M. 2014. Investigation on distribution of airborne fungi in outdoor environment in Tehran, Iran. *Journal of Environmental Health Science & Engineering* 12(1):54. <https://doi.org/10.1186/2052-336X-12-54>.
- Sharma, N., Rathore, M., and Sharma, M. 2013. Microbial pectinase: sources, characterization and applications. *Reviews in Environmental Science and Bio/Technology* 12(1):45-60. <https://doi.org/10.1007/s11157-012-9276-9>.
- Shuhada, S. N., Salim, S., Nobilly, F., Zubaid, A., and Azhar, B. 2017. Logged peat swamp forest supports greater macrofungal biodiversity than large-scale oil palm plantations and smallholdings. *Ecology and Evolution* 7(18):7187-7200. <https://doi.org/10.1002/ece3.3273>.
- Sigler, L., Bartley, J. R., Parr, D. H., and Morris, A. J. 1999. Maxillary sinusitis caused by medusoid form of *Schizophyllum commune*. *Journal of Clinical Microbiology* 37(10):3395-3398. <https://doi.org/10.1128/JCM.37.10.3395-3398.1999>.
- Singha, B. L., Hassan, Y., and Borah, R. K. 2017. Durability of traditionally treated *Bambusa tulda* towards white rot fungus using vermiculite. *International Journal of Science and Research* 6(4):967-970.
- Siqueira, J. P. Z., Sutton, D., Gené, J., García, D., Guevara-Suarez, M., Decock, C., Wiederhold, N., and Guarro, J. 2016. *Schizophyllum radiatum*, an emerging fungus from human

- respiratory tract. *Journal of Clinical Microbiology* 54(10):2491-2497.
<https://doi.org/10.1128/JCM.01170-16>.
- Sjöström, E. 1993. *Wood chemistry: Fundamentals and applications*. 2. ed. Academic Press, San Diego.
- Song, Z., Kennedy, P. G., Liew, F. J., and Schilling, J. S. 2017. Fungal endophytes as priority colonizers initiating wood decomposition. *Functional Ecology* 31(2):407-418.
<https://doi.org/10.1111/1365-2435.12735>.
- Song, Z., Vail, A., Sadowsky, M. J., and Schilling, J. S. 2015. Influence of hyphal inoculum potential on the competitive success of fungi colonizing wood. *Microbial Ecology* 69(4):758-767. <https://doi.org/10.1007/s00248-015-0588-5>.
- Speckbacher, V., and Zeilinger, S. 2018. Secondary Metabolites of Mycoparasitic Fungi in: *Secondary Metabolites - Sources and Applications*. R. Vijayakumar, and S. S. Raja, eds. InTech.
- Stajić, M., Vukojević, J., Milovanović, I., Čilerdžić, J., and Knežević, A. 2016. Role of Mushroom Mn-Oxidizing Peroxidases in Biomass Conversion. Pages 251–269 in: *Microbial Enzymes in Bioconversions of Biomass*. V. K. Gupta, ed. Springer International Publishing, Cham.
- Stalpers, J. A. 1988. Auriculariopsis and the Schizophyllales. *Persoonia - Molecular Phylogeny and Evolution of Fungi* 13(4):495-504.
- Stoilova, I., and Krastanov, A. 2008. Overproduction of laccase and pectinase by microbial associations in solid substrate fermentation. *Applied Biochemistry and Biotechnology* 149(1):45-51. <https://doi.org/10.1007/s12010-007-8013-2>.
- Stravinskienė, V., Snieškienė, V., and Stankevičienė, A. 2015. Health condition of *Tilia cordata* Mill. trees growing in the urban environment. *Urban Forestry & Urban Greening* 14(1):115-122. <https://doi.org/10.1016/j.ufug.2014.12.006>.
- Suárez, M. B., Vizcaíno, J. A., Llobell, A., and Monte, E. 2007. Characterization of genes encoding novel peptidases in the biocontrol fungus *Trichoderma harzianum* CECT 2413 using the TrichoEST functional genomics approach. *Current Genetics* 51(5):331-342.
<https://doi.org/10.1007/s00294-007-0130-5>.

- Suliaman, S. Q., AL-Khesraji, T. O., and Hassan, A. A. 2017. New records of basidiomycetous macrofungi from Kurdistan region - Northern Iraq. *African Journal of Plant Science* 11(6):209-219. <https://doi.org/10.5897/AJPS2017.1543>.
- Sun, X., Sun, Y., Zhang, Q., Zhang, H., Yang, B., Wang, Z., Zhu, W., Li, B., Wang, Q., and Kuang, H. 2014. Screening and comparison of antioxidant activities of polysaccharides from *Coriolus versicolor*. *International Journal of Biological Macromolecules* 69:12-19. <https://doi.org/10.1016/j.ijbiomac.2014.05.027>.
- Supaphon, P., Phongpaichit, S., Rukachaisirikul, V., and Sakayaroj, J. 2014. Diversity and antimicrobial activity of endophytic fungi isolated from the seagrass *Enhalus acoroides*. *Indian Journal of Geo-Marine Sciences* 43(5):785-797.
- Suprapti, S. 2002. Ketahanan kayu mangium (*Acacia mangium* Willd.) terhadap sebelas jamur pelapuk kayu (The resistance of Mangium (*Acacia mangium* Willd.) wood against eleven wood-decaying fungi). *Buletin Penelitian Hasil Hutan* 20(3):187–193 (In Indonesian).
- Suprapti, S. 2010. Decay resistance of 84 Indonesian wood species against fungi. *Journal of Tropical Forest Science* 22(1):81-87.
- Suprapti, S., and Djarwanto. 2012. Ketahanan enam jenis kayu terhadap jamur pelapuk (The resistance of six wood species against decaying fungi). *Jurnal Penelitian Hasil Hutan* 30(3):228–235 (In Indonesian).
- Suprapti, S., and Djarwanto. 2013. Ketahanan lima jenis kayu asal Cianjur terhadap jamur (The resistance of five wood species from Cianjur against decaying fungi). *Jurnal Penelitian Hasil Hutan* 31(3):193–199 (In Indonesian).
- Suprapti, S., and Djarwanto. 2014. Ketahanan lima jenis kayu asal Ciamis terhadap sebelas strain jamur pelapuk (the resistance of five wood species from Ciamis against eleven strain of decaying fungi). *Jurnal Penelitian Hasil Hutan* 32(3):189–198 (In Indonesian).
- Suprapti, S., and Djarwanto. 2015. Uji pelapukan lima jenis kayu yang dipasang sekrup logam (Decay tests on five wood species fastened with metal screw). *Jurnal Penelitian Hasil Hutan* 33(4):365–376 (In Indonesian).

- Suprapti, S., Djarwanto, and Andianto. 2016. Daya tahan enam jenis kayu asal Papua terhadap jamur perusak (Decay resistance of six wood species from Papua against destroying fungi). *Jurnal Penelitian Hasil Hutan* 34(2):157–165 (In Indonesian).
- Suprapti, S., Djarwanto, and Hudiansyah. 2007. Ketahanan lima jenis kayu terhadap tigabelas jamur perusak kayu (The resistance of five wood species against thirteen wood destroying fungi). *Journal of Forest Product Research* 25:75–83 (In Indonesian).
- Suprapti, S., Djarwanto, and Hudiansyah. 2011. Ketahanan lima jenis kayu asal Lengkong Sukabumi terhadap beberapa jamur pelapuk (The resistance of five wood species originated from Lengkong Sukabumi against some decaying fungi). *Journal Penelitian Hasil Hutan* 29(3):259–270 (In Indonesian).
- Susi, P., Aktuganov, G., Himanen, J., and Korpela, T. 2011. Biological control of wood decay against fungal infection. *Journal of Environmental Management* 92(7):1681-1689. <https://doi.org/10.1016/j.jenvman.2011.03.004>.
- Sysouphanthong, P., Thongkantha, S., Zhao, R., Soyotong, K., and Hyde, K. D. 2010. Mushroom diversity in sustainable shade tea forest and the effect of fire damage. *Biodiversity and Conservation* 19(5):1401-1415. <https://doi.org/10.1007/s10531-009-9769-1>.
- Takahashi, M. 1977. Studies on the wood decay by a soft rot fungus, *Chaetomium globosum* Kunze, Kyoto, Japan.
- Takemoto, S., Nakamura, H., Imamura, Y., and Shimane, T. 2010. *Schizophyllum commune* as a ubiquitous plant parasite. *Japan Agricultural Research Quarterly* 44(4):357-364. <https://doi.org/10.6090/jarq.44.357>.
- Tanaka, H., Takizawa, K., Baba, O., Maeda, T., Fukushima, K., Shinya, K., and Kosuge, J. 2008. Basidiomycosis: *Schizophyllum commune* osteomyelitis in a dog. *The Journal of Veterinary Medical Science* 70(11):1257-1259. <https://doi.org/10.1292/jvms.70.1257>.
- Tanesaka, E., Masuda, H., and Kinugawa, K. 1993. Wood degrading ability of basidiomycetes that are wood decomposers, litter decomposers, or mycorrhizal symbionts. *Mycologia* 85(3):347-354.

- Tang, W., Jia, R., and Zhang, D. 2011. Decolorization and degradation of synthetic dyes by *Schizophyllum* sp. F17 in a novel system. *Desalination* 265(1-3):22-27.
<https://doi.org/10.1016/j.desal.2010.07.024>.
- Tantengco, O. A. G. 2018. Ethnomycological survey of macrofungi utilized by Ayta communities in Bataan, Philippines. *Current Research in Environmental & Applied Mycology* 8(1):104-108. <https://doi.org/10.5943/cream/8/1/9>.
- Tapwal, A., Kumar, R., and Pandey, S. 2013. Diversity and frequency of macrofungi associated with wet ever green tropical forest in Assam, India. *Biodiversitas* 14(2):73-78.
<https://doi.org/10.13057/biodiv/d140204>.
- Tarasov, D., Leitch, M., and Fatehi, P. 2018. Lignin-carbohydrate complexes: properties, applications, analyses, and methods of extraction: a review. *Biotechnology for Biofuels* 11:269. <https://doi.org/10.1186/s13068-018-1262-1>.
- Tchinda, J.-B. S., Ndikontar, M. K., Belinga, A. D. F., Mounguengui, S., Njankouo, J. M., Durmaçay, S., and Gerardin, P. 2018. Inhibition of fungi with wood extractives and natural durability of five Cameroonian wood species. *Industrial Crops and Products* 123:183-191.
<https://doi.org/10.1016/j.indcrop.2018.06.078>.
- Terakawa, A., Natsume, A., Okada, A., Nishihata, S., Kuse, J., Tanaka, K., Takenaka, S., Ishikawa, S., and Yoshida, K.-I. 2016. *Bacillus subtilis* 5'-nucleotidases with various functions and substrate specificities. *BMC Microbiology* 16(1):249.
<https://doi.org/10.1186/s12866-016-0866-5>.
- The UniProt Consortium. 2019. UniProt: a worldwide hub of protein knowledge. *Nucleic Acids Research* 47(D1):D506-D515. <https://doi.org/10.1093/nar/gky1049>.
- Thorn, S., Bässler, C., Bußler, H., Lindenmayer, D. B., Schmidt, S., Seibold, S., Wende, B., and Müller, J. 2016. Bark-scratching of storm-felled trees preserves biodiversity at lower economic costs compared to debarking. *Forest Ecology and Management* 364:10-16.
<https://doi.org/10.1016/j.foreco.2015.12.044>.
- Tovar-Herrera, O. E., Batista-García, R. A., Sánchez-Carbente, M. d. R., Iracheta-Cárdenas, M. M., Arévalo-Niño, K., and Folch-Mallol, J. L. 2015. A novel expansin protein from the

- white-rot fungus *Schizophyllum commune*. PloS One 10(3):e0122296.
<https://doi.org/10.1371/journal.pone.0122296>.
- Tovar-Herrera, O. E., Martha-Paz, A. M., Pérez-LLano, Y., Aranda, E., Tacoronte-Morales, J. E., Pedroso-Cabrera, M. T., Arévalo-Niño, K., Folch-Mallol, J. L., and Batista-García, R. A. 2018. *Schizophyllum commune*: An unexploited source for lignocellulose degrading enzymes. MicrobiologyOpen 7(3):e00637. <https://doi.org/10.1002/mbo3.637>.
- Treseder, K. K., and Lennon, J. T. 2015. Fungal traits that drive ecosystem dynamics on land. Microbiology and Molecular Biology Reviews 79(2):243-262.
<https://doi.org/10.1128/MMBR.00001-15>.
- Tsujiyama, S., and Minami, M. 2005. Production of phenol-oxidizing enzymes in the interaction between white-rot fungi. Mycoscience 46(4):268-271. <https://doi.org/10.1007/s10267-005-0243-y>.
- Tudor, D., Robinson, S. C., Krigstin, T. L., and Cooper, P. A. 2014. Microscopic investigation on fungal pigment formation and its morphology in wood substrates. The Open Mycology Journal 8(1):174-186. <https://doi.org/10.2174/1874437001408010174>.
- Tzean, S. S., and Estey, R. H. 1978. *Schizophyllum commune* Fr. as a destructive mycoparasite. Canadian Journal of Microbiology 24(7):780-784. <https://doi.org/10.1139/m78-131>.
- Udochukwu, U., Nekpen, B. O., Udinyiwe, O. C., and Omeje, F. I. 2014. Bioaccumulation of heavy metals and pollutants by edible mushroom collected from Iselu market Benin-city. International Journal of Current Microbiology and Applied Sciences 3(10):52-57.
- Ujang, S., Jones, E., and Watling, R. 2002. The distribution of wood-inhabiting fungi in peninsular Malaysia. Journal of Tropical Forest Science 14(4):433-440.
- Ujang, S., Wong, A. H., and Jones, E. G. 2007. Wood degrading fungi. Pages 163–183 in: Maldysian Fungal Diversity. E. G. Jones, K. D. Hyde, and V. Sabaratnam, eds. Mushroom Research Centre, University of Malaya and Ministry of Natural Resources and Environment Malaysia.
- Ujor, V. C., Monti, M., Peiris, D. G., Clements, M. O., and Hedger, J. N. 2012a. The mycelial response of the white-rot fungus, *Schizophyllum commune* to the biocontrol agent,

- Trichoderma viride*. Fungal Biology 116(2):332-341.
<https://doi.org/10.1016/j.funbio.2011.12.008>.
- Ujor, V. C., Peiris, D. G., Monti, M., Kang, A. S., Clements, M. O., and Hedger, J. N. 2012b. Quantitative proteomic analysis of the response of the wood-rot fungus, *Schizophyllum commune*, to the biocontrol fungus, *Trichoderma viride*. Letters in Applied Microbiology 54(4):336-343. <https://doi.org/10.1111/j.1472-765X.2012.03215.x>.
- Ulyshen, M. D., Müller, J., and Seibold, S. 2016. Bark coverage and insects influence wood decomposition: Direct and indirect effects. Applied Soil Ecology 105:25-30.
<https://doi.org/10.1016/j.apsoil.2016.03.017>.
- van Suijdam, J. C., Kossen, N. W. F., and Paul, P. G. 1980. An inoculum technique for the production of fungal pellets. European Journal of Applied Microbiology and Biotechnology 10:211-221.
- Vane, C. H., Drage, T. C., and Snape, C. E. 2006. Bark decay by the white-rot fungus *Lentinula edodes*: Polysaccharide loss, lignin resistance and the unmasking of suberin. International Biodeterioration & Biodegradation 57(1):14-23. <https://doi.org/10.1016/j.ibiod.2005.10.004>.
- Vasina, D. V., Pavlov, A. R., and Koroleva, O. V. 2016. Extracellular proteins of *Trametes hirsuta* st. 072 induced by copper ions and a lignocellulose substrate. BMC Microbiology 16(1):106. <https://doi.org/10.1186/s12866-016-0729-0>.
- Veiter, L., Rajamanickam, V., and Herwig, C. 2018. The filamentous fungal pellet-relationship between morphology and productivity. Applied Microbiology and Biotechnology 102(7):2997-3006. <https://doi.org/10.1007/s00253-018-8818-7>.
- Vek, V., Oven, P., Ters, T., Poljanšek, I., and Hinterstoisser, B. 2014. Extractives of mechanically wounded wood and knots in beech. Holzforschung 68(5):529-539.
<https://doi.org/10.1515/hf-2013-0003>.
- Verma, P., and Madamwar, D. 2002. Production of Ligninolytic Enzymes for Dye Decolorization by Cocultivation of White-Rot Fungi *Pleurotus ostreatus* and *Phanerochaete chrysosporium* Under Solid-State Fermentation. Applied Biochemistry and Biotechnology 102-103(1-6):109-118. <https://doi.org/10.1385/ABAB:102-103:1-6:109>.

- Villavicencio, E. V., Mali, T., Mattila, H. K., and Lundell, T. 2020. Enzyme activity profiles produced on wood and straw by four fungi of different decay strategies. *Microorganisms* 8(1). <https://doi.org/10.3390/microorganisms8010073>.
- Viterbo, A., Ramot, O., Chemin, L., and Chet, I. 2002. Significance of lytic enzymes from *Trichoderma* spp. in the biocontrol of fungal plant pathogens. *Antonie van Leeuwenhoek* 81(1-4):549-556. <https://doi.org/10.1023/a:1020553421740>.
- Voragen, A. G. J., Coenen, G.-J., Verhoef, R. P., and Schols, H. A. 2009. Pectin, a versatile polysaccharide present in plant cell walls. *Structural Chemistry* 20(2):263-275. <https://doi.org/10.1007/s11224-009-9442-z>.
- Wald, P., Pitkänen, S., and Boddy, L. 2004. Interspecific interactions between the rare tooth fungi *Creolophus cirrhatus*, *Hericium erinaceus* and *H. coralloides* and other wood decay species in agar and wood. *Mycological Research* 108(Pt 12):1447-1457. <https://doi.org/10.1017/s0953756204001340>.
- Walsh, G. 2015. Hormones and Growth Factors Used Therapeutically. Pages 233–255 in: *Proteins: Biochemistry and Biotechnology*. G. Walsh, ed. John Wiley & Sons, Inc, Hoboken, NJ, USA.
- Wang, S., Dai, G., Yang, H., and Luo, Z. 2017. Lignocellulosic biomass pyrolysis mechanism: A state-of-the-art review. *Progress in Energy and Combustion Science* 62:33-86. <https://doi.org/10.1016/j.pecs.2017.05.004>.
- Wasser, S. P. 2002. Medicinal mushrooms as a source of antitumor and immunomodulating polysaccharides. *Applied Microbiology and Biotechnology* 60(3):258-274. <https://doi.org/10.1007/s00253-002-1076-7>.
- Weedon, J. T., Cornwell, W. K., Cornelissen, J. H. C., Zanne, A. E., Wirth, C., and Coomes, D. A. 2009. Global meta-analysis of wood decomposition rates: a role for trait variation among tree species? *Ecology Letters* 12(1):45-56. <https://doi.org/10.1111/j.1461-0248.2008.01259.x>.
- Wei, D., Schmidt, O., and Liese, W. 2013. Method to test fungal degradation of bamboo and wood using vermiculite as reservoir for moisture and nutrients. *Maderas. Ciencia y tecnología* 15(3):349-356. <https://doi.org/10.4067/S0718-221X2013005000027>.

- Wengel, M., Kothe, E., Schmidt, C. M., Heide, K., and Gleixner, G. 2006. Degradation of organic matter from black shales and charcoal by the wood-rotting fungus *Schizophyllum commune* and release of DOC and heavy metals in the aqueous phase. *The Science of the Total Environment* 367(1):383-393. <https://doi.org/10.1016/j.scitotenv.2005.12.012>.
- Wessel, D., and Flügge, U. I. 1984. A method for the quantitative recovery of protein in dilute solution in the presence of detergents and lipids. *Analytical Biochemistry* 138(1):141-143. [https://doi.org/10.1016/0003-2697\(84\)90782-6](https://doi.org/10.1016/0003-2697(84)90782-6).
- Wessels, J. G. H. 1965. Morphogenesis and biochemical processes in *Schizophyllum commune* Fr. *Wentia* 13:1-113. <https://doi.org/10.1111/j.1438-8677.1965.tb00016.x>.
- Wessels, J. G. H., Mulder, G. H., and Springer, J. 1987. Expression of dikaryon-specific and non-specific mRNAs of *Schizophyllum commune* in relation to environmental conditions and fruiting. *Microbiology* 133(9):2557-2561. <https://doi.org/10.1099/00221287-133-9-2557>.
- Wetzel, S., Demmers, C., and Greenwood, J. S. 1989. Seasonally fluctuating bark proteins are a potential form of nitrogen storage in three temperate hardwoods. *Planta* 178(3):275-281. <https://doi.org/10.1007/BF00391854>.
- White, T. C. R. 2012. *The inadequate environment: Nitrogen and the abundance of animals*. Springer-Verlag, Berlin, New York.
- Wilhelm, G. E., Liese, W., and Parameswaran, N. 1976. On the degradation of tree bark by microorganisms. *Organismen und Holz*(3):63-75.
- Win, C. C., Kyi-1, W., and Kyi-2, W. 2005. The effectiveness of BFCA and CCA wood preservatives on the durability of ten lesser-used timber species of Myanmar. Pages 386–426 in: *Proceedings of the Annual Research Conference (Forestry Sciences)*, Yangon, Myanmar, 7-9 January, 2005. Myanmar Academy of Agricultural, Forestry, Livestock and Fishery Sciences.
- Wong, D. W. S. 2009. Structure and action mechanism of ligninolytic enzymes. *Applied Biochemistry and Biotechnology* 157(2):174-209. <https://doi.org/10.1007/s12010-008-8279-z>.

- Woods, C. M., Woodward, S., and Redfern, D. B. 2005. In vitro interactions in artificial and wood-based media between fungi colonizing stumps of Sitka spruce. *Forest Pathology* 35(3):213-229. <https://doi.org/10.1111/j.1439-0329.2005.00403.x>.
- Wu, Y., and Daeschel, M. A. 2007. Lytic antimicrobial activity of hen egg white lysozyme immobilized to polystyrene beads. *Journal of food science* 72(9):M369-74. <https://doi.org/10.1111/j.1750-3841.2007.00529.x>.
- Xu, F., Shin, W., Brown, S. H., Wahleithner, J. A., Sundaram, U. M., and Solomon, E. I. 1996. A study of a series of recombinant fungal laccases and bilirubin oxidase that exhibit significant differences in redox potential, substrate specificity, and stability. *Biochimica et Biophysica Acta (BBA) - Protein Structure and Molecular Enzymology* 1292(2):303-311. [https://doi.org/10.1016/0167-4838\(95\)00210-3](https://doi.org/10.1016/0167-4838(95)00210-3).
- Xu, W., Guo, S., Gong, L., Alias, S. A., Pang, K.-L., and Luo, Z.-H. 2018. Phylogenetic survey and antimicrobial activity of cultivable fungi associated with five scleractinian coral species in the South China Sea. *Botanica Marina* 61(1):75-84. <https://doi.org/10.1515/bot-2017-0005>.
- Yamaç, M., and Bilgili, F. 2006. Antimicrobial Activities of Fruit Bodies and/or Mycelial Cultures of Some Mushroom Isolates. *Pharmaceutical Biology* 44(9):660-667. <https://doi.org/10.1080/13880200601006897>.
- Yao, J., Jia, R., Zheng, L., and Wang, B. 2013. Rapid decolorization of azo dyes by crude manganese peroxidase from *Schizophyllum* sp. F17 in solid-state fermentation. *Biotechnol Bioproc E* 18(5):868-877. <https://doi.org/10.1007/s12257-013-0357-6>.
- Yao, M., Li, W., Duan, Z., Zhang, Y., and Jia, R. 2017. Genome sequence of the white-rot fungus *Irpex lacteus* F17, a type strain of lignin degrader fungus. *Standards in genomic sciences* 12:55. <https://doi.org/10.1186/s40793-017-0267-x>.
- Yapo, B. M. 2011. Pectic substances: From simple pectic polysaccharides to complex pectins—A new hypothetical model. *Carbohydrate Polymers* 86(2):373-385. <https://doi.org/10.1016/j.carbpol.2011.05.065>.
- Yelle, D. J., Ralph, J., Lu, F., and Hammel, K. E. 2008. Evidence for cleavage of lignin by a brown rot basidiomycete. *Environmental Microbiology* 10(7):1844-1849. <https://doi.org/10.1111/j.1462-2920.2008.01605.x>.

- Yoshizawa, M., Kawarai, S., Torii, Y., Ota, K., Tasaka, K., Nishimura, K., Fujii, C., and Kanemaki, N. 2017. Eosinophilic plasmacytic conjunctivitis concurrent with gingival fistula caused by *Schizophyllum commune* in a captive cheetah (*Acinonyx jubatus*). Medical Mycology Case Reports 18:34-39. <https://doi.org/10.1016/j.mmcr.2017.09.001>.
- You, Y.-H., Yoon, H., Seo, Y., Kim, M., Shin, J.-H., Lee, I.-J., Choo, Y.-S., and Kim, J.-G. 2012. Analysis of genomic diversity of endophytic fungal strains isolated from the roots of *Suaeda japonica* and *S. maritima* for the restoration of ecosystems in Buan salt marsh. Korean Journal of Microbiology and Biotechnology 40(4):287-295. <https://doi.org/10.4014/kjmb.1207.07025>.
- Yudina, T. G., Guo, D., Piskunkova, N. F., Pavlova, I. B., Zavalova, L. L., and Baskova, I. P. 2012. Antifungal and antibacterial functions of medicinal leech recombinant destabilase-lysozyme and its heated-up derivative. Front. Chem. Sci. Eng. 6(2):203-209. <https://doi.org/10.1007/s11705-012-1277-2>.
- Zakzeski, J., Bruijninx, P. C. A., Jongerius, A. L., and Weckhuysen, B. M. 2010. The catalytic valorization of lignin for the production of renewable chemicals. Chemical reviews 110(6):3552-3599. <https://doi.org/10.1021/cr900354u>.
- Zhao, Z., Liu, H., Wang, C., and Xu, J.-R. 2013. Comparative analysis of fungal genomes reveals different plant cell wall degrading capacity in fungi. BMC Genomics 14(274):1-15. <https://doi.org/10.1186/1471-2164-14-274>.
- Zhou, X., Li, W., Mabon, R., and Broadbelt, L. J. 2017. A Critical Review on Hemicellulose Pyrolysis. Energy Technol. 5(1):52-79. <https://doi.org/10.1002/ente.201600327>.
- Zhou, Y., Yang, B., Yang, Y., and Jia, R. 2014. Optimization of manganese peroxidase production from *Schizophyllum* sp. F17 in solid-state fermentation of agro-industrial residues. Sheng wu gong cheng xue bao = Chinese journal of biotechnology 30(3):524-528.
- Zhu, N., Liu, J., Yang, J., Lin, Y., Yang, Y., Ji, L., Li, M., and Yuan, H. 2016. Comparative analysis of the secretomes of *Schizophyllum commune* and other wood-decay basidiomycetes during solid-state fermentation reveals its unique lignocellulose-degrading enzyme system. Biotechnology for Biofuels 9(42):1-22. <https://doi.org/10.1186/s13068-016-0461-x>.

Zia, A., Majcherczyk, A., and Kues, U. 2018. *Trametes versicolor* and *Schizophyllum commune* as early sapwood colonizers on wood. Accessed Jul 5, 2020.

Zolan, M. E., and Pukkila, P. J. 1986. Inheritance of DNA methylation in *Coprinus cinereus*. *Molecular and cellular biology* 6(1):195-200. <https://doi.org/10.1128/mcb.6.1.195-200.1986>.

Acknowledgements

First and foremost, I'd like to express my gratitude to Prof. Dr. Carsten Mai for being my supervisor. I appreciate all the constructive discussions and critical reviews of my data and thesis. I benefited greatly not only from your expertise, but also from your innovative research approaches. Thank you for your patience, mentoring, guidance and specially encouragement. It was a very enriching time, thank you! You are an excellent supervisor who stands by your students' side and backs them up completely. I would like also to thank Prof. Dr. Andrea Polle and PD. Dr. Markus Euring for accepting to be members of my thesis committee and for your unwavering support.

Prof. Dr. Ursula Kües deserves special thanks for allowing me to use the departmental facility for my lab work and for her guidance during the practical part of my thesis. I'm also grateful to Dr. Andrzej Majcherczyk for teaching me how to use the TripleTOF mass spectrometer and for the fruitful discussions. I want to express my sincere gratitude to Prof. Dr. Christian Ammer for your time and efforts to help with the issues I encountered during my PhD and for your participation in the examination committee. I really appreciate your continuous support.

Mrs. (Late) Karin Lange, Mr. Mojtaba Zomorodi, and Mr. Marco Winkler, lab technicians, deserve special recognition for their outstanding technical assistance during my PhD. Mr. Michael Unger assisted me with German language translation. Additionally, I appreciate all the support from my colleagues during my PhD.

My dear friend Yahya Z. A. Gaafar, you have been a tremendous personal support to me during my master's degree and, particularly, during my PhD studies. Our friendly meetings were a welcome relief "second after prayers" during the PhD period, which was full of stressful moments. I'll never forget the helpful criticism and suggestions for improving my work. Thank you, brother. I am grateful to my father, Dr. Bashir Ahmad Zia, and my mother for raising me and providing me with every opportunity to succeed. Thank you for your prayers and your infinite support. Special thanks to my brothers, brother-in-law, sister, sister-in-law, and nephew for your emotional support and prayers.

I highly acknowledge the financial support by the "Materialforschung Holz" (MaFo Holz) PhD program through the Ministry of Lower Saxony in terms of the "Georg-Christoph-

Lichtenberg-Scholarship". I am also grateful for the German Research Foundation (Deutsche Forschungsgemeinschaft; DFG) for funding the TripleTOF 5600 mass-spectrometer instrument (DFG-GZ: INST 186/1085-1 FUGG).

Thank you all for being a part of this journey with me; I wish you all the best.

Amjad Zia

Curriculum Vitae

AMJAD ZIA

born in Faisalabad, Pakistan

EDUCATION

- 09/2015 – 07/2021 PhD, Biotechnology and Mycology
University of Göttingen, Göttingen, Germany
Thesis title: Unlocking proteomic and ecological heterogeneity between *Schizophyllum commune* and *Trametes versicolor* as early sapwood colonizers on wood
- 09/2014 – 09/2012 Erasmus Mundus: European Master of Science in Nematology
Ghent University, Belgium
Thesis title: Diversity of root-knot nematodes in multiple cropping regions of Pakistan
- 08/2008 – 09/2006 M.Sc. (Hons) Agriculture – Plant Pathology
University of Agriculture, Faisalabad, Pakistan
Thesis title: Development and reproduction of *Meloidogyne incognita* on tomato cultivars & its effect on plant growth
- 07/2006 – 12/2002 B.Sc. (Hons) Agriculture – Plant pathology
University of Agriculture, Faisalabad, Pakistan

PROFESSIONAL EXPERIENCE

- 08/2021 – continue Wissenschaftlicher (PostDoc)
Institut für Klinische Chemie, Universitätsmedizin Göttingen, Georg-August-Universität, Göttingen, Germany
- 07/2011 – 09/2012 Assistant Research Officer (Plant Pathology) / Farm Manager

Plant pathology section, Ayub Agriculture Research Institute, Faisalabad, Pakistan

09/2009 – 07/2011 Plant Pathologist
Central seed testing Lab., Ministry of National Food Security and Research, Islamabad, Pakistan

09/2006 – 03/2009 Research Fellow
Department of Plant Pathology, University of Agriculture, Faisalabad, Pakistan

04/2003 – 05/2004
09/2005 – 10/2005 Science Teacher
Al-Falah Secondary School, Faisalabad, Pakistan

INTERNSHIPS

06/2006 – 08/2006 Internship (Plant Pathology)
Department of Plant Pathology, University of Agriculture, Faisalabad, Pakistan

02/2006 – 05/2006 Internship (Plant Pathology)
Plant pathology section, Ayub Agricultural Research Institute, Faisalabad, Pakistan

AWARDS & SCHOLARSHIPS

12/2008 3rd Prize in Poster Presentation “Distribution and association of root knot nematodes (*Meloidogyne* spp.) with tomato in district Faisalabad” by participating in Nematological Session of “35th All Pakistan Science Conference” at University of Karachi on 20th -23rd December 2018.

09/2012 – 08/2014 “ERASMUS MUNDUS” scholarship for two years program of “European Master of Science in Nematology”, Ghent University, Belgium

09/2015 – 08/2018

Georg-Christoph-Lichtenberg scholarship for PhD studies, Georg-August-Universität Göttingen, Göttingen, Germany